The roles of phytohormones in floral arrest and carpic dominance

Catriona Holly Walker

Submitted in accordance with the requirements for the degree of

Doctor of Philosophy

The University of Leeds

Faculty of Biological Sciences

September 2022

The candidate confirms that the work submitted is her own, except where work which has formed part of jointly-authored publications has been included. The contribution of the candidate and the other authors to this work has been explicitly indicated below. The candidate confirms that appropriate credit has been given within the thesis where reference has been made to the work of others.

Assertion of moral rights:

Acknowledgements

First and foremost, thank you to Dr Tom Bennett for your mentorship, enthusiasm and patience. Your determination to make me believe in my own abilities has been invaluable, and is something I will take with me in both my future work and life. This work would not have been possible without you. That being said, let's never forget that you initially thought 'a paper a year' was a somewhat unrealistic goal for me to set…

Alexander 'Al' Ware, Zoe Wilson and the rest of our collaborators who contributed to our publications – your input and direction was essential, and I am deeply grateful for both.

My thanks to the entire Bennett lab; Mary, Pablo, Jed, Alex, Roza, Iain, Jakub, Darren, Bianca, and especially to Cara, for all the science, friendship and cake. Thank you for all the emotional and intellectual support, it has been a pleasure to work alongside you for the last 5+ years.

I thank my family for their support and encouragement, throughout this PhD and life in general. Mum, Dad and Neen – I am infinitely grateful to you all, even though none of you understand exactly what it is that I do.

To Aisling, for all your support through the lockdown and beyond. If your total lack of boundaries, and your permanent willingness to share disturbing x-rays with me weren't going to get me though the lockdown, then nothing was.

To Rachel, for your sheer persistence in friendship, emotional support and belief in me. The snacks, prosecco and all our pets with questionable names have been a joy to share with you.

Thanks to Sammy, Evie and Bekah – for always listening and encouraging, especially when experiments seemed endless and motivation was at its lowest.

Finally, my love and thanks to Ed. Thank you for always asking how the meristems were doing, and for remaining optimistic even after I'd accidentally mashed one-too-many of them with a scalpel.

This research has been carried out by a team which has included Dr Tom Bennett, Cara Wheeldon, Dr Alexander Ware and Jan Šimura. My own contributions, and those of the other members of the group have been as follows:

Figure / Table	Data collection carried out by:	Notes
Chapter 1 – General Introduction		
Figure 1.1	Catriona Walker	
Figure 1.2	Catriona Walker	
Figure 1.3	Catriona Walker	Adapted from Michniewicz, Brewer and Friml, 2007; Balzan, Johal and Carraro, 2014
Figure 1.4	Catriona Walker	Adapted from Wheeldon and Bennett (2021); Pernisova et al. (2018); Shull, Kurepa and Smalle (2016); Kurepa, Li and Smalle (2014).
Figure 1.5	Catriona Walker	
Figure 1.6	Catriona Walker	Adapted directly from Walker and Bennett (2018), with permission
Figure 1.7	Catriona Walker	
Chapter 2 - Integrated dominance mechanisms regulate reproductive architecture in *Arabidopsis thaliana* and *Brassica napus*		
Figure 2.i	Catriona Walker	
Figure 2.1	Catriona Walker, Tom Bennett	Experimental data collection equal between both authors

Figure / Table	Data collection carried out by:	Notes
Supplementary Figure 2.1	Catriona H Walker, Cara D Wheeldon, Tom Bennett	Figure contains multiple experiments run independently by the three authors. Experiment contributions to each figure are as follows; 1A – CHW x17, TB x31, CDW x3 1B – CHW x18, TB x6, CDW x1 1C – CHW x14, TB x3 1D – CHW
Figure 2.2 B	Catriona Walker	
Figure 2.2 A,C,D,E,F	Cara Wheeldon	
Supplemental Figure 2.2	Cara Wheeldon	
Figure 2.3	Catriona Walker	
Figure 2.4	Catriona Walker	
Figure 2.5	Catriona Walker	
Figure 2.6	Catriona Walker	
Figure 2.7	Catriona Walker, Tom Bennett	Figure 7A data was collected equally by CHW and TB. Figure 7B was collected by CHW
Figure 2.8	Tom Bennett	
Supplemental Figure 2.4	Catriona Walker	
Figure 2.ii	Catriona Walker	

Figure / Table	Data collection carried out by:	Notes
Figure 2.iii	Catriona Walker	
Figure 2.iv	Catriona Walker	
Chapter 3 - A distributive '50% rule' determines floral initiation rates in the Brassicaceae		
Supplementary Table 3.1	Catriona Walker	
Supplementary Table 3.2	Catriona Walker	
Figure 3.1 A	Tom Bennett	
Figure 3.1 B,C,D,E,F,G	Catriona Walker	
Supplementary Figure 3.1	Catriona Walker	
Figure 3.2 A,B,C,D	Catriona Walker	
Figure 3.2 E	Tom Bennett	
Chapter 4 - Auxin export from proximal fruits drives arrest in temporally-competent inflorescences		
Figure 4.1	Catriona Walker	
Supplementary Figure 4.1	Catriona Walker	
Supplementary Figure 4.2	Catriona Walker	
Figure 4.2	Catriona Walker	

Figure / Table	Data collection carried out by:	Notes
Figure 4.3	Catriona Walker	
Figure 4.4	Alexander Ware	
Figure 4.5	Catriona Walker	
Figure 4.6 A,B,C	Alexander Ware	
Figure 4.6 D,E	Alexander Ware, Jan Šimura	Samples collected by AW; auxin quantification by JŠ
Figure 4.6 F	Alexander Ware, Tom Bennett	Figure designed and prepared by AW, edited by TB
Extended data Figure 4.1 A,B,D	Alexander Ware	
Extended data Figure 4.1 C,E	Catriona Walker	
Supplementary Figure 4.3	Catriona Walker	
Chapter 5 - Cytokinin signalling regulates two-stage inflorescence arrest in Arabidopsis		
Figure 5.1	Catriona Walker	
Figure 5.2	Catriona Walker	
Figure 5.3 A-G	Catriona Walker, Tom Bennett	Samples collected and prepared by CHW. Images collected by both authors.
Figure 5.3 H,M	Catriona Walker	

Figure / Table	Data collection carried out by:	Notes
Figure 5.3 I,J,K,L	Alexander Ware	
Figure 5.4	Catriona Walker	
Supplementary Figure 5.1	Catriona Walker	
Supplementary Figure 5.2	Catriona Walker	
Figure 5.5	Catriona Walker	
Figure 5.6	Catriona Walker	
Figure 5.7 A	Alexander Ware, Jan Šimura	Samples collected by AW, iP, cZ, tZ and tZR quantification by JŠ
Figure 5.7 B,C	Catriona Walker	
Chapter 6 - Cytokinin signalling regulates age-dependent changes in inflorescence morphology in Arabidopsis		
Figure 6.1	Catriona Walker	
Figure 6.2	Catriona Walker	
Figure 6.3	Catriona Walker	
Figure 6.4	Catriona Walker	
Figure 6.5	Catriona Walker	
Chapter 7 – General discussion		
Figure 7.1	Catriona Walker	

Abstract

The number of reproductive organs, and their positioning in both space and time ('reproductive architecture') are vital factors for the production of offspring in plants. We do not yet fully understand the mechanisms by which plants 'decide' how many reproductive organs to make, and where to make them, although elements are known to be controlled by long-distance hormonal signalling. Here, we have examined the control of reproductive architecture in Arabidopsis and the wider Brassicaceae; focusing on the control of inflorescence production, the quantity and positioning of fruits, and the mechanisms underlying floral arrest. We have shown that early signals control the number of inflorescences produced, and that these strongly predict the number of fruits that the plant will make. Fruit are distributed across these inflorescences in a highly predictable manner, with ~50% being supported by the secondary inflorescences, likely as a consequence of the timing of inflorescence arrest. Our examination of inflorescence arrest shows that arrest is a two-stage process, beginning with inflorescence meristem arrest, and followed by floral arrest. We clarify previous misconceptions around floral arrest, showing that it is in fact a local process, and is not regulated globally. Our data highlight the importance of both cytokinin and auxin in inflorescence arrest, with auxin export from developing fruits being required for normal arrest. In support of recent work, we have shown that cytokinin is a key promoter of inflorescence meristem activity, and that increasing cytokinin signalling can delay both inflorescence meristem and floral arrest. Development of this work highlights how the cytokinin signalling receptors ARABIDOPSIS HISTIDINE KINASE2 (AHK2) and AHK3 are differentially involved in the regulation of meristem activity in the inflorescence meristem and flowers respectively. Overall, this work provides a basis on which to develop future crop research; manipulation of cytokinin signalling and/or sensitivity shows excellent promise for yield increases without the need for increased inputs.

List of abbreviations

µL / mL / L	micro- / milli- / litre
µmol / µM	micromolar
10r / 20r	10 / 20 fruits removed
ABCB	ATP-BINDING CASETTE B
ADP / ATP	Adenosine diphosphate / triphosphate
AFB	AUXIN SIGNALING F-BOX
AHK	ARABIDOPSIS HISTIDINE KINASE
AHP	ARABIDOPSIS HISTIDINE-CONTAINING PHOSPHOTRANSFER
AM	Axillary meristem
ANOVA	Analysis of variance
AP2	APETALA2
ARE	Auxin response elements
ARF	AUXIN RESPONSE FACTOR
ARR	ARABIDOPSIS RESPONSE REGULATORS
ATS	*Arabidopsis thaliana* salts
BA	6-benzylaminopurine
BRC	BRANCHED
C / R	Secondary cauline / rosette inflorescence
C1, C2 / R1, R2	Secondary cauline 1, 2 / secondary rosette 1, 2
C1.1 / R1.1	Tertiary cauline 1 / tertiary rosette 1
C1.1.1 / R1.1.1	Quaternary cauline 1 / quaternary rosette 1
CCD7 / 8	CAROTENOID CLEAVAGE DIOXYGENASE7 / 8
cDNA	Complementary DNA
cf	Compare
CK	Cytokinin

Col	Columbia
CRE	CYTOKININ RESPONSE
cZ	*cis*-Zeatin
d	Day(s)
D14 / 27	DWARF14 / 27
DEX	Dexamethasone
DMSO	Dimethyl sulfoxide
dpa	Days post anthesis
dpb	Days post bolting
FM	Floral meristem
FUL	FRUITFULL
GA	Gibberellin
GFP	Green fluorescent protein
GH	Glasshouse
GPA	Global proliferative arrest
GPS	Global positioning system
h	Hour(s)
HSD	Honest significant difference
IAA	Indole-3-acetic acid
IM	Inflorescence meristem
inflor	Inflorescence
iP	Isopentenyladenine
ipt	Isopentenyl transferase
L*er*	Landsberg *erecta*
LOG	LONELY GUY
M	Mole
MAX	MORE AXILLARY GROWTH

miRNA	microRNA
ms	male sterile
N	Nitrogen
n	Number (of samples)
n.s.	Non-significant
NAA	1-naphthaleneacetic acid
nm / mm / cm	nano- / milli- / centi-metre
NPA	Naphthylphthalamic acid
ºC	Degrees Celsius
OSR	Oilseed rape
PAT(S)	Polar auxin transport (stream)
PDR1	PLEIOTROPIC DRUG RESISTANCE1
pg / µg / mg / g	pico- / micro- / milli- / gram
phyB	Phytochrome B
PI	Primary inflorescence
PIN	PIN-FORMED
qRT-PCR	quantitative reverse transcription polymerase chain reaction
RA	Reactivated
RBX	RINGBOX
RF	Reflowering
RRA / RRB	ARABIDOPSIS RESPONSE REGULATOR type-A / type-B
RSM	Reproductive shoot meristem
s.e.m.	Standard error of mean
SAM	Shoot apical meristem
SCF	Skp1, Cullin and F-box

SDS	Sodium diethyldithiocarbamate
SL	Strigolactone
SMXL	SMAX-LIKE
TCS	Two-component signalling sensor
TIR	TRANSPORT INHIBITOR RESPONSE
TSW	Thousand seed weight
*t*Z	*trans*-Zeatin
*t*ZR	*trans*-Zeatin riboside
UHPLC-MS/MS	Ultra-high-performance liquid chromatography tandem mass spectrometry
UK	United Kingdom
unt / untrt	Untreated
var.	Variety
WI	Walk-in controlled environment chamber
WUS	WUSCHEL

Contents

List of Figures

Chapter 1 – General Introduction

Chapter 2 - Integrated dominance mechanisms regulate reproductive architecture in *Arabidopsis thaliana* and *Brassica napus*

Chapter 3 - A distributive '50% rule' determines floral initiation rates in the Brassicaceae

Chapter 4 - Auxin export from proximal fruits drives arrest in temporally-competent inflorescences

Chapter 5 - Cytokinin signalling regulates two-stage inflorescence arrest in Arabidopsis

Chapter 6 - Cytokinin signalling regulates age-dependent changes in inflorescence morphology in Arabidopsis

Chapter 7 – General Discussion

List of Tables

Chapter 3 - A distributive ‘50% rule’ determines floral initiation rates in the Brassicaceae

Chapter 4 - Auxin export from proximal fruits drives arrest in temporally-competent inflorescences

Chapter 1

General introduction

1.1 Decision-making in plants

Plants are sessile organisms; as such, they must use information from the environment to optimise their growth with respect to prevailing conditions. While some of the observed growth responses are *reactive*, it is clear that plants are also capable of *proactive* response to their local environment, and indeed that these growth responses can be made early in their lifecycle. Such proactive responses can be characterised as 'decisions', since they occur in the absence of resource limitations, and are made in part to avoid future resource limitations. For instance, early cues that indicate future growth restraints allow plants to maximise or restrict their growth appropriately for the conditions. Plants with limited rooting substrate volume show inhibited growth early in their lifetime, for example (Wheeldon et al, 2021). The ultimate goal for all plants is the production of successful progeny in the next generation; as such, these environmental responses require forward planning and a high degree of risk-aversion.

In wild settings this strategy of risk-aversion is of particular importance, ensuring plants do not over-commit their growth and deplete resources before sufficient high-quality seeds have been produced. Many models of plant development and growth currently rely on the assumption that plant growth is driven mainly by resource availability, but a variety of evidence suggests that the answer is more complex than this. For instance, there exist multiple Arabidopsis mutants that produce greater numbers of inflorescences, biomass and/or seed than wild-type plants when grown under exactly the same conditions; as such, resource availability cannot be the sole determinant of reproductive outcome (de Freitas Lima et al, 2017). Indeed, maximising nutrient extraction, growth and reproductive effort would be a poor evolutionary strategy, particularly for those species which have a relatively short seed-dispersal distance. Offspring would be directly penalised by growing in an area already depleted of nutrients by its parent plant, and as such it is unlikely that this strategy would be maintained (Walker & Bennett, 2018). A central goal of this thesis it to understand what decisions plants make, particularly during their reproductive development, to optimise their

reproductive success, and how they actually implement these decisions during development.

1.2 Hormonal signalling

1.2.1 Long-distance signalling

In order for plants to integrate information from disparate sources and coordinate their growth in response, information must be conveyed from one part of the plant to another. In vascular plants, with distinct root and shoot systems, locally-available information often isn't sufficient to make the most appropriate growth decisions. Shoot growth, for example, is inhibited by a lack of available phosphorus in the soil (Lin et al, 2014); information which must be transferred from the root to the shoot. As plants lack a nervous system akin to that in higher animals, it therefore stands to reason that they must be able to transport signals over potentially very large distances in order to grow in the most appropriate manner.

A wide array of long-distance signals have been studied in plants, including peptides (Wheeldon and Bennett, 2021) and microRNAs (miRNAs) (Ko and Helariutta, 2017), along with a range of plant hormones. Multiple hormonal signals have been identified and characterised as conveying information over long distances. Some of these (auxin, cytokinins and strigolactones in particular) have been shown to be ancient and highly conserved within land plants (Walker and Bennett, 2018), however other hormones such as gibberellins also play a key role in developmental coordination. It is likely that rather than provision of specific instructions, these signals transfer generic environmental information around the plant body (Bennett and Leyser, 2014), enabling individual tissues and organs to locally interpret the signals and respond appropriately.

1.2.2 Strigolactones

Strigolactones (SLs) are an interesting class of signalling molecules, acting endogenously as phytohormones, while also acting as exogenous rhizosphere signals (Waters et al, 2017), having first been identified as stimulating germination in the parasitic weed *Striga lutea* (Cook et al, 1966). Strigolactones play multiple roles in plant

development, including regulation of shoot branching (Umehara et al, 2008), branch angle (Bennett et al, 2016) and internode elongation (de Saint Germain et al, 2013).

SLs are structurally diverse hormones and fall into one of two classes; canonical and non-canonical. Over 20 canonical SLs have been identified to date; they contain an ABC-ring structure which is connected to a methylbutenolide D-ring via an enol-ether bridge (Figure 1.1 A)(Yoneyama et al, 2018). The D-ring has been shown to be an essential requirement for SL biological activity (Zwanenburg et al, 2008; Magnus and Zwanenburg, 1992). Non-canonical SLs on the other hand lack the ABC structure (Figure 1.1 B), but possess the D-ring, and as such remain biologically active and function as SLs (Yoneyama et al, 2018). While the D-ring is essential to activity, it is not the defining characteristic of SLs, as possession of this structure does not mean the molecule will function as a SL (Machin, Hamon-Josse and Bennett, 2019). It has therefore been suggested that the characterisation of SLs should be defined not by the presence of a D-ring, but instead by the molecules' biosynthesis (Machin, Hamon-Josse and Bennett, 2019).

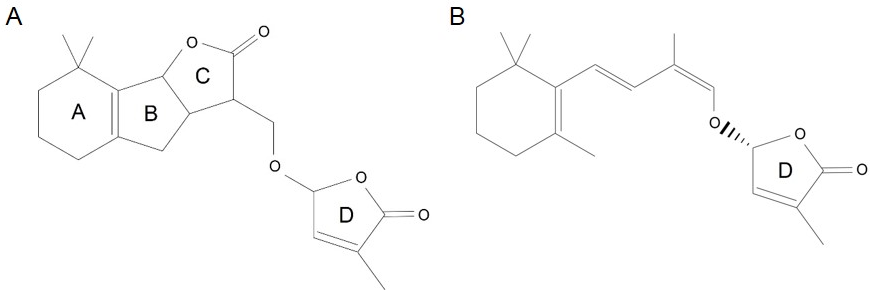

Figure 1.1 Strigolactone structure

Canonical and non-canonical strigolactone structures. (**A**) Canonical structure of strigolactone, showing the ABC structure linked to the D ring by an enol-ether bridge. (**B**) Non-canonical carlactone lacks the ABC structure, but retains the D ring, and as such displays strigolactone activity.

SL synthesis occurs in the root, where the expression of SL biosynthesis genes is very high. Despite their high concentration in the root, SL mutants display obvious

shoot phenotypes, most notably excessive branching, suggesting they can act as root-to-shoot signals. This acropetal mobility of SLs has been repeatedly supported through grafting experiments (e.g. Booker et al, 2005; Turnbull, Booker and Leyser, 2002).

The SL biosynthesis pathway is not yet fully understood, however it is known that it is initiated by β-carotene being processed via CAROTENOID CLEAVAGE DIOXYGENASE 7 (CCD7), CCD8, and DWARF27 (D27) to carlactone, an SL precursor (Alder et al, 2012)(Figure 1.1 B). Carlactone is then converted to active SLs (both canonical and non-canonical) via MORE AXILLARY GROWTH1 (MAX1)/CYP711A cytochrome P450 enzymes. While this step is likely to occur primarily in the root, MAX1 is also present and active in the shoot in Arabidopsis (Booker et al, 2005).

The method of SL transport to the shoot is still unclear, however it has been hypothesised that it could be transported shootward symplastically, or potentially apoplastically via the PLEIOTROPIC DRUG RESISTANCE 1 (PDR1) transporter family (Wheeldon and Bennett, 2021). There is not currently any evidence for rootward transportation of SL (Wheeldon and Bennett, 2021), suggesting it is primarily utilised as a root-shoot messenger. This is further supported by the recent discovery that SL was likely recruited as a phytohormone by evolution of a new signalling pathway much later in land-plant evolution than its synthesis pathway evolved. SL synthesis is conserved in land plants, however genes for the complete SL signalling pathway only evolved in angiosperms (Walker et al, 2019). In this manner, flowering plants were able to re-use an existing root exudate molecule to convey vital information over long distances.

SLs can act in the shoot by binding to the α/β hydrolase receptor DWARF14 (D14), which is then able to interact with a Skp1, Cullin and F-box protein (SCF)-type E3 ubiquitin ligase complex via the MAX2 F-box protein (Machin, Hamon-Josse and Bennett, 2019). The SCF^{MAX2} complex brings about the degradation of SMAX1-LIKE7 (SMXL7) and homologous proteins, releasing SCF^{MAX2} for further signalling (Walker et al, 2019; Machin, Hamon-Josse and Bennett, 2019). The degradation of SMXL7 allows

downstream SL signalling through a range of targets genes and proteins (Shinohara et al, 2013; Wang et al, 2020).

1.2.3 Auxin

The small, long-distance signalling molecule auxin (indole-3-acetic acid; IAA) (Figure 1.2) plays a key role in almost all areas of plant development, including organ initiation and phyllotaxis (Bartlett and Thompson, 2014), shoot branching (Bennett et al, 2006), and vascular organisation (Biedroń and Banasiak, 2018) to name but a few. Its synthesis occurs in all plant tissues, but is detected at the highest concentrations in young, actively-growing shoot tissues. While auxin is essential for plant growth, it induces different responses in different cell and tissue types, depending on their specialisation (Leyser, 2018).

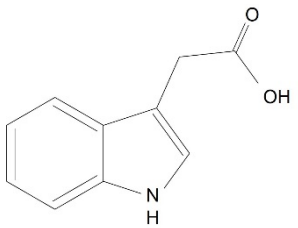

Figure 1.2. Molecular structure of indole-3-acetic acid auxin

Auxin typically brings about responses at a cellular level through the modulation of gene transcription levels (Leyser, 2018), although recent work has demonstrated several types of non-canonical auxin signalling, including ultra-fast phosphorylation at the plasma membrane (Kubeš and Napier, 2019; Huang, Zheng and He, 2019; Simonini et al, 2016). Auxin binds to F-box proteins of the TRANSPORT INHIBITOR RESPONSE1/AUXINSIGNALING F-BOX (TIR1/AFB) family, and to the Aux/IAA transcription factors. In the absence of auxin, Aux/IAA proteins bind to AUXIN RESPONSE FACTOR (ARF) proteins, preventing the ARFs from promoting transcription of auxin-response genes via ‘auxin response elements’ (AREs) in promoters (Leyser,

2018; Tan et al, 2007). The auxin/TIR1/Aux/IAA complex binds with an SCF-type ubiquitin protein ligase complex (Smalle and Vierstra, 2004). Cullin interacts with RING-BOX1 (RBX1), which ubiquitinates the target Aux/IAA proteins, labelling them for degradation by the 26S proteasome (Leyser, 2018). Since auxin strongly promotes transcription of members of the Aux/IAA family, it is therefore capable of regulating its own signalling levels via feedback and regulatory loops (Salehin, Bagchi and Estelle, 2015).

Auxin is a highly efficient shoot-to-root long-distance signal, and actively upregulates its own transportation around the plant (Bennett et al, 2016). The auxin transport system is governed by three principal components; first, auxin develops in young, growing tissues such as leaves and meristems, and is actively transported in a rootward direction (Brewer, Koltai and Beveridge, 2013). Second, auxin transport is often polar, and as such is described as polar auxin transport (PAT), moving via the polar auxin transport stream (PATS); this effect is not reversed by relocation of sinks or sources (Prusinkiewicz et al, 2009). Thirdly, the polar movement of auxin at a cellular level is proposed to occur by the chemiosmotic theory of auxin transport (Rubery and Sheldrake, 1974; Raven, 1975).

1.2.3.1 Chemiosmotic theory

Auxin is weakly acidic, and as a result is primarily neutrally charged in the acidic cell wall space (pH ~5.5). Auxin can therefore move passively within the wall space, and can diffuse through the charged plasma membrane into the cellular cytoplasm, although it can also be actively moved into the cell via auxin influx carriers (Michniewicz, Brewer and Friml, 2007) (Figure 1.3). The neutral (pH 7) cytoplasm leads to deprotonation of auxin molecules, and the proton (H^+) is transported out of the cytoplasm via an H^+ pump. To avoid being trapped in the cytoplasm, auxin is actively transported out of the cytoplasm via the PIN-FORMED (PIN) and ATP-BINDING CASETTE B (ABCB) families

of proteins. The often polarly-localised PIN proteins contribute to the polar transport of auxin (Bennett et al, 2016).

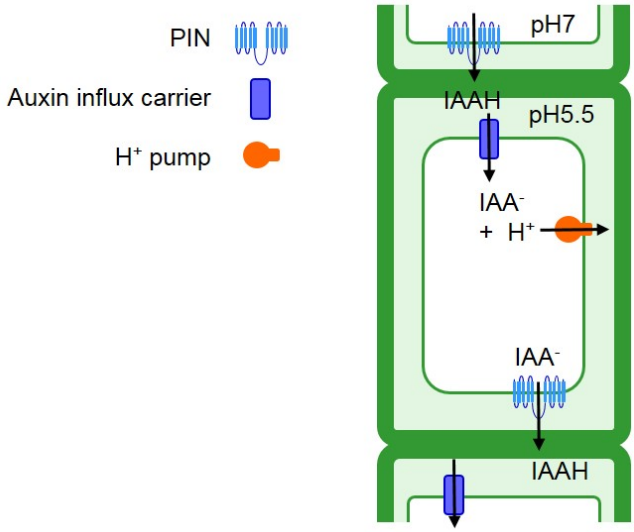

Figure 1.3. Chemiosmotic theory

Simplified diagram of polar auxin transport through cells, mediated by auxin influx carriers and PIN proteins. Acidic auxin can passively move within the cell wall space, but is deprotonated in the cytoplasm, preventing it leaving passively. PIN proteins actively transport auxin out of the cell. Adapted from Michniewicz, Brewer and Friml, 2007; Balzan, Johal and Carraro, 2014.

1.2.3.2 Auxin canalization

Plant vasculature connects organs in a coherent network, and is required for transport and communication across the plant body. The continuous and apparently self-organising formation of this network is a complex phenomenon that is driven by auxin transport. Sachs (1969) showed that auxin exported from growing leaves results in the differentiation of tissues and formation of new vascular elements. Through the application of exogenous auxin, Sachs (1969) determined that auxin presence is sufficient for new vascular elements to develop from the site of application. These elements join auxin sources (i.e. new organs) with auxin sinks (i.e. existing vasculature) by the shortest route. To explain this, Sachs (1969) proposed the canalization hypothesis, in which auxin upregulates its own transport from source to sink, resulting in

formation of ‘canals’ of high auxin transport that pattern the vascular elements. Subsequently, auxin has been shown to upregulate its own polar transport through increasing the polar localisation of PIN proteins (Bennett et al, 2014)(see Figure 1.3). Vascular patterning highlights the importance of both the source and sink strengths of auxin for canalization to occur. New vasculature will only join with the existing vascular system when both the auxin source (the developing organ) and the auxin sink (the stem) are sufficiently strong (Sachs, 1969). More generally, canalization provides a mechanism by which auxin sources and auxin sinks can be connected - and potentially regulate each other - by self-organizing auxin transport between them. These ideas have been built upon to explain the regulation of some aspects of shoot architecture (see below).

1.2.4 Cytokinin

Cytokinins (CKs) are signalling molecules derived from adenine, and play a number of developmental roles including the regulation of vasculature development, cell differentiation and shoot meristem activity (Ko and Helariutta, 2017). The main CK species have been identified as isopentenyl-adenine (iP) and *trans*- and *cis*-Zeatin (*t*Z, *c*Z) (Matsumoto-Kitano et al, 2008) (Figure 1.4). The zeatin variants are typically the most abundant, however *t*Z is active in all plants, whereas *c*Z is active in only some (Kieber and Schaller, 2018).

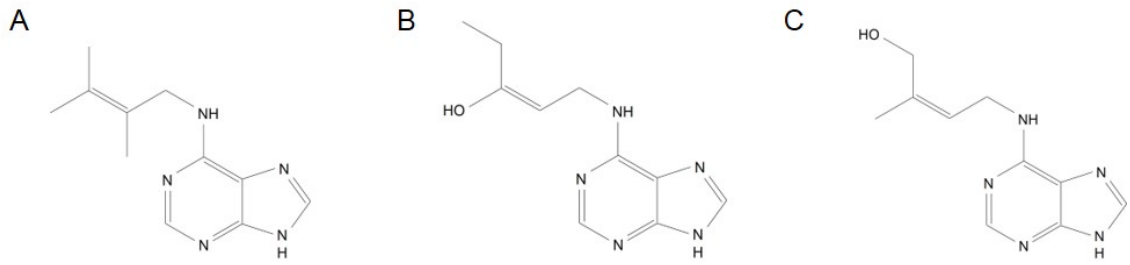

Figure 1.4. Cytokinin structures

Molecular structures of iP (A); *trans*-Zeatin (*t*Z) (B); *cis*-Zeatin (*c*Z).

CKs are synthesised from adenine derivatives in the roots via isopentenyl-transferase enzymes (IPTs) which add a prenyl group to ATP/ADP (Kieber and Schaller,

2018), producing iP ribotides. iP CKs are converted to *trans*-Zeatin via cytochrome P450 enzymes within the CYP735A class; both IPT and CYP735As are upregulated in response to nitrate in the soil (Hirose et al, 2008). iP and *t*Z CKs are converted to free base (non ribotide) active forms via LONELY GUY (LOG) enzymes. LOG enzymes are located throughout the plant tissues, suggesting that CK conversion to the active form may occur locally, allowing inactive intermediates to be transported around the plant (see Figure 1.5)(Kurakawa et al, 2007).

In Arabidopsis, cellular response to CK occurs following the binding of CK to the CHASE domain of ARABIDOPSIS HISTIDINE KINASE2 (AHK2), AHK3 or AHK4 / CYTOKININ RESPONSE1 (CRE1). Binding of CK initiates autophosphorylation of the receptors, and subsequent transfer of the phosphate group to ARABIDOPSIS RESPONSE REGULATOR (ARRs) proteins via ARABIDOPSIS HISTIDINE-CONTAINING PHOSPHOTRANSFER (AHP) protein (Pernisova et al, 2018). Activated type-B ARRs (RRBs) are capable of controlling cytokinin-responsive gene expression; type-A ARRs (RRAs) inhibit the CK signalling pathway, although the mechanism controlling this is currently unclear (Shull, Kurepa and Smalle, 2016)(Figure 1.5). As seen in the other phytohormones, CK is therefore capable of self-regulation via a negative feedback loop.

It has recently been proposed that iP and *t*Z CK forms could essentially be considered separate hormones having diverged in function at some point in vascular plant evolution, as their translocation and effects are so different (Wheeldon and Bennett, 2021). Indeed, *t*Z has been shown to move shootward via the xylem (Hirose et al, 2008), while iP moves rootward via the phloem (Bishopp et al, 2011). Additionally, the free base forms are preferentially recognised by different receptors; iP is predominantly recognised by AHK4 in the root, whereas *t*Z is more commonly recognised by AHK3 in the shoot (Wheeldon and Bennett, 2021). Interestingly, AHK2 appears to have similar affinity for both CKs, and has an element of functional redundancy it shares with both AHK3 and AHK4 (Bartrina et al, 2017).

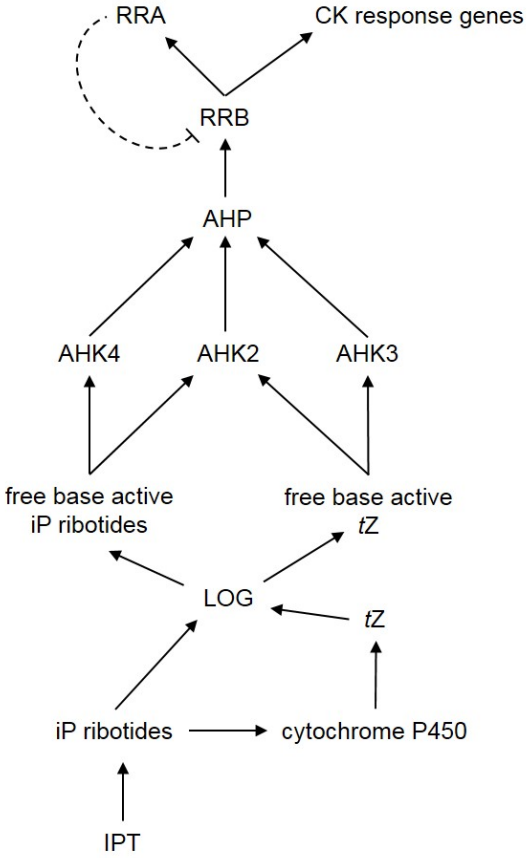

Figure 1.5. Cytokinin signalling

Diagram outlining some of the key processes involved in cytokinin (CK) signalling. Isopentenyl-transferase (IPT) enzymes generate iP ribotides in the root. Cytochrome P450 enzymes from the CYP735A class catalyse the conversion of iP CKs into *trans*-Zeatin (tZ) CKs. *t*Z and iP ribotides are both converted to free base actives via LONELY GUY (LOG) enzymes, located throughout the plant. iP CKs are predominantly recognised by ARABIDOPSIS HISTIDINE KINASE 2 (AHK2) and AHK4 in the root; *t*Z CKs are predominantly recognised by AHK2 and AHK3 in the shoot. AHK proteins phosphorylate HISTIDINE PHOSPHOTRANSFER PROTEINS (AHPs), which subsequently phosphorylate ARABIDOPSIS RESPONSE REGULATORS type-B (RRB) (Kurepa et al, 2014). RRBs regulate expression of CK response genes, including the RR type-A (RRA) proteins, which have been shown to inhibit CK signalling through an as-yet-unknown mechanism (Shull, Kurepa and Smalle, 2016; Kurepa et al, 2014). Figure adapted from Wheeldon and Bennett (2021); Pernisova et al. (2018); Shull, Kurepa and Smalle (2016); Kurepa, Li and Smalle (2014).

1.3 An example of hormonal decision-making: shoot branching

1.3.1 Shoot branching

Shoot architecture is the above-ground ordering and positioning of plant organs, including stems, leaves, vegetative branches and floral inflorescences (Wang, Smith and Li, 2018). Shoot branches are a vital component of shoot architecture, providing new axes of growth within the shoot system and allowing for a greater rate of organ production per unit time. Shoot branches arise from axillary shoot meristems; multicellular structures containing un-differentiated stem cells (Nicolas et al, 2022), allowing for plastic development. Axillary meristems are initiated in most leaf 'axils', and can arrest in early development to form an axillary bud. Most growth decisions relating to shoot branching occur as the cumulative effect of buds either individually activating or remaining dormant. In order to optimise growth, shoot branching must be carefully controlled across the whole plant. For instance, shoot branching must be correlated with root resources and grow according to the conditions at any given time. Above ground, investment into vegetative production must be appropriately balanced with reproductive output. Over- or under-production of shoot branches would be inefficient, as branch and inflorescence production are both energetically expensive processes (Walker and Bennett, 2018). This adaptive restriction of growth also allows for the replacement of lost or damaged organs, e.g. due to disease or herbivory (Karasov et al, 2017).

The regulation of shoot architecture must therefore be responsive to environmental cues, integrating local and global resources and stimuli to pattern organs and control tissue growth in the most appropriate way. Shoot branching is thus controlled both systemically and locally. Overall branch production is regulated at a whole-plant level, although the growth of individual organs is typically controlled locally (Karasov et al, 2017); regulation at multiple levels allows for fine-tuning according to the environmental conditions. In good growth conditions, shading an individual shoot branch will likely inhibit its growth, but this will not inhibit growth of branches elsewhere in the

plant (Kebrom et al, 2006). Systemic control thereby ensures the plant does not over-commit to resource usage, while local control ensures resource investment occurs within the most appropriate organs, e.g. those which are not shaded (Reddy and Finlayson, 2014; Seale et al, 2017). These decision-making processes ensure growth is continually fine-tuned to the current environment.

1.3.2 The regulation of shoot branching

Understanding the regulation of shoot branching has typically started with apical dominance. Apical dominance is a well-characterised physiological phenomenon, by which actively growing shoots inhibit the activation of secondary axillary buds (e.g. Snow, 1937; Phillips, 1975; Fisahn and Hofner, 1995; Teichmann and Muhr, 2015). It has long been recognised that auxin is responsible for axillary bud inhibition in the context of apical dominance (Thimann and Skoog, 1934), and is consequently highly important in shaping shoot architecture. In order to respond plastically to organ damage or loss, plants maintain a surplus of axillary buds (Phillips, 1975). Apical dominance acts to inhibit the growth of these buds, preventing the outgrowth of all organs, maintaining a risk-averse growth strategy. In the event that a dominant bud is lost, dominance may be released from one or more inhibited buds, allowing their outgrowth. These buds will in turn become dominant over the remaining buds.

Snow (1929; 1937) performed classic apical dominance studies, decapitating shoot apices to allow the outgrowth of axillary buds. These experiments highlighted the presence of correlative control, whereby one part of the plant can control the growth of another, through signals transmitted long-distance across the plant. These early experiments involved decapitation of the primary shoot above the cotyledonary node, thereby allowing the activation of the axillary meristems in the cotyledon axils (Snow, 1931; Leyser, 2009). In these systems, two buds may grow out, however often only one would grow; removal of the growing bud would allow the other to grow, highlighting a dominance mechanism which would require long-distance signalling between the buds.

Snow (1929) hypothesised that a substance was causing the inhibition between buds; this was later confirmed to be auxin after application to decapitated nodes maintained dominance (Thimann and Skoog, 1934). While auxin export maintains bud growth, it does not move into inhibited buds, and as such cannot be acting directly (Went, 1938; Prasad et al, 1993). Additionally, application of auxin to inhibited buds does not maintain their dormancy (Hall and Hillman, 1975; Brown et al, 1979). This, in conjunction with the indirect action of auxin suggests that there must be additional factors involved in the control of apical dominance.

Two hypotheses have been extensively debated as to explain the phenomenon of apical dominance. Initially it was posited that auxin activates a 'second messenger' which is capable of moving into the bud to activate growth (Domagalska and Leyser, 2011). The modern formulation of the model proposes that CK, SL and sugars are second messengers, regulated by auxin and which are capable of moving into the buds to regulate growth.

Auxin is believed to upregulate SL via transcription of MAX3 and MAX4, increasing SL synthesis, while inhibition of auxin dynamics decreases MAX3 and MAX4 transcription (Foo et al, 2005; Hayward et al, 2009). SLs are known to be inhibitors of bud activation, as SL mutants are highly branched, and application of SLs to buds prevents their outgrowth (Hayward et al, 2009; Domagalska and Leyser, 2011). CKs on the other hand, are downregulated by auxin via suppression of IPT gene expression. Application of CKs to a dormant bud can promote outgrowth (Sachs and Thimann, 1967), while CK mutants such as the *ipt357* mutant have decreased growth and branching, a phenotype which can be partially recovered by the application of exogenous CKs (Miyawaki et al, 2006). Sugars have also been shown to play a role in apical dominance. Following decapitation of the dominant bud, sugars accumulate rapidly within axillary buds; this occurs up to 24 hours before depletion of auxin can be detected within the stem (Mason et al, 2014). Sugars also inhibit the bud growth-repressing BRANCHED1 (BRC1), resulting in rapid growth upon their application (Mason et al, 2014). While the

second messenger model is simple and elegant, it cannot explain why some buds grow and others do not, despite exposure to the same levels of SLs, CKs and sugars (Walker and Bennett, 2018).

Subsequently, it has been suggested that the auxin canalization hypothesis can be used to explain apical dominance (Müller and Leyser, 2011). According to this model, in order to grow, buds must export auxin (Morris, 1977; Bangerth, 1989). In order for auxin export to occur, the bud must be a strong enough auxin source, and the stem a strong enough auxin sink (Prusinkiewicz et al, 2009). The bud must therefore produce a sufficient amount of auxin in order for the bud to be able to create a canalized link to the stem. However, actively growing branches reduce the source-strength of the stem by exporting auxin into it. Younger buds must therefore 'compete' with each other for canalization to the stem; those which do not produce sufficient auxin levels will be unable to grow out, unless removal of a more dominant bud sufficiently increases the sink strength of the stem for the younger bud to canalize. In this model, the roles of CK and SL are seen as respectively promoting and repressing PIN protein localization in the stem (Shinohara et al, 2013; Waldie & Leyser, 2018), thus altering stem sink-strength. While this provides a good model to explain the outgrowth of certain buds and not others, it has been highlighted that this theory fails to consider multiple factors. For instance, canalization does not account for the roles of sugar as a promoter of outgrowth, the inhibition of bud outgrowth by the bud growth-repressing BRANCHED1 (BRC1) transcription factor, nor the regulation of BRC1 by SL, CK and sugar (Brewer et al, 2015).

1.3.3 The hybrid model

It has been shown that neither the direct action model nor the canalization model can fully explain apical dominance, however neither is incompatible with the other (Seale, Bennett and Leyser, 2017; Waters et al, 2017). The two models have subsequently been combined into a single model known as the hybrid model (Walker and Bennett, 2018).

The hybrid model suggests that buds must first be 'primed' for growth by environmental cues; this information is transported systemically via CK, SL and sugar, and these inputs are integrated by control of BRC1 expression locally in the bud (Figure 1.6). High CK and sugar levels will therefore prime buds through the repression of BRC1, while SL-driven upregulation of BRC1 will inhibit growth, along with high far-red light levels that indicate shading (Devlin, Christie and Terry, 2007).

Second, these same systemic signals also alter the stem sink strength for auxin, thereby effecting the ease with which a given bud can canalize. In support of this, SLs have been shown to downregulate PIN1 proteins in the stem (Bennett et al, 2006); in effect, this reduces the sink strength of the stem, allowing more buds to canalize, and explaining the high-branching phenotype of SL mutants. CK has been shown to increase auxin biosynthesis (Jones et al, 2010), and as such is also able to confer resource information and affect the auxin strength of a bud (Waldie and Leyser, 2018).

The third tenet of the hybrid model hypothesis (Walker and Bennett, 2018), is that the bud must be a sufficiently strong auxin source, and the stem a sufficiently strong sink for the bud to be capable of canalizing to the PATS in the stem. The auxin level required for bud outgrowth is not a fixed value, but rather is a relative threshold. Through this, growth would be best optimised to the local conditions; in poor growth conditions, the outgrowth of a single bud may be sufficient to saturate the PATS, whereas a plant in excellent growth conditions may need buds to reach a much higher threshold, due to increased competition from multiple growing branches.

Finally, the hybrid model requires the auxin exported from a bud to decrease the PATS sink strength of the stem. This would result in the sink strength decreasing over time as more buds canalize. Through this process, the combination of local and systemic signals would enable the outgrowth of buds, likely resulting in the growth of the most dominant branches, until the PATS was saturated. Conveniently, this model also allows for the growth of new buds following damage or environmental changes; as the

canalization threshold is relative, improved conditions or loss of a dominant branch would allow for plastic response and additional growth.

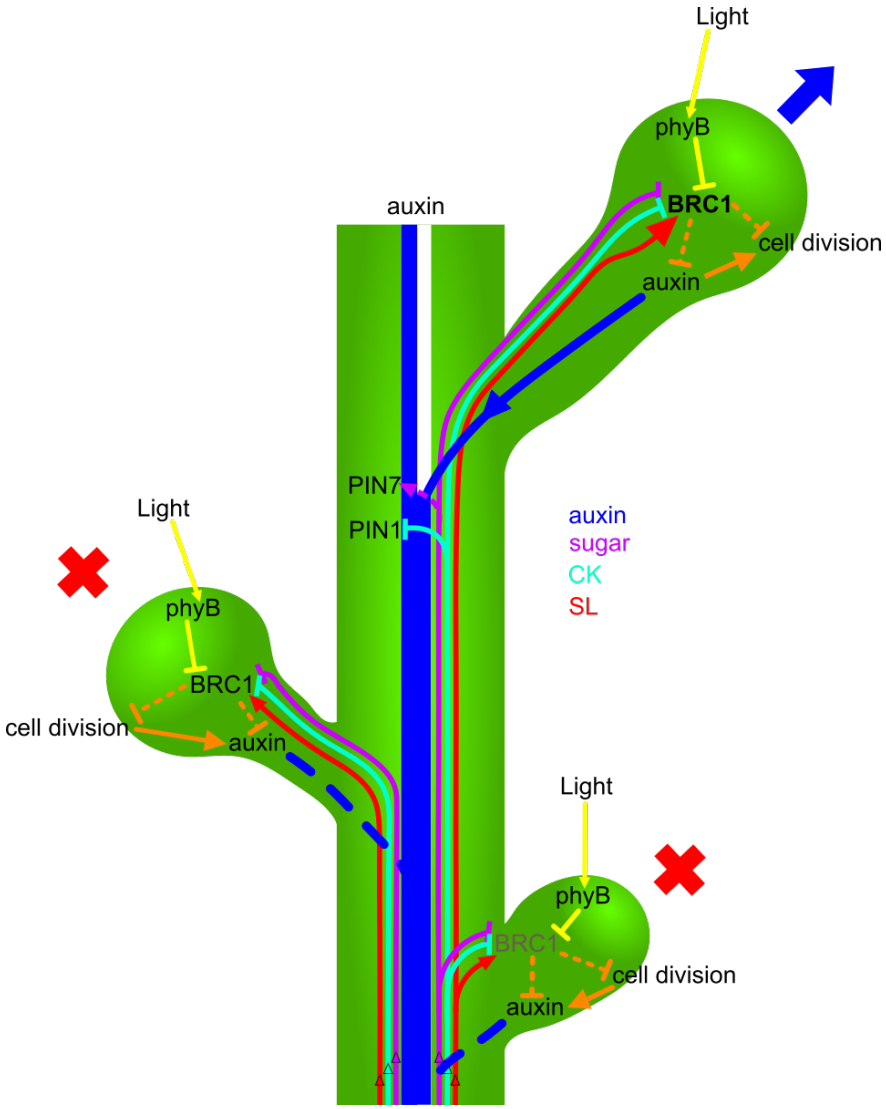

Figure 1.6. The proposed hybrid model of shoot branching

Diagram indicating how a combination of systemic and local signals control auxin export from buds, resulting in bud outgrowth or inhibition. Light is processed locally via phytochromeB (phyB), which inhibits *BRANCHED1* (BRC1). BRC1 is also inhibited by systemic sugar (purple line) and cytokinin (CK; turquoise line). Strigolactone (red line) activates BRC1. BRC1 expression may alter cell division and/or auxin (blue line) in the stem. SL and possibly CK alter PIN-FORMED (PIN) protein localisation in the stem, further affecting auxin transport. Bud outgrowth is affected by multiple parameters; the uppermost bud is able to canalize as the stem is a sufficiently strong sink and the bud is a sufficiently strong source of auxin, even considering high local *BRC1* expression. The two lower buds have lower *BRC1* expression, however neither is a sufficiently strong auxin source to canalize to the stem, and as such neither is able to grow out. Adapted directly from Walker and Bennett (2018), with permission.

1.4 Reproductive shoot architecture

Shoot architecture varies widely across flowering plants, with architecture optimised for resource capture, usage and reproduction. Shoot architecture is perhaps best recognised by the branching patterns of the plant, often made up of vegetative branches and reproductive inflorescences. Shoot architecture is determined by the positioning of the apical, axillary and inflorescence meristems, along with dominance mechanisms (e.g. apical dominance) controlling their outgrowth. Within this broader context, reproductive shoot architecture is determined by the number of inflorescences, flowers, fruit and seed produced by the plant, alongside their placement in both space and time.

Reproductive architecture can be strikingly different between species. In tomato reproduction, for example, the vegetative shoot apical meristem (SAM) is converted to a transitional meristem, and the last SAM continues shoot growth. The transitional meristem initiates a phytomer containing an inflorescence meristem (IM), leading to the development of floral meristems (FMs), which are capable of maturing into fruit (Périlleux, Lobet and Tocquin, 2014). In barley, the SAM initiates leaf primordia, and branches (tillers) form from the axillary meristems in the leaf axil (Figure 1.7). The plant then undergoes floral transition and the SAM converts to an IM, which develops into specialised branch and spikelet meristems (Tanaka et al, 2013; Gauley and Boden, 2019). In these two species, reproductive structures are positioned very differently in relation to the vegetative growth. Tomato plants produce short compound inflorescences of multiple fruits while maintaining vegetative growth of the whole plant (Figure 1.7). Barley undergoes a whole-plant transition from vegetative to floral (Tanaka et al, 2006; Gauley and Boden, 2019), with each tiller (typically) producing a single ear. Despite differing reproductive strategies, these species must both integrate environmental signals through long-distance signalling in order to optimise their reproductive development.

Reproduction is a careful balancing act of fecundity (seed number) and seed quality, determined by the resources allocated per seed (Karban, 2008). In commercial crops however, resources are typically plentiful, yet the plants still maintain a bet-hedging growth plan. This results in existing varieties retaining significant potential for yield increase, without increasing inputs (Sylvester-Bradley and Kindred, 2009). A greater understanding of the decision-making processes and mechanisms regulating reproductive architecture would therefore be of great benefit to the agricultural industry.

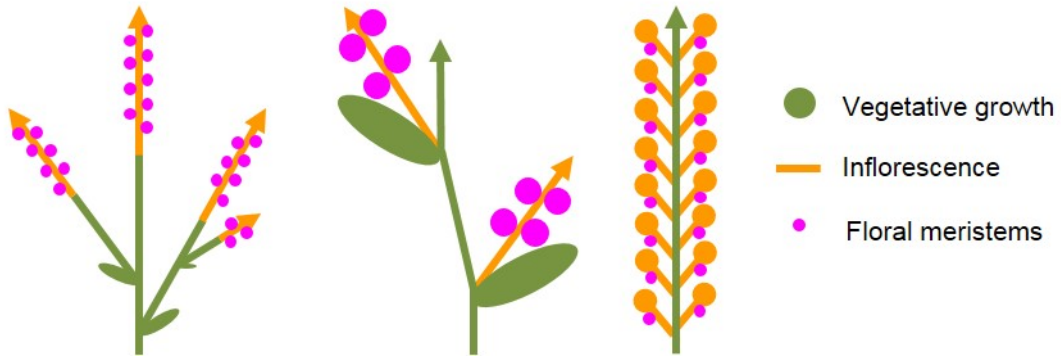

Figure 1.7. Variation in reproductive architecture

Diagram representing different reproductive strategies in (left to right) Arabidopsis (Brassicacea), tomato and barley. Vegetative growth is shown in green, inflorescences in gold, and floral meristems/fruit in pink.

1.4.1 Reproductive architecture in the Brassicaceae

The reproductive architecture of the Brassicacea is conserved across the family, with a vegetative rosette (which may or may not undergo stem extension between the leaves), and reproductive inflorescences. In these species, all branching is floral, and as such all branches are classed as inflorescences. When members of the Brassicacea undergo floral transition, the vegetative SAM converts to an IM, and a primary inflorescence (PI) develops, from which may grow multiple secondary inflorescences (see Supplementary Figure 3.1). From these may grow tertiary inflorescences, and so on and so forth. Inflorescences in the Brassicacea support flowers which are capable of

developing into fruits (often referred to as ‘siliques’ in Arabidopsis, and ‘pods’ in *Brassica napus* (oilseed rape) but called fruit throughout this work).

Brassicacea species typically produce inflorescences in a single wave at the start of the reproductive period. The production of inflorescences is energetically expensive (Walker and Bennett, 2018), and inflorescences must grow before flowers can develop, which must in turn open and be pollinated before fruits and seed can form. As such, Brassicaceae produce inflorescences a long way in advance of seed-filling. Conversely, in tomato, vegetative growth and reproductive growth are maintained simultaneously. In this manner, inflorescence development is controlled continuously, allowing reproductive effort to match existing resource availability, without the need for ‘prediction’ of future resources.

1.4.2 Reproductive decision-making in the Brassicaceae

There are still many unanswered questions regarding the ‘decision-making’ mechanisms that Brassicaceae use to correctly determine their reproductive architecture. It seems a reasonable hypothesis that there will be strong similarities with decision making during vegetative development (e.g. shoot branching, discussed above), but little research has been carried out into this, even in Arabidopsis.

As one example of this, given that the plant cannot have all of the necessary environmental information available regarding the total achievable seed-set when it starts reproductive development, plants must make early, ‘best-guesses’ as to the production of inflorescences. It would be suboptimal to produce a large number of inflorescences then be unable to fill all the resulting seed, or to make too few inflorescences and then have no time available to make more seed. While it is evident that resource availability affects the quantity of inflorescences (Salemaa and Sievänen, 2002; David et al, 2019), the process by which plants ‘decide’ on inflorescence number is not well understood. It is not currently clear how the volume of inflorescence production

is governed at a systemic level; how do plants ensure they produce the most appropriate amount of inflorescences and flowers for the environmental conditions?

As a second example, the Brassicacea produce large numbers of seeds, which can vary widely between individuals of the same species under similar conditions (Walker and Bennett, 2018). Given the resource allocation required for inflorescence and floral organ production, how do plants optimise the ratio of organ types? It may be less resource-intensive, but higher risk to support all fruits on a single inflorescence as the likelihood of severe damage and/or fruit loss would be greatly increased. Similarly, it may be more risk averse to produce a greater number of inflorescences, but the required energy inputs would surely limit resource allocation for developing fruits. How do plants therefore control the optimal number of fruits per inflorescence, and what level of plasticity is retained in order to maintain this?

Finally, these processes must be controlled (at least in part) systemically; signals from the roots will be required to moderate appropriate inflorescence growth, while light capture and photosynthate availability are similarly essential throughout the plant. Information transfer must therefore be coordinated over relatively long distances to control reproductive output, however what are the mechanisms controlling these processes?

1.5 Aims

Reflecting on the questions posed here leads to a series of aims regarding better understanding of reproductive decision-making processes in the Brassicacea, which are subsequently examined in this thesis.

1. How is the quantity of reproductive output systemically controlled? What determines the number of inflorescences and fruits produced? What determines when plants stop producing new reproductive organs, and why?
2. How is the organ ratio balanced between different organ types and stages of reproductive development? E.g. What mechanisms control the number of fruits per inflorescence?
3. What roles do phytohormones play in the regulation of reproductive architecture in Arabidopsis and the wider Brassicacea? Are there similarities (or differences) in the control of shoot branching?

The aims of this thesis are to investigate these questions, and to try to improve our understanding of reproductive architecture control in the Brassicaceae. Understanding the mechanisms controlling reproductive architecture and output in plants could be a key factor in increasing crop yield without the need for increasing inputs. Regulation of the reproductive effort is inherently risk-averse in plants; as such, understanding these processes could have significant benefits in crop breeding and yield production.

References

Alder, A., Jamil, M., Marzorati, M., Bruno, M., Varmathen, M., Bigler, P. et al. (2012). The path from β-carotene to carlactone, a strigolactone-like plant hormone. *Science*, **335**, 1348-1351.

Balzan, S., Johal, G.S. and Carraro, N. (2014). The role of auxin transporters in monocots development. *Frontiers in Plant Science,* **5**, doi:10.3389/fpls/2014.00393.

Bangerth, F. (1989). Dominance among fruits/sinks and the search for a correlative signal. *Physiologia Plantarum*, **76**, 608-614.

Bartlet, M.E. and Thompson, B. (2014). Meristem identity and phyllotaxis in inflorescence development. *Frontiers in Plant Science*, **5**, doi:10.3389/fpls.2014.00508.

Bartrina, I., Jensen, H., Novák, O., Strnad, M., Werner, T. and Schmülling, T. (2017). Gain-of-function mutants of the cytokinin receptors AHK2 and AHK3 regulate plant organ size, flowering time and plant longevity. *Plant Physiology*, **173**, 1783-1797.

Bennett, T., Sieberer, T., Willett, B., Booker, J., Luschnig, C. and Leyser, O. (2006). The Arabidopsis MAX pathway controls shoot branching by regulating auxin transport. *Current Biology*, **16**, 553-563.

Bennett, T. and Leyser, O. (2014). The auxin question: a philosophical overview. In *Auxin and its Role in Plant Development* (Zažímalová, E., Petrášek, J. and Benková, E. ed), Springer, 3-19.

Bennett, T., Liang, Y., Seale, M., Ward, S., Müller, D. and Leyser, O. (2016). Strigolactone regulates shoot development through a core signalling pathway. *Biology Open*, **5**, 1806-1802.

Biedroń, M. and Banasiak, A. (2018). Auxin-mediated regulation of vascular patterning in *Arabidopsis thaliana* leaves. *Plant Cell Reports*, **37**, 1215-1229.

Binenbaum, J., Weinstain, R. and Shani, E. (2018). Gibberellin localization and transport in plants. *Trends In Plant Science*, **23**, 410-421.

Bishopp, A., Lehesranta, S., Vatén, A., Help, H., El-Showk, S., Scheres, B. et al. (2011). Phloem-transported cytokinin regulates polar auxin transport and maintains vascular pattern in the root meristem. *Current Biology*, **21**, 927-932.

Björklund, S., Antti, H., Uddestrand, I., Moritz, T. and Sundberg, B. (2007). Cross-talk between gibberellin and auxin in development of *Populus* wood: gibberellin stimulates polar auxin transport and has a common transcriptome with auxin. *The Plant Journal*, **52**, 499-511.

Booker, J., Sieberer, T., Wright, W., Williamson, L., Willett, B., Stirnberg, P. et al. (2005). *MAX1* encodes a cytochrome P450 family member that acts downstream of *MAX3/4* to produce a carotenoid-derived branch-inhibiting hormone. *Developmental Cell*, **8**, 443-449.

Brewer, P.B., Koltai, H. and Beveridge, C.A. (2013). Diverse roles of strigolactones in plant development. *Molecular Plant,* **6**, 18-28.

Brewer, P.B., Dun, E.A., Gui, R., Mason, M.G. and Beveridge, C.A. (2015). Strigolactone inhibition of branching independent of polar auxin transport. *Plant Physiology*, **168**, 1820-1829.

Brown, B.T., Foster, C., Phillips, J.N. and Rattigann, B.M. (1979). The indirect role of 2,4-D in the maintenance of apical dominance in decapitated sunflower seedlings (*Helianthus annus* L.). *Planta*, **146**, 475-480.

Cook, C.E., Wichard, L.P., Turner, B., Wall, M.E. and Egley, G.H. (1966). Germination of witchweed (*Striga lutea* Lour.): isolation and properties of a potent stimulant. *Science*, **154**, 1189-1190.

David, L.C., Girin, T., Fleurisson, E., Phommabouth, E., Mahfoudhi, A., Citerne, S. et al. (2019). Developmental and physiological responses of *Brachypodium distachyon* to fluctuating nitrogen availability. *Scientific Reports*, **9**, doi:10.1038/s41598-019-40569-8.

de Freitas Lima, M., Eloy, N.B., de Siqueira, J.A.B., Inze, D., Hemerly, A.S. and Ferreira, P.C.G. (2017). Molecular mechanisms of biomass increase in plants. *Biotechnology Research and Innovation,* **1**, 14-25.

de Saint Germain, A., Ligerot, Y., Dun, E.A., Pillot, J-P., Ross, J.J., Beveridge, C.A. and Rameau, C. (2013). Strigolactones stimulate internode elongation independently of gibberellins. *Plant Physiology*, **163**, 1012-1025.

Devlin, P.F., Christie, J.M. and Terry, M.J. (2007). Many hands make light work. *Journal of Experimental Botany*, **58**, 3071-3077.

Dill, A., Jung, H-S. and Sun, T-p. (2001). The DELLA motif is essential for gibberellin-induced degradation of RGA. *Proceedings of the National Academy of Sciences of the USA*, **98**, 14162-14167.

Domagalska, M.A. and Leyser, O. (2011). Signal integration in the control of shoot branching. *Nature Reviews Molecular Cell Biology*, **12**, 211-221.

Fisahn, J. and Hofner, W. (1995). Influence of a plant-growth regulator on the sink capacity of oilseed rape (*Brassica napus* L.). *Journal of Agronomy and Crop Science*, **174**, 99-109.

Foo, E., Bullier, E., Goussot, M., Foucher, F., Rameau, C., Beveridge, C.A. (2005). The branching gene *RAMOSUS*$_1$ mediates interactions among two novel signals and auxin in pea. *The Plant Cell*, **17**, 464-474.

Franco, M. (1986). The influence of neighbours on the growth of modular organisms with an example from trees. *Philosophical Transactions of the Royal Society B*. **313**, 209-225.

Gauley, A. and Boden, S.A. (2019). Genetic pathways controlling inflorescence architecture and development in wheat and barley. *Journal of Integrative Plant Biology*, **61**, 269-309.

Hall, S.M. and Hillman, J.R. (1975). Correlative inhibition of lateral bud growth in *Phaseolus vulgaris* L. timing of bud growth following decapitation. *Planta*, **123**, 137-143.

Hayward, A., Stirnberg, P., Beveridge, C. and Leyser, O. (2009). Interactions between auxin and strigolactone in shoot branching control. *Plant Physiology*, **151**, 400-412.

Hedden, P. and Thomas, S.G. (2012). Gibberellin biosynthesis and its regulation. *Biochemical Journal*, **444**, 11-25.

Hedden, P. and Sponsel, V. (2015). A century of gibberellin research. *Journal of Plant Growth Regulation*, **34**, 740-760.

Hirose, N., Takei, K., Kuroha, T., Kamada-Nobusada, T., Hayashi, H. and Sakakibara, H. (2008). Regulation of cytokinin biosynthesis, compartmentalization and translocation. *Journal of Experimental Botany*, **59**, 75-83.

Huang, R., Zheng, R. and He, J. (2019). Noncanonical auxin signaling regulates cell division pattern during lateral root development. *PNAS*, **116**, 21285-21290.

Jones, B., Andersson Gunnerås, S., Petersson, S.V., Tarkowski, P., Graham, N., May, S. et al. (2010). Cytokinin regulation of auxin synthesis in *Arabidopsis* involves a homeostatic feedback loop regulated via auxin and cytokinin signal transduction. *The Plant Cell*, **22**, 2956-2969.

Kaneko, M., Itoh, H., Inukai, Y., Sakamoto, T., Ueguchi-Tanaka, M, Ashikari, M. and Matsuoka, M. (2003). Where do gibberellin biosynthesis and gibberellin signaling occur in rice plants? *The Plant Journal*, **35**, 104-115.

Karasov, T.L., Chae, E., Herman, J.J. and Bergelson, J. (2017). Mechanisms to mitigate the trade-off between growth and defense. *The Plant Cell,* **29**, 666-680.

Karban, R. (2008). Plant behaviours and communication. *Ecology Letters,* **11**, 727-739.

Kebrom, T.H., Burson, B.L. and Finlayson, S.A. (2006). Phytochrome B represses *teosinte branched1* expression and induces sorghum axillary bud outgrowth in response to light signals. *Plant Physiology,* **140**, 1109-1117.

Kieber, J.J. and Schaller, G.E. (2018). Cytokinin signaling in plant development. *Development*. **145**, doi:10.1242/dev.149344.

Ko, D. and Helariutta, Y. (2017). Shoot-root communication in flowering plants. *Current Biology*, **17**, 973-978.

Kubeš, M. and Napier, R. (2019). Non-canonical auxin signalling: fast and curious. *Journal of Experimental Botany*, **70**, 2609-2614.

Kurakawa, T., Ueda, N., Maekawa, M., Kobayashi, K., Kojima, M., Nagato, Y. et al. (2007). Direct control of shoot meristem activity by a cytokinin-activating enzyme. *Nature*, **445**, 652-655.

Kurepa, J., Li, Y. and Smalle, J.A. (2014). Cytokinin signaling stabilizes the response activator ARR1. *The Plant Journal*, **78**, 157-168.

Lacombe, B. and Achard, P. (2016), Long-distance transport of phytohormones through the plant vascular system. *Current Opinion in Plant Biology*, **34**, 1-8.

Leyser, O. (2009). The control of shoot branching: an example of plant information processing. *Plant, Cell and Environment*, **32**, 694-703.

Leyser, O. (2018). Auxin Signalling. *Plant Physiology*, **176**, 465-479.

Lin, W-Y., Huang, T-K., Leong, S.J. and Chiou, T-J. (2014). Long-distance call from phosphate: systemic regulation of phosphate starvation responses. *Journal of Experimental Botany*, **65**, 1817-1827.

Machin, D., Hamon-Josse, M. and Bennett, T. (2019). Fellowship of the rings: a saga of strigolactones and other small signals. *New Phytologist*, **225**, 621-636.

Magnus, E.M. and Zwanenburg, B. (1992). Tentative molecular mechanism for germination stimulation of *Striga* and *Orobanche* seeds by strigol and its synthetic analogues. *Journal of Agricultural Food and Chemistry*, **40**, 1066-1070.

Mason, M.G., Ross, J.J., Babst, M.A., Wienclaw, B.N. and Beveridge, C.A. (2014). Sugar demand, not auxin, is the initial regulator of apical dominance. *PNAS*, **111**, 6092-6097.

Matsumoto-Kitano, M., Kusumoto, T., Tarkowski, P., Kinoshita-Tsujimura, K., Václavíková, K., Miyawaki, K. and Kakimoto, T. (2008). Cytokinins are central regulators of cambial activity. *PNAS*, **105**, 20027-20031.

Michniewicz, M., Brewer, P.B. and Friml, J. (2007). Polar auxin transport and asymmetric auxin distribution. *The Arabidopsis Book*, **5**, doi:10.1199/tab.0108.

Miyawaki, K., Tarkowski, P., Matsumoto-Kitano, M., Kato, T., Sato, S., Tarkowska, D. et al. (2006). Roles of *Arabidopsis* ATP/ADP isopentenyltransferases and tRNA isopentenyltransferases in cytokinin biosynthesis. *PNAS*, **103**, 16598-16603.

Morris, D.A. (1977). Transport of exogenous auxin in two-branched dwarf pea seedlings (*Pisum sativum* L.). *Planta*, **136**, 91-96.

Müller, D. and Leyser, O. (2011). Auxin, cytokinin and the control of shoot branching. *Annals of Botany*, **107**, 1203-1212.

Nicolas, A., Maugarny-Calès, A., Adroher, B., Chelysheva, L., Li, Y., Burguet, J. et al. (2022). *De novo* stem cell establishment in meristems requires repression of organ boundary cell fate. *The Plant Cell*, doi.org/10.1093/plcell/koac269.

Périlleux, C., Lobet, G. and Tocquin, P. (2014). Inflorescence development in tomato: gene functions within a zigzag model. *Frontiers in Plant Science*, **5**, doi:10.3389/fpls.2014.00121.

Pernisova, M., Grochova, M., Konecny, T., Plackova, L., Harustiakova, D., Kakimoto, T. et al. (2018). Cytokinin signalling regulates organ identity via the AHK4 receptor in *Arabidopsis*. *Development*, **145**, doi:10.1242/dev.163907.

Phillips, I.D.J. (1975). Apical dominance. *Annual Review of Plant Physiology and Plant Molecular Biology,* **26**, 341-367.

Prasad, T.K., Li, X., Abdel-Rahman, A.M., Hosokawa, Z., Cloud, N.P, LaMotte, C.E. and Cline, M.G. (1993). Does auxin play a role in the release of apical dominance by shoot inversion in *Ipomoea nil? Annals of Botany*, **71**, 223-229.

Prusinkiewicz, P., Crawford, S., Smith, R.S., Ljung, K., Bennett, T., Orgaro, V. and Leyser, O. (2009). Control of bud activation by an auxin transport switch. *PNAS,* **106**, 17431-17436.

Ragni, L., Nieminen, K., Pacheco-Villalobos, D., Sibout, R., Schwechhimer, C. and Hardtke, C.S. (2011). Mobile gibberellin directly stimulates *Arabidopsis* hyposotyl xylem expansion. *The Plant Cell*, **23**, 1322-1336.

Raven, J.A. (1975). Transport of indoleacetic acid in plant cells in relation to pH and electrical potential gradients, and its significance for polar IAA transport. *New Phytologist*, **74**, 163-172.

Reddy, S.K. and Finlayson, S.A. (2014). Phytochrome B promotes branching in Arabidopsis by suppressing auxin signaling. *Plant Physiology,* **164**, 1542-1550.

Rubery, P.H. and Sheldrake, A.R. (1974). Carrier-mediated auxin transport. *Planta,* **118**, 101-121.

Sachs, T. (1969) Polarity and the induction of organised vascular tissues. *Annals of Botany*, **33**, 263-275.

Sachs, T. and Thimann, K.V. (1964). Release of lateral buds from apical dominance. *Nature*. **201**, 939-940.

Sachs, T. and Thimann, K.V. (1967). The role of auxins and cytokinins in the release of buds from dominance. *American Journal of Botany*, **54**, 136-144.

Salehin, M., Bagchi, R. and Estelle, M. (2015). $SCF^{TIR1/AFB}$-based auxin perception: Mechanism and role in plant growth and development. *The Plant Cell*, **27**, 9-19.

Salemaa, M. and Sievänen, R. (2002). The effect of apical dominance on the branching architecture of *Arctostaphylos uva-ursi* in four contrasting environments. *Flora*, **197**, 429-442.

Seale, M., Bennett, T. and Leyser, O. (2017). *BRC1* expression regulates bud activation potential but is not necessary or sufficient for bud growth inhibition in Arabidopsis. *Development*, **144**, 1661-1673.

Shull, T.E., Kurepa, J. and Smalle, J.A. (2016). Cytokinin signaling promotes differential stability of type-B ARRs. *Plant Signaling and Behaviour*, **11**, doi:10.1080/15592324.2016.1169354.

Silverstone, A.L., Ciampaglio, C.N. and Sun, T-p. (1998). The Arabidopsis *RGA* gene encodes a transcriptional regulator repressing the gibberellin signal transduction pathway. *The Plant Cell*, **10**, 155-169.

Simonini, S., Deb, J., Moubayidin, L., Stephenson, P., Valluru, M., Freire-Rios, A. et al. (2016). A noncanonical auxin-sensing mechanism is required for organ morphogenesis in *Arabidopsis. Genes and Development*, **30**, 2286-2296.

Smalle, J. and Vierstra, R.D. (2004). The ubiquitin 26S proteasome proteolytic pathway. *Annual Reviews in Plant Biology*, **55**, 555-590.

Snow, R. (1929). The transmission of inhibition through dead stretches of stem. *Annals of Botany*, **43**, 261-267.

Snow, R. (1931). Experiments on growth of inhibition. Part II.-New phenomena of inhibition. *Proceedings of the Royal Society B*, **108**, 305-316.

Snow, R. (1937). On the nature of correlative inhibition. *New Phytologist,* **36**, 283-300.

Sylvester-Bradley, R. and Kindred, D.R. (2009). Analysing nitrogen responses of cereals to prioritize routes to the improvement of nitrogen use efficiency. *Journal of Experimental Botany,* **60**, 1939-1951.

Tan, X., Calderon-Villalobos, L.I.A., Sharon, M., Zheng, C., Robinson, C.V., Estelle, M. and Zheng, N. (2007). Mechanism of auxin perception by the TIR1 ubiquitin ligase. *Nature*, **446**, 640-645.

Tanaka, M., Takei, K., Kojima, M., Sakakibara, H. and Mori, H. (2006). Auxin controls local cytokinin biosynthesis in the nodal stem in apical dominance. *The Plant Journal*, **45**, 1028-1036.

Tanaka, W., Pautler, M., Jackson, D. and Hirano, H-Y. (2013). Grass meristems II: Inflorescence architecture, flower development and meristem fate. *Plant and Cell Physiology*, **54**, 313-324.

Teichmann, T. and Muhr, M. (2015). Shaping plant architecture. *Frontiers in Plant Science,* **6**, doi:10.3389/fpls.2015.00233.

Thimann, K.V. and Skoog, F. (1934). On the inhibition of bud development and other functions of growth substance in *Vicia faba*. *Proceedings of the Royal Society B*, **114**, 317-339.

Turnbull, C.G.N., Booker, J.P. and Leyser, H.M.O. (2002). Micrografting techniques for testing long-distance signalling in *Arabidopsis*. *The Plant Journal*, **32**, 255-262.

Umehara, M., Hanada, A., Yoshida, S., Akiyama, K., Arite, T., Takeda-Kamiya, N. et al. (2008). Inhibition of shoot branching by new terpenoid plant hormones. *Nature*, **455**, 195-200.

Waldie, T. and Leyser, O. (2018). Cytokinin targets auxin transport to promote shoot branching. *Plant Physiology*, **177**, 803-818.

Walker, C.H. and Bennett, T. (2018). Forbidden fruit: dominance relationships and the control of shoot architecture. *Annual Plant Reviews,* **1**, 1-38.

Walker, C.H., Siu-Ting, K., Taylor, A., O'Connell, M.J. and Bennett, T. (2019). Strigolactone synthesis is ancestral in land plants, but canonical strigolactone signalling is a flowering plant innovation. *BMC Biology*, **17**, doi:10.1186/s12915-019-0689-6.

Wang, B., Smith, S.M. and Li, J. (2018). Genetic regulation of shoot architecture. *Annual Review of Plant Biology*, **69**, 437-468.

Wang, L., Wang, B., Yu, H., Guo, H., Lin, T., Kou, L. et al. (2020). Transcriptional regulation of strigolactone signalling in Arabidopsis. *Nature*, **583**, 277-281.

Waters, M.T., Gutjahr, C., Bennett, T. and Nelson, D.C. (2017). Strigolactone signaling and evolution. *Annual Review of Plant Biology*, **28**, 291-322.

Went, F.W. (1938). Specific factors other than auxin affecting growth and root formation. *Plant Physiology*, **13**, 55-80.

Wheeldon, C.D. and Bennett, T. (2021). There and back again: An evolutionary perspective on long-distance coordination of plant growth and development. *Seminars in Cell and Developmental Biology*, **109**, 55-67.

Yamaguchi, S., Kamiya, Y. and Sun, T. (2001). Distinct cell-specific expression patterns of early and late gibberellin biosynthetic genes during Arabidopsis seed germination. *The Plant Journal*, **28**, 443-453.

Yoneyama, K., Xie, X., Yoneyama, K., Kisugi, T., Nomura, T., Nakatani, Y. et al. (2018). Which are the major players, canonical or non-canonical strigolactones? *Journal of Experimental Botany,* **69**, 2231-2239.

Zhang, J., Mazur, E., Gallei, M., Kalousek, P., Medved'ová, Z., Li, Y. et al. (2020). Strigolactones inhibit auxin feedback on PIN-dependent auxin transport canalization. *Nature Communications*, **11**, doi:10.1038/s41467-020-17252-y.

Zwanenburg, B., Mwakaboko, A.S., Reizelman, A., Anilkumar, G. and Sethumadhavan, D. (2008). Structure and function of natural and synthetic signalling molecules in parasitic weed germination. *Pest Management Science*, **65**, 478-491.

Zweig, G., Yamaguchi, S. and Mason, G.W. (1961). Translocation of C^{14}-gibberellin in red kidney bean, normal corn and dwarf corn. *Advances in Chemistry*, **28**, 122-134.

Chapter 2

Integrated dominance mechanisms regulate reproductive architecture in *Arabidopsis thaliana* and *Brassica napus*

Originally published in *Plant Physiology*, 2021

Volume **186**, Issue 4, Pages 1985-2002

2.1 Extended introduction

The following publication focuses on dominance mechanisms controlling reproductive architecture in *Arabidopsis thaliana* (Arabidopsis), then extends this research into the related *Brassica napus* (oilseed rape). My interest in dominance mechanisms followed from Snow's (1931; 1937) apical dominance studies in *Vicia faba*, and Bangerth's (1989) review of dominance between fruits. In an early attempt to better understand dominance between fruits, I grew *Cucumis sativus* (cucumber) under glasshouse conditions. The level of dominance between fruits (hereafter carpic dominance) in this species is clearly visible, with the production of progressively smaller fruits developing, until complete inhibition of the fourth fruit on the plant (Figure 2.i). Seeing proof of carpic dominance encouraged my own further study, however cucumber was not an ideal study system. Instead I chose to work on Arabidopsis, and examined similarities and differences between this and *B. napus*.

Figure 2.i Carpic dominance inhibits fruit development

Images of developing cucumbers on a single plant. Fruits are numbered in the order in which they grew, 1-4. Fruits are progressively inhibited by earlier fruit, resulting in total inhibition of fruit 4.

A large amount of research has been carried out into apical dominance – the inhibition between branches (Snow, 1931; Domagalska and Leyser, 2011) – but much less so with regards to the relevance and importance of fruit in dominance relationships. The following publication focuses on multiple dominance factors within Arabidopsis, considering the relationships between branches and fruits.

2.1.1 Chapter Note

The following article text is replicated here as it was in the original publication. Figures are the same, but positioning within the text has been adjusted for clarity. Most obviously, supplementary figures are now included in the relevant position within the text, rather than being placed collectively together at the end of the manuscript.

Any text underlined within this chapter highlights direction to text *not included within the original publication* (located in Appendix A). These points are included to direct the reader to additional supplementary information relevant to the work but which was not included as part of the original publication (typically due to space constraints enforced by the publishing journal). Only direction to novel material has been provided; no additional discussion or data has been included within the manuscript text; all new material follows the end of the manuscript.

Please note formatting has been altered to retain consistency throughout this thesis; in no way has this affected the content of the work enclosed.

Integrated dominance mechanisms regulate reproductive architecture in *Arabidopsis thaliana* and *Brassica napus*

Catriona H. Walker, Cara D. Wheeldon & Tom Bennett*.

School of Biology, Faculty of Biological Sciences, University of Leeds, Leeds, LS2 9JT

*E-mail address: t.a.bennett@leeds.ac.uk

Running title: Control of reproductive architecture

Author contributions

CHW, CDW, TB designed and performed experiments and analysed the data. TB and CHW conceived the project. All authors contributed to writing the manuscript. TB agrees to serve as the author responsible for contact and ensures communication.

Summary

A series of negative feedback mechanisms regulates the spatio-temporal production of reproductive structures in Arabidopsis and *Brassica napus*, allowing plants to optimise seed-set relative to resource and resource-related signals.

2.2 Abstract

The production of seed in flowering plants is complicated by the need to first invest in reproductive shoots, inflorescences, flowers and fruit. Furthermore, in many species, it will be months between plants generating flowers and setting seed. How can plants therefore produce an optimal seed-set relative to environmental resources when the 'reproductive architecture' that supports seed-set needs to be elaborated so far in advance? Here, we address this question by investigating the spatio-temporal control of reproductive architecture in *Arabidopsis thaliana* and *Brassica napus*. We show that resource- and resource-related signals such as substrate volume play a key role in determining the scale of reproductive effort, and that this is reflected in the earliest events in reproductive development, which broadly predicts the subsequent reproductive effort. We show that a series of negative feedbacks both within and between developmental stages prevent plants from over-committing to early stages of development. These feedbacks create a highly plastic, homeostatic system in which additional organs can be produced in the case of reproductive failure elsewhere in the system. We propose that these feedbacks represent an 'integrated dominance' mechanism that allows resource use to be correctly sequenced between developmental stages to optimise seed set.

2.3 Introduction

In flowering plants, the vegetative phase of the life-cycle is optimised for harvesting resources from the environment; in the shoot system, the primary concern is the capture of photosynthetically active solar radiation. As such, the vegetative shoot architecture (i.e. the spatio-temporal arrangement of organs) of flowering plants tends to consist of a simple, iterative pattern of development. In contrast, the reproductive shoot architecture of flowering plants is optimised to increase reproductive success, utilising the resources acquired during the vegetative phase. As such, reproductive architecture is driven and constrained by fundamentally different factors to vegetative architecture. In particular, the acquisition of resources, while still beneficial, is less important than servicing the reproductive strategy of the plant. Thus, for insect-pollinated plants where pollinator availability is temporally limited, the need to produce flowers in a single mass display may be particularly important. For other species, the continual initiation of a small number of flowers may be a better strategy. Other plants (such as those growing in the desert) may need to take advantage of a very limited window of environmental opportunity to deposit seeds in the soil. Since flowering plant reproductive strategies are highly diverse, so too are the reproductive architectures through which plants attempt to execute these strategies.

Despite the differences in reproductive architecture between species, the basic building blocks of reproductive architecture are the same among flowering plants. These organs are produced in a hierarchical temporal sequence that is inherently more complex than vegetative architecture. After the plant undergoes the transition to the reproductive phase (i.e. flowering), many or all of the vegetative shoot meristems on the plant will be converted to reproductive shoot meristems (RSMs), which generate reproductive shoots bearing leaves (Benlloch et al, 2015). The secondary ‘axillary’ shoot meristems produced along these reproductive shoots may also be specified as RSMs, but can instead be directly specified as inflorescence meristems (IMs). Existing RSMs may also be converted to IMs during reproductive development. In pea, the main RSMs are long-

lived, and axillary meristems are directly specified as IMs (Benlloch et al, 2015). Conversely, in Arabidopsis, every axillary meristem is initially specified as a short-lived RSM, but is quickly converted to an IM after producing a few leaves; this includes the primary RSM (Schultz & Haughn, 1991; Pouteau & Albertini, 2011). IMs initiate bracts (which may be cryptic) rather than leaves, and these bracts contain floral (axillary) meristems. These floral meristems each produce a single flower bearing the male and female reproductive organs (stamens and carpels). Pollination of female gametophytes (the ova, contained within the ovules, within the carpel) by male gametophytes (pollen) leads to the formation of a zygote, and conversion of the ovules into seed. The setting of seed in turn causes the carpel to develop into a fruit, containing the seed. Thus, to produce the seeds that ultimately constitute their reproductive effort, plants must first produce reproductive shoots, inflorescences, flowers and fruits, in sequence.

The hierarchical and sequential nature of reproductive development makes it difficult for plants to correctly determine their reproductive effort (Walker & Bennett, 2018). The maximum number of seed that a plant can produce reflects the resources it has available at the point of seed-set. However, when the plant begins reproductive development, it cannot predict what level of resource will be available at seed set, since this will largely depend on the amount of solar radiation and water the plant receives between the start and end of flowering. This problem is particularly acute in spring-blooming fruit trees, which actually undergo the floral transition the previous autumn, and initiate all the inflorescences and flowers that will ‘blossom’ the following spring. In these species, the initial production of reproductive organs is separated from seed set by up to 9 months, and the resources that may be available for seed-set are essentially unknowable (Walker & Bennett, 2018). Even in plants with more straightforward reproductive cycles, there may be a large time lag between the initiation of flowering and seed-set. Reproductive strategies across species must therefore require control mechanisms to regulate seed set and adjustment of the reproductive effort may be controlled by varying mechanisms, depending on the lifecycle of the plant (Lloyd, 1980).

How then can plants possibly produce an optimal reproductive architecture, elaborated over weeks or month of growth, which maximises reproductive effort? How do plants generate the ‘correct’ number of inflorescences, flowers, fruit and seed without over- or under-committing resources to any of the developmental stages?

An important component in structuring reproductive architecture is ‘correlative inhibition’, in which older reproductive organs inhibit the growth of newer organs (Bangerth, 1989). These phenomena are well known to gardeners and horticulturists, being a prevalent feature of ornamental and horticultural crops. In many species, the earliest fruits will inhibit the development of fertilized and otherwise viable later-set fruit, resulting in reduced growth, abortion, abscission or senescence (Bangerth, 1989). Cucurbits such as cucumber provide a particularly striking example of this phenomenon, and a single fertile fruit may inhibit any subsequent fruit from developing (Zhang et al, 2015; Shnaider et al, 2018). In many other species, the presence of fertile fruit prevents ongoing flowering, and the prompt ‘dead-heading’ of flowers (in ornamental species) or regular picking of fruit (in horticultural species) is required to promote the continued initiation of inflorescences. A related phenomenon is biennial bearing, in which the presence of a heavy fruit load in spring-blooming trees can inhibit the formation of inflorescences for the next season’s flowering (Samach & Smith, 2013; Krasniqi et al, 2017). In cereal crops, there are well-known ‘yield trade-offs’, in which increasing one component of yield (e.g. number of ears) will tend to result in the decrease of other components (e.g. seed mass), such that there is no overall increase in yield (Gaju et al, 2009; Sakuma & Schnurbusch, 2020). Although not formally proven, there is reason to think that these effects are also driven by correlative inhibition mechanisms (Guo & Schnurbusch, 2019).

The traditional explanation for correlative inhibition effects has been competition for resources between organs; i.e. that plants cannot produce any more organs because the earlier organs monopolise the available supply of resources (Bangerth, 1989). There is certainly evidence that resource source-sink relationships within the plant play a role

in determining which organs grow and which do not, but also evidence that the effects are not sufficient to fully explain correlative inhibition effects (Marcelis et al, 2004; Wubs et al, 2009; Wubs et al, 2011). Furthermore, correlative inhibition of new organs often occurs before they have a high demand for resources (Bohner & Bangerth, 1988). It has therefore been suggested that correlative inhibition occurs by active 'dominance' mechanisms, in which older organs inhibit the growth of younger organs by active signalling, rather than by passive resource use (Bangerth, 1989). In the case of apical dominance - the inhibition of new shoot branches by actively growing shoots - the existence of a complex signalling network involving the hormonal signals auxin, cytokinin and strigolactone has certainly been demonstrated (Domagalska & Leyser, 2011). There is some evidence that the same principles may apply in reproductive development. For instance, auxin transport from early-set tomatoes has been implicated in the growth inhibition of later-set tomatoes on the same truss (Bangerth, 1989). In citrus and olive, auxin export from fruit has also been implicated in the inhibition of inflorescence development, and thus biennial bearing (Haim et al, 2020). However, the role of dominance mechanisms in the control of reproductive architecture has not yet been systematically investigated.

Within the Brassicaceae, we now have very clear understanding of the mechanisms that regulate floral initiation, and the identify and function of shoot meristems during flowering in Arabidopsis (Pajoro et al, 2014), and increasingly in other species including *Brassica napus* (oilseed rape / canola)(O'Neill et al, 2019) and *Arabis alpina* (e.g. Wang et al, 2009; Hyun et al, 2017; Lazaro et al, 2018; Vayssieres et al, 2020). However, despite the prominence of Arabidopsis as a model system, the control of reproductive architecture as a spatio-temporal phenomenon has generally been poorly characterised. Recent work has also started to elucidated how flowering in Arabidopsis is brought to an end, demonstrating the importance of events both in the inflorescence meristem themselves (Wuest et al, 2016; Balanzà et al, 2018), and signalling from fertile fruits (Hensel et al, 1994). Indeed, floral arrest in Arabidopsis seems to arise as a result

of fruit exerting local dominance over the inflorescence apex by auxin export, although the exact target of this dominance is still uncertain (Ware et al, 2020; Gonzalez-Suarez et al, 2020). However, our understanding of how the number of organs is controlled, and how those are distributed in time and space is lacking. In order to understand the mechanisms that control reproductive architecture in the Brassicaceae, we systematically investigated reproductive architecture control in Arabidopsis, complementing this with targeted experiments in *Brassica napus*.

2.4 Results

2.4.1 The scale of reproductive effort is predicted by early developmental decisions

To understand how reproductive architecture is controlled in Arabidopsis, we began by compiling an extensive dataset of reproductive architecture measurements from wild-type Arabidopsis (Col-0) from experiments across the past 18 years. This included experiments grown in a range of growth conditions (glasshouse, walk-in chamber), light intensities, photoperiods and soil volumes. For each experiment we had recorded the number of secondary inflorescences, i.e. the inflorescences initiated by the axillary meristems in the leaves along the primary shoot axis. This includes both cauline and rosette inflorescence branches (64 experiments; Supplementary Figure 2.1 A). For a number of these experiments we had also recorded the total number of inflorescences (i.e. including the tertiary inflorescences that branch from the secondaries, the quaternaries that branch from the tertiaries, etc.) (39 experiments; Supplementary Figure 2.1 B), and for a smaller number, the total number of fruits in addition (17 experiments; Supplementary Figure 2.1 C). Because they are easy to count, it is tempting to use the number of secondary inflorescences as a good proxy for reproductive architecture as a whole. Indeed, in studies of shoot branching in Arabidopsis, typically only the secondary inflorescences (usually referred to as ‘primary branches’ in this context) are assessed to define the overall branching levels of plants (e.g. Bennett et al, 2016; Brewer et al 2016; van Rongen et al, 2019; Fichtner et al, 2020). However, our data show the danger of this approach; while the number of secondary inflorescences does correlate with both overall inflorescence numbers as a whole, the relationship between these parameters is exponential, not linear (Figure 2.1 A). Thus, small increases in the number of secondary inflorescences can produce a dramatic increase in overall inflorescence number - and therefore reproductive effort. Conversely, while plants with more secondary inflorescences certainly tend to produce more fruit, the correlation between these parameters is not strong (Figure 2.1 C). Even total inflorescence number does not strongly predict total fruit number (Figure 2.1 E), as we

have previously discussed, because of apparent feedback between active inflorescences (Walker & Bennett, 2019). Nevertheless, it is clear that, as the earliest developmental decision in the elaboration of the reproductive system, the number of secondary inflorescences initiated at the start of flowering broadly determines the overall scale of the reproductive effort in Arabidopsis - especially since Arabidopsis inflorescences have a limited lifetime of activity (Ware et al, 2020).

In a rather smaller dataset of *Brassica napus* plants – including both field and glasshouse grown plants of several varieties – we observed similar patterns. Secondary inflorescence number was correlated with total inflorescence number in a manner also best described by an exponential function (Figure 2.1 B). Interestingly, secondary inflorescence number was much better correlated with total fruit number in *B. napus*, with a quadratic function best describing this relationship; this was also the best fit for the equivalent relationship in Arabidopsis (Figure 2.1 D). Total inflorescence number is exceptionally well correlated with total fruit number, in a clear linear relationship (Figure 2.1 F). In general, *B. napus* tends to produce a smaller proportion of higher order branches (tertiaries and above) than Arabidopsis, which might explain the better correlation between secondary inflorescence number and total fruit number. Although adequately predicting reproductive effort, these inflorescence number parameters nevertheless fail to capture the spatial complexity in the reproductive architecture of *B. napus*, a species in which many flowers do not produce a fertile fruit (discussed further below)(Tayo & Morgan, 1975). To understand how early the scale of reproductive architecture is determined in *B. napus*, we tracked the number of active secondary inflorescences in 16 individual field-grown plants from April (before any flowers opened) to July (when plants were nearing fruit ripening). We found that plants with less than 15 secondary inflorescences had essentially the same number in July as in April (Figure 2.1 G), but that those with greater than 15 had all lost inflorescences by July. These were almost all lower-canopy inflorescences; some of these were lost to damage, but the others appeared to have aborted shortly after April. Overall, the inflorescence number in

April provided a good prediction of total inflorescence number, total fruit number, and total seed mass in July (Figures 2.1 H,I). Thus, even more than in Arabidopsis, the overall scale of reproductive development in *B. napus* seems to be determined very early on after flowering; plants produce a reproductive effort completely in proportion to their size in April. Remarkably, larger plants gain no additional advantage from being large, and smaller plants suffer no additional penalty for being small. This is consistent with recent work showing that winter annual *B. napus* plants undergo floral transition, and generate much of their reproductive architecture in autumn, and not spring; their visible flowering thus largely consists of elaborating existing structures, not generation of new ones (O'Neill et al, 2019).

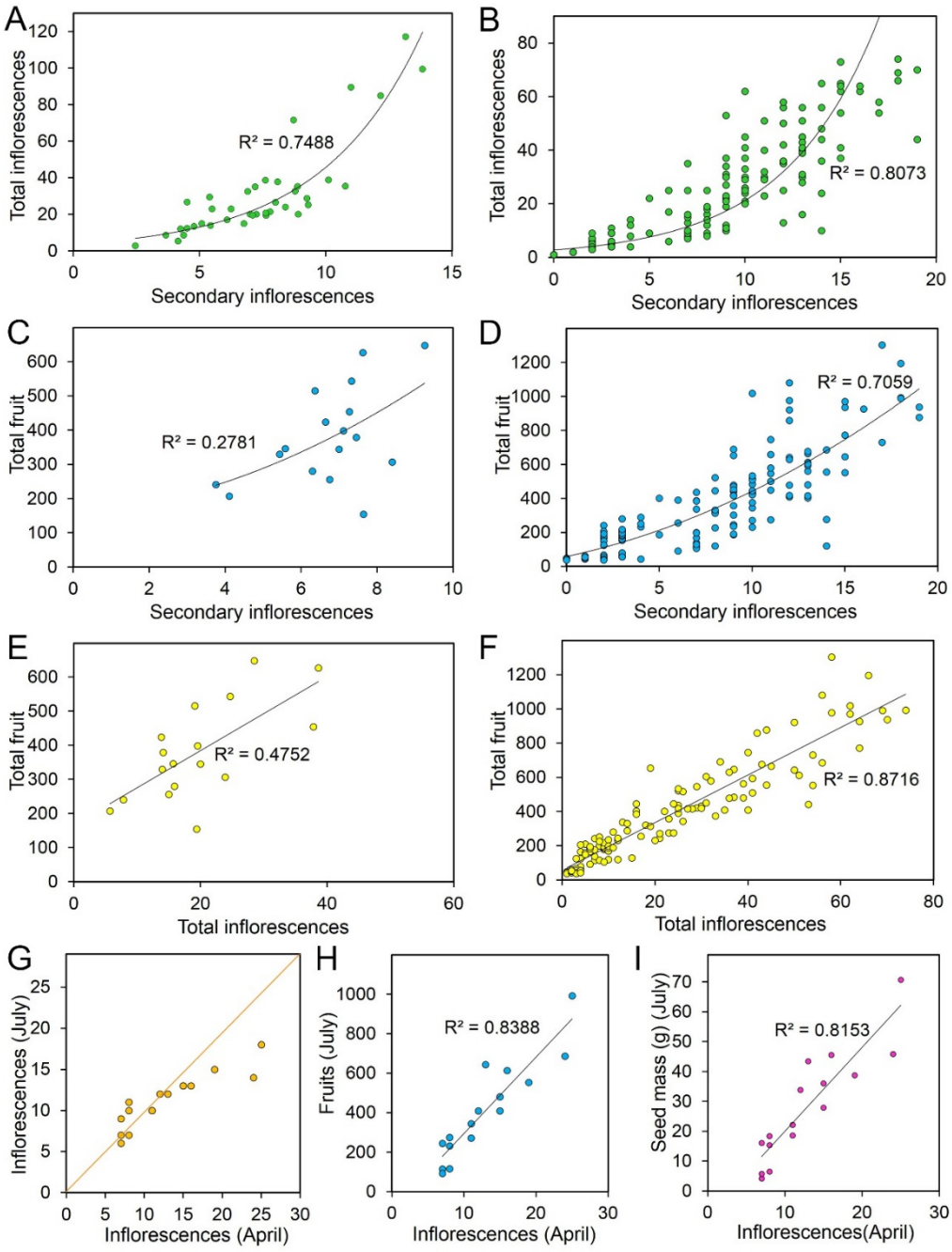

Figure 2.1. Early events determine the scale of reproductive development

Graphs showing relationship between inflorescence number reproductive development. Graphs show experimental means for multiple independent studies carried out in Arabidopsis Col-0 (A,C,E). Plants were grown on compost in either glasshouses or controlled environment chambers, in soil volumes ranging from 50ml to 2L. Following the end of flowering, all inflorescences were assessed and recorded, and in some instances total fruit counts were also obtained (C,E). Graphs B, D, F show individual plant means for various *B. napus* varieties, from a combination of glasshouse-grown plants in 500ml or 2L compost and field-collected samples from commercially-grown crops across the

UK. Whole plants were harvested from the field, and inflorescence number and total fruit number was assessed and recorded.

A,B) Graphs showing the relationship between number of secondary inflorescences and number of total inflorescences in Arabidopsis Col-0 plants (39 sets of experimental means)**(A)**, and in *B. napus* (155 individual plants, various oilseed rape varieties)**(B)**.

C,D) Graphs showing the relationship between number of secondary inflorescences and number of total fruit in Arabidopsis Col-0 plants (17 sets of experimental means)**(C)**, and in *B. napus* (142 individual plants, various oilseed rape varieties)**(D)**.

E,F) Graph showing the relationship between number of total inflorescences and number of total fruit in Arabidopsis Col-0 plants (17 sets of experimental means)**(E)**, and in *B. napus* (132 individual plants, various oilseed rape varieties)**(F)**. Data in E have been previously published in Walker & Bennett, 2019, but are shown here for the sake of completeness.

(G) Graph showing the relationship between number of secondary inflorescences in 16 individual commercially-grown *B. napus* plants (var. Campus) in April and July. Plants were tagged in April, and inflorescence number recorded. Plants were similarly assessed approximately monthly until the end of flowering (July), at which point plants were harvested and assessed. The orange line indicates the 1:1 line, so dots below the line are plants that lost inflorescences, and above the line gained inflorescences. **(H,I)** Graph showing the relationship between number of secondary inflorescences in 16 individual commercially-grown *B. napus* plants (var. Campus) in April and their total fruit number **(H)** and harvested dry seed mass in grams **(I)** in July. Plants were tagged in April, and inflorescence number recorded. Plants were similarly assessed approximately monthly until the end of flowering (July), at which point plants were harvested and assessed.

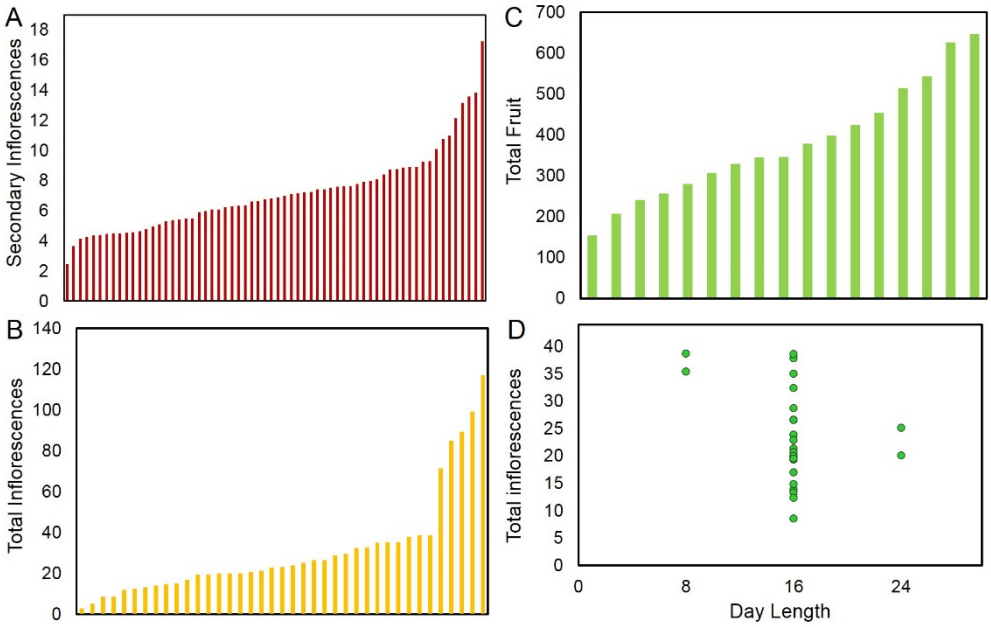

Supplementary Figure 2.1. *Arabidopsis* reproductive architecture datasets

A-C) Graphs showing the ranked experimental means for the number of secondary inflorescences (n=64 experiments)**(A)**, total inflorescences (n=39)**(B)** and total fruit (n=17)**(C)**, from a series of experiments performed with Arabidopsis Col-0 wild-type plants, from 2002-2020, using a variety of soil volumes and growth conditions. **(D)** Graph showing total inflorescences produced in Arabidopsis Col-0 in 25 experiments conducted in different day-lengths. Each data point is the mean of one experiment.

2.4.2 Resource, and resource-related information determine reproductive effort

Our data suggest that the resources available to plants during the vegetative phase, and the resulting pre-flowering developmental history of the plants, may be more important in determining the scale of reproductive effort than the resources available to plants during the reproductive phase. To try and understand which factors influenced the scale of reproductive effort most strongly in our experiments, we interrogated our datasets in more detail. Our fruit number datasets are almost all from plants nominally grown in the same conditions (16-hour day lengths, 150-200$\mu molm^{-2}s^{-1}$ light intensity, and 100ml soil volume), so we focussed on factors influencing secondary and total inflorescence number. Lighting conditions had relatively little clear effect on reproductive effort, with plants grown in controlled environment rooms versus glasshouses showing the same ranges in inflorescence number. Plants grown in 24 hours of light were in the middle of the range of those grown in 16-hour day lengths, whereas plants grown in 8-hour day lengths were at the upper end of that range (Supplementary Figure 2.1 D). However, it is difficult to disentangle this effect from the altered developmental history of these plants caused by their elongated vegetative phase. It must be noted that we were not able to systematically vary light intensity or quality across experiments to test the effect on reproductive effort, and doubtlessly light availability does play a role in determining this.

The clearest effect on inflorescence number in our dataset appeared to relate to the volume of soil the plants were grown in, with pot size clearly explaining much of the variation in inflorescence number (Figure 2.2 A). This is not especially surprising, since larger pots contain more nitrate, phosphate and other mineral nutrients. However, in many species substrate volume itself also strongly affects plant growth, independently of nutrient levels (Poorter et al, 2012; Wheeldon et al, 2020). Elsewhere, we have discussed the potential importance of soil volume as a proxy for future resource availability that allows plants to avoid resource limitations (Wheeldon et al, 2020). To test the idea that soil volume is a key determinant of the overall scale of reproductive effort

in Arabidopsis, we grew plants in 50, 100 and 500ml soil volumes. We observed a clear linear relationship between inflorescence number, biomass and pot size (Supplementary Figures 2.2 A,B). Additional nutrients had no clear effect on shoot growth parameters in these experiments, suggesting the effect is non-nutritional. To further test whether the effect of soil volume is nutritional or non-nutritional, we grew Arabidopsis in 100 and 500ml of sand/perlite mix, supplemented with low N or standard N fertiliser (7.5 or 75µmol of N/week). Even under low N treatment, plants grown in larger pots had significantly greater shoot biomass than in smaller pots (Supplementary Figure 2.2 E). We observed the same trend under standard N treatment, with plants in larger pots having increased shoot biomass relative to those in smaller pots (Supplementary Figure 2.2 E). Thus, both the volume and nutrient concentration of the substrate affect the growth of the Arabidopsis shoot system. Interestingly, when we grew Arabidopsis in pots larger than 500ml, we observed a clear saturation of soil volume on reproductive system size. Between 500ml and 1000ml there was only a marginal and statistically insignificant increase in inflorescence number despite a doubling in soil volume; and similarly between 1000ml and 2000ml (Supplementary Figure 2.2 C). We observed the same pattern for shoot biomass (Supplementary Figure 2.2 D). Thus, Arabidopsis growth seems to plateau in the range 500-1000ml, above which plants are unable to efficiently use the additional resources available. This might be because of the early flowering in long day-grown Arabidopsis; the plants may not have sufficient time to fully colonise the substrate volume before flowering is induced.

Using *B. napus*, we more clearly defined the effect of substrate volume on reproductive architecture, by growing plants in pots containing either 100ml, 500ml or 2000ml of soil (Figure 2.2 B). For every parameter we assessed – shoot biomass, inflorescence number, fruit number and fruit mass – the size of the reproductive system was clearly proportional to the substrate volume (Figures 2.2 C-F). Again, additional nutrients had no clear effect on shoot growth parameters in these experiments, suggesting the effect of substrate volume is non-nutritional, at least in part (Figures 2.2

C-F). *B. napus* plants grown in 100ml pots produced only a single primary inflorescence, while Arabidopsis typically produces ~30 inflorescences in the same soil volume. Thus, although plants are capable of adapting to any soil volume, the inherent size of the species plays a key role in determining what the reproductive architecture will be in different conditions. In 500ml pots, the *B. napus* plants produced secondary inflorescences as well, but no tertiaries, while most of the additional branches produced in 2000ml pots are tertiaries, rather than secondaries. Thus, like Arabidopsis, the complexity of *B. napus* reproductive architecture increases as overall reproductive effort increases.

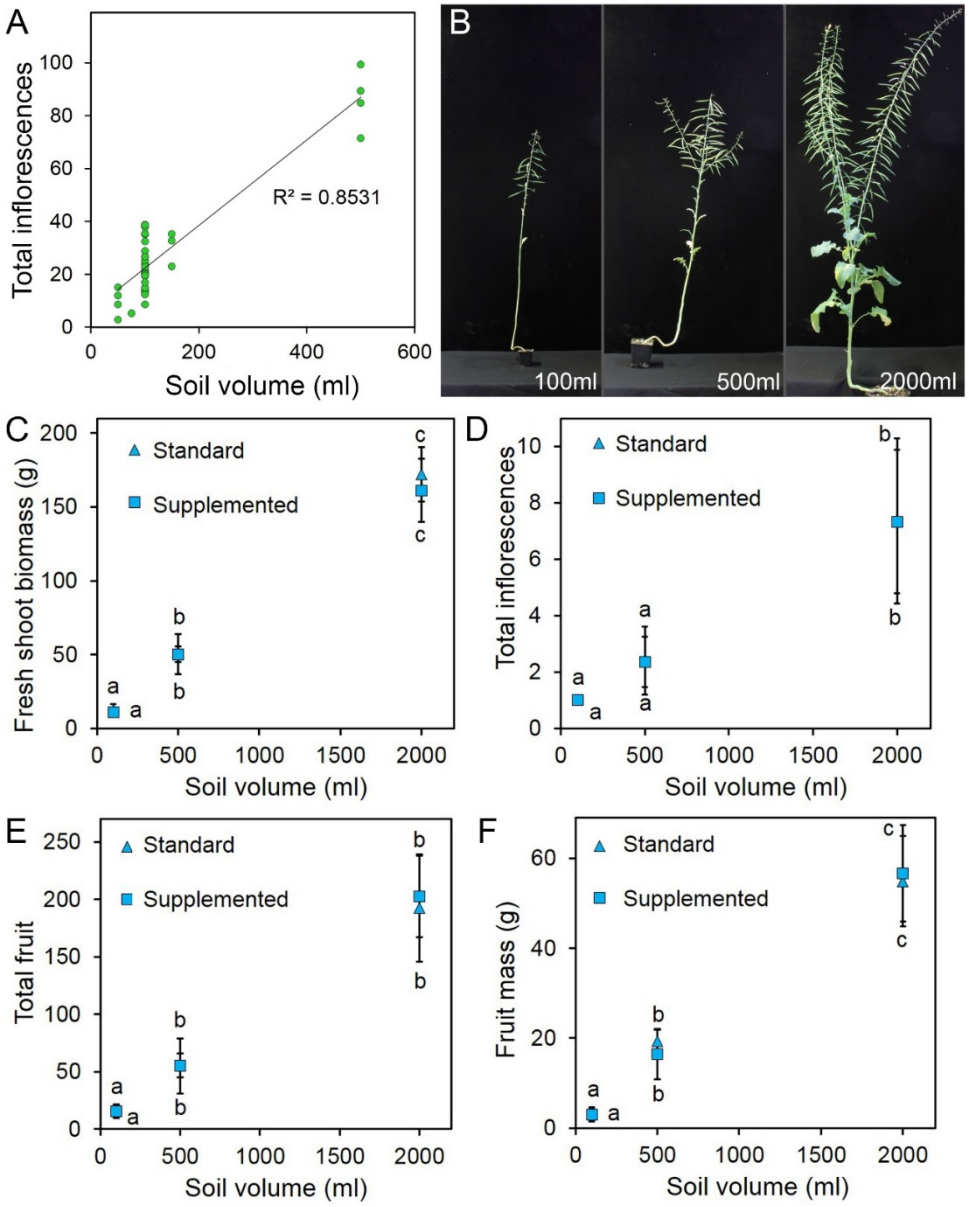

Figure 2.2. Soil volume directly influences reproductive architecture

(A) Graph showing the relationship between soil volume and total inflorescence number in 39 experiments using Arabidopsis Col-0 plants; data points are experimental means. **(B)** Final plant size in Heros spring oilseed rape plants grown in 100, 500 and 2000ml of soil (photos are to scale). **(C-F)** Graphs showing the relationship between soil volume and mean fresh shoot biomass in grams **(C)**, mean total inflorescence number **(D)**, mean total fruit number **(E)** and mean fruit dry biomass in grams **(F)** in spring oilseed rape grown in 100, 500 and 2000ml of soil, with ('supplemented') or without ('standard') additional nutrients provided. Error bars indicate s.e.m, n=6-12. Data points with the same letter are not statistically different to each other (C - ANOVA and Tukey HSD test, F=374.3; df=5; D - Kruskal-Wallis test with pairwise comparison and Bonferroni correction F=59.99, df=5; E - Kruskal-Wallis test with pairwise comparison and Bonferroni correction F=62.28; df=5; F - ANOVA and Tukey HSD test, F=167.84; df=5).

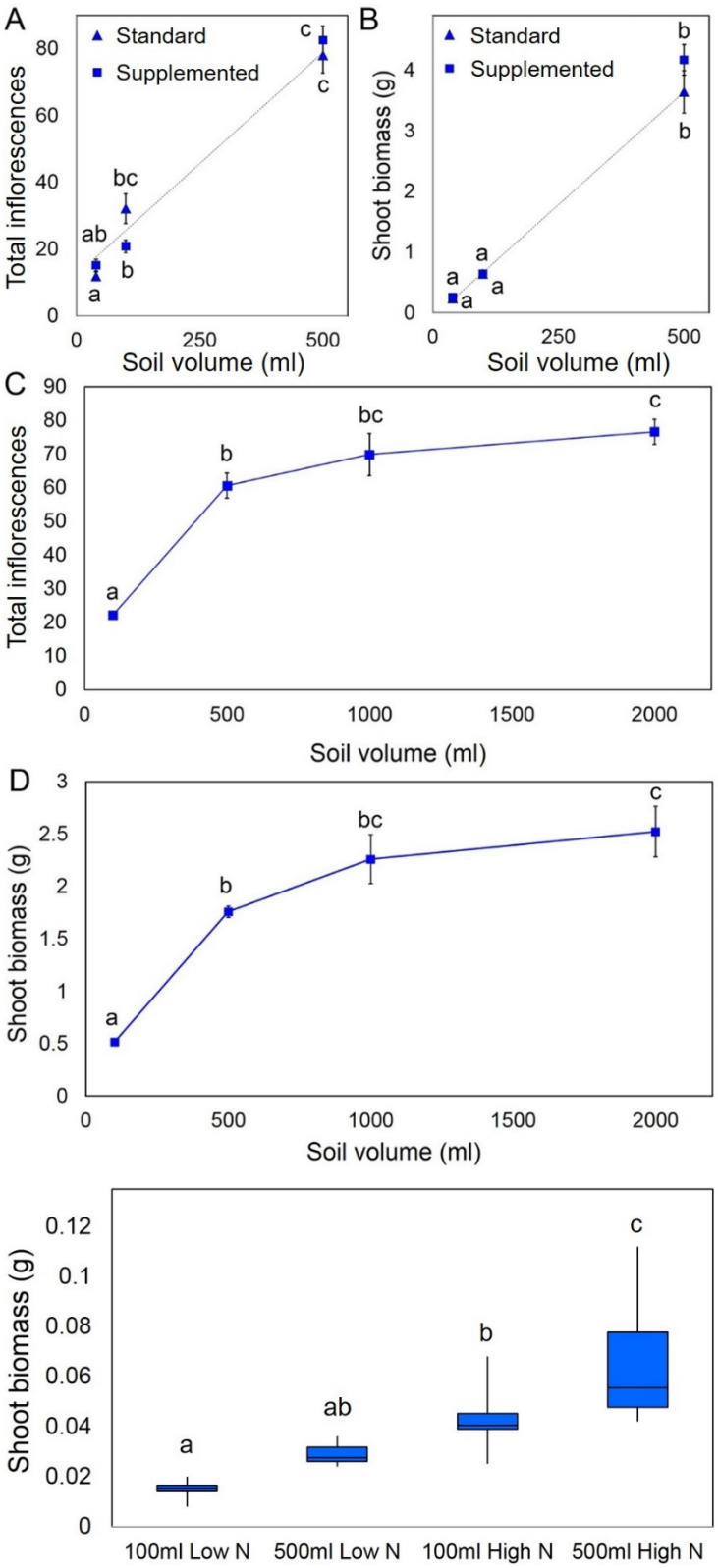

Supplementary Figure 2.2. Substrate volume determines shoot growth in Arabidopsis

(A,B) Graphs showing the relationship between soil volume and mean total branch number **(A)** and mean dry shoot biomass in grams **(B)** in Arabidopsis grown in 50, 100, and 500mL of soil, with ('Supplemented') or without ('Standard') additional nutrients. Error bars indicate s.e.m, n=10-12. Data points with the same letter are not statistically

different to each other (A - Kruskal-Wallis test, F=54.94, df=5, p>0.05; B - ANOVA + Tukey HSD, F=118.3, df=5, p>0.05). **(C)** Graph showing mean total branch number in wild-type (Col-0) Arabidopsis grown on compost, in four pot sizes (100, 500, 1000 and 2000ml). Data points show means, bars indicate ± s.e.m. n=8-12. Points with the same letter are not statistically different from each other (ANOVA+Tukey HSD, F=51.46, df=3, p>0.05). **(D)** Graph showing mean final dry shoot biomass in wild-type (Col-0) Arabidopsis grown on compost, in four pot sizes (100, 500, 1000 and 2000ml). Data points are means ± s.e.m. n=8-12. Bars with the same letter are not statistically different from each other (ANOVA+Tukey HSD, 39.69, df=3, p>0.05). **(E)** Box plots showing mean final dry shoot biomass in wild-type (Col-0) Arabidopsis grown on a sand/vermiculite mix, in two pot sizes (100 and 500ml) and supplemented with fertiliser containing either standard nitrate concentration (75µmol/week) or a low nitrate concentration (7.5µmol/week). Box represents interquartile range, and midline indicates the median. Whiskers indicate maximum and minimum. Data points are means ± s.e.m. n=10. Bars with the same letter are not statistically different from each other (ANOVA+Tukey HSD, F=24.82, df=3, p>0.05).

2.4.3 Reproductive shoot/inflorescence branching is homeostatically regulated

We next wanted to understand how Brassicaceae temporally sequence the growth of their reproductive systems in response to resource and resource-related information. In particular, we wanted to understand how plants correctly allocate resources to the early stages of reproductive development. Given that each inflorescence has an essentially fixed growth potential and lifetime (O'Neill et al, 2019; Ware et al, 2020), not making enough inflorescences will restrict maximum reproductive effort. Conversely, since each inflorescence requires an investment of nutrients that cannot be remobilised until the very end of development, and requires a constant supply of water and photosynthate, making too many inflorescences will also restrict reproductive effort. How do plants make the correct developmental 'decision' on inflorescence number, such that the resources available for flowering and fruit set later in development are maximised? We hypothesised that very strong 'dominance' effects early on in reproductive development might prevent over-allocation of resources to inflorescence development.

To test this idea, we performed a variety of inflorescence removal ('debranching') experiments using wild-type Col-0 Arabidopsis. Although Arabidopsis meristems pass through an exceptionally short-lived RSM phase, by the time any of them are visible (including the primary meristem), they have already converted to IMs. Thus, performing experiments specifically on the reproductive shoot phase of Arabidopsis development is practically impossible, and we treated it as part of the inflorescence phase in our experiments. We trialled different timings for inflorescence removal, before settling on 15 days post bolting (dpb) as an 'early-mid flowering' point. At this point, plants had typically activated most inflorescences, but had only made ~30 fruit (approximately 5% of their typical total fruit set). We performed debranching of secondary inflorescences in different positions, and of different magnitudes. Some plants had 50% of their secondary inflorescences removed, either apically or basally (50% apical, 50% basal), others had 75% removed basally (75% basal); in the most extreme treatments 100% of secondary inflorescences were removed either without (100%) or in addition to the primary inflorescence (100%+) (Figure 2.3 A). We then tracked the number of secondary inflorescences produced by these plants during the rest of normal reproductive development. Surprisingly, for all treatments, the final number of secondary inflorescences was not significantly different from the original, pre-treatment number (Figure 2.3 A), nor was there any difference relative to the original number of secondary inflorescences present in the untreated control (Figure 2.3 A). The partial exception to this was the 50% apical treatments, which initiated few new secondary inflorescences, although were not statistically different from untreated plants (Figure 2.3 A).

We also tracked the total number of inflorescences produced by these plants. Similarly to secondary inflorescences, there was no statistical difference in the total number of inflorescences between any of the treatment groups and the untreated control at the end of the experiment, including the 50% apical group (Figure 2.3 B). We did not count fruits in this experiment, but in an earlier iteration with the same basic design, we found that final fruit numbers were slightly - but not statistically significantly - lower in the

more extreme treatments (Supplementary Figure 2.3 A). We also assessed whether the regulation of inflorescence architecture changes over time by performing the same debranching experiment as in Figure 2.3 A, but in plants which had undergone arrest of the primary inflorescence (~22 days post bolting). We observed highly comparable results to the earlier time points, with the more dramatic treatments resulting in complete replacement of lost organs, while the 50% treatments prompted less strong responses (Supplementary Figure 2.3 B). Thus, as a whole, the Arabidopsis reproductive system displays a very surprising level of homeostasis to loss of organs.

These data demonstrate several key features of Arabidopsis reproductive architecture. Firstly, the initial number of inflorescences produced by the plant does not reflect resource limitations; plants retain the capacity to make the same numbers of inflorescences again, along with attendant fruit, if needed - even if the loss or organs occurs right at the end of reproductive development. Secondly, the secondary inflorescences collectively inhibit the initiation of new secondary inflorescences, in keeping with the idea of ‘dominance’ between organs. Thirdly, the system is highly homeostatic, and accurately replaces lost organs. In formal terms, the regulatory systems of the plant are calibrated so as to produce an optimal number of inflorescences for the available resources, even if the system is perturbed – but in effect, we could say that the plant has a ‘target’ inflorescence number.

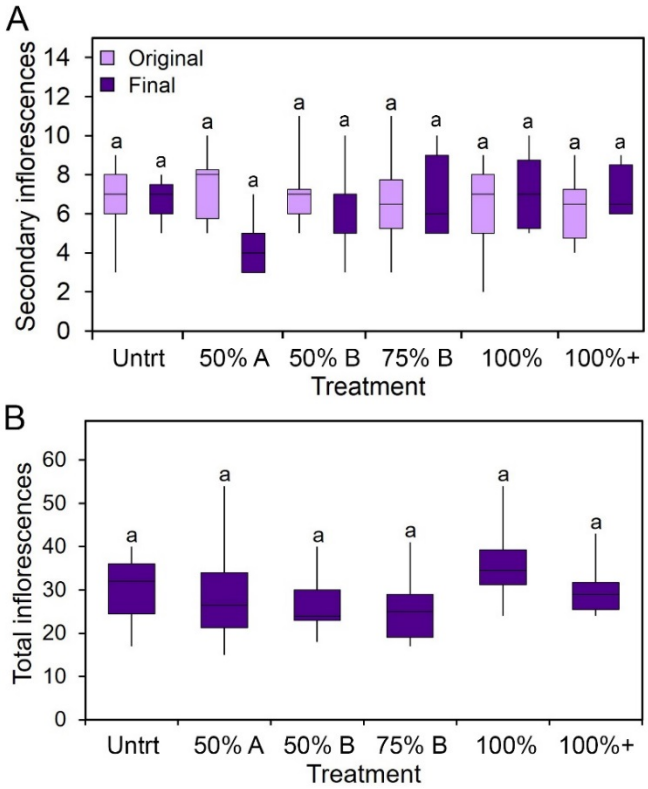

Figure 2.3. Inflorescence number is homeostatically regulated

(A) Graph showing the number of secondary inflorescences produced in Arabidopsis Col-0 plants. 15 days post bolting, when the majority of inflorescences had been produced, existing inflorescences were counted (pre-treatment, light boxes), and scissors were used to remove differing numbers of inflorescences. '50% A' had the apical 50% of existing secondary inflorescences removed, while '50% B' and '75% B' had the basal 50 or 75% of secondary inflorescences removed respectively. '100%' treated plants had all inflorescences removed, while leaving the primary inflorescence in-tact, while this was also removed in '100% +' treatments. Following recovery and when the plants had finished flowering, the number of secondary inflorescences was again counted (post-treatment, dark boxes). Bars with the same letter are not statistically different from each other (ANOVA + Tukey HSD, n=9-12 pre treatment, 3-6 post treatment; F=1.165, df=11). **(B)** Total inflorescences produced following recovery and end of flowering in Arabidopsis Col-0 plants. All treatments as described in **A**. Boxes indicate the interquartile range. The central line indicates the median, whiskers show minimum and maximum values. Bars with the same letter are not statistically different from each other (ANOVA + Tukey HSD, n=3-6; F=0.737, df=5).

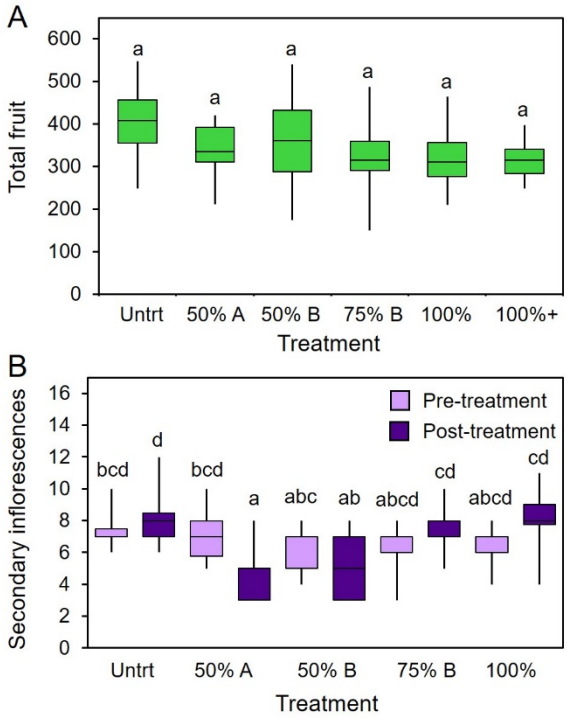

Supplementary Figure 2.3. Inflorescence and fruit number display homeostasis in Arabidopsis

(A) Box plot of total fruits produced by *Arabidopsis* Col-0 under treated conditions. Secondary inflorescences were removed during flowering, and plants were allowed to recover; following the end of flowering, the total number of fruits on the plant was recorded. '50% A' had the apical 50% of existing secondary inflorescences removed, while '50% B' and '75% B' had the basal 50 or 75% of secondary inflorescences removed respectively. '100%' treated plants had all inflorescences removed, while leaving the primary inflorescence in-tact, while this was also removed in '100%+' treatments. Bars with the same letter are not statistically different from each other (ANOVA + Tukey HSD, n=8-19, F=2.102, df=5, p>0.05). **(B)** Box plot of secondary inflorescences produced by Arabidopsis Col-0 plants. Secondary inflorescences (and any subtending higher order inflorescences) were removed from the plant with scissors following the end of flowering. Inflorescence numbers were recorded immediately prior to 5 treatment (pre-treatment, light boxes) and following a recovery period, when the plants were no longer flowering (post-treatment, dark boxes). '50% A' had the apical 50% of existing secondary inflorescences removed, while '50% B' and '75% B' had the basal 50 or 75% of secondary inflorescences removed respectively. '100%' treated plants had all inflorescences removed. Boxes indicate the interquartile range. The central line indicates the median, whiskers show minimum and maximum values. Bars with the same letter are not statistically different from each other (ANOVA + Tukey HSD, n=9-13, pre-treatment F=1.960, df=4; post-treatment F=10.046, df=4, p>0.05).

2.4.4 'Infloretic dominance' arises from all parts of the inflorescence

The clear dominance that secondary inflorescences exert over the activation of other secondary inflorescences is highly reminiscent of the apical dominance phenomenon. However, apical dominance is usually associated with vegetative branching, rather than inflorescence branching. Arabidopsis does not make elongated vegetative branches, and as such has been a poor system for 'classical' apical dominance research. Studies using Arabidopsis inflorescences as a model system for apical dominance studies have generally struggled to see the classical effects of decapitation and auxin application (e.g. Chatfield et al, 2000; Cline et al, 2001). However, our results suggest that inflorescences do exert considerable dominance. We therefore questioned whether this 'infloretic dominance' is qualitatively different from classic apical dominance in vegetative shoots. We performed experiments in which we removed different parts of the secondary inflorescences to understand how the dominance is mediated. In one treatment, we removed all the flower-bearing parts of each inflorescence, leaving the leaf-bearing nodes at base of each inflorescence ('de-crowning'). In another treatment group, we removed the inflorescence meristem and cluster of unopened flowers from the inflorescence apex ('de-capitation'), and in another group we removed all fruit present on each inflorescence ('de-fruiting'). We performed these treatments at 17dpb, and then tracked the growth of the plants until the end-of-flowering.

All three treatments promoted the activation of tertiary, quaternary and quinternary branches, although inflorescences also increased in untreated plants over the course of the experiment (Figures 2.4 A-C). This effect was strongest in the de-crowned plants (30 additional branches) and weakest in the de-fruited plants (8 additional branches), which was not statistically different from the untreated group. It should be borne in mind that de-crowned and de-capitated secondary inflorescences will not produce any more organs on existing inflorescences, but that de-fruited inflorescences will continue to produce new flowers and fruits, and therefore represent a

much less severe treatment. Intriguingly, we observed that very few new secondary inflorescences were activated in any of the treatment groups (Figures 2.4 A,B). Thus, although each treatment removed a substantial proportion of the inflorescence, the secondary inflorescences largely retained their dominance over other secondary inflorescences. It therefore appears that the activation of additional tertiary and higher order branches allows each secondary inflorescence system as a whole to maintain its overall dominance in the system. Thus, the 'infloretic dominance' that secondary inflorescences exert over other secondary inflorescences results from the combined dominance exerted by i) the inflorescence apex, ii) the fruit and iii) the higher order branches within the inflorescence system. In this context, it can be noted that while removal of the inflorescence apex (de-capitation) does not have an effect on other secondary inflorescences, it does release higher order branches subtending the apex from inhibition (Figure 2.4 B). Thus, in the reproductive system, 'classic' apical dominance effects only occur *within* inflorescence systems, and not *between* them.

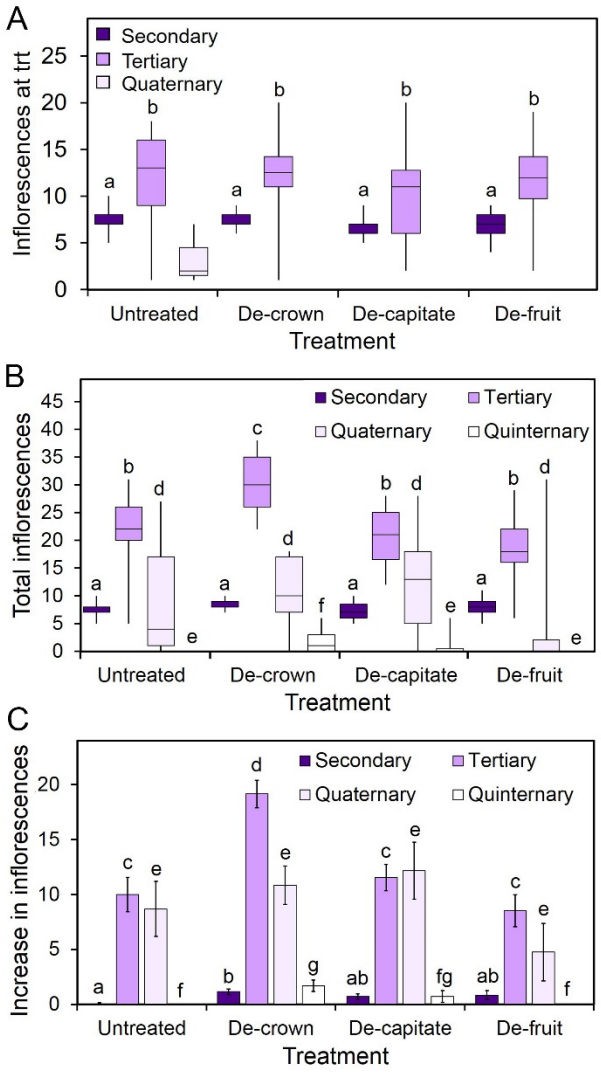

Figure 2.4. Infloretic dominance arises from a combination of organs

(A) Box plot showing the number of inflorescences of each class (secondary, tertiary and quaternary; dark, medium and light boxes respectively) present in Arabidopsis Col-0 plants immediately prior to treatment. When approximately 30 flowers had opened on the primary inflorescence (around 15dpb), plants were left untreated; had all active floral parts of the inflorescence removed from immediately below the lowest fruit (de-crown); had all bud clusters and inflorescence meristems removed (de-capitate); or had all present fruit removed (de-fruit). At the time of treatment, the number and position of each inflorescence was recorded. Bars with the same letter are not statistically different from each other, each class of inflorescence was compared separately (ANOVA + Tukey HSD, n=10-12. Secondary F=1.504; df=3; tertiary F=0.419, df=3; quaternary F=1.885; df=3). **(B)** Box plot showing the number of inflorescences of each class (secondary, tertiary, quaternary and quinternary; darkest to lightest boxes respectively) present in Arabidopsis Col-0 plants, following treatment and a recovery period. Treatments were carried out as described in A. Following recovery and the end of flowering, the total number and position of each inflorescence was recorded. Bars with the same letter are

not statistically different from each other, each class of inflorescence was compared separately (ANOVA + Tukey HSD, n=10-12. Secondary F=2.081, df=3; tertiary F=8.595, df=3; quaternary F=1.726, df=3; quinternary F=5.124, df=3). **(C)** Bar graph showing the difference secondary, tertiary, quaternary and quinternary inflorescences between arising between treatment and end-of-life in plants treated as described in A. Boxes indicate the interquartile range. The central line indicates the median, whiskers show minimum and maximum values Error bars indicate s.e.m; bars with the same letter are not statistically different to each other (comparisons only made within each inflorescence class). (ANOVA + Tukey HSD, n=10-12. Secondary F=2.891, df=3; tertiary F=11.951, df=3; quaternary F=1.830, df=3; quinternary F=5.124, df=3).

2.4.5 Fruit limit inflorescence activation in *trans* through exchangeable dominance

These data suggest that fruit play a role in the control of reproductive architecture of Arabidopsis. To understand the effect of fruit on overall reproductive architecture, we trialled the removal of different numbers of fruit from different inflorescences in Arabidopsis. We found that a wide range of minor perturbations had no effect on reproductive architecture, and that treated plants tended to produce the same number of inflorescences, flowers and fruit as untreated plants. For instance, plants treated by removal of 50% fruit from the lower part of every inflorescence at 17 dpb made the same total number of flowers and fruit as control plants (Figure 2.5 A). Conversely, more dramatic treatments, such as the removal of all branches (Supplementary Figure 2.3 A), the removal of all fruit (Figures 2.5 C,D) and the continuous removal of all fruit (Figure 2.5 C,D) seem to completely ‘reset’ the system, such that treated plants ultimately make approximately the same number of fertile fruits as treated plants. Again, this illustrates that during this later phase of reproductive development plants retain the capacity to accurately replace lost organs; we could informally say that plants also have a ‘target’ fruit number.

How is this effect of fruit on reproductive architecture mediated? We have previously shown that fruit can limit the further production of fruit on the same inflorescence (i.e. in *cis*) by triggering a time-dependent arrest of the inflorescence (Ware

et al, 2020). However, our data suggest that fruit also exert dominance over the activation of higher order inflorescences (i.e. in *trans*)(Figure 2.4 B). To explore this 'exchangeable dominance' in more depth, we performed a series of experiments with different fruit removal treatments. Continuous removal of all fruit on the plant leads to a massive increase in the number of branches produced across the plant, regardless of if a recovery period is allowed or not (Figure 2.5 E). Compared to these complete de-fruiting treatments, a single treatment removing 50% of the fruit had variable effects. In one experiment, removing the oldest 50% of fruit on each inflorescence at 17dpb produced no clear increase in inflorescence number (Figure 2.5 B). However, in other experiments, the same treatment produced quite a strong increase in inflorescence number (Figure 2.5 F), presumably reflecting differences between the developmental stages the plants in different experiments had reached at the 17dpb. There was also a clear effect of the position of the fruit removed; the removal of the youngest 50% of fruit on an inflorescence had a stronger effect than removing the oldest 50% of fruit (Figure 2.5 F). This likely reflects the timing of the treatments, rather than any major difference in the dominance of the fruits themselves; the first treatment occurring when the inflorescence meristem is still active, and the second after the arrest of the inflorescence meristem (and thereby the end of its dominance from the system). Overall, fruit therefore gradually and collectively supplant the inflorescence meristem as the main source of dominance in the inflorescence, and continue the inhibition of subtending inflorescences. However, the dominance exerted by each Arabidopsis fruit is weak, and it is only once fruit numbers reach their maximum on each inflorescence that they have a strong effect on reproductive architecture.

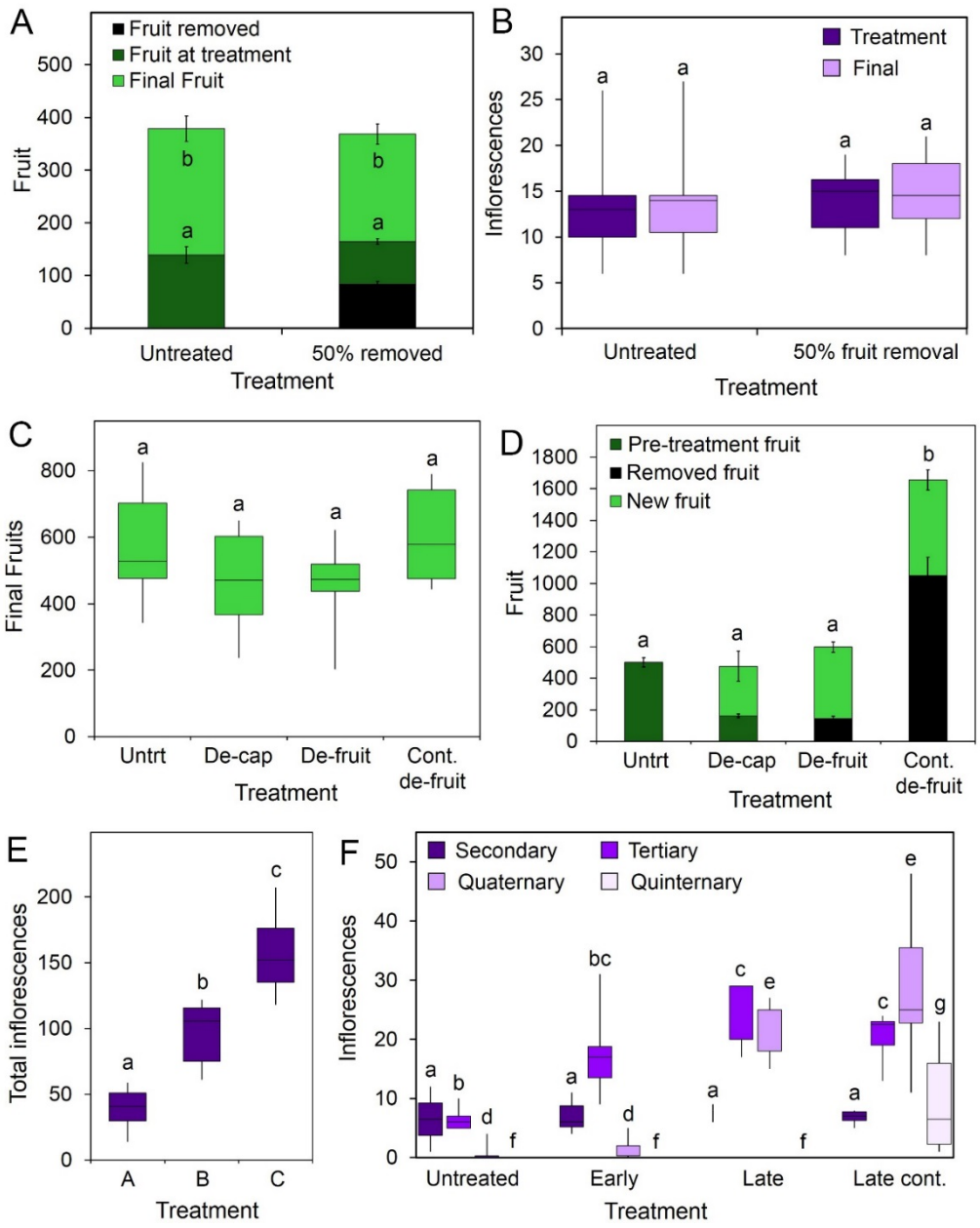

Figure 2.5. Fruit regulate inflorescence activation in *trans*

(A) Graph showing the effects of partial fruit removal on the final total fruit production in Col-0 Arabidopsis. Plants were either untreated, or had the basal 50% of fruit removed from all branches at 17dpb. The number of fruits removed were counted (fruit removed, black), alongside all remaining fruits on the plant at the time of treatment (fruit at treatment, dark green). Finally, all fruits at the time of floral arrest were counted (final fruit, light green). Bars indicate standard error. Fruit at treatment and final fruit were compared separately; bars with the same letter are not statistically different to each other (T-test, $p<0.05$, n=11-12). **(B)** Boxplot showing the number of inflorescences present following early fruit removal. The basal 50% of fruit were removed from all inflorescences 17dpb. Inflorescences were counted at the time of treatment (treatment, dark purple), and again following the end of flowering (final, light purple). Bars with the same letter are

not statistically different to each other (ANOVA+Tukey HSD, n=11-12). **(C)** Boxplot showing the final number of fruits produced in Col-0 Arabidopsis following treatment. Treatments were carried out when approximately 30 fruits were present on the primary inflorescence. At this point, all inflorescence meristems were removed from the plant (de-cap), all fruits were removed from the plant in a single event (de-fruit), or all fruits were removed, with a period of continual fruit removal, before allowing the plants to recover (cont. de-fruit). Following the end of flowering, the total number of fruits present across the whole plant was recorded. Bars with the same letter are not statistically different to each other (ANOVA+Tukey HSD, n=6-13; F=2.498, df=3). **(D)** Graph showing the total number of fruits produced and removed from Col-0 Arabidopsis following treatment. All treatments were as described in (C). Fruits were counted at the time of treatment (pre-treatment fruit, dark green). Fruits removed were counted (removed fruit, black). After the end of flowering, the total number of new fruits produced after treatment were counted (new fruit, light green). Bars indicate standard error. Bars with the same letter are not statistically different to each other (ANOVA+Tukey HSD, n=6-13; F=60.549, df=3). **(E)** Boxplot showing total final number of inflorescences in Arabidopsis Col-0 plants. Plants were untreated ('A') or had all open flowers continually removed daily. Plants had all existing fruit and open flowers removed when approximately 30 fruits were present on the primary inflorescence. Following this treatment, all open flowers were removed daily from every inflorescence for 28 days. After 28 days, the plants were allowed to recover ('B'). The final treatment ('C') was carried out in the same manner as 'B', only plants were not allowed a recovery period; instead, open flowers were removed daily from these plants until the plants finished flowering. Total inflorescence numbers for each plant were recorded following the end of flowering. Bars with the same letter are not statistically different to each other (ANOVA+Tukey HSD, n=5-13, F=50.024, df=3). **(F)** Boxplot showing the effects of severe fruit removal on higher order inflorescence production. Plants which were 'early' treated had all open flowers removed daily from all inflorescences until around 30 fruits (approximately 15dpb) were present on the primary inflorescence, then allowed to flower as normal. 'Late' treated plants had all flowers removed daily from all inflorescences, from around 30 fruits being present on the primary inflorescence; flowers continued to be removed until approximately 30 flowers (approximately 15dpb) had been removed from the primary inflorescence. 'Late cont.' treated plants were as 'Late' plants, however flowers were removed from all inflorescences until approximately 45 flowers had been removed from the primary inflorescence. At arrest, all present inflorescences within each inflorescence class were counted (secondary, tertiary, quaternary, qinternary; dark purple to light purple respectively). Box represents interquartile range, and midline indicates the median. Whiskers indicate maximum and minimum. Bars with the same letter are not statistically

different to each other; each class of inflorescence was compared separately (ANOVA+Tukey HSD, n=5-11; secondary F=0.741, df=3; tertiary F=6.131, df=3; quaternary F=40.097, df=3; quinternary F=9.292, df=3).

2.4.6 Carpic dominance is absent in Arabidopsis

As discussed above, in many species the older fruit inhibit the development of younger fruit on the same inflorescence. This 'carpic dominance' may include smaller size of younger fruit (e.g. tomato), shedding of fertile younger fruit by abscission (e.g. apple), or the inhibition or abortion of new fruit development (e.g. cucumber)(Bangerth, 1989; Walker & Bennett 2018). Within the Brassicaceae, the unusual dimorphic fruit of *Aethionema* species have been proposed to arise by carpic dominance (Lenser et al, 2018), but no such phenomena has been demonstrated in Arabidopsis. We therefore examined whether carpic dominance exists in Arabidopsis. We observed that there is a clear gradient in fruit size along each inflorescence with smaller fruit towards the apex; and also between inflorescences, with higher order inflorescences having smaller fruit than major inflorescences (Figure 2.6 A). This developmental gradient is suggestive of carpic dominance, so we tested this by removing either the 50% oldest, the 50% youngest, or 100% of fruit from the primary inflorescence at ~20 dpb, and assessed the effect on the growth of the subsequent fruit on the inflorescence. However, we observed no change in the size of post-treatment fruit, even in the strongest treatments, strongly suggesting there is no same-inflorescence carpic dominance in Arabidopsis (Figure 2.6 B) (see also Appendix 2.3.1).

We reasoned that carpic dominance might still occur in Arabidopsis if fruit on higher order branches are inhibited by fruit on the super-tending branch. We therefore removed the fruit from all secondary inflorescences, to test whether this had any effect on the size of fruit on the tertiary inflorescences. Since we have already shown the infloretic dominance of major inflorescences arises from a combination of fruit and inflorescence meristem, we also performed a de-crowning of the secondary inflorescences, to test whether this altered fruit size on tertiary branches. However, neither treatment had any effect on fruit size (Figure 2.6 C). We therefore conclude that in Arabidopsis, there is no detectable correlative inhibition of fruit by any organ type.

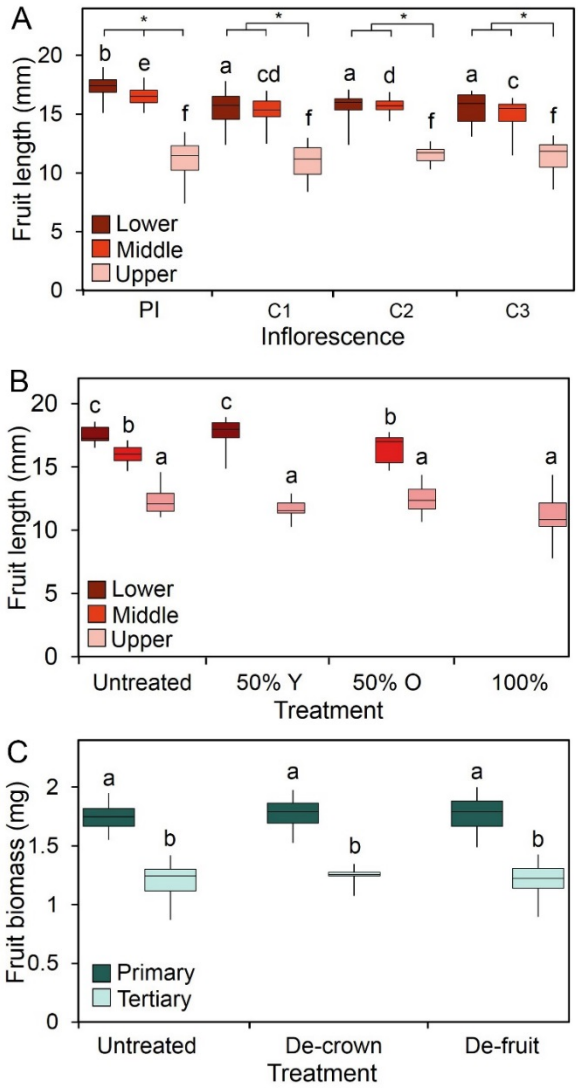

Figure 2.6. Fruit growth does not show correlative inhibition in Arabidopsis

(A) Box plot showing fruit lengths at different positions along inflorescences in Col-0 Arabidopsis. At the end of flowering in untreated plants, fruits were collected from different positions along the primary inflorescence (PI), and the uppermost 3 cauline inflorescences (C1 – C3, uppermost to lowest). On each inflorescence, 3 fruits were collected and measured with digital callipers from the lower (dark red), middle (red) or uppermost (light red) part of the inflorescence. These values were then averaged for each section, for each plant. Bars with the same letter are not statistically different to each other; lower, middle and upper sections were compared separately across inflorescences (ANOVA+Tukey HSD, n=9-12). Asterisks indicated significant differences between sections of the same inflorescence; each inflorescence was compared separately (ANOVA+Tukey HSD, n=9-12; lower F=21.318, df=3; middle F=16.473, df=3; upper F=1.262, df=3). **(B)** Box plot showing fruit lengths at different positions along the inflorescence in Col-0 Arabidopsis. When there were approximately 45 fruits on the primary inflorescence (PI), 50% of the youngest/upper fruit were removed from the PI (50% Y), 50% of the oldest/lowest fruits were removed (50% O), or all fruits present were

removed (100%). Plants were allowed to finish flowering, then 3 fruits were collected and measured with digital callipers from the lower (dark red), middle (red) or uppermost (light red) part of the PI. Values shown are the mean individual fruit length. Bars with the same letter are not statistically different to each other; the different sections of the inflorescence were compared separately (Upper: ANOVA+Tukey HSD, F=2.855, df=3; Middle and Lower, t-test; n=10-11). **(C)** Box plot showing fruit biomass in Col-0 Arabidopsis on primary and tertiary inflorescences. Secondary inflorescences were either 'de-crowned', by having only the flowering part of the inflorescence removed, or had open flowers continually removed (de-fruit). Both treatments were initiated at anthesis of the secondary inflorescence. At the end of flowering, the mean individual fruit biomass for the primary (dark green) and tertiary (light green) inflorescences was calculated. Box represents interquartile range, and midline indicates the median. Whiskers indicate maximum and minimum. Bars with the same letter are not statistically different to each other, inflorescence classes were compared separately (ANOVA+Tukey HSD, n=8-12; primary F=0.176, df=2; tertiary F=0.298, df=2).

2.4.7 Older fruit cause the abortion of younger fruit in *Brassica napus*

Brassica napus has previously been suggested to show carpic dominance (Bangerth, 1989), since fruit development is typically inhibited toward the end of inflorescences lifetimes, such that the final period of flowering in oilseed rape may not produce any fertile fruit (Tayo & Morgan, 1975). We characterised the extent and occurrence of this phenotype in our growth conditions, in plants grown in 2000ml of soil. Under these conditions, we observed that the fruit-set is generally highly successful early on in development, but begins to decline after (on average) 72% of flowers have opened. There is a short 'wobble zone' with a mixture of fertile and aborted fruit, and then the final 20% (on average) of flowers generally produce no fruit (Figure 2.7 A). The same pattern is seen on the secondary inflorescences, but the 'zone of success' is always proportionally shorter than on the primary inflorescence - and in late activating secondary inflorescences, as few as 40% of flowers may result in a fertile fruit (Figure 2.7 A) (see also Appendix 2.3.2). This pattern of development is thus highly consistent with carpic dominance effects, but as we saw in Arabidopsis, does not necessarily arise by correlative inhibition.

We therefore tested whether older fruit do indeed inhibit the formation of fruit in the later flowers on the inflorescence, by removing either the first 10, or first 20 flowers produced along the primary inflorescences of oilseed rape plants grown in 100ml of soil. Plants grown in this soil volume typically only produce a single inflorescence, removing any confounding effects of other inflorescences in this experiment. Under these conditions, 46% of the flowers in untreated plants did not lead to production of a fertile fruit (Figure 2.7 B). However, when the first 10 or 20 flowers are removed, was a strong reduction in the 'failure' of subsequent flowers to produce a fertile fruit (Figure 2.7 B). Thus, although there is no evidence for carpic dominance in Arabidopsis, this phenomenon does seem to occur in *Brassica napus* (see also Appendix 2.3.3).

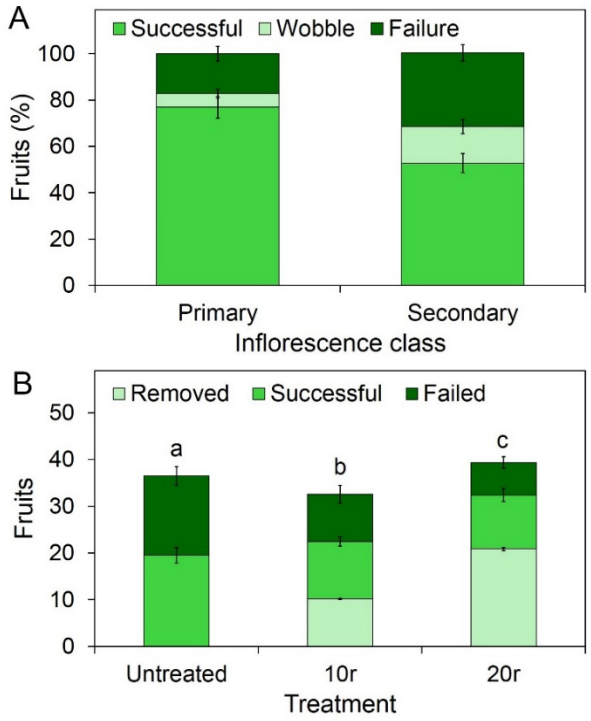

Figure 2.7. Carpic dominance effects in *B. napus*

(A) Graph showing the percentage of fruit 'zones' along inflorescences of different classes in untreated *B napus*. Plants were grown in 2000ml pots in the glasshouse under supplemental light conditions. At the end of flowering, each fruit on each inflorescence was assessed as 'successful' (fruit containing seeds) or 'failed' (a produced flower which resulted in no seeds). Percentage 'zones' of success were then determined – the successful (green) zone encompassed the lowest fruit, to the highest successful fruit, where no failed fruits were present. The 'wobble' zone encompassed the zone in which both successful and failed fruits were present. The failure zone encompassed the uppermost portion of the inflorescence where no successful fruits were present. Bars indicate s.e.m. n=6. **(B)** Graph showing number and success of fruit in *B. napus* under different treatments. Plants were grown in 100ml pots in the glasshouse under supplemented light conditions. Plants were either left untreated, or had the first 10 or 20 open flowers on the primary inflorescence (PI) removed before pollination (10r and 20r respectively). All plants were then allowed to finish flowering, at which point the fruits on the PI were counted and assessed. Fruits were scored as either removed (light green), successful (a fully-formed fruit containing seeds) (green) or failed (any flower produced which did not produce seed) (dark green). Bars represent s.e.m. Bars with the same letter indicate plants where the number of failed fruits was not significantly different (ANOVA + Tukey HSD, n=7-9; F=18.518, df=2).

2.5 Discussion

2.5.1 The control of inflorescence number and development

In this study, we set out to understand the mechanisms that shape the spatio-temporal organization of reproductive organs in Arabidopsis and *Brassica napus*. The earliest visible events during the reproductive development of both species are the activation of secondary inflorescences, which occurs immediately after floral transition. Once active, the number of secondary inflorescences remains relatively constant in both species during reproductive development (Figures 2.1 G, 2.3 B), and broadly predicts the overall scale of the reproductive effort (Figures 2.1 F,H,I). Our results indicate that secondary inflorescence number is very tightly controlled, and that we can perhaps speak of plants having a 'target inflorescence number'. When the system is pushed away from this number, the plant responds by initiating new secondary inflorescences until the original target is reached again (Figure 2.3 A). This shows that inflorescence number is controlled by the concerted dominance exerted by the secondary inflorescences over other secondary axillary meristems. Our results show that this 'infloretic dominance' is a property of the whole secondary inflorescence system; the inflorescence meristem, fruit and subtending tertiary branches (Figure 2.4 A,B). Removal of the fruit or meristem does not remove the dominance of the secondary inflorescence as a whole, but rather allows the activation of more tertiary branches, which maintain the overall dominance of the secondary inflorescence system. Our results thus show that higher order branches are regulated by both the inflorescence meristems and fruits. As fruit numbers increase, and the inflorescence meristem gradually shuts down, there is seamless 'exchangeable' dominance that continues to inhibit higher order branches. Our results stress the importance of fruit in the control of further inflorescence formation; reproductive success therefore tends to limit further flowering, while reproductive failure promotes its continuation. The importance of dead-heading and/or prompt fruit-picking to maintain flowering illustrates that fruit also play a key role in preventing the activation of new inflorescences in many other species beyond the Brassicaceae. Indeed, heavy fruiting

is even able to inhibit the formation of inflorescences for the next year's flowering, generating the biennial bearing habit seen in many fruit trees (Krasniqi et al, 2017).

2.5.2 The control of fruit number and development

In many species, fruit have been demonstrated to exert carpic dominance over the growth of other fruit (Bangerth et al, 1989). Our results clearly demonstrate that fruit exert dominance over inflorescences in Arabidopsis, but show that fruit exert no dominance over other fruit. This situation seems somewhat paradoxical, especially since *B. napus* seems to display carpic dominance, as do members of the Brassicaceae genus *Aethionema*, which have dimorphic fruits (Lenser et al, 2018). However, it is worth noting that in Arabidopsis, fruit do exert dominance over the continued opening of flowers on the same inflorescence (i.e. in *cis*) (Ware et al, 2020). Could it be the case that in Arabidopsis, carpic dominance effects are actually so strong that they act at a much earlier stage of development, and inhibit flowers from ever opening, rather than inhibiting the fruit set of opened flowers? From a different perspective, we might also question why there is this discrepancy in reproductive strategy between Arabidopsis and *B. napus*. Why does *B. napus* - and many other species besides - abort or otherwise inhibit the growth of viable fruit? One possible explanation is the pollination strategy of different organisms. Arabidopsis is highly self-fertile, to the point where it pollinates the majority of its own flowers before they open. For Arabidopsis, production of a flower essentially guarantees production of a fruit, and fruit number can be controlled as function of flower number. However, for insect-pollinated *B. napus*, opening a flower does not necessarily guarantee a fruit will be produced, and the plant may need to 'over-flower' to produce the required fruit-set. In turn, this requires the plant to have a carpic dominance mechanism to prevent excess fruit-set if pollination is more successful. The need for such a system may be particularly strong in spring-blooming fruit trees such as apple, where the inflorescences are all formed the previous autumn. Because pollinator availability in spring is unknowable, the plant must produce many more flowers than

needed to ensure a minimum fruit-set. In the event of good pollinator availability, excess fruit are removed in the remarkable ‘June drop’ (Abruzzese et al, 1995).

2.5.3 An integrated model for control of reproductive architecture in Brassicaceae

Taken together, our results suggest that there is an integrated dominance mechanism that acts throughout reproductive development in Arabidopsis and other Brassicaceae, to coordinate the growth of reproductive organs in space and time. The source and target of this central dominance mechanism may change during development, but the transitions between seem relatively ‘seamless’. We can nevertheless identify different dominance interactions that occur at different stages in reproductive development (Figure 2.8). Within this system, resources and resource-related signals such as substrate volume seem to be the main determinant of how many organs can form in total. The dominance mechanisms then determine how this growth potential is divided among different classes of organs, to determine which organs grow. Each secondary branching system shares a proportion of the overall growth potential, and this is distributed (and homeostatically re-distributed) within the branching system. Higher-order inflorescences have an inherently lower growth potential than secondary inflorescences, and only grow if there is ‘spare’ growth potential - if resource availability is high, or if the secondary ‘crown’ is damaged. In *B. napus*, the lower growth potential of higher order branches is also reflected in the much lower proportion of flowers that set a fruit, showing that the hierarchical position of an inflorescence affects more than just its growth. This integrated dominance mechanism generates a flexible, homeostatic system, allowing more organs to be produced either locally or globally, depending on changes in environmental conditions, and depending on the earlier reproductive success of the plant.

Here, we have not attempted to elucidate the molecular regulation underpinning the dominance network. However, it is very likely that a combination of hormonal signals

- and in particular, auxin, cytokinins and strigolactones - form the core of this system. An extensive body of work has identified these hormones as critical regulators of the apical dominance that occurs in vegetative shoots, in which actively growing apices repress the activation of new shoot branches (Domagalska & Leyser, 2011). Auxin exported by dominant shoot apices seems to act by occupying the auxin sink strength of the stem, which prevents dominated apices from forming a canalized auxin transport link to the stem, and from exporting their own auxin (Prusinkiewicz et al, 2009; Shinohara et al, 2013; Bennett et al, 2016; van Rongen et al, 2019). Meanwhile, cytokinins and strigolactones respectively promote and repress the activation of new branches by increasing or decreasing the abundance of PIN auxin transporters in the stem, thereby altering auxin sink strength (Shinohara et al, 2013; Waldie & Leyser, 2018) and by priming or de-priming apices for growth (Dun et al, 2012). There is reasonable evidence that the dominance mechanism(s) active during reproductive development operate on the same principles, or are indeed the same mechanism. For instance, the *cis*-effect of fruit on inflorescence activity in Arabidopsis is driven by auxin export from fertile fruit (Ware et al, 2020), and the biennial bearing effect of citrus and olive fruits is mediated by increased auxin transport from the fruits (Haim et al, 2020). Meanwhile, in *Aethionema arabicum*, cytokinin treatment increases the proportion of large ‘dominant’ fruit relative to the small ‘dominated’ fruit (Lenser et al, 2018). We thus believe that, as indeed previously proposed by Bangerth (1989), reproductive organs must export auxin in order to grow, and can be inhibited from doing so by the auxin export from actively growing organs - whether of the same type, or different. This model requires further investigation, but provides a preliminary framework for the control of reproductive architecture in Brassicaceae.

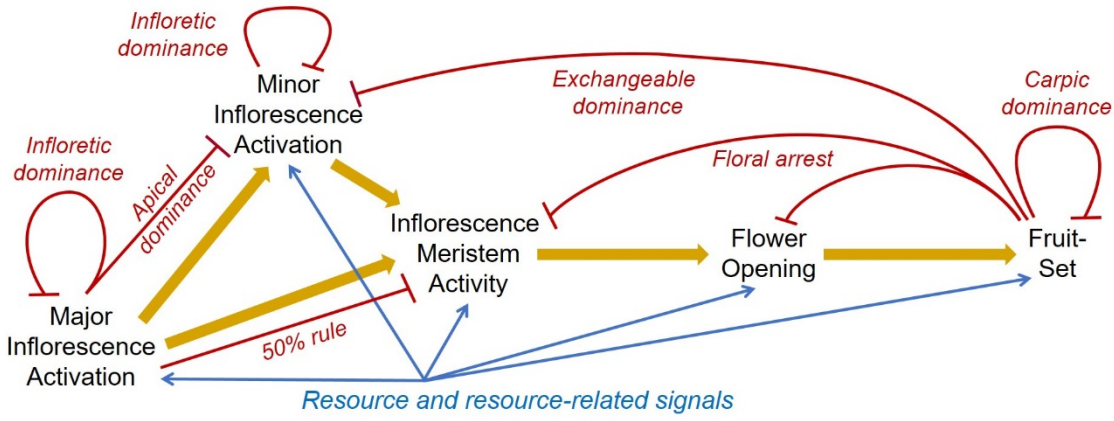

Figure 2.8. A model for spatio-temporal control of reproductive architecture

Diagram showing developmental processes in the elaboration of reproductive architecture in the Brassicaceae, and their interrelationship (gold arrows). Negative feedbacks identified in this or other studies are indicated with red arrows (50% rule: Walker & Bennett, 2019; Floral arrest: Ware et al, 2020). Positive feedback from resource or resource-related signals are shown in blue.

2.5.4 Early, resource-related developmental decisions shape reproductive architecture

For a sustainable future, crop yields must be increased without using additional land for agriculture, and indeed with reduced inputs of fertiliser, agrochemicals and oil-driven machinery. In other words, there is a pressing need to 'do more with less'. There is certainly scope to do this, given that the yields of most crop plants are generally well below the yields that are theoretically achievable given the water, sunlight and mineral nutrients available to them (Foulkes et al, 2009; Schills et al, 2018; Mitchell & Sheehy, 2018). We therefore need to understand the constraints that prevent plants from achieving such yields. Our results suggest that the scale of reproductive development is largely established very early on during the reproductive process, probably reflecting environmental conditions and developmental events during the vegetative phase. While both species can flexibly respond to environmental conditions post-flowering by making more or fewer higher order inflorescences, these are rather unproductive in *B. napus* (Figure 2.7 A), and produce smaller fruit in Arabidopsis (Figure 2.6 A), and do not

dramatically increase the overall reproductive effort. It is also notable that, at least in the case of nutrients, post-flowering increases in availability had very little effect on any aspect of reproductive development in our experiments (Figure 2.2). Our data suggest that – from a structural perspective at least – it is critical to increase the production of major inflorescences (e.g. ears in wheat, secondary inflorescences in *B. napus*), at the very start of flowering to achieve dramatic increases in yield potential of crops. However, how can this be successfully achieved in practice? Our results, along with those of others, show that simply increasing the quantity of secondary inflorescences will not necessarily increase yield, due to the homeostatic feedback in the system (Walker & Bennett, 2019).

Our data suggest that one way to achieve this increase may be to alter the way that plants respond to resource- and resource-related signals, which strongly determine the overall size of the reproductive system. In particular, we show that the substrate volume in which plants are growing strongly limits the scale of their reproductive effort, independently of the mineral nutrients available in the substrate (Figure 2.2, Supplementary Figure 2.2 A), consistent with our previous work in wheat (Wheeldon et al, 2020). Although substrate volume may seem like an abstract concept for field-grown plants, our results suggest that substrate volume and neighbour density are at least partly interchangeable, and that small pots effectively mimic high neighbour density (Wheeldon et al, 2020). Furthermore, substrate volume effects could arise under field conditions from shallow soil or compacted soil layers. Our results suggest plants may be inherently ‘cautious’ about reproductive development when substrate volume/neighbour density indicates there may be future resource limitations, and do not maximise their reproductive potential relative to the actual abundance of resources. Indeed, as we have previously discussed, this non-maximization of reproduction is a very sound strategy for wild plants (Walker & Bennett, 2018), but is maladaptive in crops where human intervention guarantees future resource availability. Thus, by changing the way plants

respond to resource-related signals, there seems to be scope to increase the scale of the reproductive effort, and ultimately crop yield potential.

2.6 Materials & methods

2.6.1 Plant growth conditions and materials

Arabidopsis plants for the experiment described in all figures were grown on a Levington's F2 or Petersfield No. 2 compost, or in a 1:1 sand/vermiculite mix under a standard 16 h/8 h light/dark cycle (20°C/16°C), primarily in controlled environment rooms with light provided by white fluorescent tubes at intensities of ~120µmol/m^2s^{-1}, unless otherwise specified. Oilseed rape plants were grown on Petersfield No. 2 compost in greenhouses with supplemental sodium lighting at an average intensity of ~250µmol/m^2s^{-1}. The lines used in this study were wild-type Col-0 (Arabidopsis), and spring oilseed rape variety Heros (*B. napus*)

We used Arabidopsis Thaliana Salts (ATS)(Wilson et al, 1990) as a standard modular fertiliser, and we varied the nitrate concentration by replacing nitrate ions with chloride. Standard N fertiliser was 0.015M nitrate, low N fertiliser was 0.0015M nitrate. Plants grown on sand/vermiculite received 5ml of ATS + 5ml water once per week in place of watering. Plants grown on compost received 5ml of standard ATS + 5ml of water (Arabidopsis) or 10ml of standard ATS (*B. napus*) every week in place of watering.

2.6.2 Sampling of field grown plants

For Figures 2.1B,D,F, *B. napus* oilseed rape plants (various varieties) grown at a variety of sites in the UK were hand-harvested at the end of their life, and measured in lab conditions. For Figures 2.1G-I, 16 plants in commercial cultivation at the University of Leeds farm were randomly selected in March and marked with tape, and a GPS location. We returned to measure these same plants *in situ* in April, May, June and July. The mature plants were hand-harvested in July and returned to the lab for final measurements. Fruit were collected and dried, and their biomass measured. Seed were subsequently harvested from the fruit and their biomass was measured separately.

2.6.3 Inflorescence nomenclature

Inflorescences are referred to typically through their positions and orders. The primary inflorescence (PI) is the main inflorescence growing first, directly from the centre of the rosette. The inflorescences which arise from the cauline leaves on the PI are referred to as secondary inflorescences, or cauline inflorescences. Inflorescences arising directly from the rosette leaves (but which are not the PI) are also classed as secondary inflorescences, and are referred to as rosette inflorescences. Any inflorescence which grows from a secondary inflorescence, regardless of whether it is a cauline or rosette, is referred to as a tertiary. Correspondingly, tertiaries give rise to quaternary inflorescences, which in some cases also produce quinternary inflorescences (Supplementary Figure 2.4).

The inflorescence initiation in Arabidopsis is basipetal (from top to bottom), with the oldest inflorescences being the caulines, with the rosettes initiating thereafter. As inflorescences grow upwards, the youngest part of the inflorescence is the top, with the oldest being the bottom.

The nomenclature used here also applies to *B. napus*. The overall growth of the two species is highly similar, only differing in that *B. napus* produces no rosette inflorescences; the descriptions are otherwise the same between both. To allow for greater clarity when making comparisons, we also refer to ‘fruits’ throughout the manuscript; these are commonly referred to as siliques in Arabidopsis and pods in *B. napus*, however they both fit the broader classification of fruit.

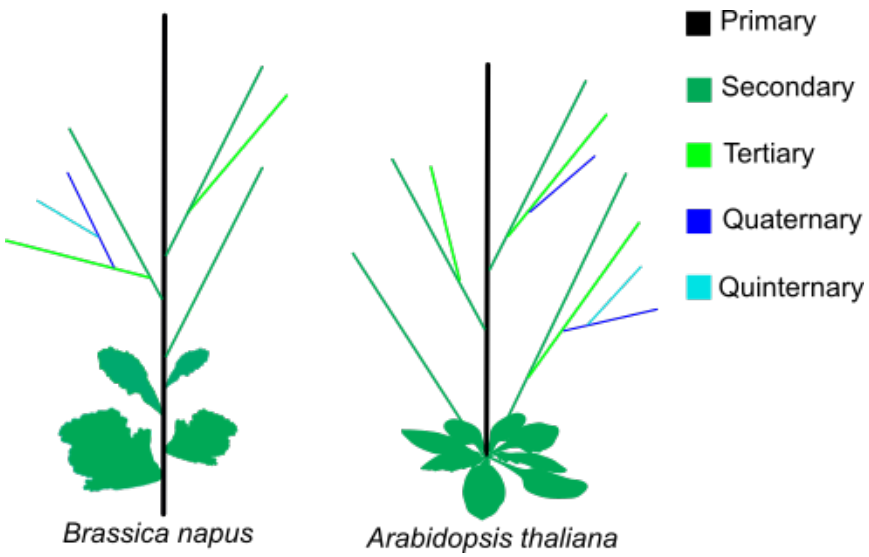

Supplementary Figure 2.4. Inflorescence nomenclature in Arabidopsis and *B. napus*

Diagram indicating the inflorescence nomenclature for Arabidopsis and *B. napus*. The primary inflorescence (black) supports the leaves (*B. napus*) or arises from the vegetative rosette (Arabidopsis). Secondary inflorescences (dark green) arise from the primary inflorescence (both species), or the rosette leaves (Arabidopsis only). Tertiary inflorescences (light green) arise from secondaries, followed by quaternaries (dark blue) and quinternaries (light blue).

2.6.4 Experimental design

2.6.4.1 Soil volume experiments (Figures 2.2B-F, Supplementary Figure 2.2)

To determine the effects of soil volume on reproductive architecture in *B. napus*, plants were grown in compost in three pot sizes; 100, 500 and 2000mL. From 3 weeks old, supplemental fertiliser was provided to half of the plants of each pot size weekly, in the form of 10ml standard ATS, following regular watering. Standard and supplemental plants were kept in separate trays to ensure any run off could not be accessed accidently by a plant undergoing different treatment. Different pot sizes were similarly kept in different trays to eliminate any effects of shading by larger plants. Plants were grown until the end of flowering, and the ripening of the final seeds. At this point, all inflorescences were recorded and fruits were harvested from the plant, with fruit number per inflorescence recorded, and biomass measurements were taken of the whole fruit mass per plant. All fresh shoot biomass above the surface of the compost was harvested and biomass measurements taken separately.

To determine the effects of root restriction and nutrition in Arabidopsis (Supplemental Figure 2.2 A,B), plants were grown in compost in three pot sizes; 50, 100 and 500ml. Standard plants received no additional fertiliser, while supplemental plants received 5ml standard ATS + 5ml water weekly in place of watering from 1 week old. Plants were grown until the end of flowering, at which point all inflorescences were recorded. The shoot was cut immediately above the rosette leaves and dried in a drying oven. Biomass was recorded using an electronic balance.

To test the uppermost limits of Arabidopsis growth (Supplementary Figures 2.2 C,D), plants were grown as above, only in compost volumes of 100, 500, 1000 and 2000ml with no supplemental fertiliser. Measurements were collected as above.

To assess the effects of fertiliser restriction on Arabidopsis shoot biomass (Supplemental Figure 2.2 E), plants were grown on a 50:50 sand:vermiculite mix, with a small (approx. 0.5cm^3) compost plug to enable germination and establishment. Plants were grown in either 100 or 500ml pots, with 5ml fertiliser (low N or high N) + 5ml water

applied weekly in place of watering from one week after sowing. Plants were grown to the end of flowering, and shoot biomass was collected as described above.

2.6.4.2 Inflorescence and fruit manipulation experiments (Figures 2.3-2.7)

For Arabidopsis experiments where inflorescence manipulations were carried out, plants were grown in 50ml compost with 24 plants per tray. Treatments were randomised across all trays using a random number generator at the beginning of the experiment. Floral transition timings (bolting, the first day of visible buds within the rosette) were recorded for each plant to ensure treatment timings were carried out at the correct time (typically 15 days post bolting, specified in the text where different).

To determine the correct inflorescences were surgically removed, all inflorescences were counted at the time of treatment. Where exact inflorescence removal could not be carried out (e.g. when the treatment called for 50% removal of an odd number of inflorescences), the effects of architecture were considered. 50% inflorescence removal typically resulted in removing all the cauline or all the rosette inflorescences – when an odd number of inflorescences were encountered, removal was generally kept to either cauline or rosette where possible.

Inflorescence removal was carried out using scissors to remove the entire inflorescence and all subtending higher order branches, by removing the inflorescence approximately 1cm from its base. De-crowning treatments differed in that they involved only the removal of the flower-bearing section of the inflorescence, leaving any subtending inflorescences and buds intact. The inflorescence was removed with scissors approximately 5mm below the lowest fruit on that inflorescence. De-capitation treatments involved using forceps to remove the bud cluster and inflorescence meristem from a treated inflorescence. The bud cluster was removed above the uppermost open flower. De-fruit treatments involved using scissors or forceps to remove every fruit and open flower. For treatments where continual flower removal was carried out, this was carried out daily on all inflorescences present, unless specified otherwise.

2.6.4.3 Fruit measurements (Figures 2.6, 2.7)

Fruits in Arabidopsis and *B. napus* were measured in the same way. Ripe fruits were removed from the plant and length was measured from where the pedicel meets the fruit to the fruit tip, using digital callipers. For biomass measurements in Arabidopsis, three fruits were grouped together and weighed using an electronic balance, before a mean individual fruit mass was calculated.

For all fruit measurements, fruits were collected when ripe; in some instances (in Arabidopsis only) this meant collecting groups of fruits from the plant at different timings to ensure all growth had finished, but seeds were not lost. When total shoot biomass was collected, all biomass above the surface of the growth medium was harvested and biomass was added to the fruit mass.

Acknowledgements

TB is supported by BBSRC grant (BB/R00398X/1). CHW and CDW are supported by BBSRC White Rose PhD studentships (BB/M011151/1). We thank Tom Rodden and George Atherden for preliminary work and data. We also thank the ADAS Yield Enhancement Network (YEN) for allowing us access to oilseed rape samples for data collection.

References

Abruzzese, A., Mignani, I., and Cocucci, S.M. (1995). Nutritional status in apples and June drop. *Journal of the American Society for Horticultural Science*, **120**, 71–74.

Balanzà, V., Martínez-Fernández, I., Sato, S., Yanofsky, M.F., Kaufmann, K., Angenent, G.C. et al. (2018). Genetic control of meristem arrest and life span in *Arabidopsis* by a FRUITFULL-APETALA2 pathway. *Nature Communications*, **9**, 565.

Bangerth, F. (1989). Dominance amongst fruits/sinks and the search for a correlative signal. *Physiologia Plantarum*, **76**, 608-614.

Benlloch, R., Berbel, A., Ali, L., Gohari, G., Millán, T. and Madueño, F. (2015). Genetic control of inflorescence architecture in legumes. *Frontiers in Plant Science*, **6**, 543.

Bennett, T., Liang, Y., Seale, M., Ward, S., Müller, D. and Leyser, O. (2016). Strigolactone regulates shoot development through a core signalling pathway. *Biology Open*, **5**, 1806-1820.

Bohner, J. and Bangerth, F. (1988). Effects of fruit set sequence and defoliation on cell number, cell size and hormone levels of tomato fruits (*Lycopersicon esculentum* Mill.) within a truss. *Plant Growth Regulation*, **7**, 141-155.

Brewer, P.B., Yoneyama, K., Filardo, F., Meyers, E., Scaffidi, A., Frickey, T. et al. (2016). LATERAL BRANCHING OXIDOREDUCTASE acts in the final stages of strigolactone biosynthesis in *Arabidopsis*. *PNAS*, **113**, 6301-6306.

Chatfield, S.P., Stirnberg, P., Forde, B.G. and Leyser, O. (2000). The hormonal regulation of axillary bud growth in *Arabidopsis*. *Plant Journal*, **24**, 159-169.

Cline, M.G., Chatfield, S.P. and Leyser, O. (2001). NAA restores apical dominance in the *axr3-1* mutant of *Arabidopsis thaliana*. *Annals of Botany*, **87**, 61-65.

Domagalska, M.A. and Leyser, O. (2011). Signal integration in the control of shoot branching. *Nature Reviews Molecular Cell Biology*, **12**, 211–221.

Dun, E.A., de Saint Germain, A., Rameau, C. and Beveridge, C.A. (2012). Antagonistic action of strigolactone and cytokinin in bud outgrowth control. *Plant Physiology*, **158**, 487-498.

Fichtner, F., Barbier, F.F., Annunziata, M.G., Feil, R., Olas, J.J., Mueller-Roeber, B. et al. (2020). Regulation of shoot branching in *Arabidopsis* by trehalose 6-phosphate. *New Phytologist*, doi: 10.1111/nph.17006.

Foulkes, M.J., Reynolds, M., Sylvester-Bradley, R., Sadras, V.O. and Calderini, D. (2009). Genetic improvement of grain crops: yield potential. In *Crop Physiology Applications for Genetic Improvement and Agronomy*, 235-256. Elsevier, Netherlands.

Gaju, O., Reynolds, M.P., Sparkes, D.L. and Foulkes, M.J. (2009). Relationships between large-spike phenotype, grain number, and yield potential in spring wheat. *Crop Science,* **49**, 961-973.

González-Suárez, P., Walker, C.H. and Bennett, T. (2020). Bloom and bust: understanding the nature and regulation of the end of flowering. *Current Opinion in Plant Biology*, **57**, 24-30.

Guo, Z. and Schnurbusch, T. (2015). Variation of floret fertility in hexaploid wheat revealed by tiller removal. *Journal of Experimental Botany*, **66**, 5945-5958.

Hensel, L.L., Nelson, M.A., Richmond, T.A. and Bleecker, A.B. (1994). The fate of inflorescence meristems is controlled by developing fruits in *Arabidopsis*. *Plant Physiology*, **106**, 863-76.

Hyun, Y., Vincent, C., Tilmes, V., Bergonzi, S., Kiefer, C., Richter, R. et al. (2019). A regulatory circuit conferring varied flowering response to cold in annual and perennial plants. *Science*, **363**, 409-412.

Krasniqi, A.-L., Blanke, M.M., Kunz, A., Damerow, L., Lakso, A.N. and Meland, M. (2017). Alternate bearing in fruit tree crops: past, present and future. *Acta Horticulturae*, **1177**, 241-248.

Lazaro, A., Obeng-Hinneh, E. and Albani, M.C. (2018). Extended vernalization regulates inflorescence fate in *Arabis alpina* by stably silencing *PERPETUAL FLOWERING1*. *Plant Physiology*, **176**, 2819-2833.

Lenser, T., Tarkowská, D., Novák, O., Wilhelmsson, P.K.I., Bennett, T., Rensing, S.A. et al. (2018). When the BRANCHED network bears fruit: how carpic dominance causes fruit dimorphism in *Aethionema*. *The Plant Journal*, **94**, 352-371.

Lloyd, D.G. (1980). Sexual strategies in plants. I. An hypothesis of serial adjustment of maternal investment during one reproductive session. *New Phytologist*, **86**, 69-79.

Marcelis, L.F., Heuvelink, E., Hofman-Eijer, L.R., Bakker, J.D. and Xue, L.B. (2004). Flower and fruit abortion in sweet pepper in relation to source and sink strength. *Journal of Experimental Botany*, **55**, 2261-2268.

Mitchell, P. and Sheehy, J. (2018) Potential yield of wheat in the United Kingdom: How to reach 20 t/ha. *Field Crops Research*, **224**, 115-125.

O'Neill, C.M., Lu, X., Calderwood, A., Tudor, E.H., Robinson, P., Wells, R. et al. (2019). Vernalization and floral transition in autumn drive winter annual life history in oilseed rape. *Current Biology*, **29**, 4300-4306.e2.

Pajoro, A., Biewers, S., Dougali, E., Leal Valentim, F., Mendes, M.A., Porri, A. et al. (2014). The (r)evolution of gene regulatory networks controlling *Arabidopsis* plant reproduction: a two-decade history. *Journal of Experimental Botany*, **65**, 4731-4745.

Poorter, H., Bühler, J., van Dusschoten, D., Climent, J. and Postma, J.A. (2012). Pot size matters: a meta-analysis of the effects of rooting volume on plant growth. *Functional Plant Biology*, **39**, 839-850.

Pouteau, S. and Albertini, C. (2011). An assessment of morphogenetic fluctuation during reproductive phase change in Arabidopsis. *Annals of Botany*, **107**, 1017-1027.

Prusinkiewicz, P., Crawford, S., Smith, R.S., Ljung, K., Bennett, T., Ongaro, V. et al. (2009) Control of bud activation by an auxin transport switch. *PNAS*, **106**, 17431-17436.

Sakuma, S. and Schnurbusch, T. (2020). Of floral fortune: tinkering with the grain yield potential of cereal crops. *New Phytologist*, **225**, 1873-1882.

Samach, A. and Smith, H. (2013). Constraints to obtaining consistent annual yields in perennials II: Environment and fruit load affect induction of flowering. *Plant Science*, **207**, 168-176.

Schills, R., Olesen, J.E., Kersebaum, K.C., Rijk, B., Oberforster, M., Kalyada, V. et al (2018). Cereal yield gaps across Europe. *European Journal of Agronomy*, **101**, 109-120.

Schultz, E.A. and Haughn, G.W. (1991). LEAFY, a homeotic gene that regulates inflorescence development in *Arabidopsis*. *Plant Cell*, **3**, 771-781.

Shinohara, N., Taylor, C. and Leyser, O. (2013). Strigolactone can promote or inhibit shoot branching by triggering rapid depletion of the auxin efflux protein PIN1 from the plasma membrane. *PLoS Biology*, **11**, e1001474.

Shnaider, Y., Mitra, D., Miller, G., Baniel, A., Doniger, T., Kuhalskaya, A. (2018). Cucumber ovaries inhibited by dominant fruit express a dynamic developmental program, distinct from either senescence-determined or fruit-setting ovaries. *The Plant Journal*, **96**, 651-669.

Snow, R. (1931). Experiments on growth of inhibition. Part II.-New phenomena of inhibition. *Proceedings of the Royal Society B*, **108**, 305-316.

Snow, R. (1937). On the nature of correlative inhibition. *New Phytologist,* **36**, 283-300.

Tayo, T.O. and Morgan, D.G. (1975). Quantitative analysis of the growth, development and distribution of flowers and pods in oil seed rape (*Brassica napus* L.). *The Journal of Agricultural Science*, **85**, 103–110.

van Rongen, M., Bennett, T., Ticchiarelli, F. and Leyser, O. (2019). Connective auxin transport contributes to strigolactone-mediated shoot branching control independent of the transcription factor *BRC1*. *PLoS Genetics*, **15**, e1008023.

Vayssières, A., Mishra, P., Roggen, A., Neumann, U., Ljung, K. and Albani, M.C. (2020). Vernalization shapes shoot architecture and ensures the maintenance of dormant buds in the perennial *Arabis alpina*. *New Phytologist*, **227**, 99-115.

Waldie, T. and Leyser, O. (2018). Cytokinin targets auxin transport to promote shoot branching. *Plant Physiology*, **177**, 803-818.

Walker, C.H. and Bennett, T. (2018). Forbidden Fruit: dominance relationships in the control of shoot architecture. *Annual Plant Reviews Online*, doi:10.1002/9781119312994.apr0640

Walker, C.H. and Bennett, T. (2019). A distributive '50% rule' determines floral initiation rates in the Brassicaceae. *Nature Plants*, **5**, 940-943.

Wang, R., Farrona, S., Vincent, C., Joecker, A., Schoof, H., Turck, F. et al. (2009). *PEP1* regulates perennial flowering in *Arabis alpina*. *Nature*, **459**, 423-427.

Ware, A., Walker, C.H., Šimura, J., González-Suárez, P., Ljung, K., Bishopp, A. et al. (2020). Auxin export from proximal fruits drives arrest in temporally competent inflorescences. *Nature Plants*, **6**, 699-707

Wheeldon, C.D., Walker, C.H., Hamon-Josse, M. and Bennett, T. (2020). Wheat plants sense substrate volume and root density to proactively modulate shoot growth. *Plant Cell and Environment*, doi: 10.1111/pce.13984.

Wilson, A.K., Pickett, F.B., Turner, J.C. and Estelle, M. (1990). A dominant mutation in *Arabidopsis* confers resistance to auxin, ethylene and abscisic acid. *Molecular Genetics and Genomics*, **222**, 377-383.

Wubs, A.M., Heuvelink, E., Marcelis, L.F.M. and Hemerik, L. (2011). Quantifying abortion rates of reproductive organs and effects of contributing factors using time-to-event analysis. *Functional Plant Biology*, **38**, 431-440.

Wubs, A.M., Ma, Y., Heuvelink, E. and Marcelis, L.F. (2009). Genetic differences in fruit-set patterns are determined by differences in fruit sink strength and a source:sink threshold for fruit set. *Annals of Botany*, **104**, 957-964.

Wuest, S.E., Philipp, M.A., Guthörl, D., Schmid, B. and Grossniklaus, U. (2016). Seed production affects maternal growth and senescence in *Arabidopsis*. *Plant Physiology*, **171**, 392-404.

Zhang, Z., Deng, Y., Song, X. and Miao M. (2015). Trehalose-6-phosphate and SNF1-related protein kinase 1 are involved in the first-fruit inhibition of cucumber. *Journal of Plant Physiology*, **177**, 110– 120.

2.7 Appendix A

2.7.1 Carpic dominance is absent in Arabidopsis: expansion

In addition to the data presented in the article, more in-depth analysis was carried out into declining fruit length along the Arabidopsis inflorescence. Having identified that the youngest fruits are significantly smaller than the older fruit (Figure 2.6), I hypothesised that removal of fruit would result in an increase in length of the remaining fruits. To do this, I treated Arabidopsis plants with 4 secondary cauline inflorescences (hereafter 'caulines'), carrying out a randomly-assigned treatment on each of the caulines. Caulines were either untreated, had every alternate fruit removed (1/2), two of every three alternate fruits removed (2/3), or four of every five alternate fruits removed (3/4). Fruits were removed continually throughout the inflorescence lifetime, and fruit number and length were assessed once all fruits had reached their full final length.

The most extreme 2/3 and 4/5 treatments increased floral duration (discussed separately in Chapter 4, Figure 4.5 A), however this extension was not sufficient to replace the fruits which were removed (Figure. 2.ii A; shown in Chapter 4, Figure 4.5 B, but reproduced here for clarity). The fruit lengths were not statistically different to the untreated, with all treatments having a mean fruit length of approximately 12mm (Figure 2.ii B). The decline in fruit size along the inflorescence was comparable between each of the treatments, with the same distribution of fruit size visible in the collected fruits (Figure 2.ii C-F).

These data therefore clarify the absence of carpic dominance in Arabidopsis. Fruit removal has no effect on the immediate neighbouring fruits, and similarly does not result in a reduction in the heteroblastic decrease seen in fruit size.

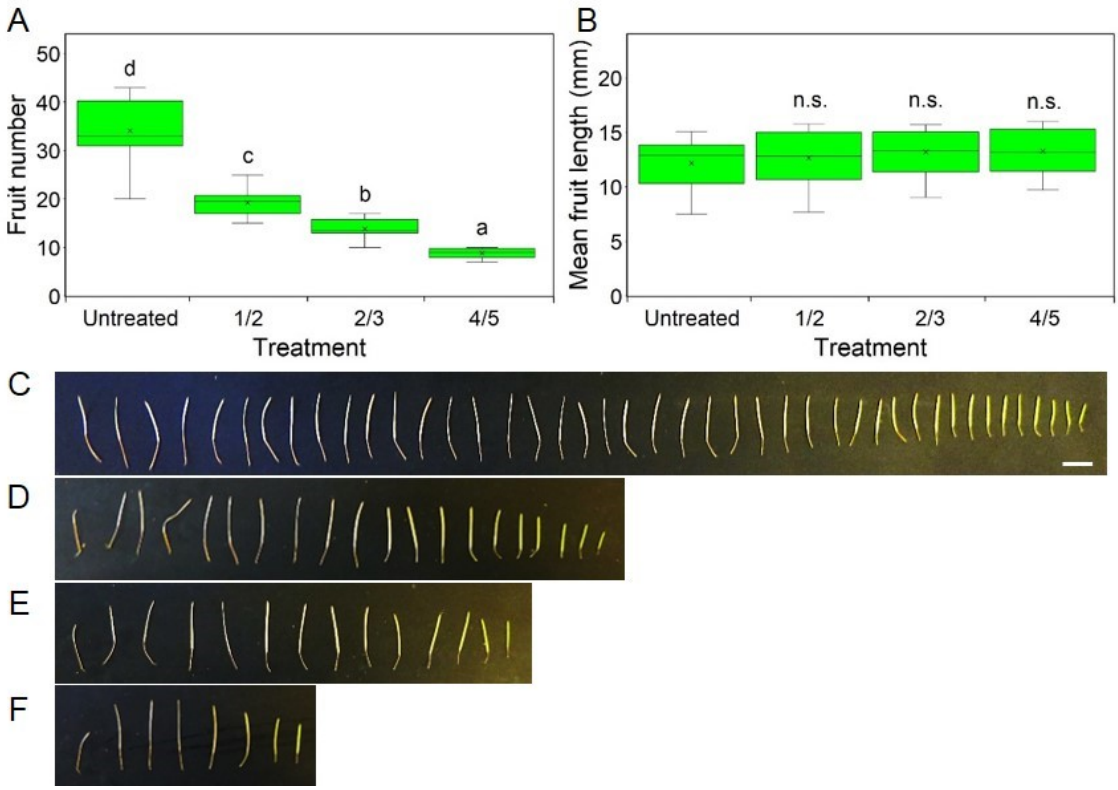

Figure 2.ii. Fruits do not compensate for local within-inflorescence fruit removal.

Box plots showing effects of within-inflorescence fruit removal on the development of remaining fruit. Treatments were carried out to the secondary cauline inflorescences of Col-0 plants. Inflorescences were untreated, had alternate (1/2), two in three (2/3) or four in five (4/5) flowers removed. Flowers were removed as they opened. Ripe fruits from the length of the inflorescence were collected and measured. **(A)** Number of developed fruit present on each inflorescence. Boxes with the same letter are not statistically different to each other (ANOVA + Tukey's HSD, $p<0.001$, $n=12$). **(B)** Mean fruit length of all fruit present on the inflorescence. n.s. = not significantly different to untreated (ANOVA + Dunnett 2-sided, $p=0.257$, $n=12$). Box indicates the interquartile range, central line is the median, central cross is the mean. Whiskers indicate maximum and minimum values, points identify outliers. **(C-F)** Representative images of all collected fruits from individual inflorescences, as described above. Images are to scale, scale bar = 1cm. **(C)** Untreated. **(D)** 1/2. **(E)** 2/3. **(F)** 4/5.

2.7.2 Older fruit cause the abortion of younger fruit in *Brassica napus*: expansion

The data presented in Figure 2.7 A shows the proportion of fruits making up the 'successful', 'wobble' and 'failure' zones in *B. napus*. This provides a good understanding of how the zones relate to each other and allows for statistical analysis between different treatments (e.g. Figure 2.7 B). Figure 2.iii shows a more visual representation of the wobble and abscission zones, providing more clarity.

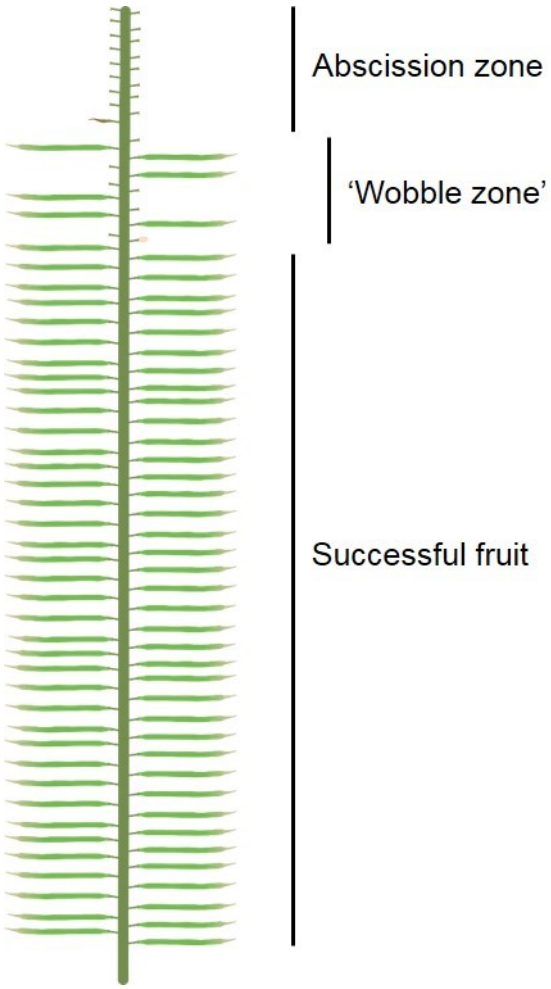

Figure 2.iii. Fruit variability in oilseed rape.

Cartoon representation of fruit success in a single representative OSR plant grown in 0.5L compost in glasshouse conditions. The first 76 fruit on the inflorescence develop successfully and produce seed (successful fruit). After this occurs a 'wobble zone', where successful fruit alternate with abscised fruit and failed flowers. The final portion of the inflorescence contains only abscised fruits (abscission zone). Not to scale.

2.7.3 Carpic dominance in *Brassica napus*

Data presented in Figure 2.7 B show the presence of carpic dominance effects in *B. napus*, however did not capture the effects observed at the seed level. Removal of the oldest 10 or 20 fruits from the inflorescence resulted in the production of more successful younger fruit than in the untreated. Similarly, these fruits typically produced a greater number of seeds than the youngest fruits in untreated plants (Figure 2.iv A).

Mirroring the pattern of fruit numbers in the 10r and 20r treatments (Figure 2.7 B), the total number of seeds produced by individual plants was significantly higher in the untreated when compared to either of the treatments, with no difference between the treatments themselves (Figure 2.iv B). Again, the compensatory response of additional fruit production in the 20r treatment resulted in the production of more seeds than would have been expected in the absence of carpic dominance.

It was hypothesised that the fruit removal treatments would increase the number of seeds per fruit. The mean number of seeds per fruit was calculated, and did not confirm this hypothesis. Instead, all three treatments produced a similar number of seeds per fruit (Figure 2.iv C). Seed biomass was next calculated for both the total plant and individual fruits. Total seed biomass for the whole plant did not significantly differ between treatments, despite untreated plants producing a slightly higher seed biomass than either the 10r or 20r treatments (0.65g, 0.48g and 0.42g respectively) (Figure 2.iv D). Interestingly, the calculated thousand seed weight (TSW) across the treatments was not statistically different, but was slightly higher in the 10r and 20r treatments (41.8g and 40.7g respectively), compared to the untreated (35.8g) (Figure 2.iv E).

When mean seed biomass per fruit was calculated, there was no significant difference between the treatments (Figure 2.iv F). When calculating TWS by fruit, the increase in 20r (5.0g) from untreated (2.1g) was approaching significance (ANOVA + Dunnett >control, P=0.052, n=6) (Figure 2.iv G). This strongly supports the presence of carpic dominance in *B. napus*, with individual seed biomass increasing in response to loss of fruit on the same inflorescence.

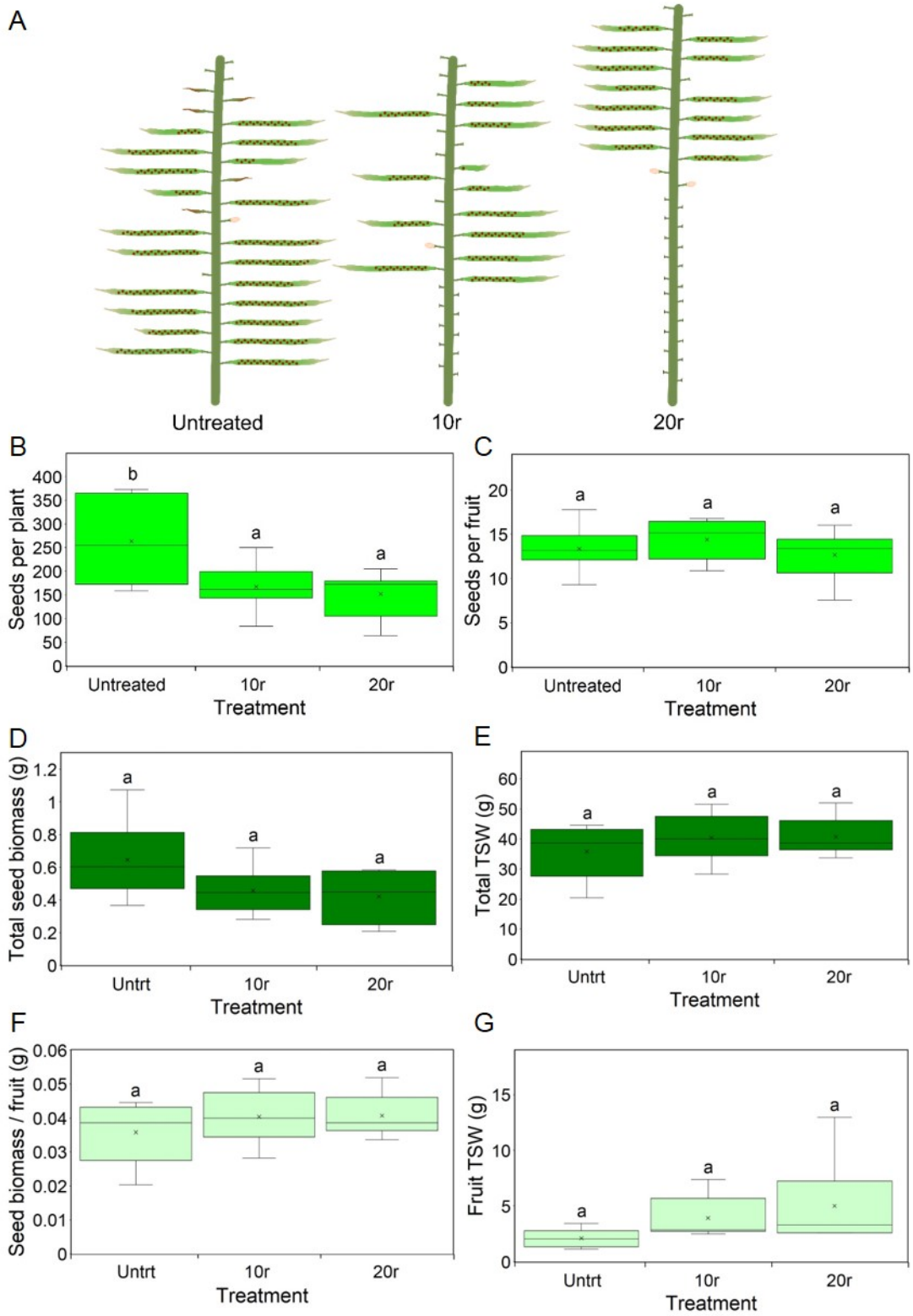

Figure 2.iv. Carpic dominance effects are present in OSR.

Carpic dominance effects in oilseed rape (OSR) following the removal of the oldest 10 (10r) or 20 (20r) flowers prior to flower opening. Plants were grown in small pots (0.1L) to restrict inflorescence growth to primary inflorescences (PIs) only. **(A)** Diagram of the three treatments, untreated, 10r and 20r. Fruit length is relative and represents individual fruit number and length. Failed flowers and fruits are indicated, as are abscised fruits. Brown circles within the fruits indicate the number of seeds per fruit. **(B)** Total number of

seeds per plant following floral arrest. (ANOVA + Tukey's HSD, p=0.006, n=8). **(C)** Mean number of seeds per fruit. (ANOVA + Tukey's HSD, p=0.388, n=8). **(D)** Seed biomass for the whole plant. (ANOVA + Tukey's HSD, p=0.290, n=8). **(E)** Calculated thousand seed weight (TSW) for the whole plant. (ANOVA + Tukey's HSD, p=0.136, n=8). **(F)** Mean seed biomass per fruit. (ANOVA + Tukey's HSD, p=0.390, n=8). **(G)** Calculated mean TSW per fruit. (ANOVA + Tukey's HSD, p=0.513, n=8). Box indicates the interquartile range, central line is the median, central cross is the mean. Whiskers indicate maximum and minimum values, points identify outliers. Boxes with the same letter are not statistically different to each other.

Chapter 3

A distributive ‘50% rule’ determines floral initiation rates in the Brassicaceae

Originally published in *Nature Plants*, 2019

Volume **5**, Pages 940-943.

A distributive '50% rule' determines floral initiation rates in the Brassicaceae

Catriona H. Walker & Tom Bennett*.

School of Biology, Faculty of Biological Sciences, University of Leeds, Leeds, LS2 9JT

*E-mail address: t.a.bennett@leeds.ac.uk

The spatio-temporal production of flowers is key to determining reproductive fitness in most flowering plants, and yield in many crop species, but the mechanisms regulating this 'reproductive architecture' are poorly characterised. Here we show that in members of the Brassicaceae, total flower number is largely independent of inflorescence number, and the proportion of flowers initiated on the secondary inflorescences represents ~50% of total floral production, irrespective of secondary inflorescence number. This '50% rule' acts as a coordinating principle for reproductive development in Brassicaceae, and similar principles may operate in other species. Our findings suggest that inflorescences continue to compete with each other for a fixed pool of meristematic potential after their activation.

Reproduction in flowering plants consists of a number of hierarchical and sequential developmental phases. Plants must first initiate reproductive branches (inflorescences), and then produce flowers, which upon pollination will give rise to fruit and ultimately seed. To produce an optimal seed set, plants must carefully control the initiation of these organ types in space and time, such that sufficient but not excessive resources are committed to each stage. In the model plant *Arabidopsis thaliana* (Arabidopsis), the control of inflorescence number is relatively well understood, and exemplifies the classic 'apical dominance' paradigm for the regulation of shoot branching (Domagalska and Leyser, 2011). The number of inflorescences that Arabidopsis initiates is controlled by the environmental conditions in which the plant is growing; greater

resource availability (including light and mineral nutrients) allows for increased initiation of inflorescences (Walker and Bennett, 2018). The exact spatio-temporal pattern of inflorescence initiation reflects both developmental history, and the inhibitory 'dominance' effect that actively-growing inflorescences exert over the activation of new inflorescences (Walker and Bennett, 2018). However, the principles that govern the number and pattern of flower initiation in Arabidopsis are essentially unknown, and we sought to understand this process.

As a null model, we hypothesised that flower number in Arabidopsis is solely determined by inflorescence number. We examined wild-type Arabidopsis (Col-0) and assessed the number of inflorescences and flowers produced in 15 separate experiments. Comparison of experimental means showed a good correlation between the total inflorescences and total flowers (Figure 3.1 B), suggesting that a plant producing more inflorescences is capable of supporting a greater number of flowers. However, this relationship only accounted for around 54% of the variation observed (R^2 = 0.544), indicating that inflorescence number is not the sole factor regulating flower number. We also examined the relationship between the total flower number and the mean number of flowers per inflorescence (as a proxy for inflorescence meristem activity), and observed no relationship between the two variables (R^2 = 0.001) (Figure 3.1 C). Thus, plants do not regulate flower number solely by altering individual inflorescence meristem activity. These results suggested that total flower number must arise from a more complex combination of both inflorescence number and inflorescence meristem activity. In attempting to understand this, we found a very strong correlation between the number of flowers produced on the secondary inflorescences (see Figure 3.1 A for definition) and total flower number (R^2 = 0.930) (Figure 3.1 D). Plants typically produced ~50% of their total flowers on the secondary inflorescences, distributing the remaining 50% across the primary inflorescence and higher order inflorescences, regardless of total inflorescence number (Supplementary Figure 3.1, Supplementary Table 3.1). We found that this 50% distribution occurs not only in the Col-0 wild type, but also in both the L*er* and Ws-2

ecotypes (Figure 3.1 E). Furthermore, we found that the 50% distribution was also maintained in the high-branching mutant *branched1-2* (*brc1-2*), and various strigolactone, cytokinin and gibberellin mutants, despite the severe alterations in inflorescence architecture in most of these lines (Figure 3.1 E).

Species	Total flowers	Primary flowers	Secondary flowers	Tertiary flowers	Quaternary flowers
A. thaliana	647.6 ± 25.1	57.0 ± 0.9	314.1 ± 8.7	276.5 ± 22.2	0
B. napus	350.0 ± 21.0	106.2 ± 3.6	175.9 ± 11.2	67.9 ± 11.6	0
B. rapa	92.1 ± 7.4	20.4 ± 1.5	38.5 ± 3.0	33.3 ± 4.2	0
C. grandiflora	454.8 ± 98.4	89.0 ± 17.2	243.8 ± 45.2	119.1 ± 44.7	2.9 ± 1.8
C. rubella	225.1 ± 45.7	67.7 ± 5.0	95.9 ± 17.6	55.3 ± 25.8	6.2 ± 4.7
Cr. hirsuta	246.7 ± 38.3	21.7 ± 1.0	128.3 ± 18.9	89.7 ± 23.8	7.0 ± 1.7

Supplementary Table 3.1. Floral distribution in Brassicaceae spp.

Table showing floral numbers from 6 examined Brassicaceae species. Values displayed show the grouped total number of flowers for each inflorescence class (primary, secondary (cauline and rosette), tertiary and quaternary). No plants examined displayed any branching orders higher than quaternary. Values for each species are means ± s.e.m. from one experiment per species; *Arabidopsis thaliana* (n=8), *Brassica rapa* (n=31), *B. napus* (n=24), *Capsella grandiflora* (n=8), *C. rubella* (n=9) and *Cardamine hirsuta* (n=6).

To assess whether this 50% distribution is robust against physical as well genetic perturbations, we removed either the upper 50%, lower 50% or lower 75% of secondary inflorescences from Col-0 plants during flowering, and allowed the plants to recover. Treated plants initiated new secondary inflorescences, and despite the highly-disruptive perturbations, the secondary inflorescence flower number still tended towards 50% of the total in all treatments, and this proportion was not significantly different from untreated plants in either of the 50% removal treatments (Supplementary Table 3.2). This indicates that the mechanism is actively homeostatic during the lifetime of inflorescences, and can correct for perturbations, at least within a certain tolerance range.

Treatment	Total flowers	Primary flowers	Secondary flowers	Tertiary flowers	% Secondary flowers
Untreated	398.4 ± 19.0	49.0 ± 2.2	205.2 ± 11.3	144.2 ± 18.3	51.5
50% upper	339.7 ± 23.2	60.9 ± 2.5	167.6 ± 10.8	111.2 ± 14.4	49.3
50% lower	357.3 ± 43.1	60.6 ± 2.2	159.6 ± 20.6	137.2 ± 24.7	44.7
75% lower	319.9 ± 34.3	63.1 ± 3.2	121.0 ± 3.2	135.8 ± 21.2	37.8*

Supplementary Table 3.2. Effect of physical perturbation of floral distribution

Table showing mean numbers of flowers produced on each inflorescence class (primary, secondary, tertiary) under surgical treatments. Entire secondary inflorescences were removed from the plant ~13 days after flowering. Three treatments were performed alongside an untreated control (n=19): the upper 50% of secondary inflorescences were removed (50% upper) (n=9), or the lower 50% of secondary inflorescences (50% lower) (n=9), or the lower 75% of secondary inflorescences (75% lower) (n=8). Values displayed are the means of multiple plants ± s.e.m, (*) indicates treatments with a significantly lower percentage of flowers on secondary inflorescences than in the untreated control (95% confidence interval; F=4.622; d.f.=3; p=0.005), ANOVA+Tukey HSD.

Collectively, these data strongly suggested that total flower number is controlled independently of inflorescence number in Arabidopsis. To confirm this, we compared flower production in two high branching mutants, *brc1-2* and *dwarf14-1* (*d14-1*) relative to Col-0 wild-type. Despite both mutants producing significantly higher numbers of inflorescences than wild type (Figure 3.1 E), all three genotypes produced the same number of flowers (Figure 3.1 F). Taken together, these data suggest that total floral potential is determined independently of inflorescence number, and that each class of inflorescence shares a proportion of the total potential, with secondary inflorescences receiving around 50%. We therefore propose that floral initiation rates between Arabidopsis inflorescences self-organize; the secondary inflorescences continue to mutually inhibit each other following activation, and the more inflorescences there are, the more the activity of each inflorescence meristem is inhibited.

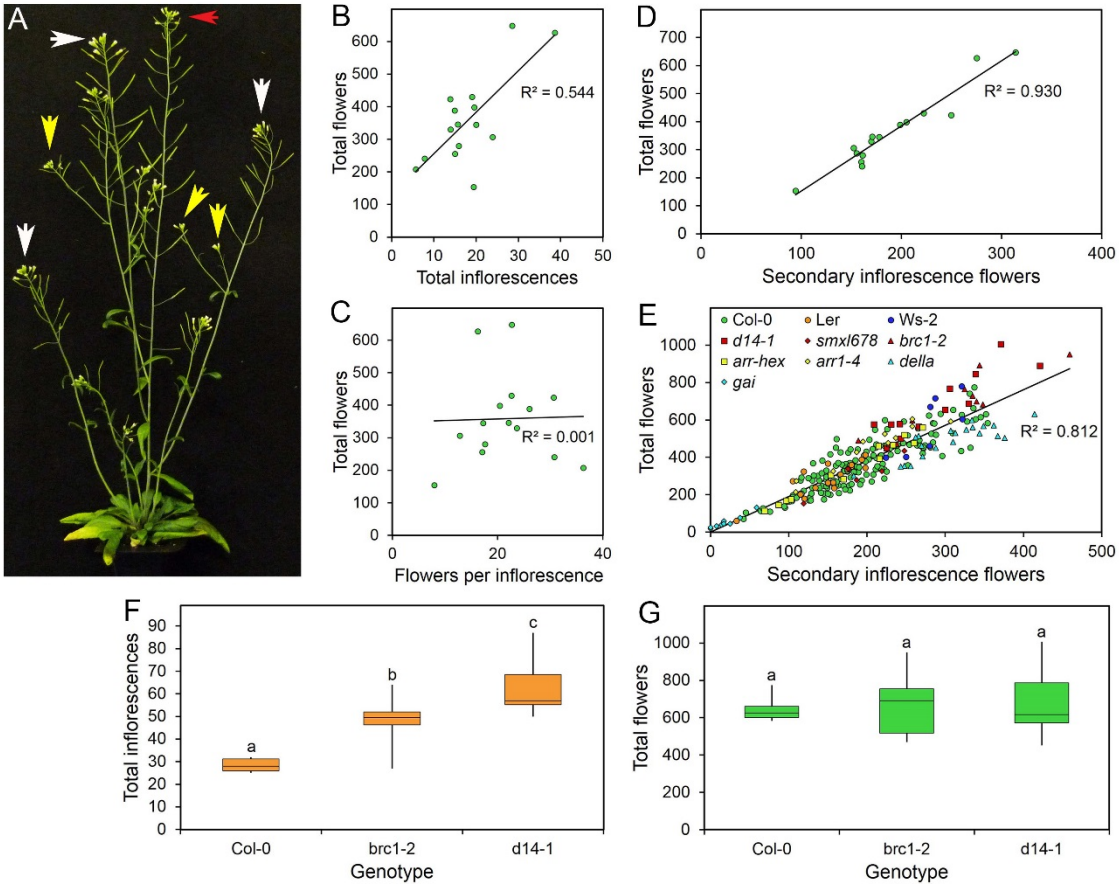

Figure 3.1. Flower number is regulated independently of inflorescence number in Arabidopsis.

(A) Reproductive architecture in Arabidopsis Col-0 WT. Arrows indicate different classes of inflorescences (red, primary inflorescence; white, secondary inflorescences; yellow, tertiary inflorescences). Secondary inflorescences include both cauline and rosette inflorescences. Following the end of flowering, each floral node (typically supporting a fruit/silique) was counted to give the number of flowers per individual inflorescence. **B-D**, Graphs showing the relationship in Arabidopsis Col-0 WT between mean total flowers and mean total inflorescences **(B)**, mean number of flowers per inflorescence **(C)** and mean number of flowers produced on the secondary inflorescences **(D)** n=15 independent experiments. Lines of best fit were calculated by the least squares approach. **(E)** Graph showing the relationship between total flower number and secondary inflorescence flower number in individual plants from 17 experiments, including Col-0 (n=161 independent samples), L*er* (n=18), Ws-2 (n=7), *d14-1* (n=12), *smxl678* (n=6), *brc1-2* (n=10), *arr-hex* (n=12), *arr1-4* (n=11), *della* (n=21) and *gai* (n=9). The line of best fit was calculated by the least squares approach across all data. **F,G**, Box plots showing total number of inflorescences **(F)** and flowers **(G)** produced by WT (Col-0) (n=8) and two branching mutants (*brc1-2* (n=10) and *d14-1* (n=12)) in a single experiment. The mid-line represents the median, the box the inter-quartile range and the whiskers the maximum and minimum values. Samples with the same letter are not

statistically different from each other (analysis of variance + Tukey's honest significant difference). Inflorescence number is significantly higher in *brc1-2* (p=0.000) and *d14-1* (p=0.000) than in WT (95% confidence interval; F=31.589; d.f.=2). Flower number is not statistically different in *brc1-2* (p=0.917) or *d14-1* (p=0.924) compared to WT (95% confidence interval; F=0.096; d.f.=2).

We questioned whether this '50% rule' was a quirk of Arabidopsis reproduction, or was more generalizable, and therefore examined a range of other Brassicaceae species. We examined *Brassica napus*, the rapid cycling ecotype *Brassica rapa*, *Cardamine hirsuta* (Cardamine), *Capsella grandiflora* and *Capsella rubella*. Like Arabidopsis, all these species produce a vegetative rosette, from which a branching system of indeterminate, racemic inflorescences then grows after the floral transition. Despite the qualitative similarities, there are strong quantitative differences in the inflorescence systems between these species, summarised in Supplementary Figure 3.1.

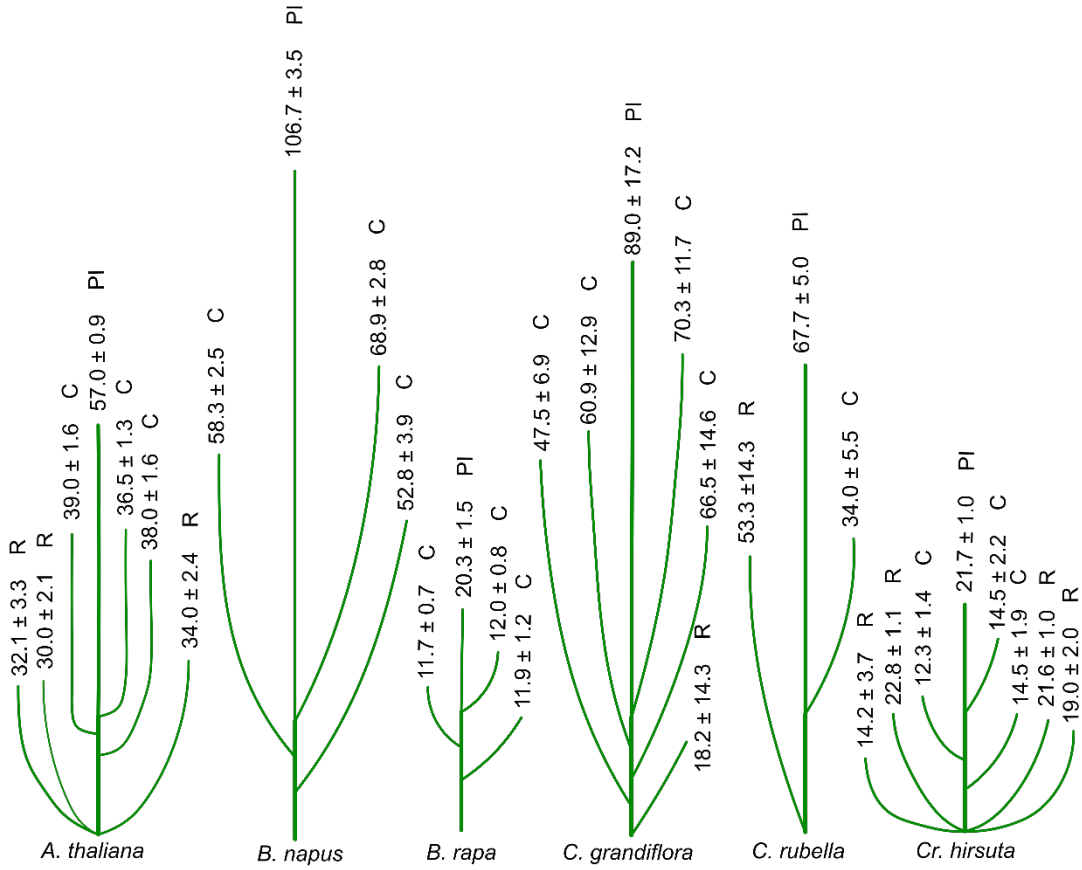

Supplementary Figure 3.1. Reproductive architecture in Brassicaceae spp.

Diagram illustrating a) the mean number and relative position (cauline/rosette) of secondary inflorescences produced in 6 different Brassicaceae species, and b) the mean number of flowers produced on those secondary inflorescences and the primary inflorescence (PI). Arabidopsis typically produces an equal number of cauline and rosette secondary inflorescences. *B. napus* and *B. rapa* only produce cauline inflorescences. Cardamine produces a lower number of flowers than the other species examined, however these are supported on a large number of rosette inflorescences which often produce almost as many flowers as the primary inflorescence, indicating the plant has multiple equally dominant axes. *C. rubella* typically produces similar numbers of cauline and rosette inflorescences, while *C. grandiflora* is obligately out-breeding and as such shows a high degree of variation in reproductive architecture between individual plants. It produces very few rosette inflorescences, and being self-incompatible, does not stop flowering unless manually cross-pollinated (which was not done in our experiments). The height of each inflorescence (from its junction with the PI) indicates the mean number of flowers per inflorescence for each species. PI height above the 2 uppermost cauline inflorescence indicates the mean number of flowers produced on the PI. Values at branch tips show the mean flower number per inflorescence ± s.e.m. Only PI and secondary inflorescence classes are shown; higher order inflorescences have been omitted for clarity, but are described in Supplementary Table 3.1. Letters above each

inflorescence indicate the inflorescence class; PI = primary inflorescence C = cauline secondary inflorescence, R = rosette secondary inflorescence. Values for each species are based on means from one experiment; *Arabidopsis thaliana* (n=8), *Brassica rapa* (n=31), *B. napus* (n=24) *Capsella grandiflora* (n=8), *C. rubella* (n=9) and *Cardamine hirsuta* (n=6).

We assessed the inflorescence and flower numbers of these species to determine if they follow the same floral distribution as seen in Arabidopsis. Total inflorescence number had no correlation with total flower number across the species (R^2 = 0.007) (Figure 3.2 A), and similarly, the number of flowers per inflorescence is not correlated with total flower number (R^2 = 0.273) (Figure 3.2 B). The lack of correlation between these parameters is unsurprising given the variation in reproductive architecture between the species. However, when we compared secondary inflorescence flower number and total flower number between these species, there was a clear correlation across species (R^2 = 0.948) with ~50% of flowers formed on the secondary inflorescences, irrespective of the underlying architecture (Figure 3.2 C). This cross-species trend is made even clearer when examining each plant individually (R^2 = 0.897) (Figure 3.2 D).

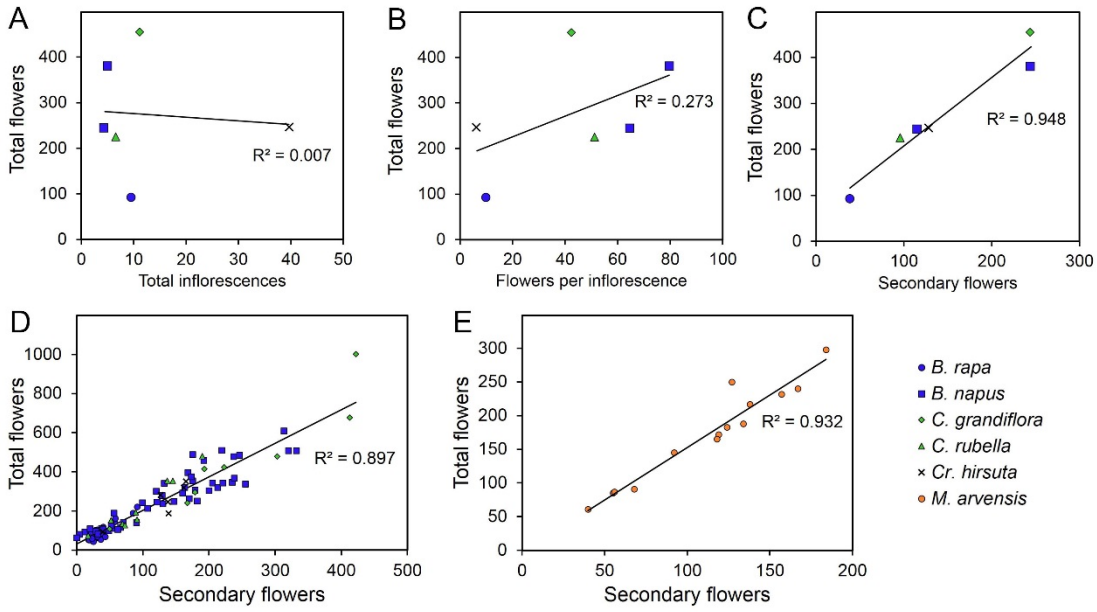

Figure 3.2. A conserved floral distribution mechanism regulates floral initiation across the Brassicaceae and beyond.

A-C, Graphs showing the relationship between mean total flowers and mean total inflorescences (n=6 independent experiments) **(A)**, mean number of flowers per inflorescence (n=6 independent experiments) **(B)** and mean number of flowers produced on secondary inflorescences in different Brassicaceae species (n=6 independent experiments): *B. rapa*, *B. napus*, *C. grandiflora*, *C. rubella* or *C. hirsuta* **(C)**. Line of best fit was calculated by the least squares approach across all data. **(D)** Graph showing the relationship between the total number of flowers and the secondary inflorescence flower number in individual plants of *B. rapa* (n=31 independent samples), *B. napus* (n=49), *C. grandiflora* (n=8), *C. rubella* (n=9) and *C. hirsuta* (n=6). Line of best fit was calculated by the least squares approach across all data. **(E)** Graph showing the relationship between the total flower number and secondary inflorescence flower number in a non-Brassicaceae species, *M. arvensis* (forget-me-not) (n=14).

Thus, as in Arabidopsis, the secondary inflorescences of all examined Brassicaceae spp. typically produced ~50% of the total flowers of the plant. Considering the large differences in reproductive architecture between the species (Supplementary Figure 3.1), this is strongly suggestive of a conserved regulatory mechanism in the Brassicaceae acting to distribute inflorescence meristem activity evenly between inflorescences of the same order, regardless how many inflorescences have been produced. Such homeostatic floral distribution cannot be universal in flowering plants, as

most species either have determinate inflorescences that produce a small number of flowers, or have unbranched inflorescence systems. However, the underlying mechanism might nevertheless be conserved across flowering plants. We therefore additionally examined flower number in *Myosotis arvensis* (forget-me-not; Boraginaceae), a distantly related species with a branching, indeterminate inflorescence system. We found the same strong correlation (R^2 = 0.932) between secondary inflorescence flower number and total flowers in this species, again irrespective of branch number (Figure 3.2 E). However, the proportion of secondary to total flowers was ~66% in this case, suggesting that the secondary inflorescences share a greater proportion of the total floral potential in forget-me-not.

The unanticipated and non-intuitive floral distribution phenomenon we describe here can be rationalized in the context of the complex temporal 'decision-making' that must occur during reproductive development. In essence, the number of secondary inflorescences represents the earliest 'estimate' of the reproductive architecture the plant should produce given the available resources. However, since resource availability varies in time, a flexible system for determining flower number independently of inflorescence number allows the plant to correct for over- or underestimates of inflorescence number. This is most strikingly illustrated by floral initiation in the strigolactone mutant *d14-1*, which makes an erroneously high number of branches, while still initiating a wild-type number of flowers (Figures 3.1 F,G). Indeed, the ability to flexibly alter reproductive effort amongst synchronously-activating inflorescences might be the selective advantage that promoted the evolution and maintenance of racemic/indeterminate inflorescences over more determinate inflorescence types. While shoot branching is typically considered a binary process in which branches are either fully inhibited or fully active (Seale, Bennett and Leyser, 2017), our data suggest that, at least in the case of inflorescences, branches may continue to exert considerable influence on each other's growth after activation. We hypothesise that these observations can be explained by extension of the canalization model for apical

dominance/shoot branching, in which auxin exported from actively growing branches is proposed to act via the self-organizing properties of the auxin transport system to inhibit canalized auxin export from new branches, thereby inhibiting their growth (Prusinkiewicz et al, 2009; Shinohara, Taylor and Leyser, 2013; Bennett, Hines and Leyser, 2014). If inflorescence meristem activity (and thus floral initiation rate) is regulated by the ongoing ability of inflorescences to export auxin, and if inflorescences continuously compete, via the self-organizing properties of the auxin transport system, to export their auxin into a shared stem, then the floral distribution rule could well be an emergent property of the same fundamental canalization mechanism (Prusinkiewicz et al, 2009; Shinohara, Taylor and Leyser, 2013). Identifying the mechanism underlying the floral distribution rule will be key to understanding the generalizability and effects of the floral distribution rule among flowering plants.

3.1 Methods

3.1.1 Plant materials

The following species were used for this work; *Arabidopsis thaliana* (Arabidopsis; Col-0, L*er*, Ws-2 ecotypes), *Brassica napus* var. *annuis* (spring oilseed rape 'Heros'), *Brassica rapa* (var. ZBC 005), *Cardamine hirsuta* (Oxford ecotype), *Capsella rubella* and *Capsella grandiflora*. The following Arabidopsis mutants were used; *brc1-2* (Aguilar-Martínez, Poza-Carrión and Cubas, 2007), *d14-1* (Waters et al. 2012), *smxl6-4 smxl7-3 smxl8-1* ('*smxl678*') (Soundappan et al. 2015), *arr3,4,5,6,7,15* ('*arr-hex'*) (Müller et al. 2015), *arr1-4* (Waldie and Leyser, 2018), *gai-t6 rga-t2 rgl1-1 rgl2-1 rgl3-1* ('*della*') (Feng et al. 2008), *gai* (Koornneef et al. 1985). *Myosotis arvensis* plants were collected from the wild on May 7th 2019, in York (UK).

3.1.2 Plant growth conditions

All plants were grown on Petersfield Growing Mediums No.2 Potting Supreme compost under a standard 16 h/8 h light/dark cycle (20ºC), primarily in controlled environment rooms with light provided by white fluorescent tubes at intensities of ~120µmol/m^2m^{-1}. Oilseed rape was grown under sodium lamp at an average intensity of ~250µmol/m^2s^{-1}.

3.1.3 Experimental design and statistics

Data in this study were gathered from a large number of independent experiments, in which each sample was a distinct plant, as described in figure legends. All data were tested for normality before statistical tests were applied. Statistical parameters are described in figure legends.

3.1.4 Phenotypic assessments

We assessed the numbers of flowers and branches at initial floral arrest in most species. In *Capsella grandiflora*, the lack of self-pollination prevents normal floral arrest, so assessments were made at the same time as for *Capsella rubella*. *Myosotis arvensis* plants of similar developmental stage were collected from the wild on 7/5/2019, and assessed at that point. Visual assessments were carried out to record the number of each class of inflorescence, and the number of floral nodes initiated on each inflorescence. All nodes where a flower had been present were counted, regardless of whether a successful fruit had been produced or not. In terms of nomenclature, the primary inflorescence (PI) is the first bolting stem, originating from the primary (i.e. embryonic) shoot meristem. Secondary inflorescences are those initiated in the axils of primary leaves (i.e. those produced by the primary SAM). In *Arabidopsis*, *Cardamine* and *Capsella*, these may either be cauline or rosette, depending on the position of the parent leaf, but were treated equally in our analyses. Any inflorescences growing directly from a secondary inflorescence was classed as a tertiary inflorescence, and so forth (see Supplementary Figure 3.1 A).

Acknowledgements

The *Cardamine hirsuta* seed were the kind gift of Angela Hay, and the *Capsella rubella* and *C. grandiflora* seed were the kind gift of Michael Lenhard.

Author contributions

CHW and TB designed and performed experiments, collected and analysed data and wrote the manuscript.

References

Aguilar-Martínez, J.A., Poza-Carrión, C. and Cubas, P. (2007). *Arabidopsis BRANCHED1* acts as an integrator of branching signals within axillary buds. *The Plant Cell*, **19**, 458-472.

Bennett, T., Hines, G. and Leyser, O. (2014). Canalization: what the flux? *Trends in Genetics*, **30**, 41-48.

Domagalska, M.A. and Leyser, O. (2011). Signal integration in the control of shoot branching. *Nature Reviews Molecular Cell Biology*, **12**, 211-221.

Feng, S. Martinez, C., Gusmaroli, G., Wang, Y., Zhou, J, Wang, F. et al. (2008). Coordinated regulation of *Arabidopsis thaliana* development by light and gibberellins. *Nature*, **451**, 475-479.

Koornneef, M., Elgersma, A., Hanhart, C.J., van Loenen-Matinet, E.P, van Rijn, L. and Zeevaart, J.A.D. (1985). A gibberellin insensitive mutant of *Arabidopsis thaliana*. *Physiologia Plantarum*, **65**, 33-39.

Müller, D., Waldie, T., Miyawaki, K., To, J.P.C., Melnyk, C., Kieber, J.J. et al. (2015). Cytokinin is required for escape but not release from auxin mediated apical dominance. *The Plant Journal*, **82**, 874-886.

Prusinkiewicz, P., Crawford, S., Smith, R.S. and Leyser, O. (2009). Control of bud activation by an auxin transport switch. *PNAS*, **106**, 17431-17436.

Seale, M., Bennett, T. and Leyser, O. (2017). *BRC1* expression regulates bud activation potential but is not necessary or sufficient for bud growth inhibition in *Arabidopsis*. *Development*, **144**, 1661-1673.

Shinohara, N., Taylor, C. and Leyser, O. (2013). Strigolactone can promote or inhibit shoot branching by triggering rapid depletion of the auxin efflux protein PIN1 from the plasma membrane. *PLOS Biology*, e1001474.

Soundappan, I., Bennett, T., Morffy, N., Liang, Y., Stanga, J.P., Abbas, A. et al. (2015). SMAX1-like/D53 family members enable distinct MAX2-dependent responses to strigolactones and karrikins in *Arabidopsis*. *Plant Cell*, **11**, 3143-3159.

Waldie, T. and Leyser, O. Cytokinin targets auxin transport to promote shoot branching. (2018). *Plant Physiology*, **177**, 803-818.

Walker, C.H. and Bennett, T. (2018). Forbidden fruit: dominance relationships and the control of shoot architecture. *Annual Plant Reviews Online*, **1**, 1-38.

Waters, M.T., Nelson, D.C., Scaffidi, A., Flematti, G.R., Sun, Y.K., Dixon, K.W. et al. (2012). Specialisation within the DWARF14 protein family confers distinct responses to karrikins and strigolactones in *Arabidopsis*. *Development*, **139**, 1285-1295.

Chapter 4

Auxin export from proximal fruits drives arrest in temporally-competent inflorescences

Originally published in *Nature Plants*, 2020

Volume **6**, Pages 699-707.

Auxin export from proximal fruits drives arrest in temporally-competent inflorescences

Alexander Ware[1]*, **Catriona H. Walker[2]***, Jan Šimura[3], Pablo González-Suárez[2], Karin Ljung[3], Anthony Bishopp[1], Zoe Wilson[1]+, Tom Bennett[2]+

[1]School of Biosciences, University of Nottingham, Loughborough, Leics, LE12 5RD.

[2]School of Biology, Faculty of Biological Sciences, University of Leeds, Leeds, LS2 9JT.

[3]Department of Forest Genetics and Plant Physiology, Umeå Plant Science Centre, Swedish University of Agricultural Sciences, 901 83 Umeå, Sweden

These authors contributed equally: Alexander Ware, Catriona H. Walker

+ Address for correspondence: t.a.bennett@leeds.ac.uk, zoe.wilson@nottingham.ac.uk.

4.1 Abstract

A well-defined set of regulatory pathways control entry into the reproductive phase in flowering plants, but little is known about the mechanistic control of the end-of-flowering despite this being a critical process for optimization of fruit and seed production. Complete fruit removal, or lack of fertile fruit-set, prevents timely inflorescence arrest in Arabidopsis, leading to a previous proposal that a cumulative fruit/seed-derived signal causes simultaneous 'global proliferative arrest'. Recent studies have suggested that inflorescence arrest involves gene expression changes in the inflorescence meristem that are, at least in part, controlled by the *FRUITFULL–APETALA2* pathway; however, there is limited understanding of how this process is coordinated at the whole-plant level. Here, we provide a framework for the communication previously inferred in the global proliferative arrest model. We show that the end-of-flowering in Arabidopsis is not 'global' and does not occur synchronously between branches, but rather that the arrest of each inflorescence is a local process, driven by auxin export from fruit proximal to the inflorescence apex. Furthermore, we show that inflorescences are competent for arrest only once they reach a certain developmental age. Understanding the regulation of inflorescence arrest will be of major importance to extending and maximizing crop yields.

4.2 Introduction

A complex series of regulatory pathways that integrate both internal and environmental signals regulate entry into the reproductive phase (the floral transition) in flowering plants (Khan, Ai and Zhang, 2014). These initiation pathways have received much attention, but relatively little is known about the mechanisms that control the end of the reproductive phase (end-of-flowering). This is somewhat surprising, since the correct timing of end-of-flowering is a critical process for optimization of fruit and seed production, and hence reproductive success. In a seminal study from 1994, Hensel et al. examined the arrest of inflorescences in the model species *Arabidopsis thaliana* (Arabidopsis) and showed that inflorescence arrest normally occurs through a regulated process in which each inflorescence ceases to open flowers and in which the inflorescence meristem enters an arrested state (Hensel et al. 1994). This process was proposed to be triggered by fruits, since complete fruit removal, or lack of fertilization in *ms1* male-sterile mutants, prevented timely inflorescence arrest anywhere on the plant. Inflorescences eventually ceased flower production, but only through terminal differentiation of the inflorescence meristem (Hensel et al. 1994). Analysis of reduced fertility and embryo-lethal mutants suggested that only fruit containing >30% fertile seed are able to trigger arrest, and that seed are an essential part of the process (Hensel et al. 1994). Finally, it was observed that post-arrest fruit removal leads to the reactivation of arrested inflorescences and the production of new fruit, suggesting that inflorescence arrest is a reversible state (Hensel et al. 1994). These observations led to a model in which inflorescence arrest was proposed to result from accumulation of a fruit/seed-derived signal that, at a threshold level, would trigger simultaneous ‘global proliferative arrest’ (GPA) in all inflorescences (Hensel et al. 1994) .

After a long gap, two recent studies have provided new insights into inflorescence arrest in Arabidopsis. Wuest et al. (2016) showed that, transcriptionally, the arrested inflorescence meristem state strongly resembles dormancy in axillary inflorescence buds, suggesting that the process of inflorescence arrest could represent a direct

reversal of bud activation. In a second study, Balanza et al. (2018) showed that *fruitfull* mutants undergo delayed inflorescence arrest and suggested that inflorescence arrest requires a FRUITFULL–APETALA2 regulatory module, which may be under the control of the miR156/ miR172 ageing pathway. However, much remains unclear about the mechanistic basis for both inflorescence arrest itself and the wider coordination of end-of-flowering across the plant. We are especially interested in understanding the mechanism by which fruits bring about inflorescence arrest, and therefore set out to understand this process in more detail.

4.3 Results

4.3.1 Inflorescence arrest is not synchronous in Arabidopsis

Our initial observations suggested that, in the Col-0 ecotype, inflorescence arrest may not be synchronous and that inflorescences may arrest at different times. Because synchronous arrest is a key tenet of the GPA model, we performed a more detailed reassessment to confirm these observations. By tracking the duration of flower production ('inflorescence duration') in each inflorescence in a cohort of Col-0 plants, we found that inflorescence arrest across plants is not synchronous, with on average ~5 d between arrest of the first and last inflorescences (Figure 4.1 A, Supplementary Figure 4.1 and Supplementary Table 4.1). We measured the duration of three orders of inflorescence: primary (PI, the main bolting stem), secondary (those arising from primary leaves, whether cauline or rosette) and tertiary (those arising from leaves on the secondary inflorescences) (Supplementary Figure 4.2). The timing of arrest followed a general basipetal pattern, with the PI and the secondary cauline (C) inflorescences arresting first at similar times, followed by a wave of arrest across the secondary rosette (R) inflorescences (Figure 4.1 A and Supplementary Figure 4.1). Tertiary inflorescences arrest at approximately the same time as their parent inflorescence (Supplementary Figure 4.1). This pattern corresponds to the general pattern of inflorescence activation observed earlier in the experiment, in which secondary cauline inflorescences activate together, followed by a basipetal wave of activation across the secondary rosette inflorescences (Figure 4.1 A and Supplementary Figure 4.1). Thus, we propose that inflorescence arrest occurs when active inflorescences reach the end of their lifetime, and this timing is largely a reflection of the timing of inflorescence activation. In instances where inflorescence activation is synchronous (probably including those in Hensel et al. 1994), end-of-flowering may also be near-synchronous, but this is not a key tenet of end-of-flowering.

We also observed an additional phenomenon of 'reflowering' in a number of experiments, whereby after the arrest of most or all inflorescences, previously dormant

axillary buds would activate, giving rise to new inflorescences (Figure 4.1 E); although this is observed relatively frequently, to our knowledge it has not previously been characterized in the literature. The reinitiation of flowering was not observed in all plants, nor indeed in all experiments, and the number of additional fruits produced through reflowering varied between experiments, but was generally greatest in those with a higher initial fruit production (Figure 4.1 D). The existence of the reflowering phenomenon, and the ability of buds to activate in *de novo* manner following systemic inflorescence arrest, further highlight the non-global, asynchronous nature of inflorescence arrest. This also implies that there may be multiple signals that are active at different stages and which are driving floral activation/arrest.

4.3.2 Inflorescence arrest is a temporally regulated process

In these analyses, we also observed that each order of inflorescence (primary, secondary, tertiary) had a distinctive duration between activation and arrest. Although the activation and arrest of individual inflorescences was not synchronous, the duration for inflorescences of the same order was generally very similar. This was true when comparing both inflorescences within individual plants and those between different plants in the same experiment (Figure 4.1 B). Furthermore we observed that, across a wide range of different experiments run under similar conditions (Supplementary Table 4.1), the primary inflorescences in Col-0 had very similar durations, being active for 22±3d post-bolting (dpb) (Figure 4.1 C). We observed that the total 'floral duration' before inflorescence arrest was also consistent among experiments, occurring at around 27±3dpb (Figure 4.1 C). These data suggest that inflorescence arrest may be a predominantly time-dependent process, requiring inflorescences to become responsive to arrest signals, rather than one purely driven by cumulative feedback inhibition from fruit-derived signals.

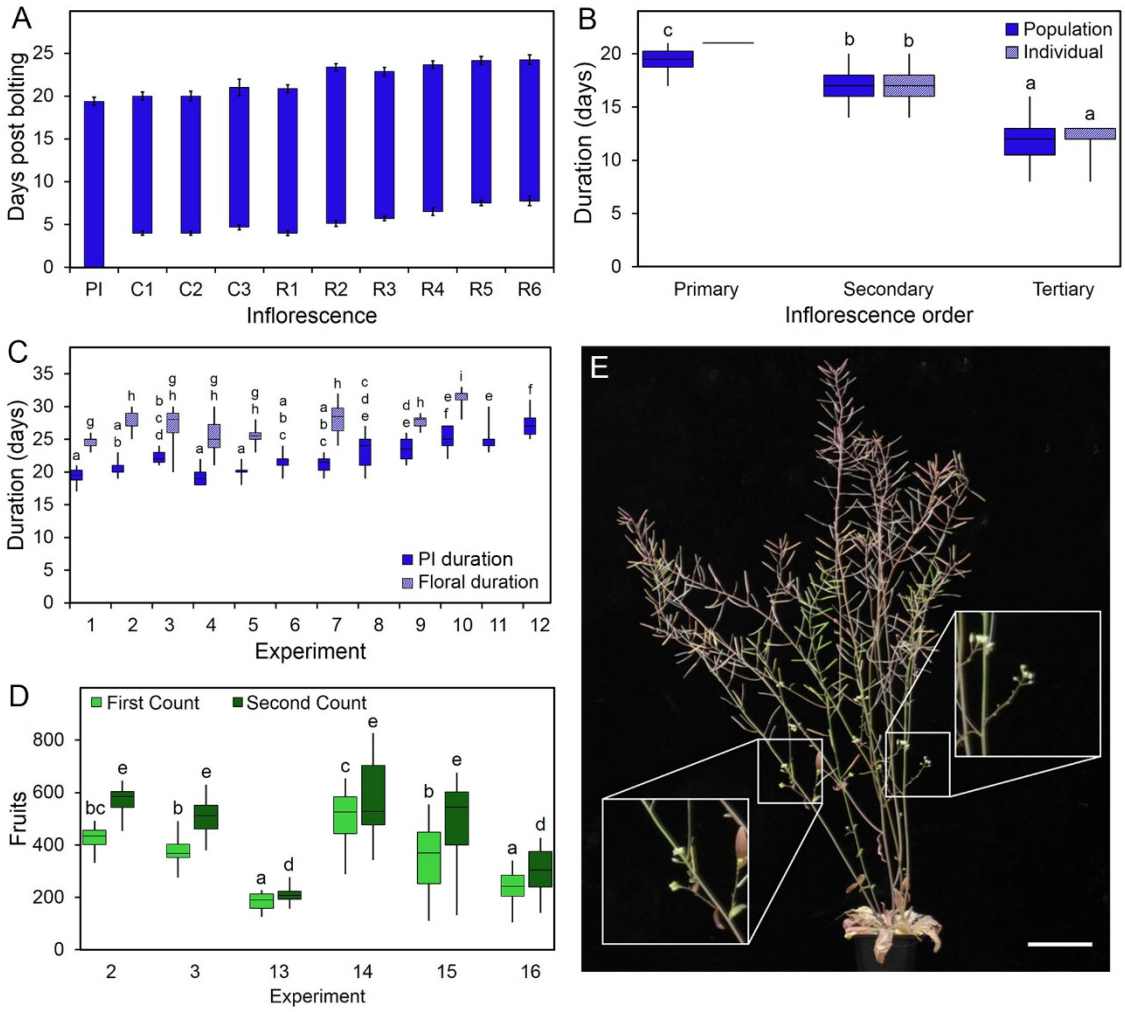

Figure 4.1. Inflorescence arrest is a temporally regulated process

(A) Timing of inflorescence activation and arrest across different branches. PI, primary inflorescence; C1, secondary cauline inflorescence 1 (the uppermost on the plant); R1, secondary rosette inflorescence 1 (the uppermost rosette inflorescence). The mean time after floral transition (bolting) until activation of each inflorescence was measured, along with the subsequent time until its arrest, for a population of Col-0 plants. The lower limit of the bar indicates the number of days after bolting when inflorescence initiated. The upper limit of the bar indicates the end-of-flowering for each inflorescence. Each bar is the mean of between three and eight plants (n=3-8 PI–R6), since not all plants had each type of inflorescence. Any inflorescence type occurring on two or fewer plants was excluded from analysis. Error bars indicate s.e.m. Bars with the same letter are not statistically different from each other (analysis of variance (ANOVA), Tukey's honest significant difference (HSD) test). **(B)** Mean duration, from activation to arrest, of different classes of inflorescence in a single Col-0 plant and across a population of Col-0 plants. For the population, n=8 plants. Bars with the same letter are not statistically different from each other (ANOVA, Tukey's HSD test). **(C)** Duration of PI as an individual inflorescence, and total time from floral transition to initial inflorescence arrest of the whole plant (floral duration), in Col-0 plants grown under long days (16 h light/8 h dark)

in 12 independent experiments. The upper and lower confines of the box indicate the interquartile range, the central line indicates the median and the whiskers represent the maximum and minimum values. n=8–24 biologically independent samples (PI duration and floral duration bars have the same n value within each experiment Bars with the same letter are not significantly different from each other (ANOVA, Tukey's HSD test). **(D)** Mean total fruit production in long-day-grown Col-0 plants across six separate experiments before reflowering (light green bars) and after reflowering ('second count', dark green bars). n=11–18; first and second count bars have the same n value within each experiment). For box plots, the upper and lower confines of the box indicate the interquartile range, the central line indicates the median and the whiskers represent the maximum and minimum values. Bars with the same letter are not significantly different from each other (ANOVA, Tukey's HSD test). **(E)** Photograph showing reflowering in Col-0, with new branches produced after initial inflorescence arrest highlighted in white boxes. Scale bar, 5 cm.

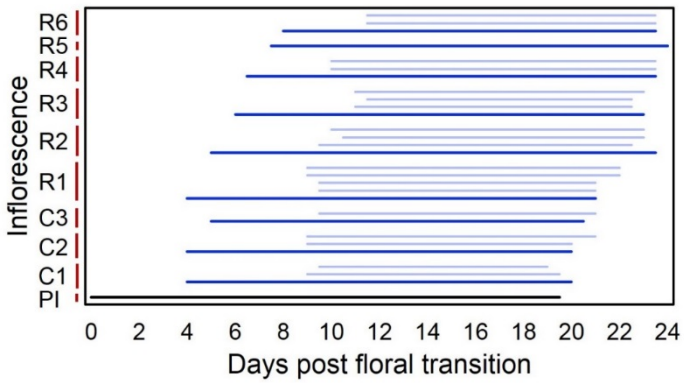

Supplementary Figure 4.1. Inflorescence classes and durations

Complete dataset for data shown in Figure 4.1 A,B. Duration of individual inflorescences in Col-0, from inflorescence activation to arrest, shown relative to the time since bolting started. The primary inflorescence ('PI') is indicated in black, secondary cauline (C1, C2, etc.) and rosette (R1, R2, etc.) inflorescences in dark blue. Tertiary inflorescences are shown in light blue above their parent secondary inflorescence. Values are derived from analysis of 8 plants. Each inflorescence duration is the mean of 3-8 plants, depending on which plants had which inflorescence type. Any inflorescence type occurring on two or fewer plants was excluded from analysis.

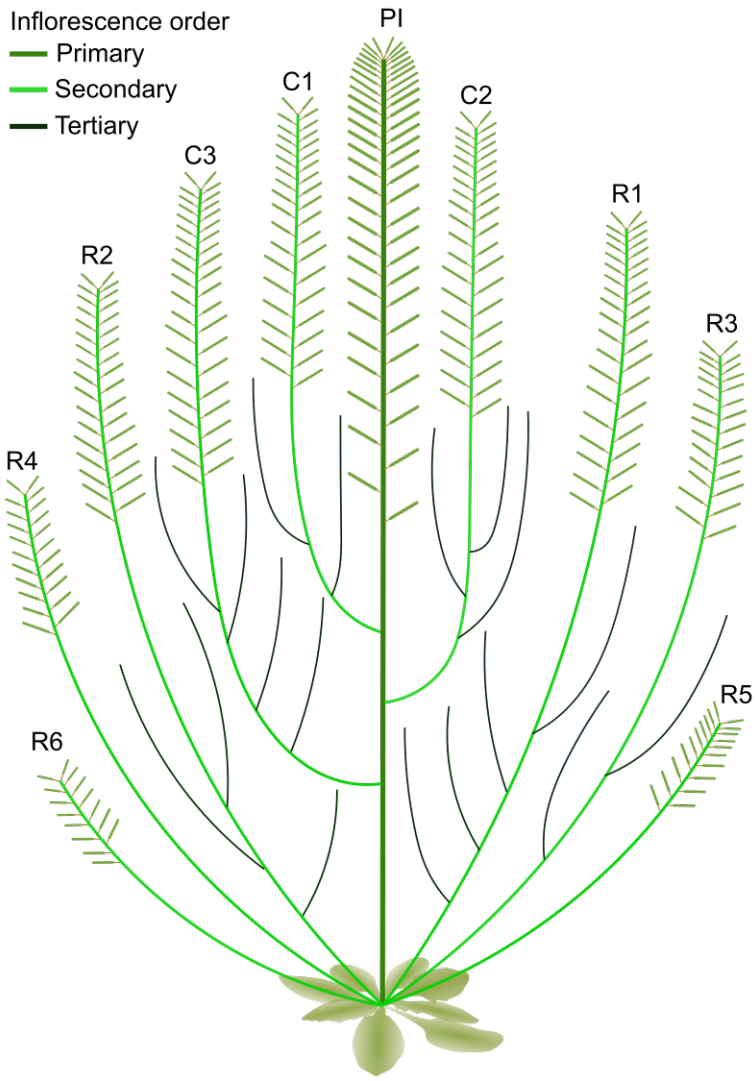

Supplementary Figure 4.2. Inflorescence architecture and nomenclature

Diagram illustrating the typical architecture of an Arabidopsis shoot system. The primary embryonic shoot apex gives rise to primary leaves and eventually forms the primary inflorescence. Flowering branches that form from axillary buds in the axils of primary leaves are secondary inflorescences. Secondary inflorescences formed from primary cauline leaves are cauline inflorescences (denoted C1 etc.), those from primary rosette leaves are rosette inflorescences (denoted R1 etc.). Secondary inflorescences are numbered in the order in which they activate, from the shoot apex downwards through the cauline nodes, and then into the rosette nodes. Thus, C1 is the apical-most cauline inflorescence, C2 is the second apical-most inflorescence, and so on. We have separated the numbering of the cauline and rosette nodes, such that R1 is the apical-most rosette inflorescence. Branches that form from secondary inflorescences are tertiary inflorescences, and are named after the parental branching system in rootward fashion (e.g. C2.1 = uppermost tertiary branch on the second cauline inflorescence).

Experiment	GH or WI	Floral duration (days)	PI duration (days)	RF duration (days)	Fruit count	RF fruit count
1	WI	24.4 ± 0.9	19.4 ± 1.3			
2	WI	27.7 ± 1.5	20.6 ± 1.1		423 ± 51	569 ± 53
3	WI	27.1 ± 1.9	22.3 ± 1.1		378 ± 62	513 ± 75
4	WI	25.4 ± 2.6	19.3 ± 1.3			
5	WI	25.4 ± 1.4	20.1 ± 1.0			
6	WI		21.3 ± 0.2			
7	WI	28.1 ± 2.5	21.3 ± 1.3		515 ± 128	
8	WI		23.2 ± 0.8			
9	WI	27.8 ± 0.3	23.5 ± 0.5			
10	WI	31.1 ± 0.6	25.1 ± 0.8			
11	WI		24.9 ± 0.4			
12	GH		27.3 ± 0.7			
13	WI				184 ± 30	208 ± 27
14	WI				501 ± 101	571 ± 149
15	WI				352 ± 129	483 ± 173
16	WI			9.9 ± 2.9	241 ± 65	301 ± 86

Supplementary Table 4.1.

Details of experiments used for flowering duration and fruit assessments. Means are presented for the untreated controls in each experiment ± standard deviation. All experiments were performed under similar long day conditions (16h day/8h night), grown in either a greenhouse with supplementary lighting (GH) or a walk-in controlled environment chamber (WI). PI = primary inflorescence, RF = after re-flowering.

4.3.3 Timely arrest in response to fruit presence is a local process in each inflorescence

The absence of synchronous arrest across inflorescences suggested that inflorescence arrest is not determined by a systemic signal. We confirmed that, as shown by Hensel et al. (1994), timely inflorescence arrest requires fertile fruit because removal of fruit everywhere on the plant was sufficient to prevent inflorescence arrest anywhere on the plant (Figures 4.2 B,C). However, when we performed localized continuous flower removal on secondary cauline inflorescences, we observed that treated inflorescences did not undergo arrest despite plants having ~90% of their normal fruit-set whilst timely arrest was observed elsewhere on the plant (Figures 4.2 D,E). Together with the lack of synchronicity, these data suggest that inflorescence arrest is not a systemically regulated process, but rather consists of the independent, locally regulated arrest of individual inflorescences.

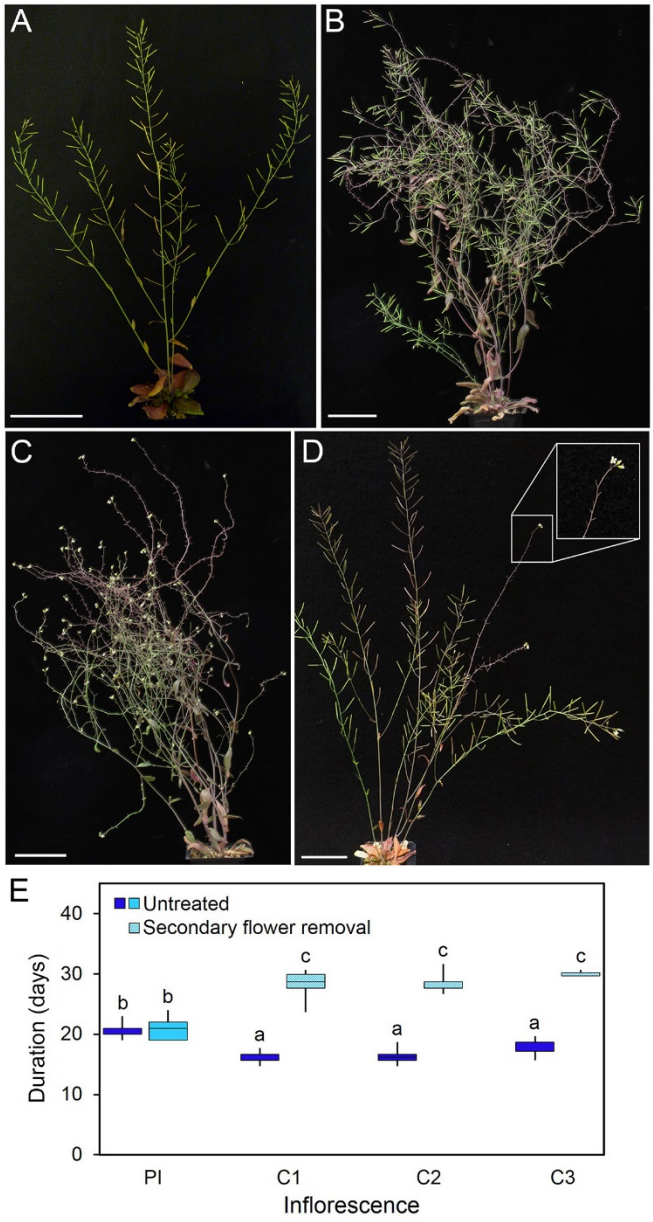

Figure 4.2. Inflorescence arrest is locally regulated by fruit presence

A-D, Inflorescence arrest is delayed by continuous flower removal. Untreated plants arrest in a predictable manner **(A)**, but continuous daily removal of flowers across all inflorescences delays arrest in wild-type Arabidopsis **(C)**. However, when treatment is ended, fruits develop and arrest occurs within a few days **(B)**. Local flower removal prevents arrest of individual inflorescences, but has no systemic effect **(D)**. Scale bars, 5 cm. **(E)** Inflorescence duration in response to local flower removal. Open flowers were removed from secondary cauline inflorescences (C1, C2, C3) every 1–2 d until 17 dpb), whereupon open flowers were removed daily. Inflorescence duration in secondary cauline inflorescences was significantly extended where flowers were removed (hatched light blue bars), relative to secondary cauline inflorescences in untreated plants (dark blue bars). However, the duration of primary inflorescences (which were not treated) was not different between treated (light blue) and untreated (dark blue). n=3–12. The upper and lower confines of the box indicate the interquartile range, the central line indicates

the median and the whiskers represent the maximum and minimum values. Bars with the same letter are not statistically different from each other (ANOVA, Tukey's HSD test).

4.3.4 Delayed inflorescence arrest in response to fruit absence occurs systemically

Contrary to this model, the results of Hensel et al. (1994) clearly demonstrated an extension of PI duration following removal of secondary inflorescences, suggesting that systemic feedback from fruits can modulate the duration of individual inflorescences. We repeated this debranching treatment and confirmed that, in the L*er* and Col-0 backgrounds, it does indeed extend inflorescence duration and fruit production of the PI relative to untreated plants (Figures 4.3 A,B). Interestingly, we observed that the duration of the PI in untreated L*er* plants was longer than that in Col-0, by approximately 7–9d (cf. Figures 4.3 A, 4.2 E), suggesting there is variation in Arabidopsis ecotypes for inflorescence duration. Similarly, when we removed tertiary inflorescences from secondary inflorescences in Col-0, we observed a small extension to the duration of secondary inflorescences and a corresponding increase in the number of fruit they produce (Figure 4.3 C). Thus, even though the global presence of fruit across the plant is not sufficient to trigger arrest of individual fruitless inflorescences, the global absence of fruit is sufficient to extend the duration of individual, fully fruited inflorescences. Collectively, our data suggest that fruit play two distinct roles in inflorescence arrest, systemically modulating inflorescence duration and locally driving inflorescences to undergo arrest. This probably indicates the existence of multiple, fruit-derived signals that are involved in the regulation of inflorescence arrest.

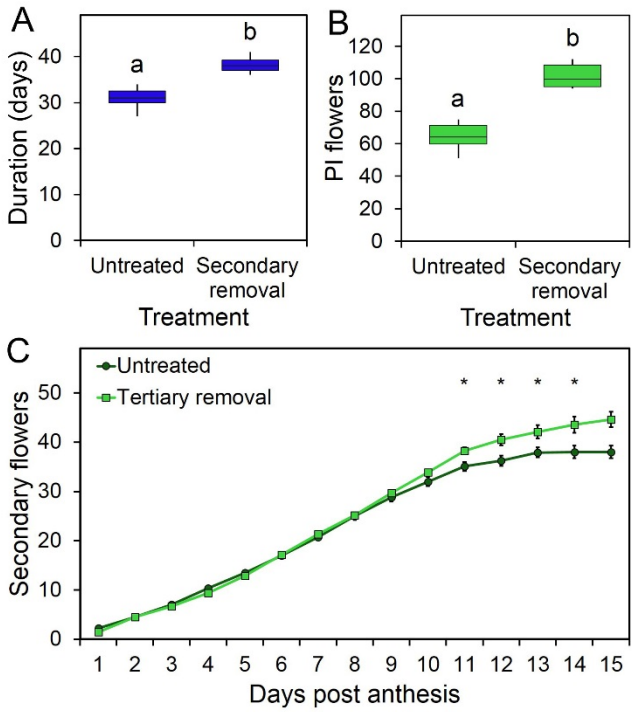

Figure 4.3. Inflorescence duration is extended by global fruit absence

A,B, Effect of secondary inflorescence removal on the duration of PI in the L*er* ecotype of Arabidopsis. In treated plants, all secondary inflorescences were removed at 7 dpb, and the timing of PI arrest was measured **(A)** as well as the number of flowers produced by the PI **(B)**. n=12. The upper and lower confines of the box indicate the interquartile range, the central line indicates the median and the whiskers represent the maximum and minimum values. Bars with the same letter are not statistically different from each other (two-tailed t-test, $p<0.001$). **(C)** Effect of tertiary inflorescence removal on the duration of secondary inflorescences in the Col-0 ecotype of Arabidopsis. In treated plants, all tertiary inflorescences were removed at 6 dpa, and the daily rate of flower opening after anthesis of the first flower on the secondary inflorescence was measured until inflorescence arrest. n=12 per treatment. The upper and lower confines of the box indicate the interquartile range, the central line indicates the median and the whiskers represent the maximum and minimum values. Asterisks indicate statistically significant differences between the treatments (t-test with Bonferroni correction, $p<0.05$).

4.3.5 Small numbers of fruit are sufficient to trigger inflorescence arrest

Each of the treatments used by Hensel et al. (1994) to support the GPA model caused a dramatic global reduction in fertile fruit, and resulted in systemic delay of inflorescence arrest. However, the intensity of these treatments precluded more nuanced understanding of the role of fruit in inflorescence arrest, and we therefore investigated

the effect of more subtle treatments. We observed that if we removed flowers continuously from inflorescences beyond their normal lifetime and then allowed plants to recover, each inflorescence arrested within a few days, despite having produced only a small number of fertile fruits (approximately six to ten per inflorescence) (Figure 4.2 B). This suggests that relatively small numbers of fruit may be sufficient to trigger inflorescence arrest. Similarly, if we used a dexamethasone (DEX)-inducible *MS1:MS1-GR* construct to restore fertile fruit formation to the *ms1-1* mutant (L*er* background), from 12 d post-anthesis (dpa) of the first flower, we observed regulated inflorescence arrest, unlike in untreated controls (Figure 4.4 A). However, the number of fertile fruit per inflorescence was around only 45% of that in wild-type plants (Figure 4.4 B).

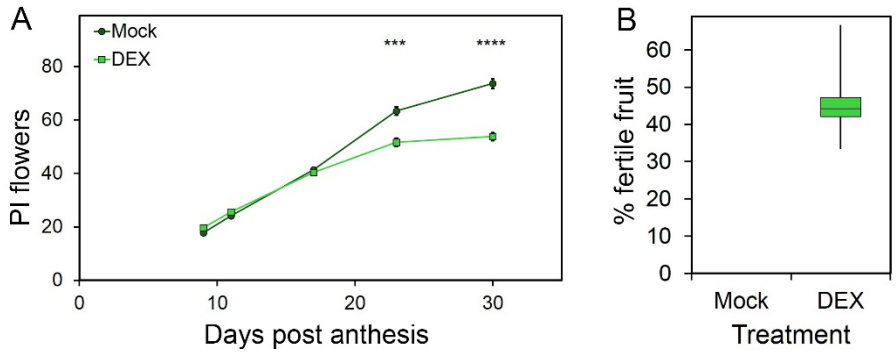

Figure 4.4. Small numbers of fruit are sufficient for local inflorescence arrest.

(A) Inflorescence arrest is delayed by male sterility. Mock-treated MS1:MS1-GR ms1-1 plants are fully sterile and do not undergo timely primary inflorescence arrest, behaving in the same way as *ms1-1* sterile plants. However, if fertility is restored by 25 μM DEX treatment at 11 and 12 dpa of the first flower on the primary inflorescence, timely inflorescence arrest occurs. n=9–12 for each time point; bars indicate s.e.m. Asterisks indicate significance as determined by Sidak's multiple comparison following fitting of a mixed-effects model (****$p<0.0001$). **(B)** Application of DEX resulted in subsequent restoration of fertility, while mock-treated plants exhibited complete sterility. n=12 for each treatment. The upper and lower confines of the box indicate the interquartile range, the central line indicates the median and the whiskers represent the maximum and minimum values.

To delineate more clearly the number of fruit needed to trigger arrest, we performed differential flower-removal treatments on secondary cauline inflorescences of

the same plant which, if untreated, typically undergo arrest at the same time (Figure 4.1 A and Supplementary Figure 4.1). On each plant, every other flower was removed from one inflorescence (1/2), three of every four flowers were removed from another inflorescence (3/4) and four of every five flowers were removed from a third inflorescence (4/5); a fourth was left untreated (Figure 4.5 F). Despite the resulting dramatic differences in fruit-set, the treated inflorescences on the same plant all underwent normal regulated arrest, although the more severe treatments delayed inflorescence arrest by 2–3 d (Figure 4.5 A). The most severely treated inflorescences arrested despite having produced only 20% of the fruit produced by untreated controls (Figure 4.5B); the average of seven fruit needed for arrest in this treatment is highly consistent with the number produced by the plants shown in Figure 4.2 B. These data thus do not support a model in which cumulative fruit-set upon each inflorescence is required for arrest. Rather, a small number of fruit (although not necessarily always as few as seven) seems sufficient for arrest to occur.

4.3.6 Proximal fruit are needed for temporally competent inflorescence arrest

These data also present a paradox: approximately seven fertile fruit are sufficient in certain circumstances to trigger arrest, but most inflorescences produce far more than seven fruit before arrest. Given our earlier observations of inflorescence duration (Figures 4.1 A,C), and that inflorescences on the same plant tend to arrest at approximately the same time despite individually producing different fruit numbers (Figures 4.5 A,B), these data reinforce the idea that temporally acquired responsiveness to a fruit-derived signal is critical, rather than a threshold level of signal being reached. We therefore tested how the timing of fruit production affects inflorescence arrest. In a first experiment, we performed two treatments; ‘early’ plants had all flowers removed, until around 30 flowers had been produced by the PI (12–13 dpb), and were then allowed to continue flowering normally. Despite producing far fewer fruit than control plants

(Figure 4.5 D), the PI of early plants underwent arrest at the same time as untreated plants (~21 dpb) (Figure 4.5 C). This mirrored the effect seen in the DEX-inducible *MS:MS1-GR* line (Figure 4.4 A). Conversely, 'late' plants were allowed to flower as normal until around 30 flowers had opened on the PI (12–13 dpb); subsequently all open flowers were removed from the plant for 20 d. Despite producing the same number of fruit as early plants during the first 21 dbp (Figure 4.5 D), late plants did not undergo timely arrest (Figure 4.5 C). However, when flower-removal treatment was ended in late plants at approximately 30 dpb, the inflorescence was active for a further 7 d, producing around seven fertile fruits before arrest (again consistent with the minimum fruit numbers established in Figures 4.2 B and 4.5 B). These data demonstrate that fruit are able to trigger arrest only when inflorescences have become temporally competent to arrest, at the end of their normal lifetime.

To further examine the relationship between timing of fruit production and arrest, we performed an experiment in which all fruit were removed from three secondary cauline inflorescences on the same plant at 17 dpb. One inflorescence per plant was subsequently allowed to produce fruit normally until it arrested (X); this approximated the '50% early' treatment (Figure 4.5 F). Another inflorescence was allowed to produce ten fruit from 17–20 dpb, but then had all subsequent flowers removed (Y) (Figure 4.5 F). The final inflorescence had additional flowers removed until 20 dpb, and was then allowed to produce ten fruit from 20–22 dpb; all subsequent flowers were also removed (Z) (Figure 4.5 F). The timing of arrest was then compared to the PI on the same plants. Treatment X inflorescences produced ~24 fertile fruit, and arrested shortly after the PI (26 dpb) (Figure 4.5 E). Neither treatment Y nor Z inflorescences underwent timely arrest, despite having produced sufficient fertile fruit (Figure 4.5 E) However, most of the Y and Z inflorescences did eventually undergo a regulated arrest (with 'bud cluster'; 8/12 inflorescences for Y and 12/13 inflorescences for Z), the Z inflorescences arresting somewhat earlier (31 dbp) than the Y inflorescences (33 dpb) (Figure 4.5 E). Together with the experiment shown in Figures 4.5 A,B, these data show that a small number of

fruit proximal to the inflorescence apex are sufficient to trigger arrest once the inflorescence is arrest-competent (Figure 4.5 F). The further away fruit are from the meristem at the point when the inflorescence becomes arrest-competent, the lower the ability of those fruit to trigger arrest (Figure 4.5 F); very distal fruit are completely unable to trigger arrest. Collectively, our data suggest that inflorescence arrest is a time-dependent process in which inflorescences become competent to arrest at a certain developmental age post-floral transition and then undergo almost immediate arrest, providing they receive an inhibitory signal from fruit they have recently produced. This developmental age does not directly reflect the absolute age of the inflorescence, with the relationship between developmental age and absolute age probably varying due to environmental influences or differences in growth history, and is reflected in the range of fruit numbers produced between plants.

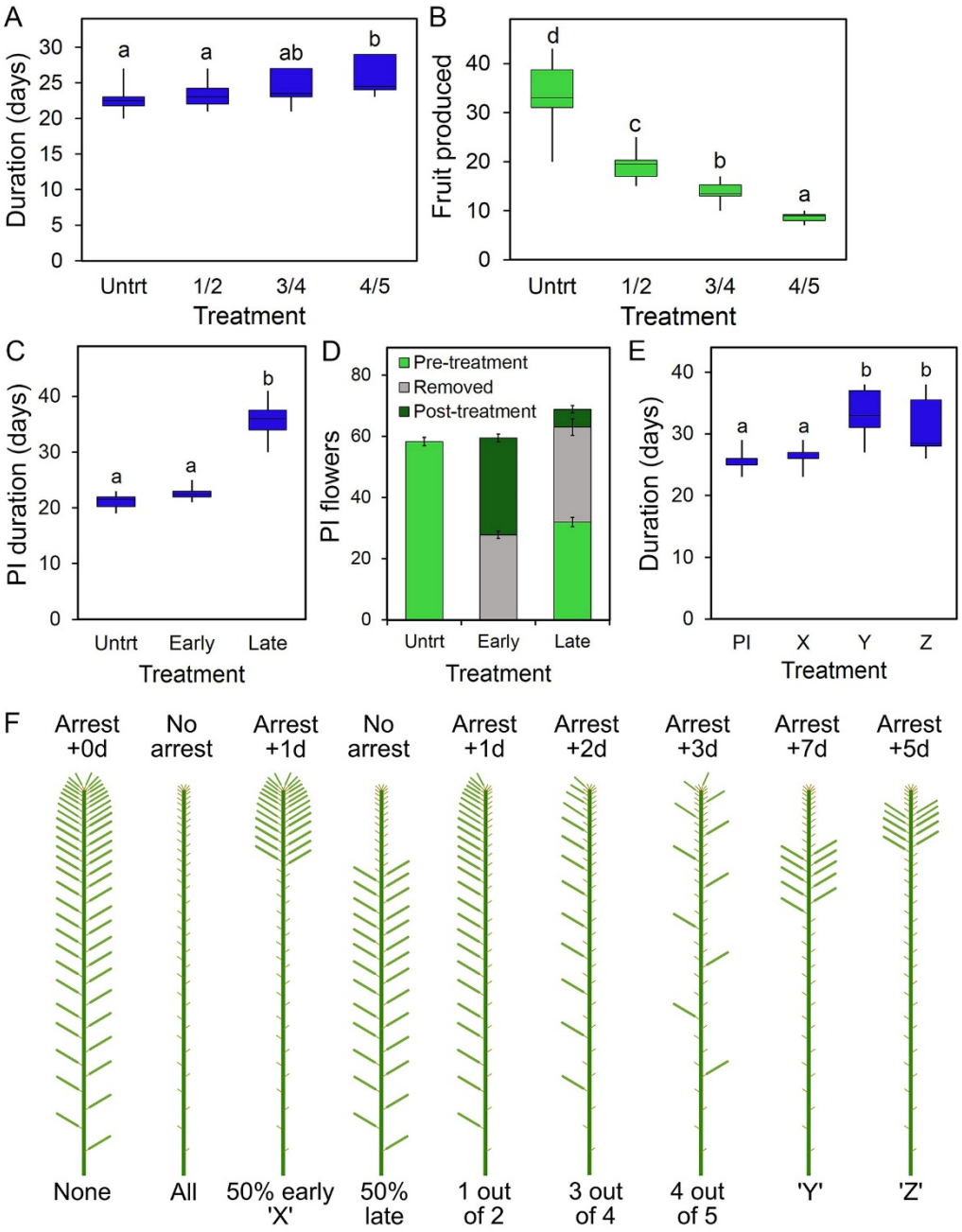

Figure 4.5. Proximal fruit drive arrest in competent inflorescences.

A,B, Effect of fruit removal on inflorescence arrest. Secondary cauline inflorescences on the same plant were subjected to four different fruit removal treatments, removing either no fruit (untrt), one out of every two fruit (1/2), three out of every four fruit (3/4) or four out of every five fruit (4/5). The timing of secondary inflorescence arrest was measured **(A)**, as well as the number of fruit produced by each inflorescence **(B)**. n=12. Bars with the same letter are not statistically different from each other (ANOVA, Tukey's HSD test). **C,D)** Effect of partial and differential fruit removal on inflorescence arrest. In 'Early' plants, open flowers were removed from the whole plant every 1–2 d until approximately 30 flowers had been produced on the primary inflorescence, following which they were allowed to flower normally. 'Late' plants were allowed to flower as normal until around 30 flowers had opened on the primary inflorescence, then all flowers subsequently produced

were removed daily until 30 dpb, when the inflorescence was allowed to produce fruit again. **(C)** The inflorescence duration of the PI for these different treatments; n=13–14. Bars with the same letter are not statistically different from each other (ANOVA, Tukey's HSD test). **(D)** The number of flowers produced by the PI in these treatments, coloured according to whether the flower was produced before (light green) or after (dark green) treatment, or whether it was removed (grey). n=14, bars indicate s.e.m. **(E)** Effect of timing of fruit production on inflorescence arrest. Secondary cauline inflorescences on the same plant were subjected to three different treatments (X, Y, Z; see F). In all treatments, fruit produced up to 17 dpb were removed. Treatment X inflorescences were then allowed to make fruit until arrest. Treatment Y inflorescences were allowed to set ten fruit from 17 dpb, and then were subjected to continuous flower removal until arrest. Treatment Z inflorescences were subjected to continuous flower removal until 20 dpb, at which point they were allowed to set ten fruit before flower removal was restarted until arrest. The primary inflorescences on the same plant acted as untreated controls. The graph shows the mean time of arrest (dpb) for inflorescences in each of these treatments. n=14 biologically independent samples. For box plots, the upper and lower confines of the box indicate the interquartile range, the central line indicates the median and the whiskers represent the maximum and minimum values. Bars with the same letter are not statistically different from each other (ANOVA, Tukey's HSD test). **(F)** Diagram summarizing the effects of fruit removal quantity and timing on inflorescence arrest, based on experiments in A-E.

4.3.7 Auxin export from fertile fruit triggers inflorescence arrest

We next questioned how fertile fruit trigger arrest. Previous authors tentatively proposed that fruit communicate with inflorescence apices by a phytohormonal signal, although provided no clear evidence supporting this (Hensel et al. 1994; Balanzà et al. 2018). A number of phytohormones could be involved in delivering the arrest signal, and multiple signals may also be involved at the various developmental stages. Gibberellin is an important regulatory signal produced during fruit development, and could act as an arrest-inducing signal. To test this, we examined the quintuple *rga-t2 gai-t6 rgl1-1 rgl2-1 rgl3-1* (*della*) mutant that lacks all DELLA proteins (Feng et al. 2008) and which, as a result, has effectively constitutive gibberellin responses. We saw a dramatic increase in fruit number per inflorescence in the *della* mutant, consistent with the known role of

gibberellin in controlling meristem size and activity (Serrano-Mislata et al. 2017) (Supplementary Figure 4.3 B). However, the *della* mutant had an identical PI duration to the L*er* wild type, suggesting that gibberellin is not a major factor regulating timely inflorescence arrest (Supplementary Figure 4.3 A). However, given the differences in the rate of flower production (florochron) between *della* and L*er*, we cannot rule out that gibberellin might play a smaller, quantitative role in arrest. The much higher fruit production in the *della* mutant does not induce premature inflorescence arrest, which further indicates that arrest does not occur upon reaching a cumulative fruit-signal threshold.

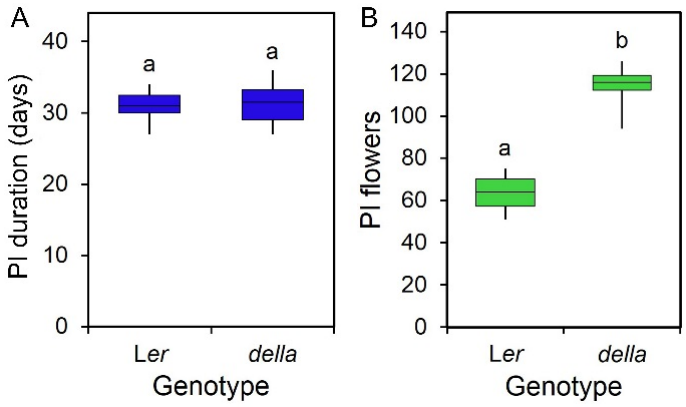

Supplementary Figure 4.3. Role of gibberellin in floral arrest

A,B) Effect of *della* quintuple mutants (which have constitutive gibberellin responses) on inflorescence arrest, relative to L*er* wild-type plants. The duration of the PI arrest was measured **(A)**, as well as the number of flowers produced by the PI **(B)**. n=12. The upper and lower confines of the box indicate the interquartile range, the central line indicates the median, and the whiskers represent the maximum and minimum values. Bars with the same letter are not statistically different from each other (two-sided t-test, $p<0.05$).

Transcriptionally, the switch between activity and arrest in inflorescence meristems mirrors the switch between activity and dormancy in axillary meristems (AMs)(Hensel et al. 1994). Because this switch in AMs is controlled in part by auxin export from the AM into the stem (Bennett et al. 2006; Prusinkiewicz et al. 2009), we hypothesized that auxin may also be a key signal in inflorescence arrest, especially given the high levels of auxin known to be produced in fruits and seeds in many species

(Gustafson, 1939; Bangerth, 1989; Serrani et al. 2010; Kanno et al. 2010). Previous work in Arabidopsis has identified a curve of hormone production in developing fruit, with a peak in auxin content at 6 dpa (Kanno et al. 2010). To confirm whether fertilization increases the auxin content of Arabidopsis fruit, sterile (*ms1-1*) and fertile (L*er*) fruit were sampled at 6 dpa, and auxin levels were quantified using ultra-high-performance liquid chromatography–tandem mass spectrometry (UHPLC–MS/ MS). This analysis showed that auxin levels are much higher in fertile fruit (392 pg mg^{-1} tissue) than in sterile fruit (16 pg mg^{-1} tissue; Figure 4.6 D), a difference further amplified by their tenfold greater mass (Extended Data Figure 4.1 A). We next ascertained whether fertile fruit indeed transport auxin into the stem, by collecting auxin exported from the pedicels of 6-dpa fertile fruit from the PI. We found that individual fertile fruit export ~75 pg of auxin in 21 h, which is 7.5-fold higher than for equivalent sterile fruit (Figure 4.6 E). Given that the equivalent pool of mobile auxin collected from the associated inflorescence stem is ~100–200 pg (Prusinkeiwicz et al. 2009), it is clear that a small number of fertile fruit make a very significant contribution to auxin levels in the inflorescence stem.

For direct testing of this model, we assessed whether exogenous application of auxin to sterile fruits could restore timely arrest of the PI. We treated sterile fruit in the *aborted microspores* (*ams*) mutant which, like *ms1*, fails to undergo normal arrest (Ferguson et al. 2017), with the auxin analogue 1-naphthaleneacetic acid (NAA) from 6 dpa. This resulted in earlier inflorescence arrest, with the PI producing ~50 fruit compared to ~80 in mock-treated plants (Figure 4.6 A). In auxin-treated *ams* plants, arrested inflorescences have the normal bud cluster morphology associated with the arrest of wild-type inflorescences (Figure 4.6 C). As expected, although auxin treatment occurred throughout flowering it induced arrest only at the time that inflorescences normally become competent to arrest, at around 20 dpa (Figure 4.6 A). When we applied NAA to the uppermost ten sterile fruit of *ams* individuals at 20 dpa (and to any fruit subsequently formed in the following 3 d), this rapidly induced a normal arrest (Figure 4.6 B) through the treatment of relatively few (~18) sterile fruit (Figure 4.6 B), consistent

with the role of proximal fruit triggering inflorescence arrest only when the inflorescence is competent to do so. To rule out the possibility that auxin application to sterile fruit activates synthesis of a 'second messenger' that actually acts as an arrest signal, we performed NAA application at 23 dpa to de-fruited pedicels in *ams* mutants. This treatment was completely effective at inducing timely inflorescence arrest, unlike the mock treatment but similar to the fruit application experiments (Extended Data Figure 4.1 B). This shows that production of a second messenger in fruit is not required for arrest, although it is still possible that a second messenger could be produced in the stem.

If auxin exported from fertile fruits triggers arrest, treatments affecting the auxin transport system might be expected to inhibit the ability of fruit to export auxin and drive arrest. To test this idea, we analysed arrest in three mutants with reduced auxin transport: (1) *pin3 pin4 pin7* (*pin347*), which lacks three members of the PIN auxin efflux carrier family (Bennett et al, 2016); (2) *aux1 lax1 lax2 lax3* (*aux1 lax123*), which lacks all members of the AUX/LAX family of auxin influx carriers (Bainbridge et al. 2008); and *smxl6 smxl7 smxl8* (*smxl678*), which has a 60% reduction in PIN1 abundance and auxin transport in the stem (Soundappan et al. 2015). These mutants have some pleiotropic phenotypes, but are broadly wild type in terms of their branching architecture (Bennett et al. 2008; Bainbridge et al. 2008; Soundappan et al. 2015). Consistent with our hypothesis, two of these lines had delayed inflorescence arrest with a clear and lengthy delay in *aux1 lax123* and *smxl678* (Extended Data Figure 4.1 C). While *aux1 lax123* does reduce fruit fertility, *smxl678* mutants are normally fertile and set seed well (Soundappan et al. 2015), showing that the effect on inflorescence arrest, in this line at least, is not due to reduced fertility. We do not believe that the arrest defect in *smxl678* mutants is connected to their primary defect in strigolactone signalling, because mutants completely deficient in strigolactone signalling and synthesis arrest at essentially the same time as wild type (Extended Data Figure 4.1 E). Taken together, our data demonstrate that auxin is probably a key signal that triggers arrest in temporally competent inflorescences.

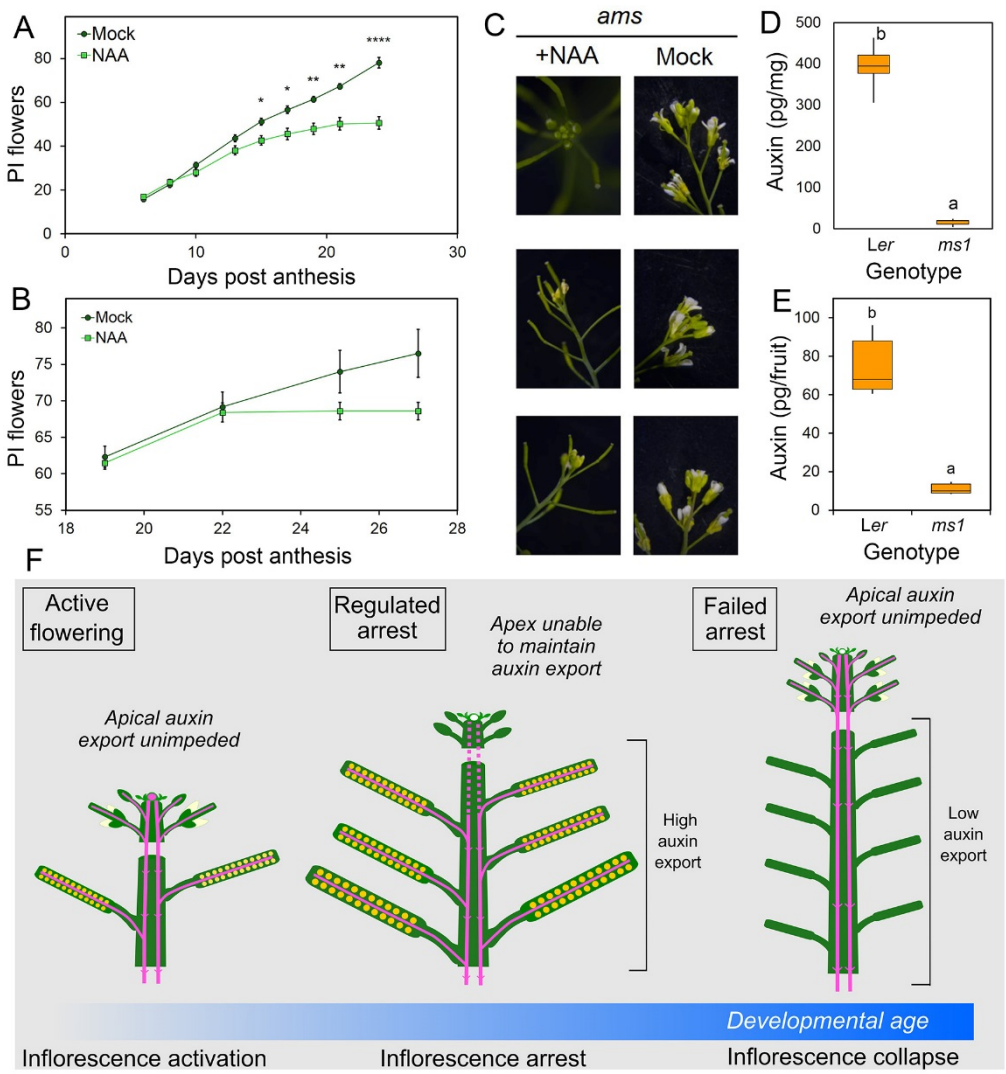

Figure 4.6. Auxin export from fruit triggers inflorescence arrest

(A) Temporal production of flowers by the PI of male-sterile *aborted microspores* (*ams*) plants following application of either 5 mg g^{-1} NAA in lanolin or a mock treatment consisting of lanolin and DMSO. Flower counts and lanolin treatment were performed every 2–3 d, starting from 6 dpa of the first flower on the primary inflorescence. n=7-12; bars indicate s.e.m. Asterisks indicate significance as determined by Sidak's multiple comparisons following fitting of a mixed-effects model; *p<0.05, **p<0.01, ***p=0.001, ****p=0.0001. **(B)** Temporal production of flowers on the PI of male-sterile *ams* following application of 5 mg g^{-1} NAA in lanolin or mock as in (A). Flower counts and lanolin treatment were performed every day, starting from 20 dpa. n=6-10; bars indicate s.e.m. **(C)** Representative photographs (three per treatment) showing inflorescence apices in *ams* mutants following NAA or mock treatment. NAA-treated plants arrested with a classic bud cluster morphology (Hensel et al. 1994), while mock-treated plants did not arrest and continued to open flowers. **(D)** Quantification of auxin content in 6 dpa fertile (L*er*) and sterile (*ms1*) Arabidopsis fruits. n=5. Bars with the same letter are not

statistically different from each other (two-tailed *t*-test, p<0.001). **(E)** Quantification of auxin eluted from fertile and sterile *Arabidopsis* fruits. n=5. For box plots, the upper and lower confines of the box indicate the interquartile range, the central line indicates the median and the whiskers represent the maximum and minimum values. Bars with the same letter are not statistically different from each other (two-tailed *t*-test, p<0.001). **(F)** Model for induction of inflorescence arrest. Initially, the apex can freely canalize to the polar auxin transport stream (PATS, pink). After a temporally defined period of flowering, inflorescences reach a critical age and become capable of arrest. In the presence of approximately six to eight fertile fruit containing seed (yellow circles), which actively export large quantities of auxin into the PATS, the apex is no longer able to canalize to the PATS. This induces inflorescence arrest, similar to bud dormancy. If fruit are sterile (or removed), the auxin export from proximal fruit is significantly reduced. This allows the apex to continue flowering beyond the point of arrest-competence, because it can still canalize to the PATS. Fertilization or auxin application at this point rapidly induces arrest. If no fertilization occurs, the meristem ultimately undergoes the terminal differentiation described in Hensel et al (1994).

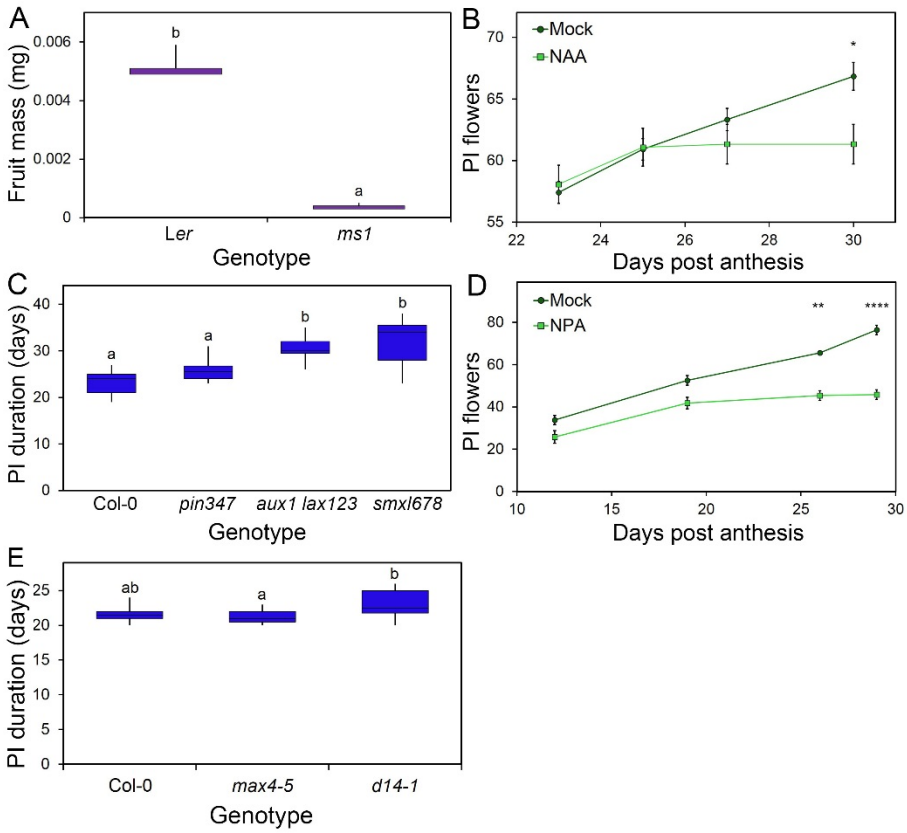

Extended Data Figure 4.1. Role of auxin transport in floral arrest

(A) Weight in milligrams of 5 fertile (L*er*) or sterile (*ms1-1)* fruits harvested at six days post anthesis. Bars with the same letter are not statistically different from each other (two-tailed T-test, p<0.001). **(B)** Temporal production of flowers by the PI of male-sterile *aborted microspores* (*ams*) plants upon application of either 5 mg/g NAA in lanolin, or a mock treatment consisting of lanolin and DMSO, to the de-fruited pedicels of the top 10 fruit in *ams* at 23 dpa; any further fruit produced were also treated in the same manner. n=12, bars indicate s.e.m. Asterisks indicate significance. **(C)** Effect of the auxin transport mutants *pin3-3 pin4-3 pin7-1* (*pin347*), *aux1 lax1 lax2 lax3* (*aux1 lax123*) and *smxl6-4 smxl7-1 smxl8-1* (*smxl678*) on primary inflorescence (PI) duration, relative to Col-0 wild-type. n=9-12. Bars with the same letter are not statistically different from each other (ANOVA, Tukey HSD test). **(D)** Effect of subapical NPA treatment on temporal flower production in the PI of the male-sterile line *ams*. An approximately 1 cm region directly below the apex of the PI was either treated with NPA (0.1 mg/g) in lanolin or a mock at 12 dpa. n=5, bars indicate s.e.m. Asterisks indicate significance as determined by Sidak's multiple comparisons following fitting of a mixed-effects model; *p<0.05; **p<0.01; ***p=0.001; ****p=0.0001. **(E)** Effect of the strigolactone mutants *max4-5 and d14-1* on primary inflorescence (PI) duration, relative to Col-0 wild-type. n=8-11. For box plots, the upper and lower confines of the box indicate the interquartile range, the central line indicates the median, and the whiskers represent the maximum and minimum

values. Bars with the same letter are not statistically different from each other (ANOVA, Tukey HSD test).

4.4 Discussion

Our research provides clearer understanding of the process of end-of-flowering in Arabidopsis, and the regulatory mechanisms that govern it. We show that end-of-flowering arises from the uncoordinated local arrest of inflorescences, rather than from a globally coordinated arrest, and that quasi-synchronicity of arrest is a natural consequence of the quasi-synchronous inflorescence activation. We show that inflorescences will arrest only when they become temporally competent to do so, which is probably a reflection of the developmental age of the inflorescence meristem. Our work thus complements the recent work of Balanzà et al. (2018), who showed that age-related up- and downregulation of the *FRUITFULL* and *APETALA2* transcription factors in inflorescence meristems is associated with delayed inflorescence arrest. FRUITFULL and APETALA2 are thus likely to be key factors determining the competence of inflorescence meristems to arrest, and may integrate external signals from the fruit (Balanzà et al. 2018).

We have shown that auxin exported from fruits triggers arrest in competent inflorescences. Auxin exported from dominant shoot apices is a potent but indirect inhibitor of AM activation (Walker and Bennett, 2018), suggesting that auxin exported from fruits might act analogously to indirectly inhibit inflorescence activity. This is corroborated by data from Wuest et al. (2016), who showed that arrested inflorescences meristems have a transcriptome similar to pre-activation AMs in Arabidopsis, supporting the idea that arrest might represent an inverse of AM/IM activation. Two major, non-mutually exclusive mechanisms have been proposed for the inhibitory effect of apical auxin on AM activation. In the second-messenger model, cytokinin and strigolactones are synthesized in the stem and are transported into buds where they promote and repress AM activation, respectively. In this model, apical auxin acts by repressing cytokinin and promoting strigolactone synthesis in the stem. Conversely, in the ‘canalization’ model of shoot branching, it is proposed that AMs need to create a canalized auxin transport link to the stem, to export auxin, and thus become active

(Prusinkiewicz et al. 2009; Shinohara, Taylor and Leyser, 2013). In this model, the presence of apical auxin reduces the auxin sink strength of the stem, limiting the number of AMs that can create a canalized link, and therefore grow (Prusinkiewicz et al. 2009; Shinohara, Taylor and Leyser, 2013). Building on this model, we propose that arrest-competent inflorescence apices become inhibited and deactivated because they are outcompeted for auxin sink strength in the stem by the considerable quantity of auxin exported from proximal fruit. This model in turn suggests that the arrest-competent state may be associated with a rapid loss of auxin source strength in the inflorescence apex (Figure 4.6 F). The result of losing the competition for auxin sink strength is that auxin transport connection between the apex and the stem is 'de-canalized', preventing further apical activity. It is important to note that in the canalization model it is not auxin accumulation in shoot apices that causes their growth inhibition, it is the loss (or lack) of a canalized auxin transport link in itself. In support of this model, we found that sub-apical application of the auxin transport inhibitor NPA, which completely blocks export of auxin from the PI, was sufficient to trigger regulated arrest in sterile *ams* inflorescences following the 20 dpa time point (Extended Data Figure 4.1 D).

Our work thus potentially expands the canalization framework to a new developmental process, but more work will be needed to test and model these ideas. We have also clearly shown that gibberellin signalling does not have a role in controlling inflorescence duration, despite the fact that it can affect fruit production. Nonetheless, this does not exclude a role for other phytohormones, as is seen in AM activation. The potential presence of additional signals is also reflected in the reinitiation of flowering that is observed in previously 'dormant' inflorescences (Figure 4.1 E). This occurs late in the plant life cycle once the seeds are maturing. At this stage the seeds/pods will have lower auxin levels, suggesting that additional signals may also be involved in this process. Overall, our model refines the GPA model of Hensel et al. (1994) and provides a mechanistic framework that would potentially allow for the duration of flowering to be extended or reduced to match local climatic conditions, whilst also containing a key

checkpoint so that flowering ceases only if fertile fruit have recently been produced. This paves the way to provide understanding of the end-of-flowering syndromes in other species which, in turn, has potential impact for extending and maximizing future crop yields.

4.5 Methods

4.5.1 Plant growth conditions

Plants for phenotypic and microsurgical experiments were grown on John Innes compost, under a standard 16/8 h light/dark cycle (20°C) in controlled environment rooms, with light provided by white fluorescent tubes at a light intensity of ~120 µmol m^{-2} s^{-1}. Plants for hormone profiling, DEX application and hormone application experiments were grown on John Innes no. 3 compost under the same light/dark cycle but at 22/18°C, with light provided by fluorescent tubes at an intensity of ~150 µmol m^{-2} s^{-1}.

4.5.2 Plant materials

Arabidopsis wild types Col-0 and L*er* were used as indicated. The following lines have previously been described: *ms1-1* (L*er* background)(Wilson et al. 2001); *AMS:AMS-GR ams* (used as *ams* mutants; Col-0 background, *ams* is SALK_152147)(Feng et al. 2008); *MS1:MS1-GR ms1-1* (L*er* background)(Ito et al. 2007); *rga-t2 gai-t6 rgl1-1 rgl2-1 rgl3-1* (*della*; L*er* background)(Feng et al. 2008); *pin3-3 pin4-3, pin7-1* (Col-0 background)(Bennett et al. 2016); *aux1 lax1 lax2 lax3* (Col-0 background)(Bainbridge et al. 2008); and *smxl6-4 smxl7-3 smxl8-1* (Col-0 background)(Soundappan et al. 2015).

4.5.3 Phenotypic assessment

We used the following nomenclature (Supplementary Figure 4.2). The primary embryonic shoot apex gives rise to primary leaves and eventually forms the primary inflorescence. Flowering branches that form from axillary buds in the axils of primary leaves are secondary inflorescences. Secondary inflorescences formed from primary cauline leaves are cauline inflorescences (denoted C1 and so on), while those from primary rosette leaves are rosette inflorescences (denoted R1 and so on). Secondary inflorescences are numbered in the order in which they activate, from the shoot apex

downwards through the cauline nodes, and then into the rosette nodes. Thus, C1 is the apical-most cauline inflorescence, C2 is the second apical-most inflorescence and so on. We have separated the numbering of the cauline and rosette nodes, such that R1 is the apical-most rosette inflorescence. Branches that form from secondary inflorescences are tertiary inflorescences, and so on, and are named after the parental branching system in rootward fashion (for example, C2.1 is the uppermost tertiary branch on the second cauline inflorescence).

For the timing data in Figures 4.1 A–C, 4.2 E, 4.3 A,C and 4.5 A,C,E, Extended Data Figure 4.1 C,E and Supplementary Figures 4.1 and 4.3 A, plants were assessed daily until visible flower buds were present at the shoot meristem. Dates of floral transition were recorded, and plants were assessed daily as appropriate for inflorescence activation (scored when buds were longer than 10 mm) and inflorescence arrest (scored when there were no more open flowers on the inflorescence). For fruit counts in Figures 4.1 D, 4.3 B and 4.5 B,D and Supplementary Figure 4.3 B, the number of inflorescences was counted and the number of fruits on each inflorescence recorded (or the number of fruits removed). Fruit counts were made at final arrest unless otherwise stated.

For the DEX-induction experiment, *MS1:MS1-GR ms1-1* plants were treated with either a solution consisting of 10 ml distilled water, 25 μM dexamethasone (from a 25 mM stock in ethanol) and 2 μl Silwet-77, or a mock containing the same but with ethanol only. Treatments were carried out at 11 and 12 dpa, and fruit number was subsequently counted at the time points indicated. Following arrest of DEX-treated plants, the percentage fertility in all plants was evaluated counting the number of fruit that had extended.

4.5.4 Microsurgical experiments

Flower removal in Figures 4.2 B–D and 4.5 A–E was performed every 1–2 d by removal of all open flowers on the plant between the stated time points. Branch removal in Figures 4.3 A–C was performed by cutting off branches at their base at the stated time point.

4.5.5 Indoleacetic acid (IAA) metabolite quantification

For quantification of IAA and IAA metabolites, 6-dpa fruits were sampled from mature flowering (~15–18 dpa) *ms1-1* and L*er* plants. Fruit age was tracked by marking their corresponding flowers with thread at 6 d previously, at anthesis. For the export assay the same strategy was used but, following excision, fruits were placed pedicel-down in closed PCR tubes containing 50 µl of 2.5 mM sodium diethyldithiocarbamate buffer and incubated for 21 h in a growth room. The samples were snap-frozen in liquid nitrogen and stored at −80°C until analysis, by either gas chromatography–MS/MS as described in Prusinkiewicz et al. (2009)(eluates) or UHPLC–MS/MS as described in Novák et al. (2012); in the latter, before UHPLC– MS/MS analysis the fruit tissues were extracted and purified according to Dobrev et al. (2002).

4.5.6 Hormone applications

For the 5 mg g^{-1} NAA lanolin treatments, 50 µl of either 100 mg ml^{-1} stock solution in DMSO or DMSO alone for the mock with 1 µl of dye was added to 1 g of molten lanolin (heated to 60°C) and subsequently shaken until completely incorporated. Sufficient paste to create a thin layer was then applied to the fruit using a micropipette tip. For the early/continual NAA application experiments, the application regimen began at 6 dpa of the first flower. For the late NAA application experiment, treatment was initiated at 20 dpa and only the top (that is, proximal to the inflorescence apex) ten fruits, and any produced above these in the subsequent 3 d, were treated. For NAA removal and

replacement treatments, plants were de-fruited of their top ten fruit at 23 dpa and the resulting cut pedicel was treated with NAA in lanolin, as in the late treatments. For NPA treatments, a region of ~1 cm directly below the apex of the PI was treated with either NPA (0.1 mg g^{-1}, from 100 mg ml^{-1} of DMSO stock) in lanolin or a mock (1 µl of DMSO in lanolin) at 12 dpa. Treatments were conducted at the same time as fruit number counts, indicated by the time points in the figures.

4.5.7 Experimental design and statistics

Sample sizes for each experiment are described in the figure legends. For plant growth experiments, each sample was a distinct plant. For auxin measurements, each sample was a set of tissues pooled from multiple plants; each sample was distinct. For data analysis, we tested data for normality to determine the most appropriate statistical test, except when mixed-effects models were used where, instead, sphericity was not assumed and the Greenhouse–Geisser correction was applied. For Sidak's multiple comparison, individual variances were calculated for each comparison.

References

Bainbridge, K., Guyomarc'h, S., Bayer, E., Swarup, R., Bennett, M., Mandel. T. et al. (2008). Auxin influx carriers stabilize phyllotactic patterning. *Genes Dev*, **22**, 810–823.

Balanzà V., Martínez-Fernández, I., Sato, S., Yanofsky, M.F., Kaufmann, K., Angenent, G.C. et al. (2018). Genetic control of meristem arrest and life span in *Arabidopsis* by a *FRUITFULL–APETALA2* pathway. *Nature Communications,* **9**, 565.

Bangerth, F. (1989). Dominance amongst fruits/sinks and the search for a correlative signal. *Physiologia Planta,* **76**, 608–614.

Bennett, T., Sieberer, T., Willett, B., Booker, J., Luschnig, C. and Leyser, O. (2006). The *Arabidopsis* MAX pathway controls shoot branching by regulating auxin transport. *Current Biology,* **16**, 553–563.

Bennett, T., Hines, G., van Rongen, M., Waldie, T., Sawchuk, M.G., Scarpella, E. et al. (2016). Connective auxin transport in the shoot facilitates communication between shoot apices. *PLoS Biology,* **14**, e1002446.

Dobrev, P.I. and Kamínek, M. (2002). Fast and efficient separation of cytokinins from auxin and abscisic acid and their purification using mixed-mode solid-phase extraction. *Journal of Chromatography A,* **950**, 21–29.

Feng, S., Martinez, C., Gusmaroli, G., Wang, Y., Zhou, J., Wang, F. et al. (2008). Coordinated regulation of *Arabidopsis thaliana* development by light and gibberellins. *Nature,* **451**, 475–479.

Ferguson, A.C., Pearce, S., Band, L.R., Yang, C., Ferjentsikova, I., King, J. et al. (2017). Biphasic regulation of the transcription factor ABORTED MICROSPORES (AMS) is essential for tapetum and pollen development. *New Phytologist,* **213**, 778–790.

Gustafson, F. (1939). Auxin distribution in fruits and its significance in fruit development. *American Journal of Botany,* **26**, 189.

Hensel, L.L., Nelson, M.A., Richmond, T.A. & Bleeker, A.B. (1994). The fate of inflorescence meristems is controlled by developing fruits in *Arabidopsis*. *Plant Physiology,* **106**, 863–876.

Ito, T., Nagata, N., Yoshiba, Y., Ohme-Takagi, M., Ma, H. and Shinozaki, K. (2007). *Arabidopsis* MALE STERILITY1 encodes a PHD-type transcription factor and regulates pollen and tapetum development. *Plant Cell,* **19**, 3549–3562

Kanno, Y., Jikumaru, Y., Hanada, A., Nambara, E., Abrams, S.R. Kamiya, Y. et al. (2010). Comprehensive hormone profiling in developing *Arabidopsis* seeds: examination of the site of ABA biosynthesis, ABA transport and hormone interactions. *Plant Cell Physiology,* **51**, 1988–2001.

Khan, M.R., Ai, X.Y. and Zhang, J.Z. (2014). Genetic regulation of flowering time in annual and perennial plants. *Wiley Interdisciplinary Reviews RNA,* **5**, 347–359.

Novák, O., Hényková, E., Sairanen, I., Kowalczyk, M., Pospíšil, T. and Ljung, K. (2012). Tissue-specific profiling of the *Arabidopsis thaliana* auxin metabolome. *The Plant Journal,* **72**, 523–536.

Prusinkiewicz, P., Crawford, S., Smith, R.S. and Leyser, O. (2009). Control of bud activation by an auxin transport switch. *PNAS,* **106**, 17431–17436.

Serrani, J., Carrera, E., Ruiz-Rivero, O., Gallego-Giraldo, L., Peres, L.E.P. and García-Martínez. J.L. (2010). Inhibition of auxin transport from the ovary or from the apical shoot induces parthenocarpic fruit-set in tomato mediated by gibberellins. *Plant Physiology,* **153**, 851–862.

Serrano-Mislata, A., Bencivenga, S., Bush, M., Schiessl, K., Boden, S. and Sablowski. R. (2017). DELLA genes restrict inflorescence meristem function independently of plant height. *Nature Plants,* **3**, 749–754.

Shinohara, N., Taylor, C. & Leyser, O. (2013). Strigolactone can promote or inhibit shoot branching by triggering rapid depletion of the auxin efflux protein PIN1 from the plasma membrane. *PLoS Biology,* **11**, e1001474.

Soundappan, I., Bennett, T., Morffy, N., Liang, Y., Stanga, J.P., Abbas, A. et al. (2015). SMAX1-LIKE/D53 family members enable distinct MAX2-dependent responses to strigolactones and karrikins in *Arabidopsis*. *Plant Cell,* **27**, 3143–3159.

Walker C. H. & Bennett T. (2018). Forbidden fruit: dominance relationships and the control of shoot architecture. *Annual Plant Reviews Online,* **1**, 1-38.

Wilson, Z.A., Morroll, S.M., Dawson, J. and Tighe, P.J. (2001). The *Arabidopsis MALE STERILITY1* (*MS1*) gene is a transcriptional regulator of male gametogenesis, with homology to the PHD-finger family of transcriptional regulators. *The Plant Journal,* **28**, 27–39.

Wuest, S.E., Philipp, M.A., Guthörl, D., Schmid, B. and Grossniklaus, U. (2016). Seed production affects maternal growth and senescence in *Arabidopsis*. *Plant Physiology,* **171**, 392–404.

Acknowledgements

A.W. was supported by BBSRC DTP grant no. BB/M008770/1. K.L. and J.S. are supported by the Knut and Alice Wallenberg Foundation, the Swedish Governmental Agency for Innovation Systems and the Swedish Research Council. We thank R. Granbom for technical assistance and the Swedish Metabolomics Centre (http://www.swedishmetabolomicscentre.se/) for access to instrumentation.

Author contributions

C.H.W., A.W., P.G.-S., J.S. and K.L. performed experiments and analysed the data. T.B., A.B. and Z.A.W. designed the study. All authors contributed to writing the manuscript.

Chapter 5

Cytokinin signalling regulates two-stage inflorescence arrest in Arabidopsis

Resubmitted to *Plant Physiology* following review, August 2022

Cytokinin signalling regulates two-stage inflorescence arrest in Arabidopsis

Catriona H. Walker[1], Alexander Ware[2], Jan Šimura[3], Karin Ljung[3], Zoe Wilson[2], Tom Bennett[1+]

[1]School of Biology, Faculty of Biological Sciences, University of Leeds, Leeds, LS2 9JT.

[2]School of Biosciences, University of Nottingham, Loughborough, Leics, LE12 5RD.

[3]Department of Forest Genetics and Plant Physiology, Umeå Plant Science Centre, Swedish University of Agricultural Sciences, 901 83 Umeå, Sweden

+ Address for correspondence: t.a.bennett@leeds.ac.uk

5.1 Abstract

To maximise reproductive success, flowering plants must correctly time entry and exit from the reproductive phase. While much is known about mechanisms that regulate initiation of flowering, the end-of-flowering remains largely uncharacterised. End-of-flowering in *Arabidopsis thaliana* consists of quasi-synchronous arrest of inflorescences, but it is unclear how arrest is correctly timed with respect to environmental stimuli and reproductive success. Here we show that Arabidopsis inflorescence arrest is a complex developmental phenomenon which includes arrest of the inflorescence meristem (IM), coupled with a separable 'floral arrest' of all unopened floral primordia; these events occur well before visible inflorescence arrest. We show that global inflorescence removal delays both IM and floral arrest, but that local fruit removal only delays floral arrest, emphasising their separability. We test whether cytokinin regulates inflorescence arrest, and find that cytokinin signalling dynamics mirror IM activity, while cytokinin treatment can delay both IM and floral arrest. We further show that gain-of-function cytokinin receptor mutants can delay IM and floral arrest; conversely, loss-of-function mutants prevent extension of flowering in response to inflorescence removal. Collectively, our data suggest that dilution of cytokinin among an increasing number of sink organs leads to end-of-flowering in Arabidopsis by triggering IM and floral arrest.

5.2 Introduction

In order to maximise reproductive success, flowering plants must simultaneously fulfil three distinct requirements. Firstly, the quantity of reproductive structures produced by the plant – inflorescences, flowers, fruits and seeds – must be carefully matched to the availability of resources (light, fixed carbon, nitrate, phosphate and water); both those already acquired by the plant, and those it might yet acquire (Walker & Bennett, 2018). Secondly, the timing of both the start and end of the reproductive phase must be optimised to occur in the correct season, and to coincide with the availability of both pollinators and crucially, potential mates. Thirdly, plants must measure their own reproductive success, and use this information to modify both the quantity of reproductive structures they produce, and the timing of their reproductive phase (Walker & Bennett, 2018). Plant typically meet all these criteria, producing a coherent and flexible 'reproductive architecture' that can react to changes in circumstance (Walker et al, 2021), but our mechanistic understanding of reproductive architecture control is still limited.

Given our knowledge of shoot branching control in flowering plants, it is very likely that the integration of long-distance hormonal signals plays a key role in determining the quantity of reproductive structures produced. For instance, soil nitrate and phosphate availability respectively upregulate cytokinin synthesis and downregulate strigolactone synthesis in the root (Takei et al, 2001; Umehara et al, 2010). Cytokinin and strigolactones are transported root-to-shoot, and are perceived in axillary buds to determine their outgrowth, respectively promoting and repressing outgrowth (reviewed in Wheeldon & Bennett, 2021), and thus connecting quantity of branches to soil resources. Apical dominance, which is driven by export of the hormone auxin from actively-growing shoot apices, also plays a key role in shoot branching regulation by inhibiting the activation of additional axillary buds through the self-organising properties of the auxin transport system (Prusinkiewicz et al, 2009; Shinohara et al, 2013; Bennett et al, 2016; van Rongen et al, 2019). Removing actively growing shoots removes this inhibition, and allows new axillary buds to activate and accurately replace the lost

branches (Walker et al, 2021); apical dominance thus acts as a mechanism by which plants can ‘measure’ their shoot branching. There is certainly evidence that both fruit and seeds can also act as sources of ‘dominance’ within the reproductive system (Bangerth, 1989), and can prevent new fruit, seed and inflorescences from developing (Walker & Bennett, 2018; Walker et al, 2021), probably also through their export of auxin (Bangerth, 1989; Lenser et al, 2018; Ware et al, 2020; Haim et al, 2021; Goetz et al, 2021). Furthermore, cytokinin has been shown to mediate the connection between soil nitrate resources and the activity of inflorescence meristems, which initiate new floral meristems at a greater rate (‘florochron’) as nitrate levels increase (Landrein et al, 2018).

The timing of reproduction – or at least its initiation – is generally very well understood in flowering plants. At least seven distinct environmental or internal cues are integrated together to regulate the floral transition that begins the reproductive phase (Cho et al, 2016; Gol et al, 2017). However, the events that contribute to end-of-flowering are generally much less studied, in part because end-of-flowering is a much more diverse phenomenon than floral transition (Gonzalez-Suarez et al, 2020). While floral transition is a single process, there are at least four different developmental processes by which end-of-flowering can occur, and different species use them in different combinations to end their reproductive phase (Gonzalez-Suarez et al, 2020). For instance, in Arabidopsis, end-of-flowering occurs because plants cease to initiate new inflorescences early in flowering, and because each inflorescence has a finite developmental lifetime (Ware et al, 2020). End-of-flowering in Arabidopsis was initially proposed to be a synchronised ‘global proliferative arrest’ (Hensel et al, 1994), but recent work demonstrates that each inflorescence stops opening new flowers through a locally-mediated process (‘inflorescence arrest’) that occurs independently of other inflorescences (Ware et al, 2020). The quasi-synchronous nature of inflorescence arrest in Arabidopsis is mostly explained by the quasi-synchronous initiation of inflorescences (Ware et al, 2020). The timing of inflorescence arrest can be modified by both local and systemic feedback from fertile fruit and inflorescences, forming a flexible system in which

developmental timing and measurement of reproductive success are coupled (Hensel et al, 1994; Ware et al, 2020; Wuest et al, 2016).

Most studies have viewed inflorescence arrest as resulting from the arrest of the inflorescence meristem (IM) itself (Hensel et al, 1994; Wuest et al, 2016; Balanzà et al, 2018; Merelo et al, 2022). Certainly the IM decreases in size and mitotic activity over the course of flowering (Wang et al, 2020; Merelo et al, 2022), before undergoing a regulated arrest toward end-of-flowering (Balanzà et al, 2018; Merelo et al, 2022), entering a quiescent 'dormancy-like' state (Wuest et al, 2016) and then undergoing a gradual senescence (Wang et al, 2020). It is also the case that extending the activity of the IM through genetic manipulations in key regulatory genes such as *FRUITFULL* can delay overall inflorescence arrest (Balanza et al, 2018; Martínez-Fernández et al, 2020; Merelo et al, 2022). However, it is unclear whether the normal end of flower opening in inflorescences is directly caused by IM arrest. Certainly, the floral meristems (FMs) in Arabidopsis can also undergo their own arrest (Lenhard et al, 2001; Lohmann et al, 2001; reviewed in Xu et al, 2019), and visible inflorescence arrest could be a result of this process, rather than directly due to IM arrest. Hensel et al (1994) showed that male sterility, and inflorescence/fruit removal (both before and after inflorescence arrest) could extend the lifetime of inflorescence development, either by delaying inflorescence arrest, or undoing arrest if it had already occurred. However, it is unclear how the changes in inflorescence arrest in these treatments are actually mediated at a developmental level. In our previous work, we showed that auxin exported from fertile fruits is required for timely inflorescence arrest (Ware et al, 2020), but again, did not identify which tissue is responding to this signal. In the present study, we therefore aimed to define the developmental processes underlying inflorescence arrest in Arabidopsis, and to understand in particular the mechanisms by which local and systemic measurement of reproductive success is integrated into these developmental processes.

5.3 Results

5.3.1 Arabidopsis inflorescence arrest consists of separate inflorescence meristem and floral arrest events

To define how Arabidopsis inflorescences arrest, we grew a large population of wild-type Col-0 plants. Each plant was sampled at a given timepoint after visible floral transition (days post bolting, dpb) and was destructively analysed to determine 1) the number of opened flowers; 2) the number of as-yet-unopened floral primordia and buds; and 3) the total number of floral nodes (i.e. the sum of 1 and 2) on the primary inflorescence (PI) at each timepoint. In this experiment, we observed that flower opening is a strongly linear process, with plants opening ~3 flowers/day from 6dpb (i.e. anthesis) until 17dpb (Figure 5.1 B), at which point the inflorescence arrests. We found that the initiation of floral nodes proceeds at the same linear rate, indicating that flowers mature at a constant rate after initiation (Figure 5.1 A). At the 0dpb timepoint, we found that inflorescences had already formed ~18 primordia, suggesting floral transition actually occurred 6 days before visible bolting. The initiation of floral nodes continued at 3/day, until it plateaued at 12dpb (Figure 5.1 A). This demonstrates that the IM stops initiating new floral primordia 5 days before visible inflorescence arrest, and that in the final phase, the inflorescence is only opening existing floral buds, and not initiating new ones. Our data thus indicate that Col-0 inflorescence lifetime consists of two overlapping stages; an IM-driven flower initiation phase which ends in IM arrest, and an independent flower-opening phase that ends in a ‘floral arrest’ event (Figures 5.1 A,B).

Consistent with these data, the number of as-yet-unopened floral primordia initially increases until 6dpb, at which point it plateaus; thereafter, new initiation of primordia is balanced by opening of flowers (Figure 5.1 C). The number of primordia then begins to decline from 12dpb, since no new floral primordia are being initiated, but flowers continue to open. Primordia number then plateaus again at 17dpb, after the opening of the final flowers, and the inflorescence arrests with cluster of ~15 unopened buds/primordia (Figures 5.1 C, E). Thus, the final set of floral primordia initiated from 8-

12dpb do not open, and the timing of IM arrest does not determine the timing of visible inflorescence arrest.

We also examined the morphology of the IM along this time-course. We found that distinct changes in meristem size coincide with changes in flowering (Figure 5.1 D). Interestingly, IM diameter is constant until approximately 6dpb (i.e. anthesis) and then shows two distinct stages of decline in diameter, with the first occurring between 7-12dpb, until the point of IM arrest. After IM arrest, there is a short plateau before a second decline between 15-17dpb, until the point of inflorescence arrest. Thus, physical changes in the IM mirror the discrete stages of inflorescence arrest we have identified. Our results are consistent with recent work which shows the same decline in IM size over inflorescence lifetime (Wang et al, 2020; Merelo et al, 2022), but provide a more high-resolution time-sequence and more nuanced results.

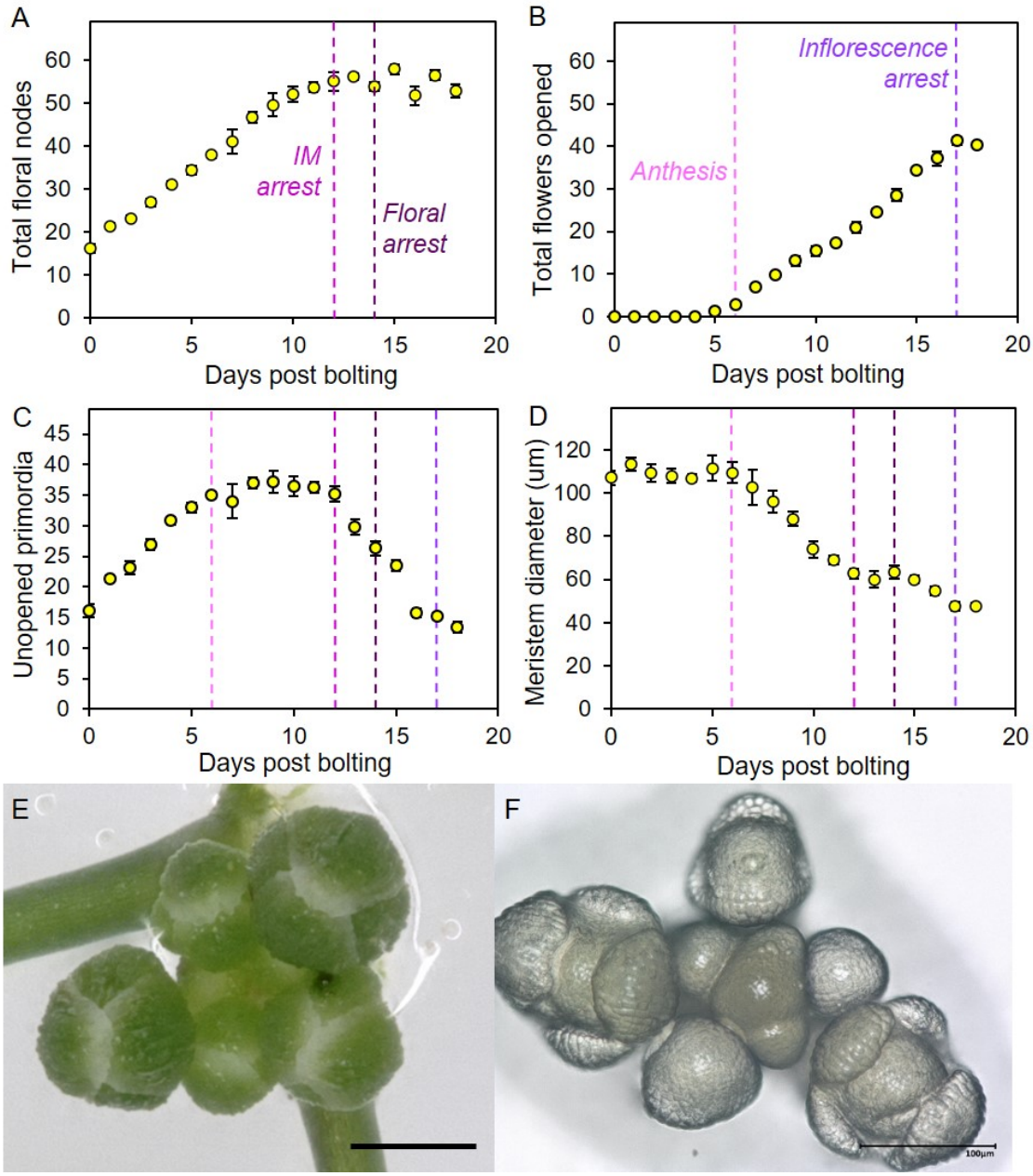

Figure 5.1. Inflorescence arrest is a two-stage process

Plants were grown in a controlled environment chamber and assigned randomised collection dates. Samples were collected daily from the primary inflorescence from 0 days post bolting (dpb) onwards. (A-C) Scatter graphs showing number of floral nodes **(A)**, the number of opened flowers (including previously opened flowers)**(B)** and the number of unopened floral buds and primordia **(C)** present along the primary inflorescence on each day post bolting. **(D)** Scatter graph showing mean IM diameter on each day post bolting. Error bars indicate s.e.m. The dashed vertical lines indicate the key points in inflorescence lifetime highlighted by this analysis: anthesis (6 dpb), IM arrest (12 dpb), floral arrest (14dpb) and inflorescence arrest (17 dpb). **(E)** Image showing a typical example of floral buds present within the bud cluster following the final flower opening. Scale bar = 500µm. **(F)** Image showing IM and remaining attached floral

primordia. The meristem is in the centre of the bud cluster, with progressively older floral primordia spiralling outwards. Scale bar = 100μm.

5.3.2 Floral arrest is a complex, non-meristematic phenomenon

A surprising outcome of our time-course data is the observation that the last flower to open at 17dpb was initiated at 7dpb (based on node number), just after anthesis and ~5 days *before* IM arrest (Figure 5.1). Thus, all subsequently-initiated flowers do not normally open, giving rise instead to the distinctive bud-cluster. Arabidopsis flowers develop and mature in a characteristic and predictable sequence, and thus the stage of development of a given flower reveals its approximate age (Smyth et al, 1990). While Smyth et al (1990) found that flowers took 13 days to open, flowers only took 10 days to mature under our growth conditions, implying each stage of development occurred at a faster rate. We reasoned that by examining the stage of development of the un-opened buds, we could establish approximately when floral arrest occurs, and we therefore dissected the oldest 6-9 floral primordia from arrested bud clusters. We found that the oldest primordia in the cluster are at stage 9 (‘*petal primordia stalked at base*’), with the stage of development reducing as we moved to progressively younger primordia, consistent with the timeline of Smyth et al, (1990) (Figure 5.2 A). Based on these data, it appears that when floral arrest occurs, all buds at stage 9 or younger halt at their current developmental stage. Stage 9 occurs at approximately 70% of the flower development time-course (Smyth et al, 1990), which in our conditions would be about 7 days after initiation. Given that the oldest flower in the cluster must have initiated at 7-8 dpb, this places the moment of floral arrest at 14-15dpb in the above experiment.

An interesting ramification of these data are that flowers older than stage 9 are ‘immune’ to floral arrest, and go on to fully develop and open. Thus, the final phase of flowering from 15-17dbp consists of the maturation of flowers that were at stages 10-12 when floral arrest occurred, but which were not ‘frozen’ at that development stage. The partial developmental stasis that results from floral arrest is unanticipated, and difficult to

explain. It does not seem to reflect changes to the activity of the floral meristem (FM), since FM activity ceases early in flower development once the stamen and carpel primordia form (stage 5-6)(Xu et al, 2019). Thus, the arrest of flowers at stages 6-9 cannot be explained by arrest of the FM.

5.3.3 Floral arrest is partially reversible, with stages 5 and 9 as developmental checkpoints

We observed that, if left undisturbed and continually watered after inflorescence arrest, up to 50% of Col-0 plants will naturally re-initiate flower opening on the primary inflorescence (after a delay of 5-10 days). These tend to be plants which opened a smaller proportion of their flowers in the first place, and may therefore still have available resources to produce more fruit (Figure 5.2 B). These newly-opened flowers are always preceded by a run of 6-9 ‘failed flowers’ produced by the oldest primordia in the bud cluster. These were also observed after inflorescence re-activation in the classic study of Hensel et al (1994). To gain more insight into this process, we dissected the flowers produced during inflorescence re-activation. We observed that all the ‘failed flowers’ were uniformly at stage 9 of development, with subsequent flowers being in a normal range from stage 17 downwards (Figure 5.2 C). Given that when floral arrest occurs, primordia are halted in their current stage, these data imply that upon inflorescence re-activation, the oldest 6-9 primordia recommence development, but become ‘stuck’ at stage 9. However, the younger primordia are able to complete development successfully. Based on the number of failed flowers after re-opening, and on our staging of bud clusters (Figure 5.2 A), the failed flowers very likely correspond to the primordia that were at stages 6-9 when floral arrest occurred, with flowers at stages 5 and below being able to form normal, fertile flowers.

These data suggest the unexpected existence of two distinct developmental checkpoints during flower development at stages 9 and 5. Flowers above stage 10 seem to be irreversibly committed to opening, but any flower below stage 9 can be halted in

development. Flowers below stage 5 can successfully re-initiate complete development, but flowers that have passed stage 5 can only re-initiate development as far as stage 9, before becoming 'stuck'. Given that the FM arrests shortly after stage 5, it is likely that the stage 5 checkpoint relates to the ability to re-initiate FM activity, but the stage 9 checkpoint lacks a clear explanation.

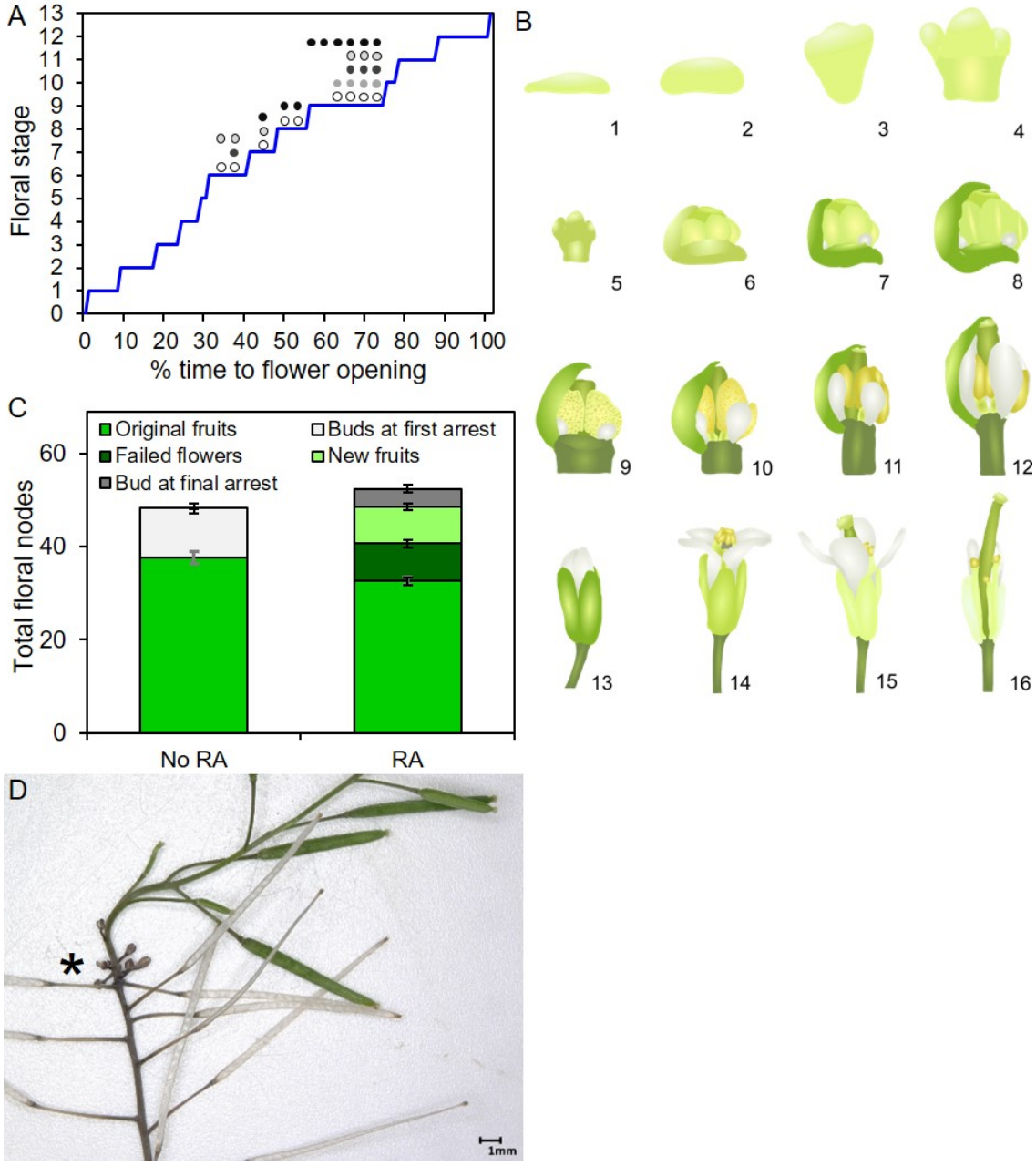

Figure 5.2. Floral arrest is a complex developmental phenomenon

(A) Line graph showing the timing of different floral development stages in Arabidopsis up to flower opening (stage 13), in relative developmental time. After Smyth et al, 1990; see panel B for illustrations). Superimposed are the developmental positions of the oldest floral primordia in the arrested bud clusters of 5 plants (each circle represents one

primordium). **(B)** Cartoon illustrating the floral development stages in Arabidopsis, after Smyth et al, 1990. Stages 6-12 are shown in cutaway view, without the enclosing sepals. Key stages for this work are 5 (petal and stamen primordia arise), 6 (sepals enclose bud), 7 (long stamen primordia stalked at base), 8 (locules appear in long stamens), 9 (petal primordia stalked at base) and 10 (petals level with short stamens). **(C)** Stacked bar graph, showing the number of floral nodes on the PI produced in Col-0 plants left untreated for sufficient time, which either reactivated (RA) or did not (No RA). The total floral nodes (i.e. the height of the full stack) is broken down into fruit produced on the PI during initial flowering (mid-green, lower bars), plus either a) the number of buds and primordia remaining in the bud cluster at first arrest (light grey)(untreated plants only), or b) the number of failed flowers (dark green), new fertile fruits (light green) and the number of buds and primordia remaining in the bud cluster at final arrest (dark grey)(treated plants only). Error bars indicate s.e.m, n = 21 (no RA), 20 (RA). **(D)** Photo showing within-inflorescence reflowering in Col-0, with older fruit dehisced, a small cluster of characteristic failed flowers (asterisk) and then resumption of fertile flower opening.

5.3.4 Cytokinin signalling regulates inflorescence arrest

We previously showed that auxin export from fruit formed late in flowering is required for inflorescence arrest (Ware et al, 2020); given the data presented here, we are therefore confident that this auxin export is a key regulator of **floral** arrest. However, IM arrest occurs too early to be caused by late-formed fruit, and we have previously shown that early-formed fruit have no impact on inflorescence arrest (Ware et al, 2020). It therefore appears unlikely that auxin dynamics regulate IM arrest. Cytokinin is an important root-shoot signal, the availability of which has previously been shown to regulate IM activation and activity in relation to environmental stimuli (Landrein et al, 2018; Müller et al, 2015). We therefore reasoned that IM arrest might be regulated by cytokinin dynamics in the shoot system.

To test this idea, we firstly examined cytokinin signalling dynamics in the IM by confocal microscopy, using the *TCSn:GFP* reporter line (Liu & Müller, 2017) to visualise the magnitude of cytokinin signalling over the course of IM lifetime. In untreated plants, we saw a marked decrease in cytokinin signalling in the IM between 3dpb and 15dpb, the time-frame in which the IM typically arrests (Figures 5.3 A-H). Consistent with this, using qRT-PCR we also observed concomitant reductions in the expression of *ARR5* and *ARR7*, two primary cytokinin response genes, in inflorescence apices over the same time frame (Figures 5.3 I,J). Thus, changes in the IM activity are closely mirrored by changes in CK signalling in the IM.

We next tested whether cytokinin treatment is sufficient to delay inflorescence arrest. We applied 1mg/g cytokinin in lanolin to specific siliques at 12 days post anthesis. We observed a clear delay of inflorescence arrest, with treated plants continuing to produce and open flowers long after control plants had ceased to do so (Figure 5.3 K). Application of 0.1mg/g CK however had no obvious effect, with inflorescence arrest and fruit number being the same as untreated plants, showing the effect is strongly dose-dependent on cytokinin concentration (Figure 5.3 L). Cytokinin at sufficiently high levels is therefore able to extend flowering duration.

We then tested whether mutants with altered cytokinin signalling showed altered inflorescence arrest. We were particularly interested in the *rock2* and *rock3* mutants, which have increased cytokinin sensitivity, and have previously been described as producing more fruit along the main inflorescence before arrest; however, it was not entirely clear whether this was due to increased rate of development, or delayed arrest (Bartrina et al, 2017). We observed that *rock2* arrested ~5 days later than the WT under our conditions, while *rock3* arrests an additional 5 days later that *rock2* (Figure 5.3 M). Taken together, our results therefore strongly suggest that cytokinin regulates the duration of inflorescence activity.

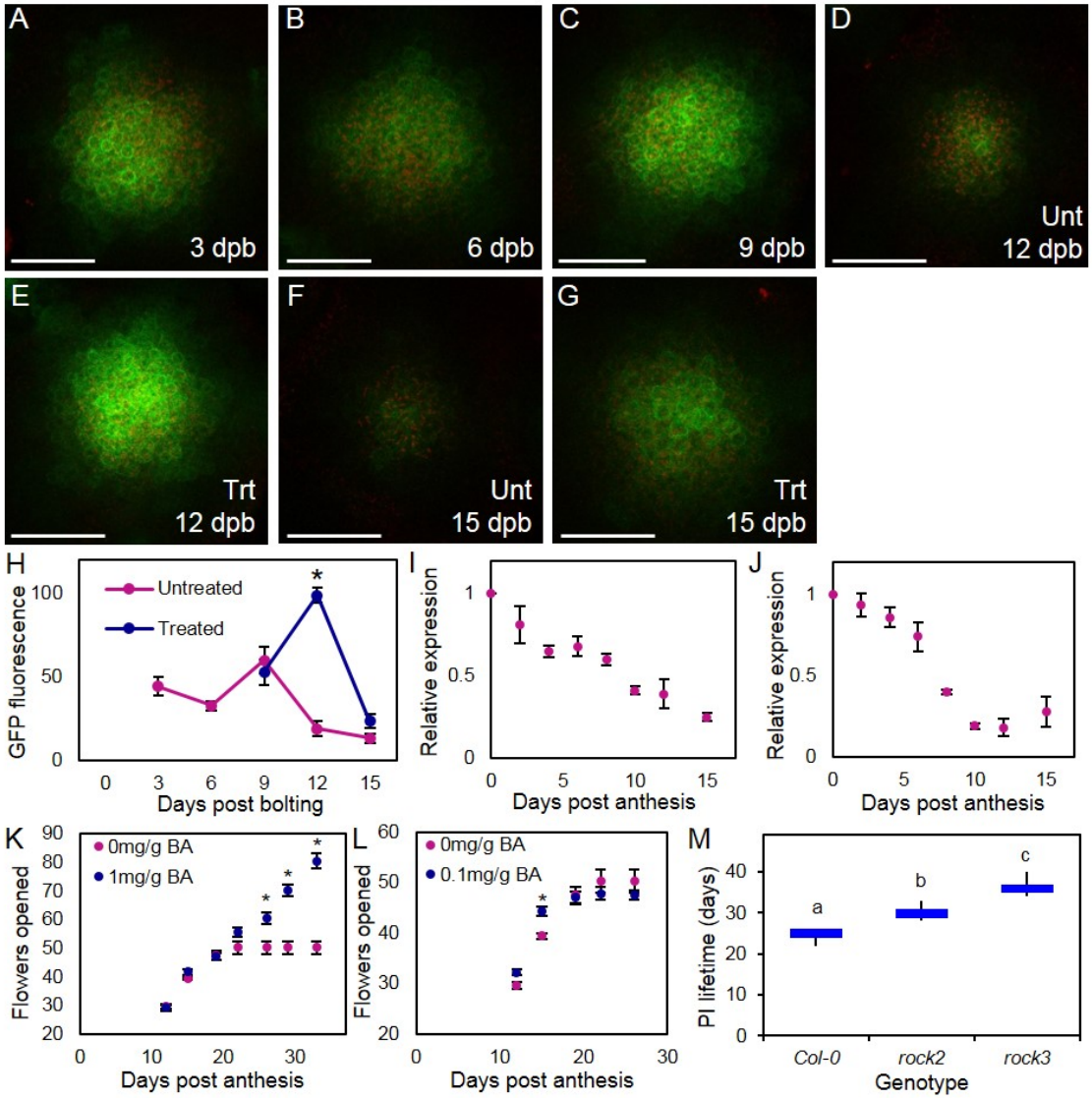

Figure 5.3. Cytokinin signalling regulates IM arrest

(A-G) Confocal microscopy images of primary IMs in Arabidopsis *TCSn:GFP* plants. GFP fluorescence is shown in green, chloroplast autofluorescence in red. Images taken from

IMs dissected at 3 **(A)**, 6 **(B)**, 9 **(C)**, 12 **(D,E)**, 15 **(F,G)** days post bolting (dpb). Plants were either untreated **(A-D,F)** or treated with removal of all secondary inflorescences at 6dpb **(E,G)**. Scale bars = 50μm. **(H)** Quantification of relative GFP fluorescence (in arbitrary units) in primary IMs of Arabidopsis *TCSn:GFP* plants between 3 and 15dpb, in untreated plants, or plants treated with removal of all secondary inflorescences at 6dpb. Data are means of n=5-6 meristems (except 9dpb treated, n=2), error bars show s.e.m. Asterisks indicate significant difference in treated samples from untreated control (t-test, n=5-6 $p<0.005$); other timepoints are not significantly different. (I,J) Relative expression of *ARR5* **(I)** and *ARR7* **(J)** in inflorescence apices at different days post anthesis. Quantification of the relative abundance of the transcript of *ARR5* and *ARR7* in inflorescence apices (all unopened buds) in wild-type Col-0 plants harvested following the anthesis of the first flower (day 0) until inflorescence arrest (day 15) by qRT-PCR. Data are means of 4 biological replicates, error bars show s.e.m. **(K,L)** Effect of cytokinin application to fruits on the primary inflorescence (PI) on the duration of flowering, as measured by rate of fruit production. Fertile L*er* plants were treated from 12 days post anthesis with 6-benzlyaminopurine (BA) dissolved in lanolin treatment at 1mg/g **(K)**, 0.1mg/g **(L)**, or a mock treatment of lanolin only. Significant differences between treatments at the same timepoint are indicated by asterisks (Sidak's multiple comparisons, on a mixed-effects model, $p<0.05$, n=8 (mock), 9 (0.1mg/g), 7 (1mg/g)). All other timepoints were not significantly different between treated and control groups. **(M)** Box plot showing primary inflorescence lifetime (days) of Arabidopsis cytokinin mutants. Bars with the same letter are not significantly different from each other (ANOVA, Tukey HSD test, n=4-12). Box indicates the interquartile range, internal line shows the median. Whiskers indicate maximum and minimum values.

5.3.5 Cytokinin signalling adjusts both IM and floral arrest

Our results indicated cytokinin was likely a very important factor in regulating inflorescence arrest, but did not indicate exactly where cytokinin acts. To understand this, we carefully examined the arrest phenotype in *rock2*, *rock3* and *ahk2-2 ahk3-3* (hereafter *ahk2/*3) mutants. The mutants *rock2* and *rock3* have gain-of-function mutations in the cytokinin receptors ARABIDOPSIS HISTIDINE KINASE2 (AHK2) and AHK3 respectively, which confer increased cytokinin sensitivity (Bartrina et al, 2017); the *ahk2 ahk3* double mutant has a loss of function in both receptors, resulting in reduced cytokinin sensitivity (Nishimura et al, 2004; Higuchi et al, 2004).

As in our earlier experiment (Figure 5.1), we tracked the number of floral nodes initiated, the number of opened flowers and the number of unopened buds and primordia on the PI for each genotype, over the course of inflorescence lifetime. Control Col-0 plants in this experiment underwent anthesis at ~7dpb (Figure 5.4 A), IM arrest at ~15dbp (Figures 5.4 B,C) and inflorescence arrest at ~24dpb (Figures 5.4 A,C). IM diameter decreased between anthesis and IM arrest, as also previously observed (Figure 5.4 D).

We found that *ahk2/3* mutants behave in a similar manner to Col-0 in terms of inflorescence lifetime, undergoing anthesis at ~7dpb, IM arrest at ~15dpb, and inflorescence arrest at ~24dpb. The major effect of *ahk2/3* was a reduction in the rate of IM activity, with fewer nodes initiated each day, leading to fewer flowers opening per day (2.3 vs 1.8 per day in Col-0 and *ahk2/3* respectively), and ultimately less nodes and flowers being formed (day 24: ANOVA + Dunnett's, $p<0.05$, $n=4$). This is highly consistent with previous data showing that cytokinin controls the activity of the IM in response to environmental conditions (Landrein et al, 2018).

The PIs of *rock3* behaved very similarly to Col-0 until inflorescence arrest, although they likely underwent slightly earlier IM arrest than Col-0 (Figure 5.4 B,C) producing less floral nodes in total (day 24: ANOVA + Dunnett's, $p<0.05$, $n=4-5$). However, *rock3* plants continued opening flowers for longer than Col-0, until the bud cluster was almost extinct (Figure 5.4 C), opening ~10 more flowers in total (Figure 5.4 A). The phenotype of *rock3* therefore clearly decouples the two stages of inflorescence arrest; there is no increase in IM activity, but a clear increase in flower-opening. We also observed that 30% of IMs in *rock3* also terminated in a terminal flower/fruit, a phenotype never observed in untreated Col-0 (Supplementary Figures 5.1 A,B).

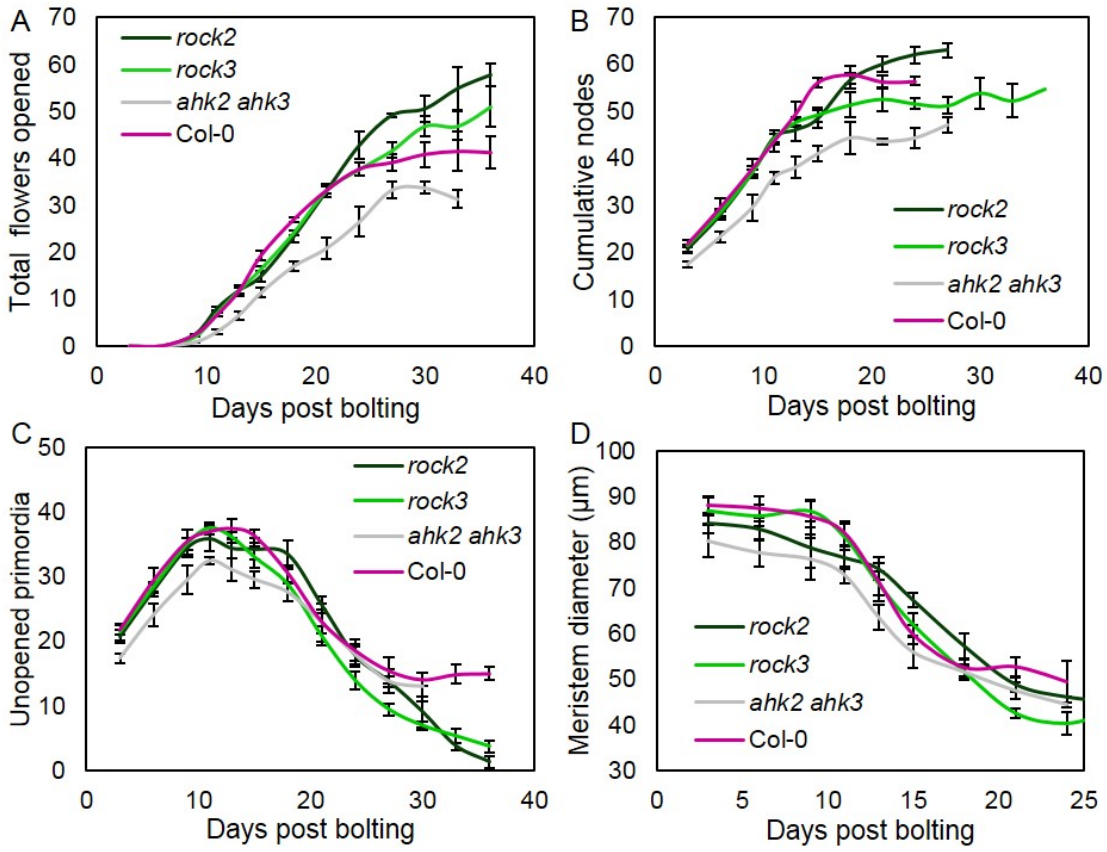

Figure 5.4. Cytokinin signalling regulates IM and floral arrest

(A-D) Large populations of Col-0, *ahk2-2 ahk3-3* (*ahk2/3*), *rock2* and *rock3* plants were grown under controlled conditions. The timing of visible bolting was recorded for each plant. Plants were randomly assigned to be sampled on a given number of days post-bolting, and then destructively sampled at that timepoint. Timepoints were spaced every 2-3 days, and 3-12 plants sampled for each timepoint. Error bars for all graphs show standard error of the mean. The data presented in Figures 5.4 A-D are two-timepoint rolling averages of the raw data presented in Supplementary Figures 5.2 A-D respectively, in order to show slightly smoothed versions of the data, illustrating the overall trend. (A) Scatter graph showing mean opened flowers, at each timepoint from 0-33/36dpb for each genotype. (B) Scatter graph showing the number of total floral nodes present at each timepoint from 0-24/27/36dpb for each genotype. (C) Scatter graph showing the number of unopened primordia present in the inflorescence apex at each timepoint from 0-30/36dpb for each genotype. (D) Scatter graph showing the inflorescence meristem diameter at each timepoint from 0-30/36dpb for each genotype.

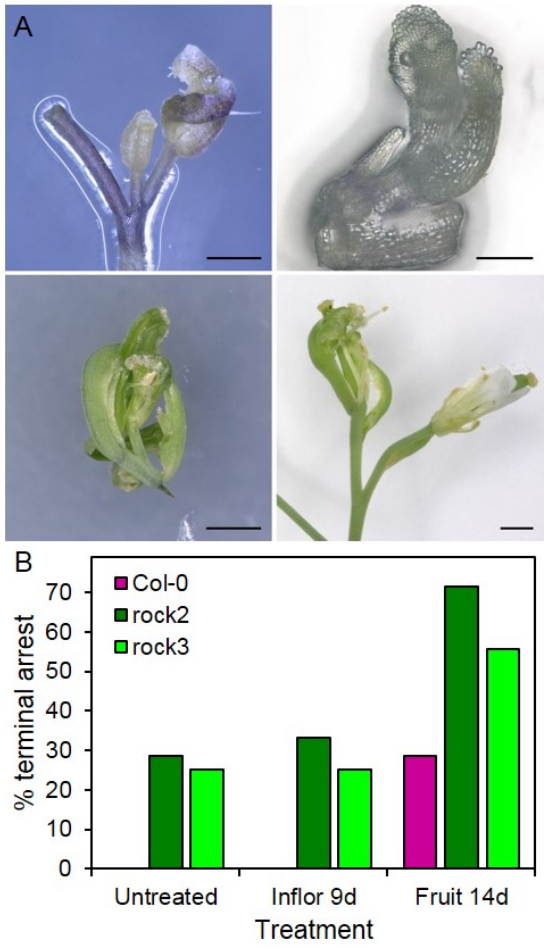

Supplementary Figure 5.1. Systemic and local stimuli increase and extend flower opening

(A) Light micrographs showing terminal flowers/fruit resulting from terminal differentiation of the IM in plants treated with fruit removal at 14 days post bolting (dpb) and continuously thereafter. Bar indicates 500µm (top left), 100µm (top right), or 1000µm (bottom left and right). **(B)** Bar graph showing frequency of terminal flower/fruit occurrence in Col-0, *rock2* and *rock3* plants either untreated, or treated by removal of all inflorescences apart from the primary inflorescence (PI) at 9dpb (Inflor 9d) or removal of all fruits from the PI at 14dpb and continuously thereafter (Fruit 14d).

The PIs of *rock2* also behaved very similarly to Col-0 for the first 10 days of the experiment (Figures 5.4 A,B,C), at which point the rate of IM activity seemed to slow down slightly compared to Col-0, (Figure 5.4 B). However, they continued to initiate new floral nodes for longer than Col-0, with IM arrest delayed until ~22dpb (Figures 5.4 B,C), and eventually produced significantly more floral nodes that Col-0 (day 24: ANOVA + Dunnett's, $p<0.05$, n=3-5)(Figure 5.4 B). Furthermore, *rock2* mutants also continued

opening flowers for longer than Col-0, even taking into account the delay in IM arrest (Figures 5.4 A,C). They open flowers for ~14 days after IM arrest, compared to ~9 days in Col-0, until the bud cluster was almost extinct. Overall, the phenotype of *rock2* mutants is therefore qualitatively different to the effect of *rock3*; there is both a delay in IM arrest, with more floral nodes initiated in total, and a subsequent additive delay in floral arrest, with a greater proportion of flowers ultimately opened. Flowers opened until extinction in *rock2*, and we again observed that 30% of IMs in *rock2* terminated in a terminal flower/fruit.

The phenotype of *rock2* and *rock3* indicate that cytokinin might not only control the rate of activity in the IM (Landrein et al, 2018), but also the timing of both IM and floral arrest in inflorescences. The phenotypes of *rock2* and *rock3* are highly consistent with the expression patterns of *AHK2* and *AHK3*. *AHK2* is strongly expressed in both IMs and flowers, and *rock2* affects the arrest of both IMs and flowers; *AHK3* is primarily expressed in flowers, and *rock3* primarily affects the arrest of flowers (Schmid et al, 2005).

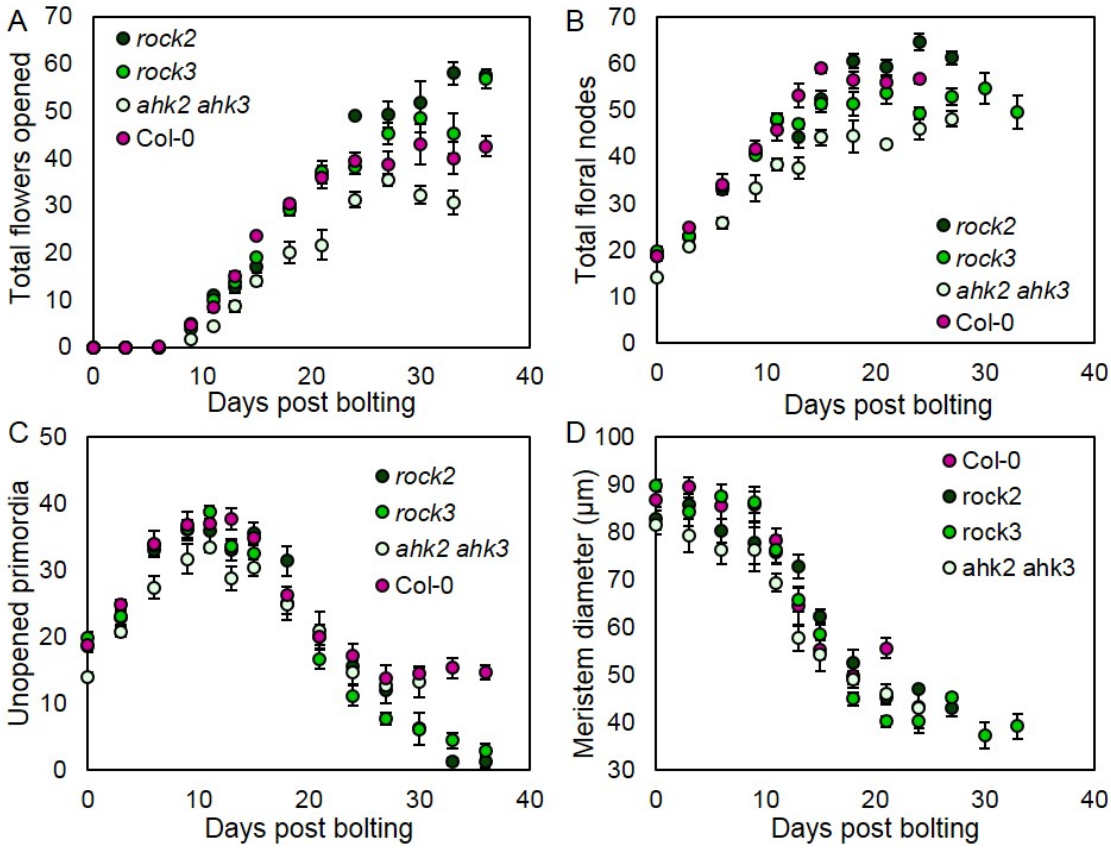

Supplementary Figure 5.2. Cytokinin signalling regulates IM and floral arrest

(A-D) Large populations of Col-0, *ahk2/3*, *rock2* and *rock3* plants were grown under controlled conditions. The timing of visible bolting was recorded for each plant. Plants were randomly assigned to be sampled on a given number of days post-bolting, and then destructively sampled at that timepoint. Timepoints were spaced every 2-3 days, and 3-12 plants sampled for each timepoint. Error bars for all graphs show standard error of the mean. These are the raw data, which are re-drawn in Figures 5.5 A-D as two-timepoint rolling averages of this data. **(A)** Scatter graph showing mean opened flowers, at each timepoint from 0-33/36dpb for each genotype. **(B)** Scatter graph showing the number of total floral nodes present at each timepoint from 0-24/27/36dpb for each genotype. **(C)** Scatter graph showing the number of unopened primordia (floral buds and primordia) present in the inflorescence apex at each timepoint from 0-30/36dpb for each genotype. **(D)** Scatter graph showing the inflorescence meristem diameter at each timepoint from 0-30/36dpb for each genotype.

5.3.6 Global inflorescence removal prolongs IM activity; local fruit removal prolongs flower opening

Collectively, our data (Figures 5.1-5.2) show that visible inflorescence arrest is an unexpectedly complex phenomenon that occurs as a result of separate IM arrest and floral arrest events that occur prior to visible inflorescence arrest. Our data also indicate that these events are separable, since *rock2* and *rock3* mutants affect these processes differentially. However, our data do not establish the functional relevance of these different events. The phenotypes of *rock2* and *rock3* mutants are qualitatively similar to those described by Hensel et al (1994) in both male sterile mutants and in plants treated by inflorescence or fruit removal. We thus hypothesised that floral arrest and IM arrest are separable processes that allow plants to flexibly and homeostatically respond to changes in the plants' reproductive success either locally (on the same inflorescence) or globally (on all inflorescences). To test this idea, we performed different treatments on Col-0 plants that, based on previous reports, we hypothesised would delay the timing of either IM arrest or floral arrest on the PI. Firstly, we continuously removed all inflorescences except the PI from plants 6dpb onwards, prior to IM arrest (Hensel et al, 1994), and secondly, we continuously removed fruit from the PI alone from 14dpb, prior to visible inflorescence arrest (Ware et al, 2020).

We firstly examined the rate of flower opening on the PI of Col-0 plants, which showed that both these treatments indeed increased the floral duration of the PI compared to untreated plants, which in this experiment again underwent inflorescence arrest at ~24dpb (Figure 5.5 A). Removing inflorescences from 6dpb resulted in an additional ~25 flowers opening, due to prolonged duration (by ~8 days), rather than increased rate of opening (Figure 5.5 A). Removing fruit from 14dpb also resulted in prolonged duration (~10 days), but with a slower rate of flower opening (~15 additional flowers at ~1.5/day)(Figure 5.5 A).

The qualitative differences between these treatments suggested that their effects arose from different developmental events. We therefore examined the timing of IM and inflorescence arrest in plants subjected to these treatments, using the same basic experimental design as in Figure 5.1. In this experiment, untreated plants underwent IM arrest at ~18dpb (Figures 5.5 C-F), and visible inflorescence arrest at ~22dpb (Figure 5.5 C). Plants treated with inflorescence removal from 6dpb showed a clear delay in IM arrest, continuing to initiate floral nodes for 5-6 days after control plants, and ultimately producing significantly more floral nodes (e.g. day 26: t-test, $p<0.05$, n=5)(Figures 5.5 C,D). Consistent with this, plants also showed a delay in reduction of IM size between 8-16dpb (Figure 5.5 B). Intriguingly, these plants also showed a clear delay in floral arrest; even accounting for the delay in IM arrest, the plants continued to open new flowers for 10 days after IM arrest (until ~32dpb), and arrested with a bud cluster of only 5 primordia. Thus, compared to control plants, the treated plants flowered for 10 days longer, initiated an additional 15 flowers, and opened an additional 25 (Figures 5.5 A-F).

In contrast, plants treated with local fruit removal after 14dpb showed no clear alteration in the timing of IM arrest (Figures 5.5 C,D), but did have a small and statistically non-significant increase in floral node number (by ~4 nodes)(e.g. day 26: t-test, $p>0.05$, n=5)(Figures 5.3 C,D). Conversely, they showed a very clear delay in floral arrest, continuing to open flowers for an additional ~14 days until 36dpb, resulting in the opening of an additional ~15 flowers, at which point the bud cluster was essentially exhausted (Figures 5.5 E,F). The nature of inflorescence arrest was different in these plants compared to plants with global inflorescence removal, in the sense that they opened flowers until the bud cluster was essentially exhausted. Furthermore, in ~30% of de-fruited plants, the IM was visibly consumed into a terminal flower or fruit (Supplementary Figure 5.1 A), which was never seen in untreated plants, or those treated with global inflorescence removal, but was previously observed in *rock2* and *rock3* (Supplementary Figure 5.1 B).

Thus, global inflorescence removal and local fruit removal both delay inflorescence arrest, but do so in qualitatively (and quantitatively) different ways. Early global inflorescence removal delayed both IM and floral arrest, but plants eventually underwent a ‘normal’ inflorescence arrest. Conversely, local fruit removal only delayed floral arrest, with no obvious change in IM activity (Figure 5.5 C,D), and led to an inflorescence arrest by extinction, with some terminal flower formation. These data therefore show that the two stages of inflorescence arrest are functionally distinct, and respond to different internal stimuli. Floral arrest is a highly sensitive process, which can be delayed by local deficits in reproductive success, whereas IM arrest is only sensitive to large deficits in reproductive success at the level of the whole plant. The separability of the two processes therefore likely gives plants two distinct strategies to flexibly respond to changes in their own reproductive success.

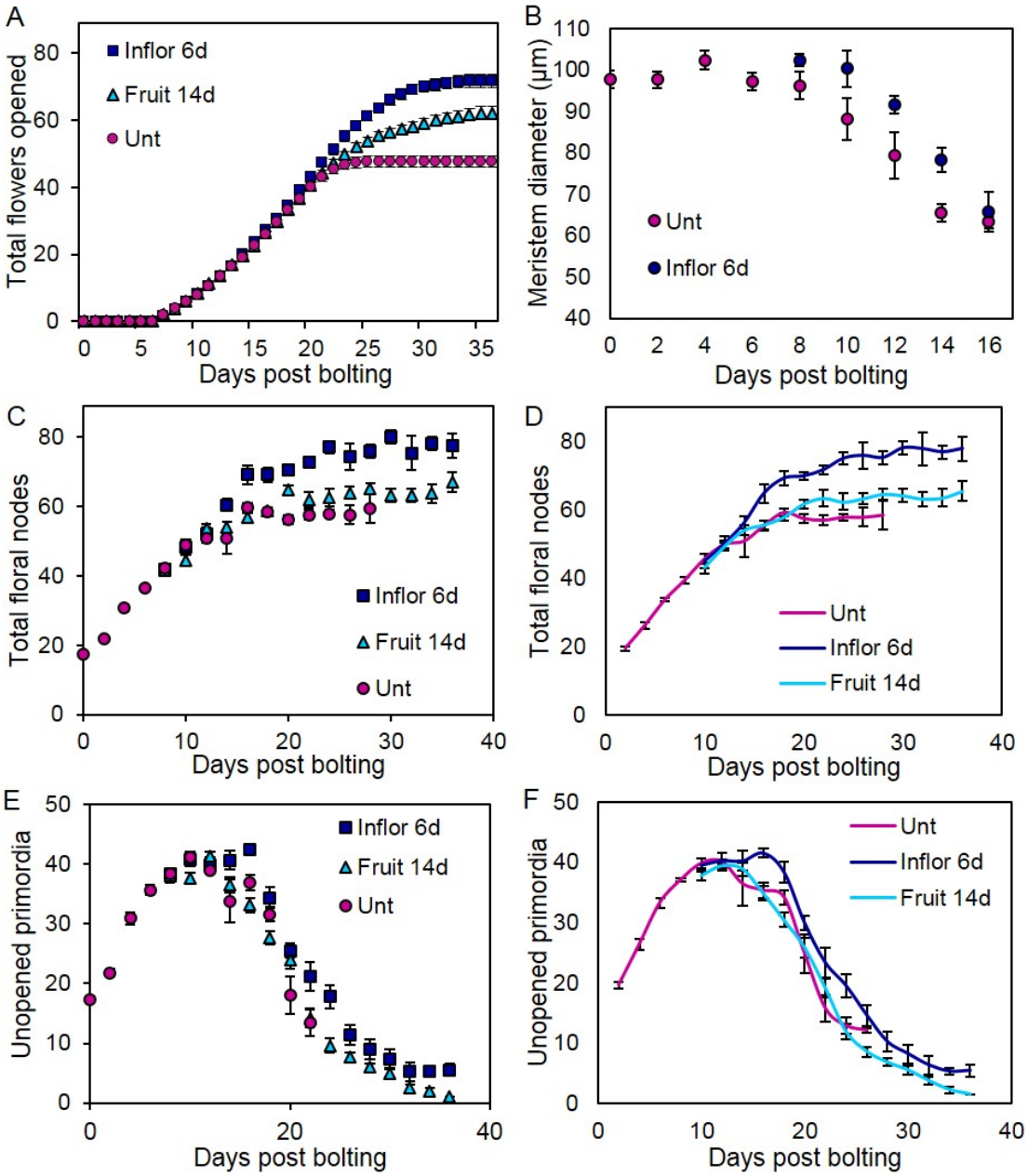

Figure 5.5. Systemic and local stimuli increase and extend flower opening

Based on observations in Figure 5.1, we performed 4 different treatments on flowering Col-0 plants. Firstly, we removed all inflorescences apart from the primary inflorescence (PI) from the plant at 6 days post bolting (Inflor 6d). This timepoint was chosen as the earliest timepoint at which secondary inflorescences are visibly elongating. We also removed all fruits from the PI at 14 days post bolting and continuously thereafter (Fruit 14d). This timepoint was chosen as the earliest timepoint at which sufficient numbers of developed fruit are present in order for their removal to potentially make a difference. **(A)** Scatter graph of cumulative flowers opened on the PI of each treatment each day post bolting; data collected non-destructively from individual plants. Error bars show s.e.m., n=10-13. **(B-F)** A large population of Col-0 plants were grown under controlled conditions. The timing of visible bolting was recorded for each plant. Plants were randomly assigned to be sampled on a given number of days post-bolting, and then

destructively sampled at that timepoint. Timepoints were spaced every two days, and 3-12 plants sampled for each timepoint. Error bars for all graphs show s.e.m. **(B)** Scatter graph showing mean IM diameter, from 0-16dpb for control plants, and day 6-16 from plants treated from day 6 with inflorescence removal. **(C)** Scatter graph showing the number of total floral nodes present from 0-28dpb for control plants, and from day 6-36/38 dpb for plants treated from day 6 with inflorescence removal or day 14 with fruit removal. **(D)** Scatter graph showing the data from **(C)** plotted as a two-timepoint rolling average in order to show a slightly smoothed version of the data illustrating the overall trend. **(E)** Scatter graph showing the total number of unopened floral primordia present in the inflorescence apex from 0-30dpb for control plants, and from day 6-36/38 dpb for plants treated from day 6 with inflorescence removal or day 14 with fruit removal. Buds and primordia were counted by dissecting buds from the bud cluster under a dissecting microscope. **(F)** Scatter graph showing the data from **(E)** plotted as a two-timepoint rolling average in order to show a slightly smoothed version of the data illustrating the overall trend.

5.3.7 Global inflorescence and local fruit removal can reactivate IM and FM activity

Hensel et al (1994) showed that individual inflorescences can also be induced to reactivate after inflorescence arrest in response to inflorescence or fruit removal. Given our new data, we questioned whether this occurs by reactivation of IM activity, flower opening, or both. We therefore treated Col-0 plants with global inflorescence removal after arrest of the PI, which promoted re-activation after an ~8 day delay, beginning with ~4 of the characteristic ‘failed’ flowers (Figure 5.2 D), before successful opening of ~9 new fertile flowers (Figure 5.6 A). Treated plants did not produce any additional floral nodes in total (Figure 5.6 A)(t-test, $p>0.05$, n=6-10), showing these changes are achieved by re-activation of flower opening without new IM activity. We also found that local fruit removal after arrest in Col-0 was able to trigger the same level of re-activation of FM activity, although the process occurred more quickly (within ~4 days)(Figure 5.6 C). Again, this occurs without any significant increase in the number of floral nodes initiated between treated and untreated plants (e.g. day 28, Mann-Whitney U-test, $p>0.05$, n=3-6) (Figure 5.6 D).

We also tested global inflorescence removal after arrest of the PI in the L*er* ecotype, in which Hensel et al (1994) performed their experiments. In contrast to Col-0, we found that inflorescence re-activation in L*er* involved reactivation of both IM and FM activity, with treated plants opening an additional ~33 new fertile flowers (and 9 failed flowers), but also showing a clear increase of ~17 total floral nodes over untreated plants (t-test, $p<0.0001$, $n=9$-11)(Figure 5.6 B). This unexpected ecotypic difference in IM reactivation potential between Col-0 and L*er* is intriguing, and might reflect the known roles of ERECTA in meristem maintenance (Mandel et al, 2014; Mandel et al, 2016; Zhang et al, 2021); it is possible that it is the *erecta* mutation itself that contributes to the difference between the ecotypes. Irrespectively, these data again emphasise the separability of IM and floral arrest as developmental processes.

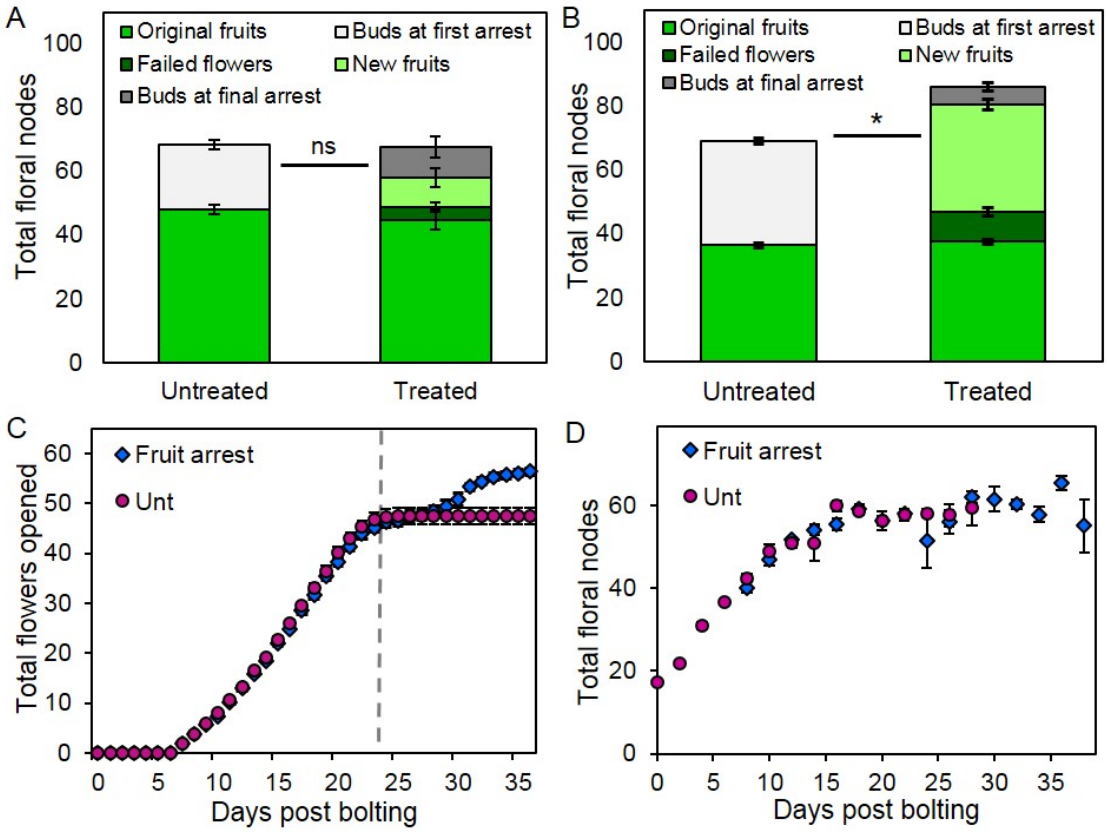

Figure 5.6. Reactivation of flower opening by inflorescence removal

(A) Stacked bar graph, showing the number of floral nodes on the PI produced in Col-0 plants either left untreated, or treated by removal of all other inflorescences after arrest of the PI. The total floral nodes (i.e. the height of the full stack) is broken down into fruit

produced on the PI during initial flowering (mid-green, lower bars), plus either a) the number of buds and primordia remaining in the bud cluster at first arrest (light grey)(untreated plants only), or b) the number of failed flowers (dark green), new fertile fruits (light green) and the number of buds and primordia remaining in the bud cluster at final arrest (dark grey)(treated plants only). Error bars indicate s.e.m, n=6-10. ns = no significant difference (t-test, $p>0.05$) between total floral node number between treated plants and untreated controls. **(B)** Stacked bar graph, showing the number of floral nodes on the PI produced in L*er* plants either left untreated, or treated by removal of all other inflorescences after arrest of the PI. The total floral nodes (i.e. the height of the full stack) is broken down into fruit produced on the PI during initial flowering (mid-green, lower bars), plus either a) the number of buds and primordia remaining in the bud cluster at first arrest (light grey)(untreated plants only), or b) the number of failed flowers (dark green), new fertile fruits (light green) and the number of buds and primordia remaining in the bud cluster at final arrest (dark grey)(treated plants only). Error bars indicate s.e.m, n=9-11. Asterisk indicates significant difference (t-test, $p<0.0001$) between total floral node number between treated plants and untreated controls. **(C)** Scatter graph of cumulative flowers opened on the PI of each treatment. Data collected non-destructively from 11 individual plants per treatment, assessed daily post bolting. 'Fruit arrest' plants were treated from 1 day after their arrest by the removal of all fruit on the primary inflorescence, then left to respond; 'Unt' plants were left untreated. The point of treatment for fruit arrest plants has been normalised to 24 days post anthesis (grey dashed line), such that day 25 shows plants 1 day post-treatment, etc. Error bars show s.e.m. **(D)** Scatter graph of total floral nodes present on the PI of each treatment. A large population of Col-0 plants were grown under controlled conditions; 'Fruit arrest' plants were treated from 1 day after PI arrest by the removal of all fruit on the PI, then left to respond. 'Unt' plants were left untreated. The timing of visible bolting was recorded for each plant; plants were then randomly assigned to be sampled on a given number of days post-bolting (or post-arrest), and then destructively sampled at that timepoint. Timepoints were spaced every two days, and 5-7 plants sampled for each timepoint. Error bars for all graphs show standard error of the mean. The point of treatment for fruit arrest plants has been normalised to 24 days post bolting (blue dashed line), such that day 25 shows plants 1 day post-treatment, etc. Error bars show s.e.m.

5.3.8 Cytokinin signalling is needed for homeostatic regulation of inflorescence arrest

Our data reveal some clear similarities between *rock2* and *rock3* mutants, and treatments which affect whole-plant reproductive success. The phenotype of *rock3*

mutants is very similar to the effect of local fruit removal, with a delay in floral arrest, including the formation of terminal flowers in ~30% of IMs (Supplementary Figure 5.1 B). The phenotype of *rock2* on the other hand, is similar to the effect of global inflorescence removal, with a delay in both IM arrest and floral arrest. However, *rock2* mutants also showed terminal flowers in ~30% of IMs, which was never seen in plants treated with global inflorescence removal. Thus the phenotype of *rock2* seems analogous to the effects of global inflorescence removal **and** local fruit removal.

Overall, our data suggest a model in which inflorescences and fruits act as sinks for cytokinin, and that their effect governs the timing of IM arrest and PI arrest. In support of this idea, we found that wild-type fertile fruit have much higher levels of *trans*-Zeatin riboside (*t*ZR) (the main transport form of *t*Z)(Hirose et al, 2008), and the signalling-active *t*Z form itself, compared to sterile fruit of the *male sterile1* (*ms1*) mutant (Figure 5.7 A). Conversely, sterile and fertile fruit contained similar quantities of isopentenyladenine (iP) and *cis*-Zeatin (*c*Z) cytokinins, showing there is not a general reduction in cytokinin in sterile fruit (Figure 5.7 A). We thus hypothesise that, as new inflorescences and fruits initiate during flowering, there is a resultant progressive dilution of cytokinin across the shoot system, which leads to reduced cytokinin levels in the IM of the primary inflorescence (Figures 5.3 A-H). This reduction in cytokinin contributes to inflorescence arrest by decreasing IM activity and flower opening (Figure 5.4). Conversely, if cytokinin sinks are removed (Figure 5.5), or if cytokinin sensitivity is increased (Figure 5.4), IM arrest and floral arrest in the PI are delayed. Consistent with this model, we found that plants treated with inflorescence removal at 6dpb showed a dramatic increase in cytokinin signalling in the IM at 12dpb consistent with the prolonged activity of these IMs, before returning to pre-treatment levels by 15dpb (Figures 5.3 A-H).

As a critical test of this model, we therefore hypothesised that *ahk2/3* should fail to respond to either inflorescence or fruit removal, and that conversely *rock2* and *rock3* should over-respond to inflorescence removal - but not to fruit removal, since they already open almost all flowers they produce. To test these hypotheses, we performed

inflorescence removal at 9dpb and fruit removal at 14dpb treatments in *ahk2/3*, *rock2* and *rock3* mutants. Consistent with our hypothesis, we found that *ahk2/3* showed very little response to either treatment, and no statistically significant difference in either the number of flowers opened or the overall lifetime of the PI (Figures 5.7 B,C). Similarly, we saw no significant difference in flowers opened or PI lifetime in *rock2* and *rock3* in response to fruit removal (Figure 5.7 B,C). However, we saw an increase the number of flowers opened in both *rock2* and *rock3* compared to Col-0, thus strongly supporting our hypothesis (Figure 5.7 B).

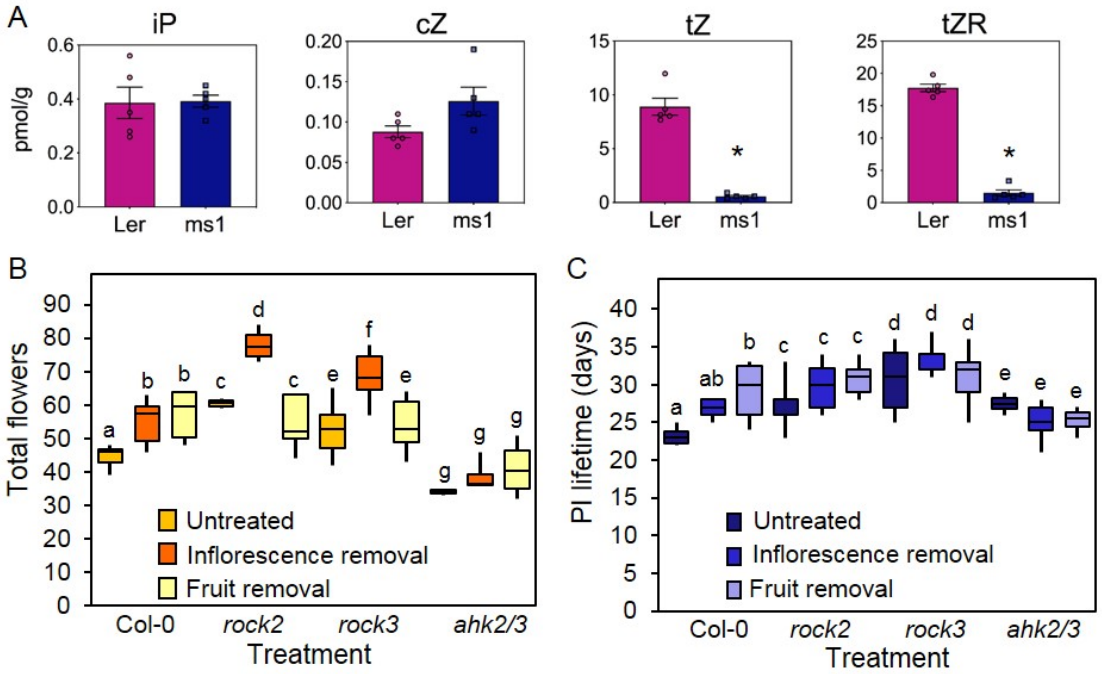

Figure 5.7. Cytokinin signalling is needed for homeostatic regulation of inflorescence arrest

(A) Concentration (pmol/g fresh weight) of the free cytokinin bases isopentenyladenine (iP), *cis*-Zeatin (cZ), *trans*-Zeatin (tZ) (biologically active cytokinins) and *trans*-Zeatin riboside (tZR) (major root-to-shoot transport form) in the fertile or sterile fruit of L*er* and *ms1* plants. n = 5 biologically independent samples (shown by overlying circles), error bars show s.e.m. Asterisk indicates significant difference from L*er* control (Mann-Whitney U-test, $p<0.05$, n=5). **(B)** Box plots showing the total number of opened flowers on the primary inflorescence of Col-0, *ahk2/3*, *rock2*, *rock3*, either untreated (yellow boxes), or treated with inflorescence removal at 9dpb (orange boxes), or fruit removal at 14dpb (beige boxes). Bars with the same letter are not statistically different from each other, (ANOVA + Tukey HSD, calculated separately within each genotype, n=2-9). **(C)** Box plots showing the inflorescence lifetime in days of the primary inflorescence of Col-0,

ahk2/3, *rock2*, *rock3*, either untreated (dark yellow boxes), or treated with inflorescence removal at 9dpb (orange boxes), or fruit removal at 14dpb (light yellow boxes). Boxes indicates the interquartile range, internal line shows the median. Whiskers indicate maximum and minimum values. Bars with the same letter are not statistically different from each other, (ANOVA + Tukey HSD, calculated separately within each genotype, n=2-9).

5.4 Discussion

5.4.1 Inflorescence arrest in Arabidopsis is a complex developmental phenomenon

Previous work has tended to view inflorescence arrest in Arabidopsis as a process driven by changes in the activity of the inflorescence meristem (IM) (Hensel et al, 1994; Wuest et al, 2016; Balanzà et al, 2018; Merelo et al, 2022). However, the fact that Arabidopsis inflorescences arrest with a cluster of unopen flowers calls into question this idea. If IM arrest directly led to inflorescence arrest, then inflorescence arrest should occur because of a lack of new flowers to open (as is indeed the case in many species). The results presented here clearly demonstrate that inflorescence arrest in Arabidopsis usually involves the arrest of both IMs and developing flowers, and show that that the timing of inflorescence arrest is more directly determined by the timing of floral arrest, rather than IM arrest. Our results show that IM and floral arrest are separate and separably-regulated processes, which can be delayed in response to global inflorescence and local fruit removal. A surprising aspect of our results is just how early the events that lead to inflorescence arrest occur. IM arrest occurs 5-9 days before visible inflorescence arrest, and the last flower to fully mature is typically initiated just after anthesis, ~5 days *before* IM arrest (Figure 5.1). Floral arrest seems to occur shortly after IM arrest, suggesting that both processes might occur in response to the same external stimuli, which are present during this phase in flowering.

Our results also provide important new information about the reversibility of arrest. Consistent with earlier reports, we show that IMs in L*er* enter a quiescent state upon arrest (Wuest et al, 2016), from which they can be reactivated in response to a loss of reproductive structures globally (Hensel et al, 1994; Merelo et al, 2022). However, we find that although Col-0 IM activity can be extended by global loss of reproductive structures (Figure 5.5), Col-0 IMs cannot be reactivated after IM arrest (Figure 5.6). The reason for this difference between Col-0 and L*er* ecotypes is unclear, but it represents a promising avenue for future investigation.

5.4.2 Auxin and floral arrest

While the process of IM arrest has previously been described (Wang et al, 2020; Merelo et al, 2022), our results define for the first time the process of floral arrest. Remarkably, we show that floral arrest only affects flowers at stage 9 or below, and has the effect of halting them in their current developmental stage. We also show that floral arrest is reversible in response to both global and local loss of reproductive structures in both Col-0 and L*er*. We show that all unopened flowers can re-initiate development after arrest, but that those that initially arrested between stages 6-9 cannot develop further than the 'checkpoint' at stage 9. Flowers that arrested at stage 5 and younger can however fully develop and go on to produce fertile fruit.

As we discussed above, the stage 5 checkpoint likely relates to the fact that the FM is still active in flowers younger than stage 5. These flowers can thus probably reactivate at the level of FM activity and complete their development. But what about the stage 9 checkpoint? One possibility is that this checkpoint relates to organ and stem elongation. Stage 9, following Smyth et al (1990), is the stage at which the floral organs begin to rapidly elongate towards their full sizes. Stage 9 additionally signifies the developmental point at which commitment to tissue specification initiates, including stigmatic tissue, transmitting tract, ovules and anther development. It is notable that there is very little internode elongation between the flowers in the arrested bud cluster (Figure 5.1 E), and that this remains the case even when there is reactivation of the inflorescence (Figure 5.2 D). In general, there is a marked reduction in internode elongation towards the end of inflorescence development (Goetz et al, 2021), culminating in the arrested bud-cluster. It thus seems that floral arrest takes place in an environment of extremely reduced stem/organ elongation, and indeed, as a developmental process, might largely constitute the absence of such elongation.

This becomes particularly interesting in the light of our previous study, which showed that later-produced fruit (i.e. those formed in the later 50% of the period between anthesis and inflorescence arrest) are locally required for inflorescence arrest, and that

auxin export from these late fruit is key to this effect (Ware et al, 2020). In this study, our new developmental analysis clarifies that this auxin-related mechanism likely specifically relates to floral arrest and not IM arrest, given that we show here that local fruit removal does not significantly affect IM activity (Figure 5.5). Furthermore, by the point in flowering that these late fruit begin to form, the IM has usually already arrested. We previously proposed that auxin exported by fruit acts by preventing the export of auxin from other organs via a canalization-dependent mechanism (Ware et al, 2020). It is also notable that auxin transport in the inflorescence diminishes towards the end of inflorescence development, and that auxin appears to build up in the inflorescence stem (Goetz et al, 2021). This therefore suggests a model in which the cumulative auxin exported by fruit triggers floral arrest by preventing the further export of auxin from flowers at stage 9 or younger, which in turn prevents both organ elongation in the flower and elongation in the adjacent internode. Flowers above stage 10 presumably already have a well-established, canalized auxin export into the stem, and so are immune to this effect (Figure 5.2), while flowers at stage 5 or below with an active FM can re-establish auxin export if nearby fruit are removed. However, those between stages 6-9 are unable to re-form a link, and therefore fail to fully develop. This model therefore provides a testable hypothesis for the nature and regulation of floral arrest for future studies.

5.4.3 The role of cytokinin in inflorescence arrest

Our results clearly demonstrate that cytokinin is an important regulator of two-stage inflorescence arrest in Arabidopsis. Our results show that there is a clear decline in cytokinin signalling in the IM in the lead-up to IM arrest, that cytokinin treatment can delay IM and FM arrest, and that cytokinin mutants show strong perturbations in the progression of inflorescence lifetime, including an inability of *ahk2 ahk3* mutants to respond to inflorescence or fruit removal (Figures 5.3 K, 5.7 B,C). Our results are consistent with the recent publication of Merelo et al (2022), who also demonstrated that cytokinin signalling diminishes over IM lifetime, and that cytokinin treatment can delay

IM arrest. However, our results provide additional information relative to those of Merelo et al (2022), by 1) providing clear genetic evidence for the role of cytokinins in IM arrest, 2) demonstrating the role of cytokinins in floral arrest as well as IM arrest and 3) placing the role of cytokinin within a clear developmental framework, namely the re-distribution of reproductive effort based on reproductive success elsewhere on the plant.

In particular, we show that the *rock2* and *rock3* mutants, previously implicated in inflorescence arrest (Bartrina et al, 2017), differentially regulate IM and FM arrest, consistent with the high expression of *AHK2* in IMs and FMs, and of *AHK3* in FMs. Remarkably, our results show that *rock2* and *rock3* phenotypes closely resemble the effect of global inflorescence and local fruit removal respectively, implicating cytokinin in the coordination of arrest events across the plant in response to systemic and local reproductive success. Consistent with this, we show that the cognate loss-of-function *ahk2 ahk3* mutants are unable to respond to inflorescence or fruit removal by extending the duration of IM or flower opening activity.

We propose that both inflorescences and fertile fruit might act as sinks for *trans*-Zeatin (*tZ*) cytokinin from the root system (Figure 5.7 A), and that the continued production of these new cytokinin sinks during flowering causes a progressive dilution in root-derived *tZ* availability in the shoot. This reduces cytokinin levels in any given inflorescence, which leads to a reduction in IM size and ultimately IM arrest, followed shortly after by floral arrest. This hypothesised re-distribution of *tZ* cytokinin between sinks in the shoot would present an elegantly simple system for plants to adjust inflorescence lifetime to compensate for reduced reproductive success. In particular, it can be seen that a local failure of external pollination – not a factor in highly self-fertile Arabidopsis, but a key consideration in most other Brassicaceae – would trigger the compensatory maturation of additional flowers by preventing cytokinin sinks/auxin sources developing. A more dramatic loss of inflorescences by e.g. herbivory would trigger both the development of additional inflorescences (Walker et al, 2021) and prolong the lifetime of existing inflorescences.

5.5 Materials & methods

5.5.1 Plant growth conditions

Plants for phenotypic and microsurgical experiments were grown on John Innes compost under a standard 16h/8h light/dark cycle (20ºC) in either controlled environment rooms with light provided by fluorescent tubes at a light intensity of ~120µmol/m^2s^{-1}, or in glasshouses with supplemental lighting. Plants for cytokinin application experiments were grown on John Innes No. 3 compost under the same light/dark cycle but at 22ºC/18ºC, with light provided by fluorescent tubes at an intensity of ~150µmol/ m^2s^{-1}.

5.5.2 Plant materials

Arabidopsis wild-types Col-0 and L*er* were used as indicated. The following lines are all in a Col-0 background and have previously been described; *TCSn:GFP* (Liu & Müller, 2017); *rock2*, *rock3* (Bartrina et al, 2017); *ipt3-2 ipt5-2 ipt7-1* (Miyawaki et al, 2006); *ahk2-2 ahk3-3* (Higuchi et al, 2004).

5.5.3 Flowering assessments and meristem measurements

To define the manner in which Arabidopsis inflorescences arrest, we grew a large population of wild-type Col-0 Arabidopsis under long day conditions. Each plant was pre-allocated to be sampled at a given timepoint after its primary shoot axis had 'bolted'. In this way ~6 plants were sampled for each timepoint, with the timepoints being at 1 day intervals post bolting. Sampling was destructive, so we could not just measure the same plants each day post bolting (dpb). For each plant we recorded 1) the number of open and previously opened flowers; 2) the number of as-yet-unopened floral buds including all floral primordia visible by dissecting the inflorescence apex under a microscope (Figure 5.1 F); and 3) the cumulative number of floral nodes initiated by each inflorescence at that timepoint (i.e. the sum of 1 and 2).

Genotypes (where relevant) and age of collection were randomised across trays, and date of bolting recorded for each plant. When ready for collection, the entire bud cluster above the uppermost open flower (where present) was removed from the plant with forceps. In the event of collection prior to anthesis, the entire bud cluster was collected. All open flowers on the primary inflorescence (PI) were counted prior to collection. The apex of the inflorescence (containing all unopened flowers) was removed from each plant and mounted into a plate containing solidified water agarose to prevent desiccation, with the meristem facing upwards. These were then dissected under a dissecting microscope using forceps and micro-scalpel. The total number of unopened flowers and floral primordia were counted, with as many as possible being removed. The dissected apices were imaged under a Keyence VHX-7000 digital microscope, using a VH-Z100R RZx100-x1000 real zoom lens. Images were loaded into ImageJ (Schneider et al, 2012), where the mean of three meristem diameters was calculated, using methodology adapted from Landrein et al (2015).

5.5.4 Micro-surgical experiments

Inflorescence removal as described in Figures 5.3, 5.4, 5.5 5.6, 5.7, Supplemental Figure 5.1 was carried out by removing all inflorescences except the PI with scissors at 6dpb. Plants were then monitored every subsequent 2-3 days and newly developed branches were removed until sample collection. Fruit removal treatments were carried out at either 14dpb or on the day of final flower opening as indicated. All developed fruits and open flowers were removed from the PI using forceps. Plants were monitored every 1-3 days, with all additional flowers being removed until sample collection.

5.5.5 Confocal imaging

Inflorescence apices of *TCSn:GFP* plants were prepared, mounted and dissected as described above. The agar plates were then flooded with distilled water to allow water-dipping lenses to be used to image the meristem. Meristems were imaged using a Zeiss LSM880 with a 20x water dipping lens. Excitation was performed using 488 nm (10% laser power) and 555 nm (5%) lasers. Chloroplast autofluorescence was detected above 600 nm, and GFP fluorescence below 555 nm. Z-stacks were taken of each meristem, covering the whole depth of the meristem dome, and then a maximum intensity projection was made of the z-stack. Quantification was performed on these projections using ImageJ (Schneider et al, 2012). The same microscope settings were used for all meristems.

5.5.6 qPCR

Col-0 plants were grown and their date of anthesis recorded. Inflorescence apices (including all unopened buds) of the PI (4-8 individual plants pooled per biological replicate) were subsequently harvested, snap frozen, and stored at -80˚C until RNA extraction. RNA was extracted from samples using a QIAGEN RNeasy plant mini kit as per manufacturer's instructions (including DNAse treatment). cDNA was synthesised using Superscript IV reverse transcriptase with 1microgram of input RNA per sample. qRT-PCR was performed on an Analytik-Jena qTOWER using PowerUp SYBR Green mastermix (Thermo-Fisher), with 10μl reactions containing 0.25μl forward and reverse primers (100μM stock), 5μl SYBR green mastermix, 1μl cDNA and 3.5μl water. Cp values were calculated using the manufacturer's software and subsequently compared via the $2^{-\Delta\Delta Ct}$ method, normalised to the average 0dpb values, with the housekeeping gene PP2A3 as an internal control. Results presented are the average of four biological replicates with three technical replicates each.

Primers:

ARR5-F – tcagagaacatcttgcctcgt; ARR5-R – atttcacaggcttcaataagaaat;

ARR7-F – ccggtggagatttgactgtt; ARR7-R – tccactctctacagtcgtcacttt;

PP2A3-F – tccgtgaagctgctgcaaac; PP2A3-R – caccaagcatggccgtatca.

5.5.7 Cytokinin applications

Cytokinin applications were performed via application in lanolin to emerged fruits of L*er* plants using a micropipette tip, the same methodology as in Ware et al (2020). Either 10µl (1mg/g treatment) or 1µl (01.mg/g treatment) of 100mg/ml 6-benzlyaminopurine stock in DMSO was added to lanolin with 1µl dye to ensure even incorporation, or DMSO and dye alone for the corresponding mock treatments. Treatments were performed at the same points as measurements, and the treatment regimen was initiated at 12 days after anthesis of the first flower.

5.5.8 Cytokinin measurements

For the cytokinin analysis of the fertile or sterile fruit of L*er* and *ms1* plants approximately 10 mg of fresh weight material was used per sample (n=5). Samples were extracted in modified Bieleski buffer (methanol/water/formic acid, 15/4/1, (v/v/v)) with a mixture of stable isotopically labelled internal standards added to each sample for precise quantification (Hoyerova et al, 2006). The purification of isoprenoid CKs was carried out according to Dobrev et al, (2002) using the MCX column (30 mg of C18/SCX combined sorbent with cation-exchange properties). Analytes were eluted by two-step elution using a 0.35 M NH_4OH aqueous solution and 0.35 M NH_4OH in 60% MeOH (v/v) solution. Samples were afterwards evaporated to dryness under vacuum at 37°C. Prior to analysis the samples were dissolved in 40µl 10% MeOH (v/v). MS analysis and quantification were performed using an UHPLC-MS/MS system consisting of a 1290 Infinity Binary LC System coupled to a 6490 Triple Quad LC/MS System with Jet Stream and Dual Ion Funnel technologies (Agilent Technologies, Santa Clara, CA, USA. UHPLC-ESI-MS/MS method parameters were adapted from (Svačinová et al, 2012).

5.5.9 Experimental design and statistics

Sample size for each experiment is described in the figure legends. For plant growth experiments, each sample was a distinct plant. For cytokinin measurements, each sample was set of tissue pooled from multiple plants; each sample was distinct. For data analysis, we tested data for normality to determine the most appropriate statistical test, except when mixed-effects models were used, where instead sphericity was not assumed and the Greenhouse-Geisser correction was applied. The statistical tests performed for each experiment are described in the text and/or in the figure legends. For Sidak's multiple comparisons, individual variances were calculated for each comparison.

Acknowledgements

CHW is supported by BBSRC White Rose PhD studentship (BB/M011151/1). AW is supported by BBSRC DTP grant BB/M008770/1. JS and KL are supported by the Knut and Alice Wallenberg Foundation (KAW), the Swedish Foundation for Strategic Research (Vinnova), and the Swedish research council (VR). We also acknowledge the Swedish Metabolomics Centre (http://www.swedishmetabolomicscentre.se/) for access to instrumentation.

Author contributions

CHW, AW and TB performed experiments and analysed the data. JS, KL carried out the cytokinin analysis. CHW, TB & ZW designed the study. All authors contributed to writing the manuscript.

References

Balanzà, V., Martínez-Fernández, I., Sato, S., Yanofskym M.F., Kaufmann, K., Angenent, G.C. et al. (2018) Genetic control of meristem arrest and life span in Arabidopsis by a *FRUITFULL-APETALA2* pathway. *Nature Communications*, **9**, doi: 10.1038/s41467-018-03067-5.

Bangerth, F (1989). Dominance amongst fruits/sinks and the search for a correlative signal. *Physiologia Plantarum*, **76**, 608-614.

Bartrina, I., Jensen, H., Novák, O., Strnad, M., Werner, T. and Schmülling, T. (2017). Gain-of-function mutants of the cytokinin receptors AHK2 and AHK3 regulate plant organ size, flowering time and plant longevity. *Plant Physiology*, **173**, 1783-1797.

Bennett, T., Hines, G., van Rongen, M., Waldie, T., Sawchuk, M.G., Scarpella, E. et al. (2016). Connective auxin transport in the shoot facilitates communication between shoot apices. *PLoS Biology*, **14**, e1002446.

Cho, L-H., Yoon, J. and An, G. (2016). The control of flowering time by environmental factors. *The Plant Journal*, **90**, 708-719.

Dobrev, P.I. and Kamínek, M. (2002). Fast and efficient separation of cytokinins from auxin and abscisic acid and their purification using mixed-mode solid-phase extraction. *Journal of Chromatography A*, **950**, 21–29.

Goetz, M., Rabinovich, M. and Smith, H.M. (2021). The role of auxin and sugar signaling in dominance inhibition of inflorescence growth by fruit load. *Plant Physiology*, **187**, 1189-1201.

Gol, L., Tomé, F. and von Korff, M. (2017). Floral transitions in wheat and barley: interactions between photoperiod, abiotic stresses, and nutrient status. *Journal of Experimental Botany*, **68**, 1399-1410.

González-Suárez, P., Walker, C.H. and Bennett, T. (2020). Bloom and bust: understanding the nature and regulation of the end of flowering. *Current Opinion in Plant Biology*, **57**, 24-30.

Haim, D., Shalom, L., Simhon, Y., Shlizerman, L., Kamara, I., Morozov, M. et al. (2021). Alternate bearing in fruit trees: fruit presence induces polar auxin transport in citrus and olive stem and represses IAA release from the bud. *Journal of Experimental Botany*, **72**, 2450-2462.

Hensel, L.L., Nelson, M.A., Richmond, T.A. and Bleecker, A.B. (1994). The fate of inflorescence meristems is controlled by developing fruits in Arabidopsis. *Plant Physiology*, **106**, 863-76.

Higuchi, M., Pischke, M.S., Mähönen, A.P., Miyawaki, K., Hashimoto, Y., Seki, M. et al. (2004). In planta functions of the Arabidopsis cytokinin receptor family. *PNAS*, **101**, 8821-8826.

Hirose, N., Takei, K., Kuroha, T., Kamada-Nobusada, T., Hayashi, H. and Sakakibara, H. (2008). Regulation of cytokinin biosynthesis, compartmentalization and translocation, *Journal of Experimental Botany,* **59**, 75–83,

Hoyerová, K., Gaudinová, A., Malbeck, J., Dobrev, P.I., Kocábek, T., Šolcová, B. et al. (2006). Efficiency of different methods of extraction and purification of cytokinins. *Phytochemistry*, **67**, 1151–1159.

Landrein, B., Refahi, Y., Besnard, F., Hervieux, N., Mirabet, V., Boudaoud, A. et al. (2015). Meristem size contributes to the robustness of phyllotaxis in *Arabidopsis*. *Journal of Experimental Botany,* **66**, 1317-1324.

Landrein, B., Formosa-Jordan, P., Malivert, A., Schuster, C., Melnyk, C.W., Yang, W. et al. (2018). Nitrate modulates stem cell dynamics in *Arabidopsis* shoot meristems through cytokinins. *PNAS*, **115**, 1382-1387.

Lenhard, M., Bohnert, A., Jürgens, G., Laux, T. (2001). Termination of stem cell maintenance in Arabidopsis floral meristems by interactions between WUSCHEL and AGAMOUS. *Cell*, **105***,* 805-814.

Lenser, T., Tarkowská, D., Novák, O., Wilhelmsson, P.K.I., Bennett, T., Rensing, S.A. et al. (2018). When the *BRANCHED* network bears fruit: how carpic dominance causes fruit dimorphism in *Aethionema*. *Plant Journal*, **94**, 352-371.

Lohmann, J.U., Hong, R.L., Hobe, M., Busch, M.A., Parcy, F., Simon, R. et al. (2001). A molecular link between stem cell regulation and floral patterning in *Arabidopsis*. *Cell,* **105**, 793-803.

Liu, J. and Müller, B. (2017). Imaging *TCSn::GFP*, a synthetic cytokinin reporter, in *Arabidopsis thaliana*. *Methods in Molecular Biology*, **1497**, 81-90.

Mandel, T., Moreau, F., Kutsher, Y., Fletcher, J.C., Carles, C.C. and Williams, L.E. (2014). The ERECTA response kinase regulates Arabidopsis shoot apical meristem size, phyllotaxy and floral meristem identity. *Development*, **141**, 830-841.

Mandel, T., Candela, H., Landau, U., Asis, L., Zelinger, E., Carles, C.C. et al. (2016). Differential regulation of meristem size, morphology and organization by the ERECTA, CLAVATA and class III HD-ZIP pathways. *Development*, **143**, 1612-1622.

Martínez-Fernández, I., Menezes de Moura, S., Alves-Ferreira, M., Ferrándiz, C. and Balanzà, V. (2020). Identification of players controlling meristem arrest downstream of the FRUITFULL-APETALA2 pathway. *Plant Physiology*, **184**, 945-959.

Miyawaki, K., Tarkowski, P., Matsumoto-Kitano, M., Kato, T., Sato, S., Tarkowska, D., et al. (2006). Roles of Arabidopsis ATP/ADP isopentenyltransferases and tRNA isopentenyltransferases in cytokinin biosynthesis. *PNAS*, **103**, 16598-16603.

Merelo, P., González-Cuadra I. and Ferrándiz, C. (2022). A cellular analysis of meristem activity at the end of flowering points to cytokinin as a major regulator of proliferative arrest in *Arabidopsis*. *Current Biology*, **32**, 749-762.

Müller, D., Waldie, T., Miyawaki, K., To, J.P.C., Melnyk, C.W., Kieber, J.J. et al. (2015). Cytokinin is required for escape but not release from auxin mediated apical dominance. *The Plant Journal*, **82**, 874–886.

Nishimura, C., Ohashi, Y., Sato, S., Kato, T., Tabata, S. and Ueguchi, C. (2004). Histidine kinase homologs that act as cytokinin receptors possess overlapping functions in the regulation of shoot and root growth in *Arabidopsis*. *The Plant Cell*, **16**, 1365-1377.

Prusinkiewicz, P., Crawford, S., Smith, R.S., Ljung, K., Bennett, T., Ongaro, V. et al. (2009). Control of bud activation by an auxin transport switch. *PNAS*, **106**, 17431-17436.

Schmid, M., Davison, T.S., Henz, S.R., Pape, U.J., Demar, M., Vingron, M. et al. (2005). A gene expression map of *Arabidopsis thaliana* development. *Nature Genetics,* **37**, 501-506.

Schneider, C.A., Rasband, W.S., and Eliceiri, K.W. (2012). NIH Image to ImageJ: 25 years of image analysis. *Nature Methods*, **9**, 671–675.

Shinohara, N., Taylor, C. and Leyser, O. (2013). Strigolactone can promote or inhibit shoot branching by triggering rapid depletion of the auxin efflux protein PIN1 from the plasma membrane. *PLoS Biology,* **11**, e1001474.

Smyth, D.R., Bowman, J.L. and Meyerowitz, E.M. (1990). Early flower development in *Arabidopsis*. *Plant Cell,* **2**, 755-767.

Svačinová, J., Novák, O., Plačková, L., Lenobel, R., Holík, J., Strnad, M. et al. (2012). A new approach for cytokinin isolation from *Arabidopsis* tissues using miniaturized purification: pipette tip solid-phase extraction. *Plant Methods*, **8**, doi:10.1186/1746-4811-8-17.

Takei, K., Sakakibara, H., Taniguchi, M. and Sugiyama, T. (2001). Nitrogen-dependent accumulation of cytokinins in root and the translocation to leaf: implication of cytokinin species that induces gene expression of maize response regulator. *Plant and Cell Physiology*, **42**, 85-93.

Umehara, M., Hanada, A., Magome, H., Takeda-Kamiya, N. and Yamaguchi, S. (2010). Contribution of strigolactones to the inhibition of tiller bud outgrowth under phosphate deficiency in rice. *Plant and Cell Physiology*, **51**, 1118-1126.

van Rongen, M., Bennett, T., Ticchiarelli, F. and Leyser, O. (2019). Connective auxin transport contributes to strigolactone-mediated shoot branching control independent of the transcription factor *BRC1*. *PLoS Genetics*, **15**, e1008023.

Walker, C.H. and Bennett, T. (2018). Forbidden fruit: dominance relationships and the control of shoot architecture. *Annual Plant Reviews Online*, doi: 10.1002/9781119312994.apr0640.

Walker, C.H., Wheeldon, C.D. and Bennett, T. (2021). Integrated dominance mechanisms regulate reproductive architecture in *Arabidopsis thaliana* and *Brassica napus*. *Plant Physiology*, **186**, 1985-2002.

Wang, Y., Kumaishi, K., Suzuki, T., Ichihashi, Y., Yamaguchi, N., Shirakawa, M. et al. (2020). Morphological and physiological framework underlying plant longevity in *Arabidopsis thaliana*. *Frontiers in Plant Science,* **11**, 600726.

Ware, A., Walker, C.H., Šimura, J., González-Suárez, P., Ljung, K., Bishopp, A. et al. (2020). Auxin export from proximal fruits drives arrest in temporally competent inflorescences. *Nature Plants*, **6**, 699-707.

Wheeldon, C.D. and Bennett, T. (2021). There and back again: an evolutionary perspective on long-distance coordination of plant growth and development. *Seminars in Cell & Developmental Biology*, **109**, 55-67.

Wuest, S.E., Philipp, M.A., Guthörl, D., Schmid, B., Grossniklaus, U. (2016) Seed production affects maternal growth and senescence in *Arabidopsis*. *Plant Physiology*, **171**, 392-404.

Xu, Y., Yamaguchi, N., Gan, E.S. and Ito, T. (2019). When to stop: an update on molecular mechanisms of floral meristem termination. *Journal of Experimental Botany*, **70**, 1711-1718.

Zhang, L., DeGennaro, D., Lin, G., Chai, J. and Shpak, E.D. (2021). ERECTA family signaling constrains *CLAVATA3* and *WUSCHEL* to the center of the shoot apical meristem. *Development*, **148**, doi:10.1242/dev.189753.

Chapter 6

Cytokinin signalling regulates age-dependent changes in inflorescence morphology in Arabidopsis

In preparation

Cytokinin signalling regulates age-dependent changes in inflorescence morphology in Arabidopsis

Catriona H. Walker[1], Tom Bennett[1+]

[1]School of Biology, Faculty of Biological Sciences, University of Leeds, Leeds, LS2 9JT.

+ Address for correspondence: t.a.bennett@leeds.ac.uk

6.1 Abstract

Reproductive success in flowering plants depends on the successful integration of external signals to regulate reproductive development. Multiple developmental parameters alter with phase change (e.g. from vegetative to reproductive) in an age-dependent manner known as heteroblasty. Given the importance of heteroblasty in appropriate timing of physiological and morphological characteristics, we examined Arabidopsis for evidence of heteroblasty occurring within the reproductive period. We identified that fruit length and internode spacing both decrease with age along the inflorescence. Furthermore, we have shown that these heteroblastic changes are at least in part controlled by cytokinin signalling via the ARABIDOPSIS HISTIDINE KINASE2 (AHK2) and AHK3 cytokinin receptors. We therefore propose that changes in cytokinin signalling through the inflorescence lifetime have substantial ramifications for seed production and yield, and identify this as a key area for future crop research.

6.2 Introduction

Reproductive success in flowering plants relies on the integration of multiple parameters. First, plants must actively and proactively respond to environmental conditions to produce the most appropriate number of seed. Seed must be contained within fruits, which develop from flowers, which are supported by inflorescences. As such, much of this 'decision-making' around seed production must be made well in advance of pollination, and yet must be optimal for the available resources (Walker and Bennett, 2018). In addition to this, floral timing must be carefully controlled; flowering must occur in an appropriate temporal window. Flowering in the correct season, coinciding with other members of the same species and when any necessary pollinators are present are all essential. The end of flowering, whilst potentially less critical, is a large determining factor for yield. Arresting too early will dramatically reduce the amount of seed produced, while continuing to flower past optimal conditions may result in resource wastage. Finally, plants must proactively monitor and modify their reproductive output through the coordination of long distance signalling (Walker and Bennett, 2018). Whilst they evidently modulate their growth and reproduction relative to their environment (Walker, Wheeldon and Bennett, 2021), we do not yet fully understand the mechanisms controlling development in flowering plants.

Plant growth is controlled through the integration of multiple signals across the plant, which are interpreted locally by specific tissues and organs (Domagalska and Leyser, 2011). Growth, however, is not a uniform process, with necessary developmental changes occurring throughout the plant lifetime. The age-dependent morphological and physiological changes of organs ('heteroblasty') appears to be a mechanism by which plants can appropriately time key developmental stages. These changes do not necessarily rely on environmental conditions, and are instead controlled autonomously (Forster and Bonser, 2009; Tsukaya et al, 2000). Heteroblasty is perhaps best recognised and studied in the change of leaf size and shape over time (Wang et al, 2019). There is evidence that heteroblasty in leaves co-ordinates leaf development with

flowering timing, and as such acts to appropriately regulate resource acquisition (Cartolano et al, 2015). In Arabidopsis, this can be observed in the clear discrepancy between the wide-tipped rosette leaves with long petioles, and the much smaller cauline leaves, which lack petioles (Forster and Bonser, 2009). In other species such as the related *Brassica napus*, juvenile plants have simple leaves, while mature plants have complex leaves containing multiple leaflets. It is therefore clear that underlying developmental mechanisms must be differentially regulated over time in order to appropriately modify organ growth.

Heteroblastic effects are related to the relative, but not the actual age of the plant. In *Cardamine hirsuta*, leaf morphology changes with respect to the developmental stage, rather than absolute time; early flowering plants display the same leaf morphology at flowering as later-flowering plants (Cartolano et al, 2015). These changes appear to occur as a result of miRNA signalling cascades. For instance, Arabidopsis trichome development on the abaxial (lower) side of the leaf occurs in later leaves and is repressed by miR156, which decreases in concentration with age (Cartolano et al, 2015). Acting through a signalling cascade, miR156 negatively regulates transcription of multiple genes, including *APETALA2* (*AP2*), resulting in repression of trichome development (Cartolano et al, 2015). Similarly, miRNA signalling has been identified as regulating the heteroblastic effects associated with reproductive phase change in leaf development (Silva et al, 2019; Zheng et al, 2019). miR156 inhibits SQUAMOSA PROMOTER BINDING PROTEIN-LIKE15 (SPL15), the result of which is a smaller number of larger cells in the leaves (Usami et al, 2009). miR156 levels are regulated by photosynthetic sugars, and as such decline as the plant ages (Yu, Lian and Wang, 2015); over time this results in leaf heteroblasty.

In addition to regulating heteroblasty in trichome and leaf development, miRNAs are known to be critical in the gene regulation of multiple flowering parameters (Waheed and Zeng, 2020); for example, miRNA-controlled transcription of AP2 has been described as an important part of floral arrest (Balanzà et al, 2018). As miR156 levels

decrease with age they exert less inhibition on SPL, which upregulates miR172, bringing about its concurrent increase as the plant ages (Balanzà et al, 2018). The action of the resulting signalling cascade results in the gradual inhibition of the flowering promoter AP2 over time (Ripoll et al, 2015; Aukerman and Sakai, 2003). Given the same signalling systems are in use in both leaf heteroblasty and floral arrest, we therefore questioned whether heteroblastic processes were also present in reproductive architecture. There is some evidence that this does occur; casual observation of Arabidopsis inflorescences appears to show that fruits decrease in size along the inflorescence, along with a reduction in internode spacing. Related traits also appear to be evident in other species; in *Aethionema arabicum*, two distinct fruit morphs are produced on a single plant, with the larger morph generally being the earliest to develop. Furthermore, the ratios of large: small fruit on individual inflorescences can be increased by removal of other reproductive organs, suggestive of carpic dominance effects (Lenser et al, 2018). In crops such as wheat, seed size is often inconsistent within a single ear, with larger seeds in the middle, decreasing towards the top and bottom of the ear (Schmidt et al, 2020). This follows the order of anthesis of the spikelets, beginning in the middle of the ear (Rawson and Evans, 1970). Despite an indication that reproductive parameters are not consistent across the flowering period in multiple species, we do not understand how this process is regulated. Understanding how heteroblastic regulation of reproductive architecture affects seed production and yield could have major benefits for agriculture. Identification of genetic targets that regulate heteroblastic effects would have great potential for breeding crop lines capable of increased seed production without increasing inputs. We therefore aimed to understand age-dependent changes in Arabidopsis, and to identify potential underlying mechanisms.

6.3 Results

6.3.1 Multiple developmental parameters alter with inflorescence age

Arabidopsis inflorescences are visibly inconsistent along their length, with decreasing fruit length and internode spacing between the fruits. To quantify the changes occurring with age, morphological measurements of the primary inflorescence (PI) of wild-type Col-0 Arabidopsis were carried out. Firstly, internode length was measured between successive fruits along the PI. A clear exponential decrease in internode length was seen along the inflorescence, from the first (node position 1) to the final flower (Figure 6.1 A).

Fruit length was next assessed, examining the apparent decrease in organ size as the PI ages. A population of 66 plants was pre-randomised, with each plant allocated to a specific sampling day post bolting. At the time of sampling, the bud cluster above the uppermost open flower was collected and the nodal position recorded. The two oldest floral buds (n0 and n+1) were collected and measured. The immature fruits (n-1 and n-2) were allowed to fully mature before collection.

Assessing these plants, there was a clear decline in fruit length which did not precisely follow the recorded node position (Figure 6.1 B). Instead of an exponential decrease in length, the first 10 fruits were highly variable in size, likely as a result of low fertility and correspondingly poor seed set, which in turn determines fruit length. From the ~10th fruit, there was a broadly linear decrease in fruit length, decreasing from approximately 18mm to 10mm over ~40 nodes. It was hypothesised that the decrease in fruit length arose from changes in earlier organ development, or from changes in flower fertility along the inflorescence. Plotting floral bud size against position showed that buds decrease in a similar manner to fruit length, decreasing in a linear fashion to ~40 nodes (Figure 6.1 C). From around 40 nodes, bud size shows a sudden dramatic decrease and a plateau; these buds are those within the bud cluster which do not open into flowers. Given the decrease in bud size, the small size of the fruits at node 40 is almost certainly linked to the small size of the flower that generates them, rather than from reduced fertility

of the fruit. This argument however is unlikely to be the case in the first 10 fruits, where the floral buds are largest, but produce some of the smallest fruit. In this case, the small size of the fruits is likely to arise from low fertility.

It was next hypothesised that decreasing organ size might also lead to changes in seed size or number along the inflorescence. The number of seeds per fruit closely follows the trend of fruit length, decreasing along the inflorescence, with the first fruits having a low number of seeds (Figure 6.1 D). Conversely, while individual seed size showed a slight decrease along the inflorescence, this did not correspond precisely with the change in fruit size (Figure 6.1 E). It therefore seems likely that the decrease in organ size along the inflorescence arises from the decrease in size of the floral buds early in their development. This has knock-on effects on ovule number per fruit, which in turn causes changes in fruit size and seed number per fruit, but has minimal effect on seed size.

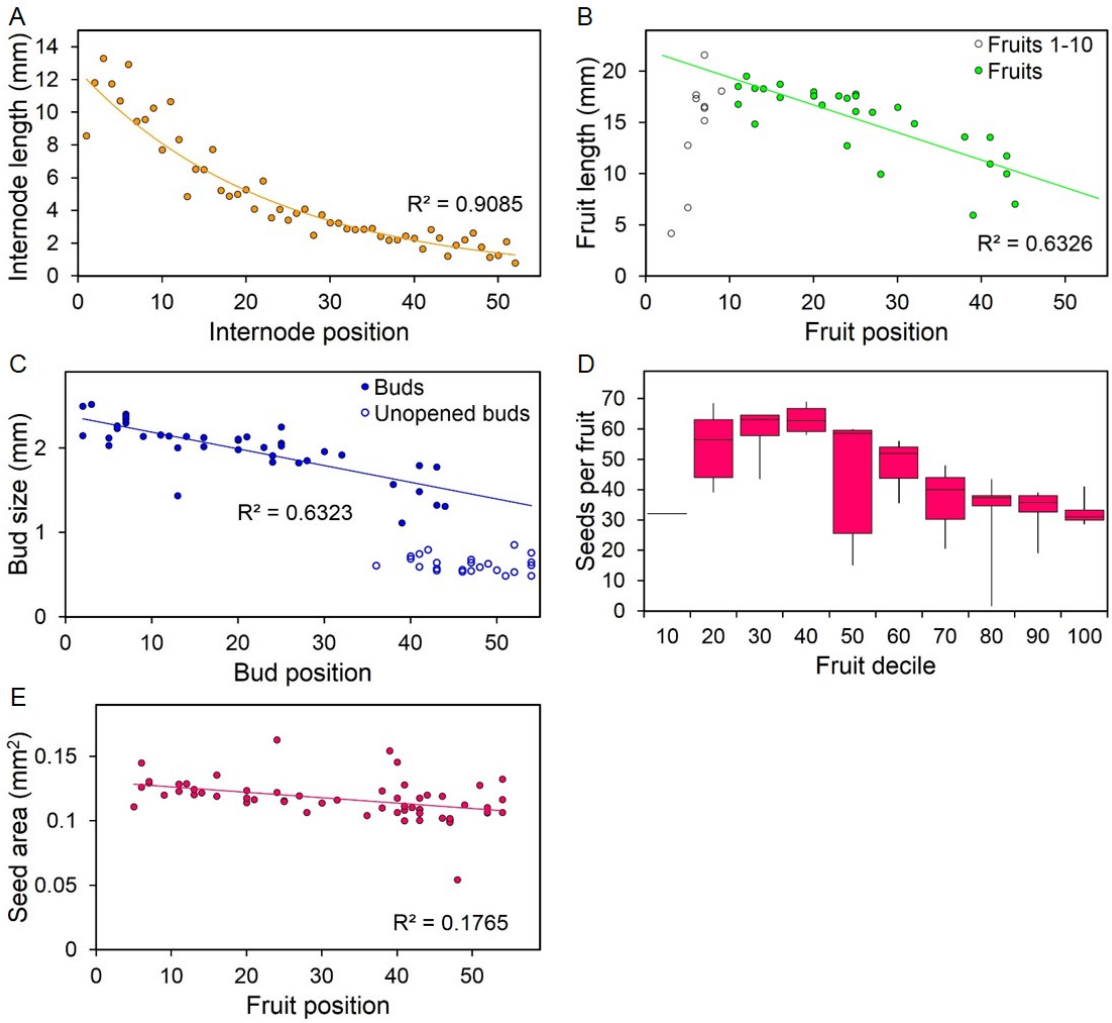

Figure 6.1. Developmental inflorescence parameters alter over time

Scatter plots of developmental parameters of the primary inflorescence (PI) of a population of wild-type Col-0 Arabidopsis. **(A)** Internode length from the rosette to each successive fruit. **(B)** Length of ripe fruits. The trend line is fitted through fruits (green filled circles), including the youngest fruits (open green circles), but is not fitted to the oldest 10 fruits (open black circles) due to their variability in size. **(C)** Bud size along the PI. The two oldest unopened buds were destructively sampled at collection, and mean bud length calculated. The trend line is fitted to bud size (closed purple circles), but not to those buds which were sampled after inflorescence arrest, and which did not open into flowers (open purple circles). **(D)** Box plot of seed number per fruit along the PI. Data is presented by decile to allow comparison across multiple plants with differing fruit numbers. Box shows interquartile range, central line indicates median, whiskers indicate maximum and minimum values. **(E)** Scatter plot of seed area along the PI by fruit position. Trend line is best fit.

6.3.2 Feedback from fruits plays a minor role in regulating inflorescence heteroblasty

Fruits are a well-established source of correlative inhibition in the shoot system (Bangerth, 1989), and we have recently shown how Arabidopsis fruits exert dominance to bring about floral arrest (Ware et al. 2020). We therefore hypothesised that the age-related change in development in the inflorescence (i.e. heteroblasty) was the result of earlier fruit inhibiting the development of later-formed fruit or flowers. To test this idea, we performed a series of differential fruit removal treatments. We used a population of 11 plants that each had 4 secondary cauline inflorescences, allowing us to perform 4 differential treatments between the inflorescences of the same plants. We have previously anecdotally observed that secondary inflorescences show the same heteroblastic pattern as primary inflorescences (PIs), and we confirmed this observation in the untreated inflorescences from this experiment (Figures 6.2 A,B). The treatments performed removed either no fruit (untreated), every second fruit (1/2), two out of every three fruits (2/3) or four out of every five fruits (4/5), thus leaving either 100, 50, 33, or 20% of fruits evenly spaced along the inflorescence. The treatments were performed continually throughout the life of the inflorescence, to give the treatments the maximum window for effect. Assessment of internode spacing and fruit size was carried out following inflorescence arrest, once all fruits were ripe.

Fruit removal treatments had minimal effect on fruit length along the inflorescence, although the more severe treatments (2/3 and 4/5) did appear to increase fruit length slightly. It was however difficult to accurately compare these differences between fruit length at equivalent fruit positions in different treatments, given that treated inflorescences also had an increase in number of flowers opened relative to untreated inflorescences. Interestingly, internode spacing did appear to be affected by fruit removal (Figure 6.2 B). Inflorescences with removal of 1/2 flowers did not differ from the untreated inflorescences, with the exception of the production of some additional flowers. However, the more severe treatments (2/3 and 4/5), showed reduced internode spacing (and therefore reduced cumulative inflorescence distance to each fruit) at equivalent fruit

positions. Untreated and 1/2 inflorescences were approximately 150mm long by node 30, compared to approximately 120mm in the 2/3 and 4/5 treatments. It should be noted that all inflorescences reached a similar final inflorescence length of approximately 150mm, regardless of fruit numbers, suggesting that the presence of fruit plays a role in homeostatic control of internode elongation.

In order to take differences in fruit number into account, we analysed fruit length and internode spacing by decile, allowing us to compare the treatments relative to each other, regardless of fruit number. From this analysis it appeared that fruit removal has a subtle effect on fruit length (Figure 6.2 C), however additional analysis of total mean fruit length did not significantly differ between treatments (ANOVA + Dunnett's; $P>0.05$).

Taken together, these data suggest that while fruit length is not entirely dependent on fruit presence, fruit presence does play a minor role in internode elongation. Our previous work has shown that export of auxin, a hormone well known for cellular elongation (Cleland, 1987; Velasquez et al, 2016), from seed-containing fruit is high (Ware et al. 2020). Removal of these auxin sources therefore likely prevents internodes from reaching their full potential length.

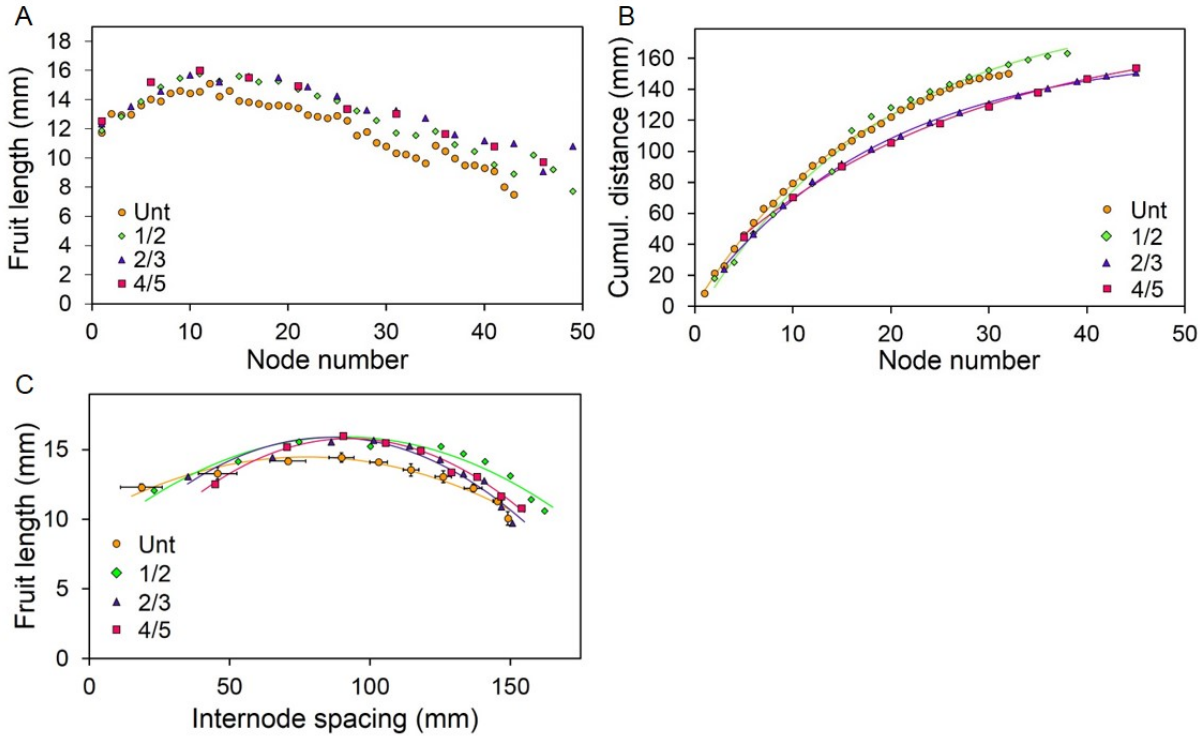

Figure 6.2. Fruit feedback subtly alters inflorescence heteroblasty

A population of wild-type Col-0 plants with 4 secondary cauline inflorescences were subject to one randomly-assigned treatment per cauline. Alternate (1/2)(green diamonds), two of every three (2/3)(purple triangles) or four of every five (4/5)(pink squares) fruits were removed from the inflorescence, or were left untreated (orange circles). **(A)** Scatter plot of fruit length along the inflorescence by node position, where node 1 is the oldest fruit. **(B)** Scatter plot of cumulative internode distance along the inflorescence, measured as accumulated distance from the first fruit. **(C)** Scatter plot of fruit length against cumulative internode length along the inflorescence. Points shown are plotted by decile to compensate for different fruit numbers between treatments. Lines show best fit, bars show s.e.m.

6.3.3 Change in developmental rate does not cause inflorescence heteroblasty

We next hypothesised that a change in the rate of development might explain inflorescence heteroblasty. If the rate of organ production increased towards the end of inflorescence lifetime, the reduced timeframe of organogenesis might lead to the production of progressively smaller organs, spaced progressively closer together. To test this idea, we measured the rate of organogenesis during the lifetime of the PI. We firstly tracked the opening of flowers from anthesis (typically 5-7 days post bolting). In multiple

experiments, we found that individual wild-type Arabidopsis typically opens flowers at a constant rate on the PI until inflorescence arrest (Figure 6.3 A), giving no indication of an acceleration in developmental rate during the lifetime of the inflorescence. The rate varies between experiments (in the range of ~2-3 flowers per day), but is consistent within experiments. However, we reasoned that it was possible that the rate of flower opening is disconnected from the rate of initiation of floral primordia, which could accelerate during development.

In a separate experiment, we thus dissected wild-type Col-0 PIs every 2-3 days post bolting to establish the number of floral nodes (fruit + opened flowers + unopened floral buds + floral primordia) present (Figure 6.3 B), compared to the cumulative number of open flowers (Figure 6.3 C). We found that on the first day of visible bolting, there were already a mean of 19 floral primordia present around the inflorescence meristem (IM), and that the number of floral nodes steadily increased at ~2.5 per day until IM arrest (Figure 6.3 B). Anthesis occurred 7 days post bolting, after which the rate of flower opening was also ~2.5 per day (Figure 6.3 C), thus matching the rate of floral initiation we observed. Our data therefore do not indicate any significant change in floral developmental rate (‘florochron’) during inflorescence development, and as such this cannot explain inflorescence heteroblasty.

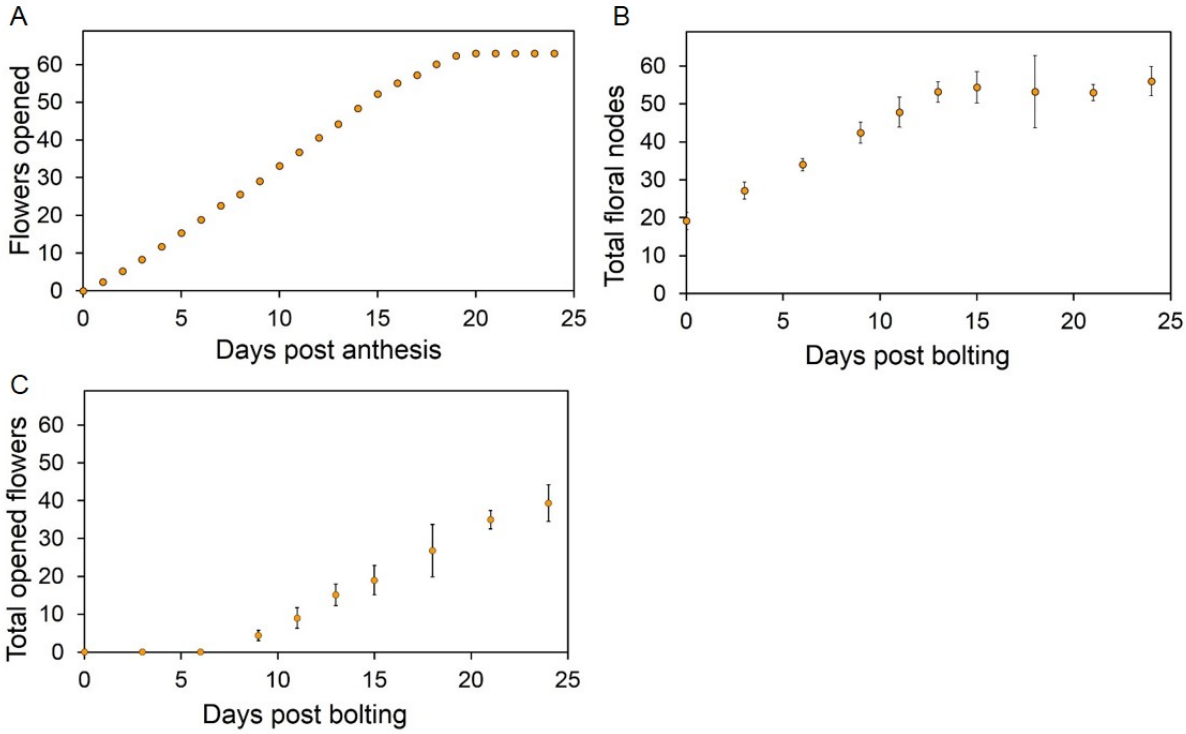

Figure 6.3. Inflorescence heteroblasty is not a result of changing florochron

(A) Scatter plot of the cumulative number of open flowers on the primary inflorescence (PI) assessed daily from a population of wild-type Col-0 Arabidopsis. **(B)** Scatter plot of the total number of floral nodes (fruits + open flowers + unopened buds + primordia) in a population of wild-type Col-0 plants, assessed every 2-3 days. **(C)** Scatter plot of the total number of flowers opened as in B). Error bars show s.e.m.

6.3.4 Change in meristem size is an effect, not a cause of inflorescence heteroblasty

We next hypothesised that the change in organ size and internode length might be caused by changes in the size of the IM over the course of the inflorescence lifetime. We have previously shown that the IM undergoes a reduction in size (Walker et al. 2022, in review), and hypothesised that this might explain the equivalent reduction in the organ and internode size. To test this idea, we measured the size of the IM daily from bolting using high-resolution light microscopy, in the same experiment shown in Figure 6.3 A. Consistent with our previous findings, we found IM size was consistent for the first 7 days post-bolting (corresponding to the initiation of ~21 floral nodes), before declining until day 13 (corresponding to an additional 18 nodes), plateauing until day 15, then declining again and plateauing until inflorescence arrest (Figure 6.4 A). This decline in meristem size thus displayed a similar heteroblastic pattern to that which we have observed for flower/fruit and internode size.

In the same experiment, the changes in IM size were echoed by the change in fruit size. We recorded fruit length as a function of the day post bolting on which its parent flower opened. Ignoring the variable earliest fruit (see Figure 6.1 B), fruit size remained consistent until 11 days post bolting (dpb), and then gradually declined until 17 dpb; a pattern closely resembling that observed in the IM (Figure 6.4 B). It is thus tempting to conclude that changes in the meristem lead to changes in fruit size. However, when we re-plotted both sets of data against the cumulative number of nodes initiated, it becomes clear that the decline in fruit size actually occurs too early to be caused by a change in size of the IM. By the time the IM begins to decrease in size at 7 dpb, it has already initiated ~40 nodes (Figure 6.4 C). Therefore, if the activity of a smaller IM caused inflorescence heteroblasty, the first fruits to show a decline in size should be those occurring after node 40. However, the first fruits to show a decline in size are those located just after node 20 (Figure 6.4 D). Thus, rather than changes in IM size causing changes in fruit size, it is likely that both tissue types are responding to the same external stimulus at the same time.

If this model is correct, it implies that in this experiment, the external stimulus began to change at around 7 dpb, when meristem size began to decrease. At this time point, the floral primordia around node 20 (the first to display a clear reduction in size) are around 5 days old, having been initiated at ~2 dpb. At approximately this time point, the carpel primordia are initiated by the floral meristem (Smyth et al. 1990). This could suggest that the reduction in fruit size and ovule number are caused by a reduction in the size of the carpels, in turn caused by a reduction in the size of the floral meristems at this time point.

It is also notable that changes in internode length occur in much earlier nodes than the changes in meristem size, and therefore cannot arise because the internode is ‘created small’, since the IM is at its largest at this point.

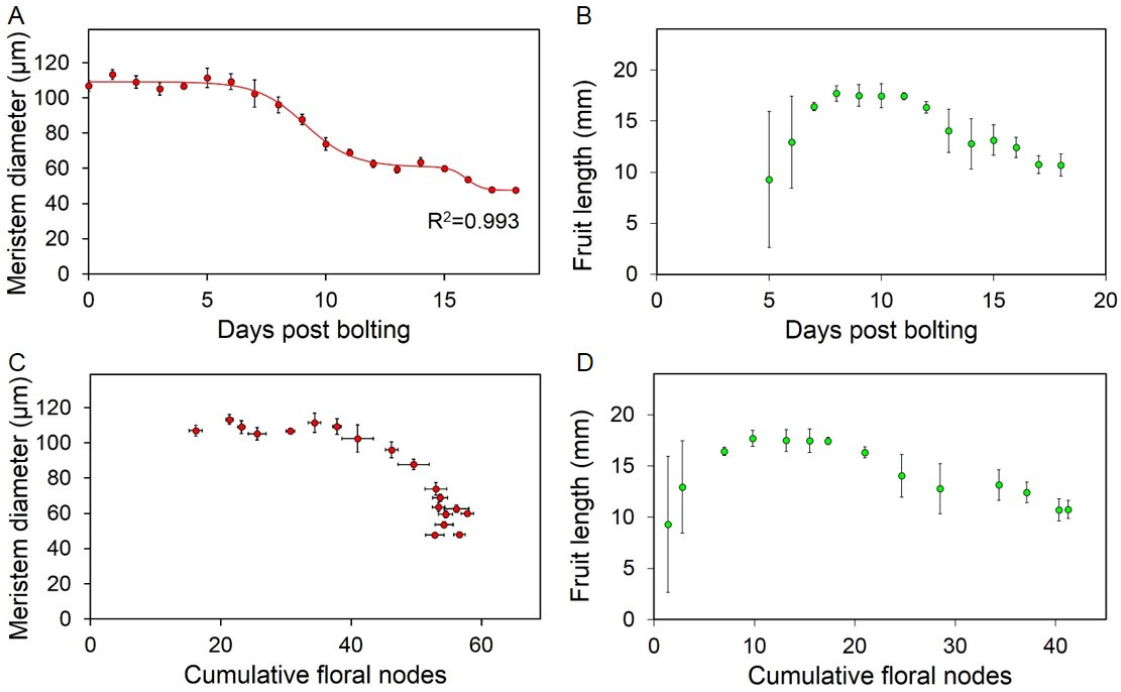

Figure 6.4. Meristematic changes are a result of inflorescence heteroblasty

A population of wild-type Col-0 Arabidopsis was grown and primary inflorescences (PIs) were destructively sampled daily for meristem assessments. The youngest opened flower was left in-tact on the inflorescence and fruit was collected once ripe. **(A)** Scatter pot of meristem diameter throughout the active flowering period of the PI. Each point is the mean of 3-8 meristems of the same developmental age (days post bolting). Line shows best fit. Bars show s.e.m. **(B)** Scatter plot of the length of the youngest fruit remaining on the PI sampling, after reaching maturity. Plotted against the time of meristem collection, days post bolting. Bars show s.e.m. **(C)** Scatter plot of meristem diameter when plotted alongside the number of cumulative floral nodes (fruits + open flowers + unopened buds + primordia) at the time of sampling. Bars show s.e.m. **(D)** Scatter plot of fruit length alongside the number of cumulative floral nodes (fruits + open flowers + unopened buds + primordia) at the time of sampling plotted against number of floral node. Bars show s.e.m.

6.3.5 Cytokinin signalling regulates inflorescence heteroblasty

Taking these data together, we therefore hypothesised that inflorescence heteroblasty arises because different tissues respond simultaneously to temporal changes in the same external factor over the course of inflorescence lifetime. Given the well-established role of plant hormones in the control of development, we speculated that the external factor controlling inflorescence heteroblasty might be a hormonal signal. We therefore screened through a collection of hormone mutants looking for any obvious differences in inflorescence heteroblasty.

In this context, we found the phenotype of the *rock2* mutant, a gain-of-function mutant in the *AHK2* receptor that confers enhanced cytokinin sensitivity (Bartrina et al. 2017), to be particularly interesting. Anecdotally, we observed that *rock2* has longer internodes in the apical part of its inflorescences than wild-type, and we therefore focussed our attention on cytokinin as a possible driver of heteroblasty. We firstly analysed the phenotype of *rock2* in more detail, along with that of *rock3*, an equivalent gain-of-function mutant in the *AHK3* receptor that also confers enhanced cytokinin sensitivity (Bartrina et al. 2017). Consistent with our initial observations, we observed that *rock3* and *rock2* undergo the same general decline in internode length, although to a lesser extent in *rock3*. *rock2* shows consistently longer internodes than Col-0, while both *rock2* and *rock3* have longer apical internodes (Figure 6.5 A). Both mutants open more flowers than Col-0, but the later internodes are longer than those in Col-0 whether compared either in absolute terms (i.e. comparing the same internode numbers) or when comparing in relative terms (i.e. comparing the last fruits of each genotype) (Figure 6.5 A).

To confirm the involvement of AHK2 and AHK3-mediated cytokinin signalling in inflorescence morphology, we also examined the phenotype of the receptor double mutants *ahk2 ahk3* (*ahk23*), *ahk2 ahk4* (*ahk24*), and *ahk3 ahk4* (*ahk34*). Consistent with the phenotypes of *rock2* and *rock3*, we found that *ahk23* and *ahk34* had a slightly shorter apical internodes than Col-0, while *ahk24* was comparable to the wild type (Figure 6.5

B). These data suggest that AHK3-mediated cytokinin signalling is particularly important in determining internode length and fruit size towards the end of inflorescence lifetime. *ahk23* and *ahk24* also have shorter internodes than Col-0 between the oldest fruit, in addition to these fruits generally being shorter. Interestingly, *ahk34* shows the opposite pattern in terms of internode length, with longer older internodes and shorter younger internodes compared to Col-0. Taken together, these data suggest that AHK2-mediated signalling might be important in promoting internode length and size at the start of inflorescence lifetime, but conversely that AHK4-mediated signalling may repress internode elongation during the same period.

Interestingly the earliest fruits in *rock3* are slightly shorter than in Col-0, although the uppermost fruits are highly comparable in size. *rock2* on the other hand consistently displays the shortest fruits of all examined genotypes, despite having the largest internode spacing and bud length (Figures 6.5 C,E). Fruit length is slightly reduced in *ahk23* mutants compared to Col-0, while both *ahk24* and *ahk34* have slightly larger fruits in the middle of the inflorescence, although they are comparable in the oldest and youngest fruits. As previously seen, fruit size is mirrored by the bud lengths in Col-0, *rock2*, *rock3*, and *ahk23*, indicating that fruit length is a direct consequence of flower size. Collectively, these data strongly support a role for cytokinin signalling in the regulation of inflorescence heteroblasty, although they suggest a complex picture of non-linear redundancy between the different cytokinin receptors in this process, with the importance of cytokinin signalling varying over developmental time.

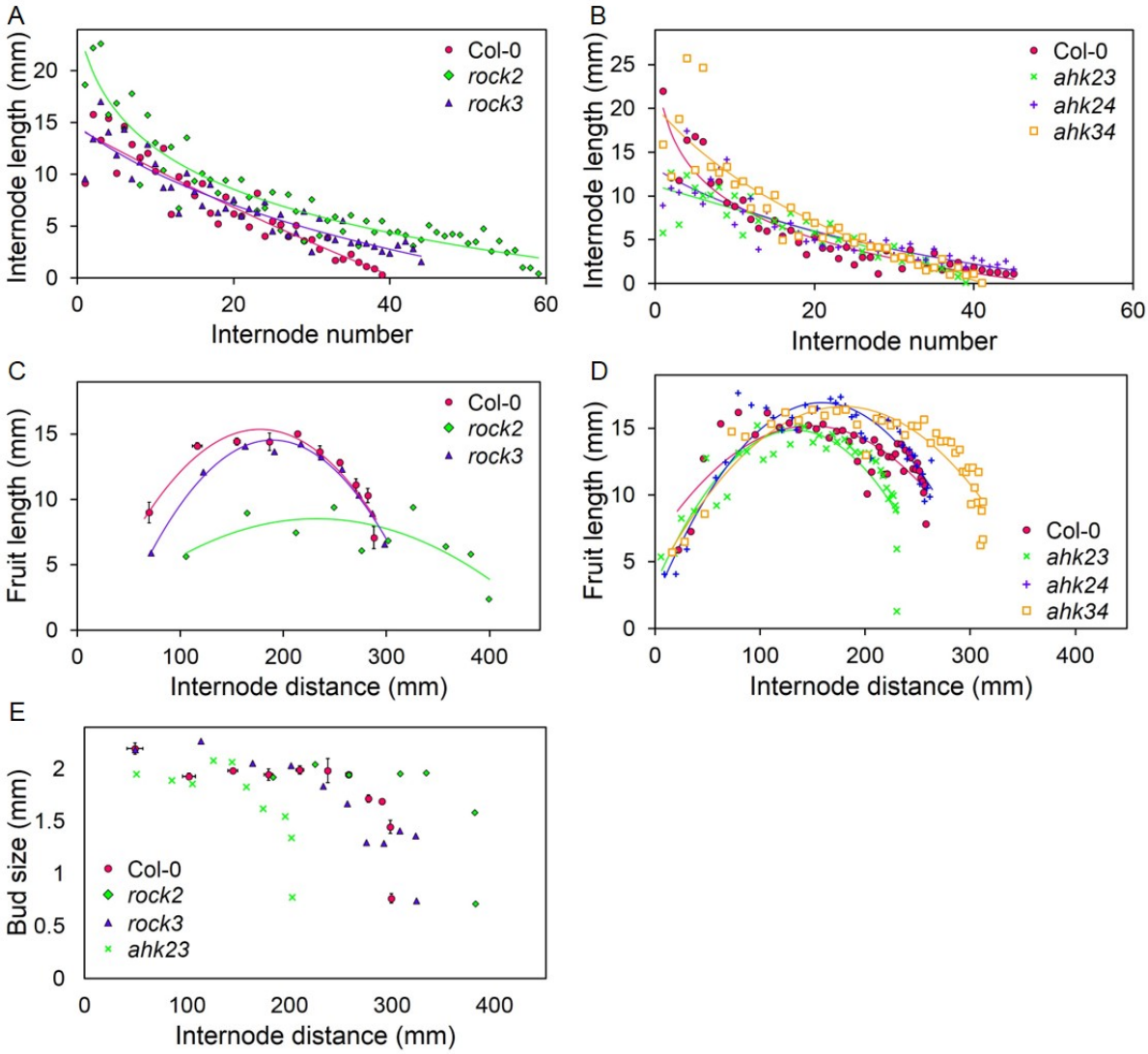

Figure 6.5. Cytokinin dynamics regulate inflorescence heteroblasty.

A population of cytokinin (CK) mutants were grown until end of flowering; wild-type Col-0 (pink circles), *rock2* (green diamonds), *rock3* (purple triangles), *ahk2ahk3* (*ahk23*; green Xs), *ahk2ahk4* (*ahk24*; blue +s), *ahk3ahk4* (*ahk34*; yellow squares). When all fruits were ripe, internode length and fruit length were recorded. **(A,B)** Scatter plots of internode length along the primary inflorescence (PI) in the CK mutants. Lines show best fit. **(C,D)** Scatter plots of fruit length along the PI in the CK mutants. Lines show best fit. **(E)** Scatter plot of bud size (calculated as distance from pedicel to the bud tip) in Col-0, *rock2*, *rock3* and *ahk23* against internode distance. Points are calculated by decile to allow comparison across multiple plants with different floral node numbers and internode distances. Bars show s.e.m.

6.4 Discussion

The data presented here highlight the importance of cytokinin regulation of inflorescence development. We have previously shown that cytokinin signalling in the IM declines over time (Walker et al, 2022), supporting recent work by Merelo et al (2022). Here we have expanded this knowledge to show that in addition to proper floral arrest, cytokinin signalling strongly affects inflorescence development through its lifetime. Furthermore, we have highlighted the importance of signalling via the AHK2 and AHK3 cytokinin receptors. We have shown that AHK2 signalling appears to be of particular importance in promoting fruit size and internode elongation early in development, while AHK3 acts towards the end of inflorescence lifetime. Our results strongly support the previous hypothesis that meristematic sink strength for cytokinin regulates meristem activity (Werner et al, 2008). Through this mechanism, the declining levels of cytokinin over time (Walker et al, 2022) will therefore result in the inflorescence heteroblasty responses described here. Considering this body of work alongside our understanding of the role cytokinin plays in the regulation of floral arrest (Walker et al, 2022), it is evident that changes in cytokinin signalling are responsible for the regulation of multiple aspects of reproductive development. In addition to regulating inflorescence number (Domagalska and Leyser, 2011) and floral arrest timing, cytokinin dynamics also constantly regulate the development of fruit and reproductive output.

From a functional perspective, these heteroblastic changes highlight potential ecological strategies. In particular, the decline in flower size over time may have distinct ramifications for pollination strategies. Arabidopsis is typically accepted to be a self-pollinated plant (Hoffmann et al, 2003), and indeed our data support that; despite no manual pollination in our controlled growth environments, almost all flowers opened produced seed (Figure 6.1 E). The exception to the rule is the first few flowers to open on the primary inflorescence (PI), which are notably larger, but produce smaller fruits (Figure 6.1 B). We hypothesise that the larger flowers are the result of increased cytokinin signalling early in reproductive development (Walker et al, in review, Chapter

5). In support of this, *rock2* mutants produce larger flowers along a greater length of the inflorescence than Col-0, but also produce smaller fruits than Col-0 in this region (Figure 6.5 C). This supports findings by Bartrina et al (2017), who showed that *rock2* mutants have disproportionately elongated gynoecia when compared to the stamen, and as such have decreased self-fertilization. Interestingly, decreased spacing between the reproductive organs of smaller flowers has been shown to be an evolutionary strategy to increase the rate of self-fertilization (Vallejo-Marín et al, 2014). This therefore leads us to postulate that high early cytokinin levels in the inflorescence result in the production of flowers that are optimised towards outcrossing, as a result of increased floral organ size that prevents self-pollination. This is supported by previous work showing that approximately 0.3-2.5% of Arabidopsis flowers in natural populations outcross (Bomblies et al, 2010); under our conditions plants typically produced ~400 fruits, with the first ~5 of these being unfertilized. Approximately 1.25% of flowers on our plants therefore may have tended towards outcrossing, fitting within outcrossing rates of natural populations. Whilst additional study is needed to confirm our hypothesis, we can identify two major benefits of maintaining a system where both outcrossed and self-fertilized flowers are produced. First, maintaining additional genetic diversity within the population decreases evolutionary diversion between lineages (Steinecke et al, 2022), maintaining a larger pool of potential mates. Second, this mechanism would maintain two distinct seed types. The larger, more genetically diverse seeds produced first would be shed from the plant earlier, and would therefore be most likely to take advantage of current growth conditions. The later-produced, smaller, self-fertilized seeds could act as a ‘reserve’, remaining in the seed bank to await future suitable growth conditions. This strategy is recognised in the dimorphic *Aethionema arabicum*, where the large fruit morph immediately dehisces, releasing seed to take advantage of immediate conditions, whilst the smaller fruit morph in indehiscent, and abscises intact from the plant, thereby repopulating the seed bank for future seasons (Lenser et al, 2016; 2018).

Our results provide a solid base on which to build future research. In conjunction with our earlier work, we have outlined a model in which changing cytokinin dynamics through the inflorescence lifetime control both the number of flowers produced by regulating floral arrest (Walker et al, in review, Chapter 5), and seed quantity and quality (e.g. seed number per fruit, seed size and perhaps even genetic diversity). Despite their dramatically different architecture, floral duration and seed quality in the grasses appear to be controlled in much the same manner. IM arrest in Arabidopsis determines the maximum number of flowers that may open on that inflorescence; in the grasses, spike meristem arrest determines the maximum number of spikelets that may develop (Dixon et al, 2018). Floret development determines the number of seeds per spikelet, comparable to the number of seeds developed per fruit in Arabidopsis. Work in barley has shown that the *SIX-ROWED SPIKE* (*VRS*) genes affect specific temporal windows of spikelet development and abortion (Zwirek et al, 2018), and that, at least in the case of *VRS1,* act to increase spikelet sensitivity to cytokinin (Shen et al, 2020). It is therefore possible that the mechanisms we have identified here are also relevant in the heteroblastic development of grass inflorescences. Increasing the sensitivity of spike and spikelet meristems to cytokinin thus has potential to increase yields in cereal crops, meeting a growing demand for increased crop yields without increasing inputs.

6.5 Materials and Methods

6.5.1 Plant growth conditions

Plants were grown on John Innes compost in glasshouses supplemented with LED lighting. Temperature was controlled to 20˚C as far as possible.

6.5.2 Plant lines

Arabidopsis Col-0 was used throughout the study as the wild-type. All genotypes used are in a Col-0 background and have been previously described; *rock2*, *rock3* (Bartrina et al, 2017); *ahk2 ahk3* (*ahk2-2 ahk3-3)*, *ahk2 ahk4* (referred to as *cre1-10 ahk2-1* in the original text), *ahk3 ahk4* (referred to as *cre1-10 ahk3-1* in the original text) (Higuchi et al, 2004).

6.5.3 Phenotypic measurements

Monitoring of inflorescence heteroblasty was carried out on a population of Arabidopsis plants, with genotypes used as required in individual experiments. Sampling dates were pre-allocated to individual plants, so plants would be sampled a set number of days post bolting.

Vegetative plants were examined every 1-2 days for visible bolting, and were destructively sampled at the relevant date. At sampling, the entire primary inflorescence (PI) bud cluster was removed from the plant with forceps; any open flowers on the PI were counted, but were left intact for the fruits to mature on the plant. The bud cluster was mounted into a 0.5% water agarose plate to prevent organs from desiccation. Buds were removed and counted from the cluster under a dissecting microscope using a micro-scalpel until no more buds could be removed. The remaining apex was mounted back into a fresh 0.5% agarose plate for imaging. IMs were imaged using a Keyence VHX-7000 digital microscope, using a VH-Z100R RZx100-x1000 real zoom lens, and resulting images were analysed in ImageJ (Schneider et al, 2012). The mean of three

meristem diameter measurements was calculated, using methodology adapted from Landrein et al (2015). The two largest buds from the cluster were additionally measured in the same manner.

When fruits left on the plants were ripe, but prior to dehiscence, the uppermost two fruits were collected. The dry valves were carefully removed from the fruit with micro forceps, and the seeds were collected on filter paper. This was again imaged using the Keyence VHX-7000 digital microscope, and the images were analysed in ImageJ (Schneider et al, 2012); in this manner, seed number and seed area could be calculated.

Plants which arrested prior to their sampling date were also used for fruit length and internode measurements. The entire PI was removed from the plant with scissors from just above the rosette. Digital callipers were used to measure the distance between each fruit (internode). Digital callipers were also used to measure individual fruit length; in fruits which had already dehisced, the replum was measured instead of the entire fruit.

References

Aukerman, M.J. and Sakai, H. (2003). Regulation of flowering time and floral organ identity by a MicroRNA and its APETALA2-like target genes. *Plant Cell*, **15**, 2730-2741.

Balanzà, V., Martínez-Fernández, I., Sato, S., Yanofsky, M.F., Kaufmann, K, Angenent, G.C. et al. (2018). Genetic control of meristem arrest and life span in *Arabidopsis* by a *FRUITFULL-APETALA2* pathway. *Nature Communications*, **9**, doi: 10.1038/s41467-018-03067-5.

Bangerth, F. (1989). Dominance among fruits/sinks and the search for a correlative signal. *Physiologia Plantarum*, **76**, 608-614.

Bartrina, I., Jensen, H., Novák, O., Strnad, M., Werner, T. and Schmülling, T. (2017). Gain-of-function mutants of the cytokinin receptors AHK2 and AHK3 regulate plant organ size, flowering time and plant longevity. *Plant Physiology*, **173**, 1783-1797.

Bomblies, K., Yant, L., Laitinen, R.A., Kim, S-T., Hollister, J.D., Warthmann, N. et al. (2010). Local-scale patterns of genetic variability, outcrossing and special structure in natural stands of Arabidopsis thaliana. *PLOS Genetics*, **6**, e1000890.

Cartolano, M., Pieper, B., Lempe, J, Tattersall, A., Huijser, P., Tresch, A. et al. (2015). Heterochrony underpins natural variation in *Cardamine hirsuta* leaf form. *PNAS*, **112**, 10539-10544.

Cleland, R.E. (1987). Auxin and cell elongation. In Davies, P.J. (eds) *Plant Hormones and their Role in Plant Growth and Development*. Springer, Dordrecht. doi:10.1007/978-94-009-3585-3_8.

Dixon, L.E., Greenwood, J.R., Bencivenga, S., Zhang, P., Cockram, J., Mellers, G. et al. (2018). *TEOSINTE BRANCHED1* regulates inflorescence architecture and development in bread wheat (*Triticum aestivum*). *The Plant Cell*, **30**, 563-581.

Domagalska, M.A. and Leyser, O. (2011). Signal integration in the control of shoot branching. *Nature Reviews Molecular Cell Biology*, **12**, 211-221.

Forster, M.A. and Bonser, S.P. (2009). Heteroblastic development and the optimal partitioning of traits among contrasting environments in *Acacia implexa*. *Annals of Botany*, **103**, 95-105.

Higuchi, M., Pischke, M.S., Mähönen, A.P., Miyawaki, K., Hashimoto, Y., Seki, M. et al. (2004). In planta functions of the Arabidopsis cytokinin receptor family. *PNAS*, **101**, 8821-8826.

Hoffmann, M.H., Bremer, M., Schneider, K., Burger, F., Stolle, E. and Moritz, G. (2003). Flower visitors in a natural population of *Arabidopsis thaliana*. *Plant Biology*, **5**, 491-494.

Landrein, B., Refahi, Y., Besnard, F., Hervieux, N., Mirabet, V., Boudaoud, A. et al. (2015). Meristem size contributes to the robustness of phyllotaxis in *Arabidopsis*. *Journal of Experimental Botany,* **66**, 1317-1324.

Lenser, T., Graeber, K., Cevik, Ö.S., Adigüzel, N., Dönmez, A.A., Grosche, C. et al. (2016). Developmental control and plasticity of fruit and seed dimorphism in *Aethionema arabicum*. *Plant Physiology*, **172**, 1691-1707.

Lenser, T., Tarkowská, D., Novák, O., Wilhelmsson, P.K.I., Bennett, T., Rensing, S.A. et al. (2018). When the BRANCHED network bears fruit: how carpic dominance causes fruit dimorphism in *Aethionema*. *The Plant Journal*, **94**, 352-371.

Mason, M.G., Ross, J.J., Babst, M.A., Wienclaw, B.N. and Beveridge, C.A. (2014). Sugar demand, not auxin, is the initial regulator of apical dominance. *PNAS*, **111**, 6092-6097.

Merelo, P., González-Cuadra, I. and Ferrándiz, C. (2022). A cellular analysis of meristem activity at the end of flowering points to cytokinin as a major regulator of proliferative arrest in *Arabidopsis*. *Current Biology*, **32**, 749-762.

Rawson, H.M. and Evans, L.T. (1970). The pattern of grain growth within the ear of wheat. *Australian Journal of Biological Sciences*, **23**, 753-764.

Ripoll, J.J., Bailey, L.J., Mai, Q-A., Wu, S.L., Hon, C.T., Chapman, E.J. et al. (2015). microRNA regulation of fruit growth. *Nature Plants*, **1**, doi:10.1038/nplants.2015.36.

Schmidt, J., Claussen, J., Wörlein, N., Eggert, A., Fleury, D., Garnett, T. and Gerth, S. (2020). Drought and heat stress tolerance screening in wheat using computed tomography. *Plant Methods*, **16**, doi:10.1186/s13007-020-00565-w.

Schneider, C.A., Rasband, W.S., and Eliceiri, K.W. (2012). NIH Image to ImageJ: 25 years of image analysis. *Nature Methods*, **9**, 671–675.

Shen, L., Liu, Y., Sun, Z., Wang, Z., Zhang, L., Cai, Y. et al. (2020). Mining the potential of *VRS1-5* gene to raise barley grain yield. *bioRxiv*, doi:10.1101/2020.09.22.307867.

Silva, P.O., Batista, D.S., Cavalcanti, J.H.F., Koehler, A.D., Vieira, L.M., Fernandes, A.M. et al. Leaf heteroblasty in *Passiflora edulis* as revealed by metabolic profiling and expression analyses of the microRNAs miR156 and miR172. *Annals of Botany*, **123**, 1191-1203.

Steinecke, C., Gorman, C.E., Stift, M. and Dorken, M.E. (2022). Outcrossing rates in an experimentally admixed population of self-compatible and self-incompatible *Arabidopsis lyrata*. *Nature*, **128**, 56-62.

Takei, K., Sakakibara, H. and Sugiyama, T. (2001). Identification of genes encoding adenylate isopentenyltransferase, a cytokinin biosynthesis enzyme, in *Arabidopsis thaliana*. *Journal of Biological Chemistry*, **276**, 26405-26410.

Tsukaya, H., Shoda, K., Kim, G-T. and Uchimiya, H. (2000). Heteroblasty in *Arabidopsis thaliana*. *Planta*, **210**, 536-542.

Umehara, M., Hanada, A., Magome, H., Takeda-Kamiya, N. and Yamaguchi, S. (2010). Contribution of strigolactones to the inhibition of tiller bud outgrowth under phosphate deficiency in rice. *Plant and Cell Physiology*, **51**, 1118-1126.

Usami, T., Horiguchi, G., Yano, S. and Tsukaya, H. (2009). The *more and smaller cells* mutants of *Arabidopsis thaliana* identify novel roles for *SQUAMOSA PROMOTER BINDING PROTEIN-LIKE* genes in the control of heteroblasty. *Development*, **136**, 955-964.

Vallejo-Marín, M., Walker, C.H., Friston-Reilly, P., Solís-Montero, L. and Igic, B. (2014). Recurrent modification of floral morphology in heterantherous Solanum reveals a parallel shift in reproductive strategy. *Philosophical Transactions of the Royal Society B*, **369**, doi:10.1098/rstb.2013.0256.

Velasquez, S.M., Barbez, E., Kleine-Vehn, J. and Estevez, J.M. (2016). Auxin and cellular elongation. *Plant Physiology*, **170**, 1206-1215.

Waheed, S. and Zeng, L. (2020). The critical role of miRNAs in regulation of flowering time and flower development. *Genes*, **11**, doi:10.3390/genes11030319.

Walker, C.H. and Bennett, T. (2018). Forbidden fruit: dominance relationships and the control of shoot architecture. *Annual Plant Reviews,* **1**, 1-38.

Walker, C.H., Ware, A., Šimura, J., Ljung, K., Wilson, Z. and Bennett, T. (2022) Cytokinin signalling regulates two-stage inflorescence arrest in Arabidopsis. *Plant Physiology*, in review.

Walker, C.H., Wheeldon, C.D. and Bennett, T. (2021). Integrated dominance mechanisms regulate reproductive architecture in *Arabidopsis thaliana* and *Brassica napus*. *Plant Physiology*, **186**, 1985-2002.

Wang, L., Zhou, C-M., Mai, Y-X., Li, L-Z., Gao, J., Shang, G-D. et al. (2019). A spatiotemporally regulated transcriptional complex underlies heteroblastic development of leaf hairs in *Arabidopsis thaliana*. *The EMBO Journal*, **38**, doi:10.15252/embj.2018100063.

Werner, T., Holst, K., Pörs, Y., Guivarc'h, A., Mustriph, A, Chriqui, D. et al (2008). Cytokinin deficiency causes distinct changes of sink and source parameters in tobacco shoots and roots. *Journal of Experimental Botany*, **59**, 2659-2672.

Yu, S., Lian, H. and Wang, J-W. (2015). Plant developmental transitions: the role of microRNAs and sugars. *Current Opinion in Plant Biology*, **27**, 1-7.

Zheng, C., Ye, M., Sang. M. and Wu, R. (2019). A regulatory network for miR156-SPL module in *Arabidopsis thaliana. International Journal of Molecular Sciences*, **20**, doi:10.3390/ijms20246166.

Zwirek, M., Waugh, R. and McKim, S.M. (2018). Interaction between row-type genes in barley controls meristem determinacy and reveals novel routes to improved grain. *New Phytologist*, **221**, 1950-1965.

Chapter 7

General discussion

7.1 Homeostatic control of reproductive shoot architecture

The data presented in this thesis have provided novel information regarding the roles of phytohormones in the control of dominance mechanisms within Arabidopsis and the wider Brassicaceae. It has been shown that plants are capable of regulating their reproductive architecture through the integration of signals from a relatively small number of long-distance signalling molecules (reviewed in Wheeldon and Bennett, 2021). The work presented here supports this, and provides an additional level of understanding to the process of homeostatic control in reproductive architecture.

7.1.1 Systemic control of inflorescence number

The Brassicaceae utilise signals early in their growth to accurately determine the appropriate number of inflorescences to invest resources into (Figures 2.1, 2.2). These early decisions are strongly influenced by the substrate rooting volume available to the plant, and also to nutrient limitation (Figure 2.2, Supplemental Figure 2.2). Recent studies have demonstrated that strigolactones (SLs) in the rhizosphere are involved in communicating information regarding neighbours and substrate volume to the shoot system (Wheeldon et al, 2022; Yoneyama et al, 2022). As such, it is likely that the early determination of inflorescence number is controlled at least in part by SLs, both those detected in the rhizosphere, and those synthesised within the plant in response to nutrient deficiency (Umehara et al, 2010; de Jong et al, 2014).

Inflorescence outgrowth has previously been shown to be inhibited through apical dominance (Snow, 1937; Phillips, 1975; Fisahn and Hofner, 1995; Teichmann and Muhr, 2015), resulting in the inhibition of some inflorescences by the dominance of other inflorescences. Our work expands on this existing knowledge, by highlighting the contribution of all parts of the inflorescence, including the inflorescence meristems (IMs) and fruit to this correlative control process, which we termed ‘infloretic dominance’ (Figure 2.4). The action of inflorescences, IMs and fruit collectively inhibits the outgrowth

of new inflorescences; loss of these organs either individually or in combination allows for the development of new inflorescences (see Figure 2.4).

The *quantity* of inflorescences produced is most likely controlled via signalling from the roots. *Which* inflorescences grow out however are most likely controlled via infloretic dominance. This method of signalling would allow the available nutrients and root volume to determine the overall scale of reproductive output by root-to-shoot SL and CK signalling. Infloretic dominance would then ensure that the most 'promising' inflorescences, i.e. those which are oldest/largest and have the greatest light availability, are those that access the growth potential defined by this root-to-shoot signalling.

Through this process it is also possible to explain the phenomenon of reflowering. This growth of late, new inflorescences in Arabidopsis only begins once the earliest fruits begin to dehisce. Fruit dehiscence in Arabidopsis is controlled by multiple hormonal signals, one of which includes a reduction in auxin (Ogawa et al, 2009); indeed, application of auxin to ripe fruits in *Brassica* results in delayed dehiscence (Ferrándiz, 2002). The outgrowth of these new inflorescences suggests that that the loss of auxin during seed shedding results in the release of infloretic dominance within the system. Arabidopsis thereby controls its inflorescence number through carefully balanced integration of environmental signals and dominance mechanisms between multiple organs simultaneously.

7.1.2 Systemic control of fruit number

Based on the data presented here, fruit number appears to be regulated principally by three parameters. The number of inflorescences is the first key determining factor; generally a plant with more inflorescences produces more fruit (Figures 2.1 D,F, 2.2, 3.1 A,D,E). The second key factor is IM activity that is responsible for the production of floral primordia. The longer the duration of IM activity, the larger the number of potential flowers within that inflorescence (Figures 5.4, 5.5). We have shown that

cytokinin dynamics are key to regulating IM activity (Figures 5.3 A-H); our data therefore support the recent findings of Merelo et al (2022), who have also shown that IMs arrest following a decline in CK levels in the shoot. Increasing the IM activity increases the number of floral primordia within the inflorescence, however that does not automatically lead to the development of more fruits on that inflorescence; the production of floral primordia does not guarantee flower opening and ultimate production of seeds.

The third controlling factor of fruit number is therefore the development of floral meristems (FMs). Arabidopsis inflorescences typically arrest with a cluster of unopened floral buds (Hensel et al, 1994). Under certain conditions however (e.g. local fruit removal) at least some of these buds are capable of opening (Figures 5.2 C,D). We have further extended this existing knowledge by showing that increased CK signalling also promotes the opening of floral primordia, especially via the ARABIDOPSIS HISTIDINE KINASE2 (AHK2) and AHK3 receptors (Figures 5.4 A,C). Interestingly, the rate of flower opening (florochron) in flowers opening after floral arrest is significantly lower than in pre-arrest conditions (Figures 5.6 C, 5.4 A). Merelo et al (2022) observed that WUSCHEL (WUS), a major regulator of meristem activity, shows a low level of reactivation following IM arrest, which might explain the slower development of these flowers.

We have previously postulated that correlative inhibition between fruits ('carpic dominance') is absent in Arabidopsis (Walker and Bennett, 2018; Figure 2.6). Fruit removal within an inflorescence does not affect the *size* of the remaining fruits (Figures 2.6, 2.ii), however fruit *number* increases when fruits are removed proximal to the inflorescence meristem, by preventing floral arrest. The removal of older fruits allowing the continued growth of younger flowers therefore appears to be phenomenologically equivalent to the correlative inhibition described between fruits in other species (Walker and Bennett, 2018; Bangerth, 1989), and as such could in effect be the same process as carpic dominance.

To better understand the relationship between carpic dominance and floral arrest, we can consider the effects of fruit removal in *Brassica napus*. Tayo and Morgan (1975)

showed that flower opening continues after the final seeds have been set in *B. napus*, while our work has expanded on that and shown that early fruit removal allows these flowers to set seed (Figure 2.iv). In untreated plants however, the youngest fruits are typically aborted very early in their development after a 'wobble zone', where successful fruits are interspersed with aborted fruits (Figure 2.iii). In both Arabidopsis and *B. napus* the number of final fruits therefore appears to be controlled by fruit-mediated correlative inhibition. This presents differently in both species however; in Arabidopsis, the dominance effect occurs very early in the floral development process, before fruit is ever formed, and flowers are inhibited from fully developing. In *B. napus* however, the dominance effect occurs later in flower development, after flower opening, but prior to seed development, and as such is more visible. It is thus probable that fruit-mediated correlative inhibition is a conserved mechanism controlling total fruit number per inflorescence in the Brassicaceae, but it manifests differently in different species. In Arabidopsis this occurs in the form of floral arrest, accounting for our initial suggestion that carpic dominance is not present in this species.

The findings presented here provide a solid framework on which to develop future study. The timing of floral arrest is a key determinant of yield, as it determines the end of seed production. Early arrest will shorten the window for developing seed, reducing yield; delayed arrest conversely increases the time frame in which seed can develop, increasing potential yield. Extension of IM and FM activity should increase the amount of seed produced by any one plant (as seen in the *rock2* and *rock3* mutants (Bartrina et al, 2017)). IM activity maintenance or reactivation are therefore excellent points of focus for future translational work.

One interesting observation is that we were unable to get Col-0 IMs to reactivate under our growth conditions, although existing immature FMs did reactivate following local fruit removal or global inflorescence removal. However, we saw that when the FMs reactivated, the IM typically terminally differentiated (Supplementary Figure 5.1 A), as described in Hensel et al (1994) in the context of *male sterile1* mutants, which never

occurred in untreated plants. This suggests that the IM may have tried and failed to reactivate. Interestingly, the same phenotype was often seen in *rock2* and *rock3* mutants, where the whole bud cluster opened without an initial arrest (Supplementary Figure 5.1 B). These terminally-differentiated IMs display some floral organs, but clearly in a highly disorganised manner. While we initially considered that this may have occurred due to a lack of CK, this now seems unlikely. Floral organ boundaries are regulated by APETALA2 (AP2) (Ó'Maoiléidigh, Graciet and Wellmer, 2013), which is downregulated via FRUITFULL (FUL) as the plant ages (Yant et al, 2010; Balanzà et al, 2018). A dramatic reduction in AP2 therefore seems the most likely cause of terminal differentiation of the IM, although this requires further examination. Future work aimed at extending flowering duration should also consider the regulation of CK and FUL/AP2, as both pathways have discrete but dramatic impacts on floral arrest. Upregulation of CK extends the flowering duration, while suppression of AP2 should allow for improved IM maintenance.

7.2 Homeostatic control of reproductive distribution

Organ ratios are an important component of reproductive output; producing too many fruits per inflorescence could increase risk of damage, while too few fruits per inflorescence would be a wasteful use of resources. The 50% rule appears to be an important mechanism conserved at least across the Brassicaceae, controlling the proportion of fruits developed on each inflorescence (Figure 3.1). As a result, the 50% rule controls the reproductive organ ratio.

Initially we hypothesised that the 50% rule could be explained as an extension of canalization-based competition between inflorescences, in which the rate of IM activity is regulated by continued competition between inflorescences post-activation. That is to say, they do not only compete to activate, but they also compete for ongoing 'growth potential' during the course of flowering. This may mean that the 50% rule is simply an emergent property of canalization-mediated competition between inflorescences. However, combining our findings regarding the 50% rule with those regarding the initiation of inflorescences (Supplementary Figure 4.1), an alternative possibility is that this phenomenon is linked to floral duration instead. In the data presented here, approximately 40% of the total floral duration of the plant (i.e. the combined floral duration of every inflorescence) was accounted for by that of the combined secondary inflorescences. Additionally, it was shown that secondary inflorescence duration was extended following removal of the subtending tertiary inflorescences (Figure 4.3). Higher order inflorescences therefore clearly shorten the duration of their parent inflorescence. It is thus probable that the homeostatic control of IM and floral arrest between inflorescences also indirectly results in the controlled '50% rule' distribution of fruits across the plant. Additionally, the rate of flowering (florochron) is the same across all inflorescences of the plant, almost certainly as a result of the same long-distance signals providing consistent information across the plant with regards to resource availability. Floral durations per inflorescence in the gibberellin mutant *della* follow the same pattern as those in the wild type, despite a significantly higher florochron (Supplementary Figure

4.3 A,B). Neither the gibberellin mutants, nor any others examined, deviated from the 50% distribution of flowers across the secondary inflorescences (Figure 3.1 E), regardless of florochron. All mutants examined across this body of research however did all follow the same ‘wave’ pattern of inflorescence initiation and arrest (see Supplementary Figure 4.1).

Whilst more work would be required to prove this hypothesis, there is good evidence that the 50% rule is an emergent property of individual inflorescence durations. As floral duration is controlled through auxin and cytokinin concentrations in the IM and stem, these correlative controls likely also indirectly regulate the number of fruits per inflorescence.

7.3 Control of reproductive shoot architecture by long-distance signals

Long-distance hormonal signalling is clearly essential for the control of reproductive architecture in plants. Integration of signals providing critical information regarding resource availability allows for optimised growth according to the current environmental conditions. Our identification of the key roles auxin and cytokinin play in the maintenance and development of IMs and FMs significantly contribute to the existing understanding of reproductive control.

7.3.1 A hypothetical model for control

While auxin and CK are long-established players regulating shoot architecture, this work highlights the importance of the interplay between these two hormones in the specific regulation of reproductive architecture. Here, a model is presented explaining floral duration and reproductive effort given the interplay between these two factors.

Initially there are high CK levels in the IMs and FMs, resulting from root-shoot transport of CK, and relatively low auxin levels, which allows for IM activity and FM opening (Figure 7.1 A). As fruits start to form, there is an increase in auxin in the inflorescence. Fruits and seeds are well-known to export significant amounts of auxin, which is required for their growth (Bangerth, 1989). As the number of fruits increases, auxin export likely causes inhibition of CK synthesis in the shoot. It is highly unlikely that CK levels decrease due to depleted resources in the soil as plants are able to re-flower, or indeed replace all inflorescences following their loss. As such, CK levels in the shoot are most likely to decrease as a result of local rather than systemic regulation. Previous work has shown that auxin represses the synthesis of *tZ* CKs, while iP CK biosynthesis is less affected (Nordström et al, 2004). Increasing numbers of fertile fruit will therefore increase the auxin levels in the stem (Goetz et al, 2021), decreasing *tZ* synthesis in the shoot. Over time the accumulation of auxin will decrease CK levels sufficiently to bring about arrest first in the IM, followed by floral arrest some days later (Figures 7.1 B, 5.1

A,B). AHK2 and AHK3 have differing affinities for the CK bases (Bartrina et al, 2011), with AHK3 having a higher affinity for *tZ* than iP, compared to AHK2 which has a similar affinity for both *tZ*s and iPs (Stolz et al, 2011; Spíchal et al, 2004). These differences could explain our observation that IM arrest occurs prior to, not simultaneously with, floral arrest. AHK2 expression occurs in both IMs and FMs, while AHK3 is most highly expressed in the FMs. As such, FMs are likely more sensitive to *tZ* when compared to IMs, allowing lower CK levels to maintain FM activity, even when levels are insufficient to maintain activity in the IM.

A second and not mutually-exclusive suggestion for the delay between IM and floral arrest is that of floral development. Flowers appear to be committed to growth once they reach stage 10 (Smyth et al, 1990)(Figure 5.2); potentially this is the stage at which they have canalized to the PATS. Therefore, even if IM arrest and floral arrest occur simultaneously, it may simply take floral arrest longer to become visible, because flowers that have reached stage 10 are able to continue developing even after the IM has visibly arrested.

The differences between AHK2 and AHK3 CK affinity likely explain the activity differences seen in the *rock2* and *rock3* mutants. Enhanced CK sensitivity in *rock2* IMs allows them to remain active for longer, while *rock3* plants lack this enhanced sensitivity in the IM, and therefore produce fewer floral nodes (Figure 5.4 B). Both genotypes maintain FM activity for longer than the wild type (Figure 5.4 A,C) due to increased sensitivity to CKs, despite their presumed declining concentrations. Additionally, this may explain the slower rate of flower opening seen late on in *rock3* inflorescences and reactivated wild type inflorescences (Figures 5.4 A, 5.6 C); *tZ* levels in the shoot will be much lower due to high auxin export from the fruits, and as such development of flowers will likely be slower, even if not prevented entirely. Enhanced sensitivity to CK, or increased CK availability through the removal of sinks such as inflorescences or fruits, will allow for extended meristem activity despite very high levels of auxin. This provides

plants with a mechanism to override their risk-averse growth strategies and compensate for organ loss (Figure 7.1 D).

Arabidopsis appears to use these same mechanisms to regulate tertiary inflorescence outgrowth; sufficient CK levels and a strong enough auxin sink strength in the inflorescence will allow for tertiary outgrowth (Figure 7.1 E), while a lack of CK and low auxin sink strength will inhibit growth (Figure 7.1 F).

In summary, it is likely that a combination of long distance CK and auxin signalling are therefore responsible for a large number of correlative controls seen in Arabidopsis and the Brassicacea. Altering the ratio of these hormones results in different outcomes, all of which result in the plant optimising growth for the existing conditions.

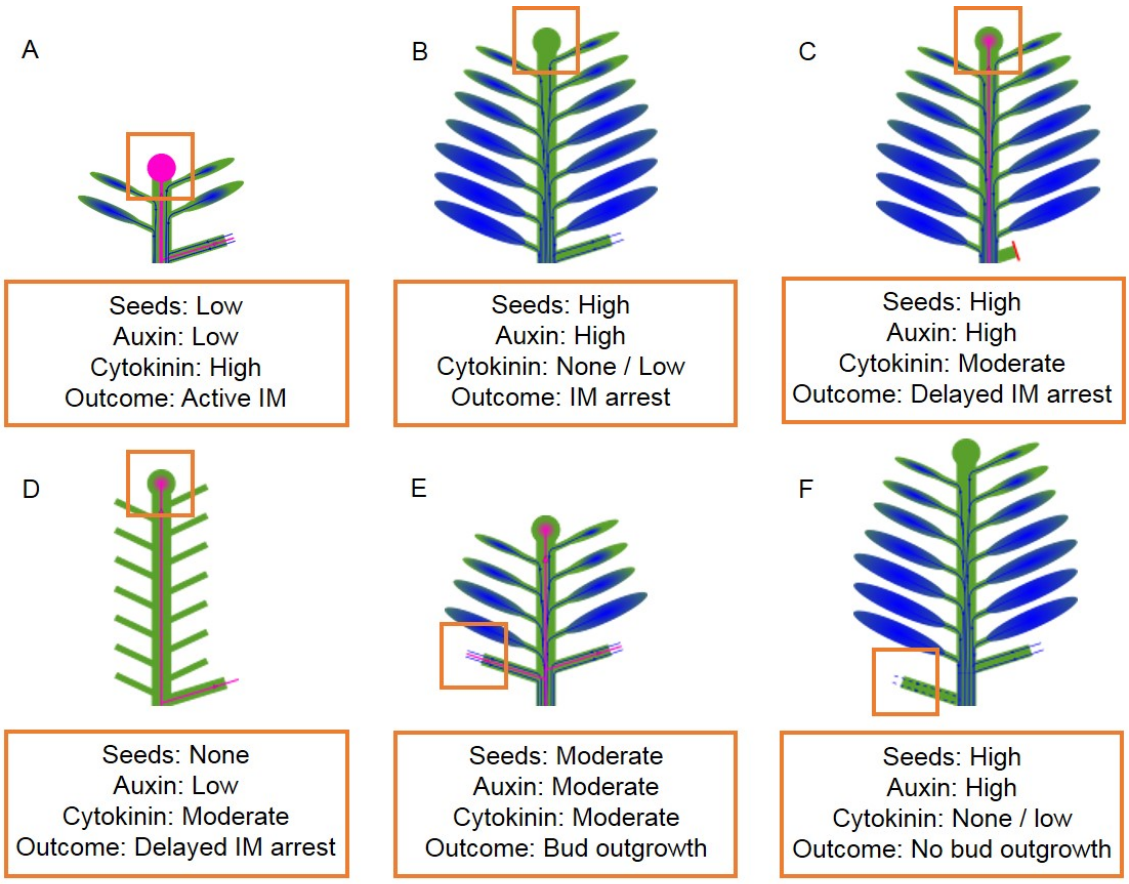

Figure 7.1. Roles of auxin and cytokinin signalling in reproductive development

Diagrams representing relative auxin (blue) and cytokinin (CK)(pink) levels under different growth conditions in Arabidopsis. In each case, the orange box indicates the location of interest in the inflorescence. **(A)** An actively-growing inflorescence meristem (IM); high CK expression, and is not inhibited by the auxin exported from the small number of local fruits. **(B)** An arrested IM; no CK expression, inhibited in part by high auxin expression in the fruits. **(C)** Global inflorescence removal; removal of additional CK sinks increases CK expression in the IM, extending IM activity despite high auxin export from fruits on the inflorescence. **(D)** Local fruit removal prevents high levels of auxin export to the stem, and as such CK is not downregulated, extending IM activity. This treatment will similarly allow the reactivation of existing floral meristems (FMs) if removed within several days of inflorescence arrest. **(E)** Bud outgrowth occurs when sufficient CK signalling occurs within the bud, and the stem sink strength is sufficiently high to allow auxin in the bud to canalize to the polar auxin transport stream (PATS). **(F)** Bud outgrowth is inhibited when auxin concentration in the stem is too high for the bud to canalize; high auxin concentration additionally reduces CK signalling, further inhibiting outgrowth.

7.4 Conclusions

The papers presented here collectively highlight the importance of correlative control across Arabidopsis reproductive shoot architecture. In particular, the roles of auxin in the control of floral arrest had been posited but unproven until now. The role of CK in the maintenance of IM activity supports recent similar discoveries (Merelo et al, 2022), however our work has taken this research one step further to highlight the two-stage process of arrest, occurring at both the IM and FM levels. Identification of the roles of AHK2 and AHK3 in maintaining activity in the inflorescence and floral meristems is of particular interest. This body of work has identified the AHK CK-signalling pathway as one of particular interest for future study. Modification of this pathway may allow us the ability to extend IM and FM activity in plants without the need for increased resources; in essence, it will allow us to override the risk-averse growth behaviour that inhibits yield production in crops.

References

Balanzà, V., Martínez-Fernández, I., Sato, S., Yanofsky, M.F., Kaufmann, K., Angenent, G.C. et al. (2018). Genetic control of meristem arrest and life span in *Arabidopsis* by a *FRUITFULL-APETALA2* pathway. *Nature Communications*, **9**, doi:10.1038/s41467-018-03067-5.

Bangerth, F. (1989). Dominance among fruits/sinks and the search for a correlative signal. *Physiologia Plantarum*, **76**, 608-614.

Bartrina, I., Otto, E., Strnad, M., Werner, T. and Schmülling, T. (2011). Cytokinin regulates the activity of reproductive meristems, flower organ size, ovule formation, and thus seed yield in *Arabidopsis thaliana. The Plant Cell*, **23**, 69-80.

Bartrina, I., Jensen, H., Novák, O., Strnad, M., Werner, T. and Schmülling, T. (2017). Gain-of-function mutants of the cytokinin receptors AHK2 and AHK3 regulate plant organ size, flowering time and plant longevity. *Plant Physiology*, **173**, 1783-1797.

de Jong, M., George, G., Ongaro, V., Williamson, L., Willetts, B, Ljung, K. et al. (2014). Auxin and strigolactone signaling are required for modulation of Arabidopsis shoot branching by nitrogen supply. *Plant Physiology*, **166**, 384-395.

Ferrándiz, C. (2002). Regulation of fruit dehiscence in *Arabidopsis*. *Journal of Experimental Botany*, **53**, 2031-2038.

Fisahn, J. and Hofner, W. (1995). Influence of a plant-growth regulator on the sink capacity of oilseed rape (*Brassica napus* L.). *Journal of Agronomy and Crop Science*, **174**, 99-109.

Goetz, M., Rabinovich, M. and Smith, H.M. (2021). The role of auxin and sugar signaling in dominance inhibition of inflorescence growth by fruit load. *Plant Physiology*, **187**, 1189-1201.

Hensel, L.L., Nelson, M.A., Richmond, T.A. and Bleecker, A.B. (1994). The fate of inflorescence meristems is controlled by developing fruits in Arabidopsis. *Plant Physiology*, **106**, 863-876.

Merelo, P., González-Cuadra, I. and Ferrándiz, C. (2022). A cellular analysis of meristem activity at the end of flowering points to cytokinin as a major regulator of proliferative arrest in *Arabidopsis*. *Current Biology*, **32**, 749-762.

Nordström, A., Tarkowski, P., Tarkowska, D., Norbaek, R., Åstot, C., Dolezal, K. and Sandberg, G. (2004). Auxin regulation of cytokinin biosynthesis in *Arabidopsis*

thaliana: a factor of potential importance for auxin-cytokinin-regulated development. *PNAS*, **101**, 8039-8044.

Ó'Maoiléidigh, D.S., Graciet, E. and Wellmer, F. (2013). Gene networks controlling *Arabidopsis thaliana* flower development. *New Phytologist*, **201**, 16-30.

Ogawa, M., Kay, P., Wilson, S. and Swain, S.M. (2009). ARABIDOPSIS DEHISCENCE ZONE POLYGALACTURONASE1 (ADPG1), ADPG2, and QUARTET2 are polygalacturonases required for cell separation during reproductive development in *Arabidopsis*. *The Plant Cell*, **21**, 216-233.

Phillips, I.D.J. (1975). Apical dominance. *Annual Review of Plant Physiology and Plant Molecular Biology*, **26**, 341-367.

Prusinkiewicz, P., Crawford, S., Smith, R.S., Ljung, K., Bennett, T., Orgaro, V. and Leyser, O. (2009). Control of bud activation by an auxin transport switch. *PNAS*, **106**, 17431-17436.

Smyth, D.R., Bowman, J.L and Meyerowitz, E.M. (1990). Early flower development in *Arabidopsis*. *The Plant Cell*, **2**, 755-767.

Snow, R. (1937). On the nature of correlative inhibition. *New Phytologist,* **36**, 283-300.

Spíchal, L., Rakova, N.Y., Riefler, M., Mizuno, T., Romanov, G.A., Strnad, M. and Schmülling, T. (2004). Two cytokinin receptors of *Arabidopsis thaliana*, CRE1/AHK4 and AHK3, differ in their ligand specificity in a bacterial assay. *Plant and Cell Physiology*, **45**, 1299-1305.

Stolz, A., Riefler, M., Lomin, S.N., Achazi, K., Romanov, G.A. and Schmülling, T. (2011). The specificity of cytokinin signalling in Arabidopsis thaliana is mediated by differing ligand affinities and expression profiles of the receptors. *Plant Journal*, **67**, 157-168.

Tayo, T.O. and Morgan, D.G. (1975). Quantitative analysis of the growth, development and distribution of flowers and pods in oil seed rape (*Brassica napus* L.). *The Journal of Agricultural Science*, **85**, 103-110.

Teichmann, T. and Muhr, M. (2015). Shaping plant architecture. *Frontiers in Plant Science,* **6**, doi:10.3389/fpls.2015.00233.

Umehara, M., Hanada, A., Magome, H., Takeda-Kamiya, N. and Yamaguchi, S. (2010). Contribution of strigolactones to the inhibition of tiller bud outgrowth under phosphate deficiency in rice. *Plant and Cell Physiology*, **51**, 1118-1126.

Wheeldon, C.D. and Bennett, T. (2021). There and back again: An evolutionary perspective on long-distance coordination of plant growth and development. *Seminars in Cell and Developmental Biology*, **109**, 55-67.

Wheeldon, C.D., Hamon-Josse, M., Lund, H., Yoneyama, K. and Bennett, T. (2022). Environmental strigolactone drives early growth responses to neighbouring plants and soil volume in pea. *Current Biology*, **32**, 3593-3600.

Yant, L., Mathieu, J., Dinh, T.T., Ott, F., Lanz, C., Wollmann, H. et al. (2010). Orchestration of the floral transition and floral development in *Arabidopsis* by the bifunctional transcription factor APETALA2. *The Plant Cell*, **22**, 2156-2170.

Yoneyama, K., Xie, X., Nomura, T., Yoneyama, K. and Bennett, T. (2022). Supra-organismal regulation of strigolactone exudation and plant development in response to rhizospheric cues in rice. *Current Biology*, **32**, 3601-3608.